Quantification of Oxygen Dynamics in the Grand River Using a Stable Isotope Approach

by

Terra Stephanie Jamieson

A thesis
presented to the University of Waterloo
in fulfilment of the
thesis requirement for the degree of
Doctor of Philosophy
in
Earth Sciences

Waterloo, Ontario, Canada 2010

Author`s Declaration

I hereby declare that I am the sole author of this thesis. This is a true copy of the thesis, including any required final revisions, as accepted by my examiners.

I understand that my thesis may be made electronically available to the public.

Abstract

The current study monitored DO, stable isotopes of O_2 ($\delta^{18}O$-O_2 and $\delta^{18}O$-H_2O) along with water quality parameters on both a diel and day-time only basis in the Grand River over several seasons and locations. A dynamic dual mass-balance model was developed to quantify rates of community respiration (CR), gross primary production (GPP), and gas exchange coefficients (k) in the Grand River, Ontario, Canada. Monitoring was conducted at three locations along a longitudinal gradient: 1) West Montrose (WM), located upstream of the cities of Kitchener and Waterloo in a predominately agricultural landscape; 2) Bridgeport (BRPT), located downstream from WM and the Conestogo tributary confluence, and 3) Blair (BLR), located downstream of the cities of Kitchener and Waterloo.

Values of k in the Grand River ranged from 3.6 to 8.6 day^{-1}, over discharges ranging from 5.6 to 22.4 $m^3 s^{-1}$, with one high-flow event of 73.1 $m^3 s^{-1}$. The k values were relatively constant over the range of discharge conditions studied. The range in discharge observed in this study is representative of non-storm and summer low-flow events; a greater range in k might be observed under a wider range of hydrologic conditions. Overall, k values obtained with the isotope model for the Grand River were found to be lower than predicted by the traditional approaches evaluated, highlighting the importance of determining site-specific values of k.

Metabolism results indicated that the Grand River is negatively impacted by both agricultural and urban inputs from the surrounding catchment. Metabolism rates in the Grand River (GPP = 2.2 to 19.9 and CR = 4.0 to 29.6 g O_2 m^{-2} d^{-1}) were found to be greater than published estimates for relatively undisturbed systems. Rates of GPP were seasonally variable at all three sampling locations, that were mainly correlated with changes in incoming radiation. The CR rates were more consistent seasonally, exhibiting moderate declines from May to December in both 2003 and 2004, likely related to decreases in temperature. The greatest rates of CR, on average 7.2 g O_2 m^{-2} d^{-1}, were measured at BLR, due to the additional input of nutrients and DO consuming substances from the urban catchment. Autotrophic production appears to be a more important energy base upstream (WM and BRPT sampling locations), as indicated by greater P:R values, as well as more positive net production rates. Net production at BLR was consistently below zero, indicating that DO inputs are not sufficient to overcome the oxidative demand upstream of this location.

Laboratory bottle incubations, submerged chamber trials, and model simulations yielded a wide range of α_r values. An overall mean of 0.994 was calculated from bottle incubation experiments. In the submerged chambers, there was little to no isotopic enrichment detected with respect to $\delta^{18}O$-O_2, despite declines observed in DO concentrations, potentially due to diffusion limitation. The model-derived α_r values mainly ranged from 0.942 to 0.998. The modeled α_r values tended to be closer to one at BLR, as compared to WM and BRPT, which exhibited similar α_r. Higher α_r values at the BLR site may be due to DO consumption reactions that have little to no fractionation, or respiration in diffusion limited sediments. Model derived α_r values found from modeling night conditions appeared to be greater than α_r derived from day data. The discrepancy of α_r among the day and night model simulations may be related to DO concentration regime or consumption characteristics under day conditions that are not captured in the model.

The addition of an isotopic mass balance provides for a corroboration of the input parameter estimates between the two balances, and constrains the range of potential input values to allow for a better estimate of GPP, CR and k. Input parameter uncertainty and sensitivity most likely reflect the dynamic processes occurring in the Grand River watershed. In this study, model error appears to be primarily linked to the ability of the isotopic mass balance to describe observed $\delta^{18}O\text{-}O_2$ data. A better understanding of processes affecting $\delta^{18}O\text{-}O_2$ would improve the capability of the model to replicate observed data, and provide more confidence in predicting metabolic processes in impacted rivers.

Acknowledgements

I would like to take this opportunity to express my gratitude to my supervisors, Dr. Sherry Schiff, and Dr. Bill Taylor, for their support during my doctoral studies. They have challenged me and helped me develop my critical thinking skills, become a more effective writer, and become a better scientist. I would also like to extend my thanks to the other members of my supervisory committee, Dr. Len Wassenaar, Dr. Ramon Aravena, for your support, feedback, and interest in my research. We are all works in progress, and I thank you for "helping me progress." Another thank-you goes to Mark Anderson and the Grand River Conservation Authority, who provided me with data, site accessibility, and feedback.

I cannot express enough thanks to the people who provided me with field and laboratory support; you made this research possible. Thank you to Kevin, Brianna, Stuart, Ashley, Andrea, Paul, Matt, Simon, Cameron, and Dave, to mention a few. An extra-special thank you to Richard Elgood for being a fantastic laboratory manager, and being the glue that holds us, and the research, together. Another huge thank you goes to Sue Fisher for her outstanding administrative support. I am grateful to my fellow graduate students who have been great friends and colleagues, and have provided me with personal and professional support. Last, but not least, I am grateful to my family for their continued support, not to mention patience, throughout my academic endeavours. In particular, I would like to express my utmost thanks to my husband, Rob. You were a somewhat capable field assistant, an excellent sounding board, and I couldn't ask for a more wonderful partner. Thank you for luring away the bats at West Montrose at dawn so I could collect my samples.

This research was supported by the Natural Sciences and Engineering Research Council, Ontario Graduate Scholarship Program, the University of Waterloo Provost's Faculty of Science Graduate Women's Incentive Fund, and the Ontario Centres of Excellence.

Table of Contents

List of Tables

List of Illustrations

List of Abbreviations

$^{18:16}O$	Ratio of ^{18}O to ^{16}O in dissolved oxygen
α_p	Fractionation effect of photosynthesis
α_r	Fractionation effect of respiration
δ, δ_0	Isotopic signature of dissolved oxygen in delta notation, and at time zero (Rayleigh Distillation Equation)
$\delta^{18}O\text{-}H_2O$	Isotopic signature of molecular oxygen in water, in delta notation
$\delta^{18}O\text{-}O_2$	Isotopic signature of dissolved oxygen, in delta notation
APHA	American Public Health Association
BLR	Blair sampling location
BRPT	Bridgeport sampling location
CCME	Canadian Council of Ministers of the Environment
CR	Community respiration
CR_T, CR_{20}	Community respiration at a given temperature (C), and at 20 C
D	Mean depth of the river channel
DIC	Dissolved inorganic carbon
DOC	Dissolved organic carbon
DO	Dissolved oxygen concentration
DOsat	Dissolved oxygen concentration at atmospheric equilibrium
f	Fraction of dissolved oxygen remaining (Rayleigh Distillation Equation)
G or GE	Gas exchange
GPP	Gross primary production
GRCA	Grand River Conservation Authority
k	Gas transfer coefficient
k_T, k_{20}	Gas transfer coefficient at a given temperature (C), and at 20 C

NP	Net production (GPP-CR)
NPRI	Environment Canada National Pollutant Release Inventory
P	Photosynthesis
Pmax	Maximum gross primary production rate
PWQMN	Ontario Ministry of the Environment Provincial Water Quality Monitoring Network
Q	River discharge
R	Respiration
RCC	River Continuum Concept
RMS	Root mean squared error
TIN	Total inorganic nitrogen
TN	Total nitrogen
TON	Total organic nitrogen
TP	Total phosphorus
V	Mean river velocity
VSMOW	Vienna Standard Mean Ocean Water
WM	West Montrose sampling location

1.0 Dissolved Oxygen and Community Metabolism in Rivers

1.1 Introduction

Oxygen (O_2) is the second most abundant gaseous constituent in the atmosphere, after nitrogen, making up 21% on a volume basis at sea level (Cole, 1994). Oxygen mediates biogeochemical cycles, acting as an oxidizing agent and supporting respiration by aerobic organisms. Minimum concentrations are required to support aerobic organisms. In streams and rivers, dissolved O_2 (DO) is a primary criterion for assessing water quality, with minimum concentrations of at least 5.5 mg L^{-1} for the protection of aquatic biota (CCME, 2007).

In aquatic ecosystems, the main controls on DO concentrations are diffusion from the atmosphere, photosynthesis, and respiration. Photosynthesis introduces DO into the water column, whereas community respiration, along with abiotic oxidative processes, is responsible for DO consumption. In waters impacted by excess nutrients, the resultant proliferation of phototrophic biomass can lead to large daily DO fluctuations. High levels of photosynthesis can induce supersaturation during the day, followed by depleted DO concentrations, sometimes anoxia, during the night due to respiration. Gas exchange dampens these daily oscilliations by driving net O_2 gain or loss, depending on concentration relative to aqueous solubility, with O_2 solubility declining with increases in temperature and salinity, and decreases in pressure. As DO is a key indicator of water quality, it is therefore of interest to quantify gas transfer, primary production and respiration rates in a system and to understand the processes responsible for the variation observed. Understanding these processes is imperative for evaluating the metabolic balance of an aquatic ecosystem, as well as for developing strategies for managing impacted river systems.

1.2 Gas Exchange

Two theories are widely used to describe gas transfer in natural waters: the two-film model, mainly applied to standing waters, and the surface-renewal model, commonly used in flowing waters (Chapra, 1997). In the two-film model (Lewis and Whitman, 1924) it is assumed that gas travels through two adjacent laminar films at the air-water interface, where the atmosphere and liquid on either side of the films are well-mixed by turbulence. This theory assumes that the greatest resistance is in the two laminar boundary layers where flux is governed by molecular diffusion. The surface-renewal theory, however, assumes that in an agitated liquid, as in rivers, turbulence extends to the surface and, therefore, no laminar boundary layer exists (Danckwerts, 1951). The gas transfer velocity for O_2 entering the water column is then dependant on the surface renewal rate, or turbulence, as well as the diffusion rate of the gas in water (Chapra, 1997).

The mass flux of O_2 in rivers is generally assumed to be a product of the deviation of DO from saturation in the water column, multiplied by a mass-transfer coefficient:

$$GE = k(DO_{sat} - DO) \tag{1.1}$$

Where GE is gas exchange, the mass flux of O_2 in DO concentration time^{-1}, k is the gas transfer coefficient, and DO_{sat} is the concentration of DO at equilibrium. To obtain a surface transfer coefficient on a length time^{-1} basis, k would have to be multiplied by mean depth, but for rivers k value is typically treated as a first order rate constant expressed on time^{-1} basis. The water column is assumed to be well-mixed with a homogeneous DO concentration. The deviation of DO from atmospheric saturation controls the direction and magnitude of O_2 moving into or out of solution.

Obtaining accurate measurements of k is essential for modeling DO and determining the assimilation capacity of rivers receiving organic effluents. There are more than 34 empirical, semi-empirical, and theoretical formulas that have been proposed to predict k in rivers (McCutcheon, 1989). Comprehensive reviews and critiques of the many formulas have been provided elsewhere (Bowie et al., 1985; McCutcheon, 1989). These models are usually parameterized in terms of water velocity and mean depth, and sometimes bed slope. Choosing a gas exchange formula then depends on the geometric similarity between the river under examination and the river used to calibrate the empirical relationship (Bennett and Rathburn, 1972). Gas exchange coefficient formulas have commonly been developed and calibrated using tracer techniques, including gaseous tracers (e.g., methyl chloride, ethylene, propane, SF_6; Wilcock, 1988; Wanninkhof et al., 1990; Clark et al., 1992), radioactive tracers (^{85}Kr; Tsivoglou and Neal, 1976), and following the reaeration of deoxygenated water (Churchill et al., 1962; Owens et al., 1964). One of the most commonly used models, the O'Connor-Dobbins formula (O'Connor and Dobbins, 1956) was derived theoretically from the surface renewal theory and the diffusivity of oxygen in natural waters. Radioactive tracer techniques tend to yield the most accurate k values (Bowie et al., 1985) but have been limited in application due to the potentially hazardous effects of radiation (Bicudo and James, 1989). The use of inert gas tracers is also subject to controversy regarding the accuracy and reproducibility of the data (Bowie et al., 1985).

Additional approaches have also been developed from DO mass balance modeling techniques. Odum and Hoskin (1958) developed a method for calculating k, also recommended by Owens (1974), where the DO deficit (i.e., DO_{sat}-DO) is regressed against the rate of change in DO (i.e., dDO/dt) after sunset, the slope of which is k. Chapra and Di Toro

(1991) have also developed an analytical solution for determining k from a single diel DO monitoring station, showing that k is a function of the time lag between solar noon and DO maximum, and day length. This function is sensitive to temperature changes during the day, data errors for sites with short time lags (i.e., high reaeration rates), and assumes that primary production follows a half-sinusoidal curve. Chapra and Di Toro's (1991) approach would mainly be useful for cloudless days at sites where there is only one DO maximum occurring after solar noon, when photosynthesis is not limited by nutrients, and when photosynthesis is linearly dependent on light.

1.3 Respiration and Photosynthesis

Living organisms in lotic ecosystems drive the production/decomposition cycle, which in turn cause, along with temperature which affects DO solubility, DO fluctuations on a temporal basis. Autotrophic organisms convert inorganic nutrients into more complex organic molecules via photosynthesis (i.e., primary production). In turn, the organic material serves as an energy source for heterotrophic organisms to return the organic matter back to the inorganic state via decomposition. Together, autotrophs and heterotrophs in river ecosystems make organic energy available to organisms at higher trophic levels (Allan, 1995). The cycle can be represented in very basic terms by the following expression:

$$6CO_2 + 6H_2O \underset{\leftarrow\text{respiration}}{\overset{\text{photosynthesis}\rightarrow}{\rightleftharpoons}} C_6H_{12}O_6 + 6O_2 \qquad (1.3)$$

The major phototrophs of running waters are aquatic plants (macrophytes) and algae. Algae are small autotrophs that are referred to as periphyton when found on substrates, and phytoplankton when in suspension within the water column (Allan, 1995). The relative abundance of the various groups of primary producers depends on river size and condition (Allan, 1995; Chapra, 1997). In larger lowland rivers, phytoplankton would tend to develop during times of moderate flow. Macrophytes are more abundant in shallower, mid-sized rivers or within marginal backwaters. Attached periphyton tends to be found on all substrates and surfaces, particularly in shallower depths where light is available. Stream biomass is controlled by the main factors of light, flow, temperature, grazing, as well as availability of nutrients (Giller and Malmqvist, 1998; Uehlinger et al., 2000). Nutrient additions may enhance primary production when ambient concentrations are low; however, in rivers draining urban and agricultural basins, nutrient concentrations usually do not limit algal growth or primary production (Uehlinger et al., 2000).

In most systems, when not subjected to physical disturbances or nutrient limitation, primary production parallels the temporal variations of solar radiation (Servais, 1984; Uehlinger et al., 2000). The influence of light on photosynthesis and primary production can be substantial. Generally speaking, Cosby and Hornberger (1984) describe the relationship between light and photosynthesis as follows: photosynthesis increases linearly with light at low light intensities, becomes constant at higher intensities (i.e., photosaturation), and, in some instances, can begin to decline when light is particularly intense (i.e., photoinhibition). Community respiration in rivers generally refers to the heterotrophic oxygen-consuming processes of the biomass; this includes the respiratory pathways of microorganisms, plants, and animals. In addition to the autochthonous inputs from primary production, allochthonous

inputs from surrounding terrestrial, wetland, and riparian ecosystems, as well as from anthropogenic sources (e.g., agriculture, domestic, industrial) contribute to the energy base. In unimpacted lotic ecosystems, the largest respiratory O_2 demand is considered to be primarily attributable to the microbial (e.g., bacteria and fungi) utilization of organic matter (Fuss and Smock, 1996).

A number of studies have looked at the physical and chemical controls on respiration rates in streams and rivers. Bott et al. (1985) found, in a survey of sixteen systems in the United States, that variation in community respiration was mainly attributable to temperature, and secondarily due to the quality and particle size of organic matter. Community respiration rates also reflected both the amount and quality of substrates, where rates were inversely correlated with detrital size. Howarth et al. (1992) also found that respiration rates in the Hudson River, NY, were highly correlated with temperature.

Other researchers, however, have found weak respiration-temperature relationships (Fuss and Smock, 1996; Hill et al., 2002). Even though Fuss and Smock (1996) had found that water temperature was a significant factor in predicting respiration, its addition as an independent variable improved the regression model only slightly. Other significant explanatory variables included nitrogen and organic matter content of stream sediments. The effect of factors varied according to substratum and season. Hill et al. (2002) measured benthic microbial respiration in 214 streams in the northeastern United States via DO consumption and dehydrogenase activity (which would include both aerobic and anaerobic microbial respiration). Canonical correlation analyses found that increases in microbial respiration, measured as DO consumption, were positively correlated with pH, riparian zone

agriculture, and stream depth; respiration was negatively correlated with DOC and stream elevation. However, only 17% of the variability in DO consumption was explained by these variables and respiration was relatively insensitive to environmental stressors.

Whole stream respiration is usually assumed to be independent of light (Odum, 1956; Odum and Hoskin, 1958; Owens, 1974; Pearson and Crossland, 1996), and the influence of photorespiration is generally ignored by DO modelers. Photorespiration involves the uptake of O_2 during photosynthetic O_2 evolution (Osmond, 1981). Osmond and Grace (1995) describe photorespiration as an inefficiency in the metabolism of plants that enhances their ability to photosynthesize under conditions of excessive solar input. Parkhill and Gulliver (1998) found that by including photorespiration in the whole-system analyses of experimental streams, photosynthesis estimates could increase by greater than 30% as compared to analyses that excluded photorespiration. In this case, photorespiration was estimated by empirically fitting a photorespiration coefficient as a function of photon flux density and was not measured directly. Photorespiration in the experimental streams was also positively correlated with photosynthesis rate, but could not be consistently observed in cases of low productivity or actively developing plant communities.

1.4 River Metabolism

River system metabolism and functioning are generally dependant on local characteristics of the drainage basin, such as geographic region, land-use, hydrology, season, and watershed vegetation. Rates of gross primary production, respiration, and P:R vary by orders of magnitude depending on the watershed conditions (Table 1.1). Since the work of Odum

(1956), analyses of river metabolism have traditionally emphasized the ratio of gross primary production to community respiration, or P:R, as a predictor of functioning (Servais et al., 1984; Allan, 1995). The P:R has been considered to indicate whether a lotic ecosystem is a net producer or consumer of organic matter. A system that respires all energy fixed via photosynthesis has a P:R ratio of 1, and is considered "balanced". Ratios greater than 1 would imply that the system is predominately autotrophic, and that export or accrual of energy is occurring. Therefore, heterotrophic systems would have a P:R of less than 1, relying on additional, or imported, energy. Rosenfeld and Mackay (1987) have argued that P:R is inadequate and misleading as an index of the relative contributions of allochthonous and autochthonous inputs in supporting stream metabolism. The error lies in that P:R=1 is not necessarily the transition point between an autochthonous and allochthonous based ecosystem. However, it was conceded that P:R is a useful summary statistic for characterizing whether a system is a net producer or consumer of organic matter.

Table 1.1 Gross primary production (GPP), community respiration (CR), both in g O_2 m^{-2} d^{-1}, along with P:R values from various river metabolism studies.

River(s)	Description	Sampling Period	Quantification Method	GPP	CR	P:R
Boreal forested watersheds, QC:		Apr-Nov	*In situ* benthic Chambers			
First Choice Creek	1st order		containing	<0.5	<0.5	-
Beaver Creek	2nd order		macrophytes,	0.3-1.5	0.3-2.0	-
Muskrat River	5th order		periphyton, moss,	0.3-1.5	1.0-1.5	-
Matamek River	6th order		and detritus	0.3-4.0	0.3-3.0	-
Moisie River	9th order			0.3-5.0	0.3-3.0	-
(Naiman, 1983*)						
Pennsylvania, PA	Eastern deciduous forest (1st-5th order)	Seasonal	*In situ* benthic Chambers	0.66-2.02	1.11-2.17	-
Michigan, MI	Eastern deciduous forest (1st-5th order)		containing colonized natural	0.28-3.37	0.71-2.88	-
Idaho, ID	High desert (2nd-6th order)		substrates operated for 3-4 days.	0.68-1.63	0.59-1.25	-
Oregon, OR	Coniferous forest (1-7th order)			0.16-0.65	0.36-0.51	-
(Bott et al., 1985)						
Cow Creek, OK (Hunter and Carroll, 1985)	5th order stream receiving municipal and industrial effluents.	Jul	DO modeling using DO and BOD data to calculate diffusion rates	1.9-37	26.2-50.0	0.06-1.14
Ogeechee River, GA (Edwards and Meyer, 1987)	6th order blackwater river.	Monthly over 4 y	Single station DO open channel, diffusion calculated by Owens et al. (1964)	0.49-13.99	3.7-11.5	0.09-1.3
Walker Branch, TN	1st order forested stream.	Apr-Nov	Two station DO open channel, diffusion calculated via tracer study	0.12-1.74	1.06-2.48	0.05-1.02
(Marzolf et al., 1994**)						
Vermilion River, IL (Wiley et al., 1990)	Mixed land-use watershed: 90-93% agricultural.	Jul-Sept	Single station DO open channel, diffusion calculated via night-time regression	<.1-44.2	6.2-41.6	-
Waikato Region, NZ (Wilcock et al., 1998)	23 lowland streams under intensively grazed agricultural land use	Summer	Single station DO open channel, diffusion calculated using productivity analysis***	0.5-29.2	3.5-55.0	0.11-1.87
Taieri River, NZ (Young and Huryn, 1999)	Tussock grassland	Seasonal	Two station DO	.83	4.59	0.2
	Native forest		open channel,	.59	5.36	0.1
	Pasture		diffusion calculated	1.36	2.03	0.7
	Exotic forest		via tracer study	1.48	2.33	0.7
	Grassland/pasture			3.7	2.68	1.5

Table 1.1 continued. Gross primary production (GPP), community respiration (CR), both in g O_2 m^{-2} d^{-1}, along with P:R values from various river metabolism studies.

River(s)	Description	Sampling Period	Quantification Method	GPP	CR	P:R
Thames, UK Pang, UK Kennet, UK (Williams et al., 2000**)	Predominately rural river reaches. Mean flows of 31.0, 0.6, and 1.3 m^3s^{-1} for Thames, Pang, and Kennet, respectively.	Aug-Oct	Single station DO open channel, diffusion calculated using delta method****	9.4 2.6 14.5	19.1 4.3 15.8	0.5 0.6 0.9
Eight N. American streams from several biomes located in PR, AZ, TN, NM, KS, MI, OR, and NH (Mulholland et al., 2001)	Undisturbed 1st -3rd order streams	Once / stream Jan (PR) - August	Two station DO method (Marzolf et al., 1994)	<0.1-15	2.4-11	0.01-1.8
2 Lowland Streams near Berlin, DE (Gucker et al., 2006)	1st and 3rd order streams, impacted by wastewater treatment plant and agricultural inputs	Winter/ Spring/ Summer	Modified, two station DO method (Marzolf et al., 1994)	<0.1-59	6-59	<0.01-1.1
Fosse Bagnatore, IT (Ruggiero et al., 2006)	3rd order stream, impacted by wastewater treatment plants	Monthly Feb - Jul	Two station DO method (Marzolf et al., 1994)	<0.1-1.8	2.1-47.8	-
River Thur, CH (Uehlinger, 2006)	7th order, gravel bed tributary of the Upper Rhine	15 yrs of daily DO data	Single station DO open channel, diffusion calculated via night-time regression	5.0±0.6	6.2±1.4	0.53-1.0

* estimated from figure presented in paper
* calculated from data results presented in paper
** Hornberger (1975)
*** Chapra and Di Toro (1991)

Streams receiving inputs from agricultural, municipal, and industrial activities (Table 1.1) tend to exhibit higher rates, and a wider range, in both photosynthesis and respiration (Hunter and Carroll, 1985; Wiley et al., 1990; Wilcock et al., 1998; Williams et al., 2000) compared to less impacted systems (Bott et al., 1985; Marzolf et al., 1994; Young and Huryn, 1999). Streams and rivers affected by agriculture often become more autotrophic due to reduced shading and enhanced nutrient levels (Allan, 1985). In stream reaches receiving discharges from wastewater treatment plants, respiration can be substantially elevated producing low P:R values, due to increased concentrations of DO-consuming substances (Paul and Meyer, 2001; Gucker et al., 2006; Ruggiero et al., 2006). Oxygen depletion downstream of combined sewer overflows has also been attributed to increases in bacterial loads, biodegradable organic carbon inputs, as well as toxicity to phytoplankton communities, causing depressed photosynthesis (Even et al., 2003).

In an attempt to develop a conceptual framework to describe the function of a watershed from headwaters to mouth, Vannote et al. (1980) developed the river continuum concept (RCC). The basic premise of the RCC is that downstream changes in hydrology and geomorphology produce predictable changes in the structure and functioning of the biological community. According to the RCC, a watershed can be divided into three main sections, the headwater, middle, and lower reaches, as represented by stream order (Table 1.2). The continuous gradient of physical conditions, in theory, should result in predictable biotic responses with consistent patterns of loading, transport, utilization, and storage of organic matter along the length of the river (Vannote, 1980).

Table 1.2 Summary of general watershed characteristics under the river continuum concept.

Watershed Section	**Stream Orders**	**Characteristics according to the RCC**
Headwater Reaches	1-2	• narrow and highly shaded • allochthonous production: the energy base of biota is mainly coarse particulate organic matter from terrestrial sources (leaves and wood) • primary biota are shredders and collectors • very little plant growth • respiration > photosynthesis
Middle Reaches	3-6	• less shading as stream becomes wider • autochthonous production: due to an abundance of photosynthesis by plants and algae • the invertebrate community shifts from shredders to grazers (which feed on periphyton) • most biologically diverse part of the river system • photosynthesis ≥ respiration
Lower Reaches	> 6	• large, wide rivers • high turbidity and unstable bed material**,** leading to therefore less light penetration and fewer photosynthetic plants. • phytoplankton are the predominate autotrophs • allochthonous production: the transport of dissolved organic matter and fine particulate organic matter from upstream and the floodplain is the primary source of food • respiration > photosynthesis

In the watershed headwaters, dense shading from the surrounding forest restricts primary productivity and results in P:R of less than one. As the channel widens downstream in the middle reaches, the increased exposure to incoming radiation promotes more photosynthesis, increasing P:R to one or greater. In the lower part of larger rivers, increased depth and turbidity limit light and photosynthesis, driving P:R values to less than one. The basic premise of the RCC has been generally supported mainly by data obtained from temperate forested watersheds in North America (Minshall, 1983; Naiman et al., 1983; Bott et al., 1985; Minshall et al., 1992).

The RCC theory presents an idealized scheme, and is challenged in some watersheds that are structurally different than forested rivers. Longitudinal patterns in vegetation, productivity, and stream temperature have been found to be inverted in grassland systems relative to RCC concepts (Wiley et al., 1990; Young and Huryn, 1999). Upper portions of the watershed drain open, unforested, prairie lands allowing for greater incoming light, higher stream temperatures, and higher rates of autotrophic production. Light availability due to riparian shading and turbidity decrease in the lower reaches, driving P:R down. Watersheds strongly affected by floodplains can become more dependent on allochthonous organic inputs with increased reach size, despite concurrent increases in primary productivity due to proportionally higher increases in respiratory demands (Meyer and Edwards, 1990).

In landscapes affected by human alteration, activities such as deforestation, agriculture, and urbanization cause watershed changes that affect stream metabolism. Catchments subjected to increased urbanization tend to be characterized by more severe high flow events and elevated concentrations of contaminants and nutrients, altered channel morphology and

stability, and less biodiversity (Meyer et al., 2005; Walsh et al., 2005). Human modification of rivers for hydrologic regulation by dams and levees can also negate the expected longitudinal sequence of energy inputs and metabolic changes and natural flow regimes (Allan, 1995). Despite criticisms of the RCC, the paradigm that streams and rivers are integrated systems and that energy inputs vary along streams with predictable consequences for the ecosystem processes and biota is heuristic, providing a framework for viewing watersheds in a holistic manner (Minshall et al., 1985; Allan, 1995).

1.5 Quantifying DO Dynamics in Rivers

A number of techniques have been developed to quantify the sources and sinks of DO in rivers. Approaches that have been commonly employed to quantify photosynthesis and respiration include light and dark bottle incubations (Cole 1994), as well as the use of chamber studies in which a portion of the benthic community is enclosed, and changes in DO, pH, or uptake of radioactive isotopes are monitored (Marzolf et al., 1994). Chamber studies have advantages that include: i) replicability, ii) the ability to prevent gas exchange, and iii) the ability to isolate components of the system and/or specific biota (Marzolf et al., 1994). However, problems associated with chamber studies include: (i) non-representative sampling of the ecosystem, (ii) creation of an unnatural environment where the community is isolated from the influences of water velocity and turbulence, (iii) prevention of nutrient and DO exchange with the rest of the system, and (iv) errors associated with scaling up the results to represent the entire system (Marzolf et al., 1994).

With respect to quantifying river metabolism, one of the most common approaches is to measure DO and temperature over a diel period at either one or at two sampling locations over a given reach. Changes in DO during night time are assumed to be attributable to respiration, taking into account reaeration due to gaseous diffusion. The rate of respiration found from night time measurements is subtracted from the total day time rate of DO change, corrected for diffusion, to determine the total diel photosynthesis of a system (Odum, 1956; Odum and Hoskin, 1958; Owens, 1974; Pearson and Crossland, 1996). One of the main advantages of the open-water approach is that metabolism measurements can be obtained relatively easily and cheaply, over a large heterogeneous area, while not disturbing the ecosystem (Kosinski, 1984). These measurements of metabolism are representative of all the components of ecosystem (e.g., benthic, water column, and hyporheic communities; Marzolf et al., 1994). Observations on the changes can also be conducted over a long period of time, whereas enclosed experiments are limited in time by changes in metabolite concentration, changes in biotic assemblages, and enclosure effects on the biota (Westlake, 1978).

However, there are several disadvantages to the open-water approach that should be noted. Unlike enclosure methods, even though repeated measurements can be taken, no true replication can be performed. The assumption that whole stream respiration is relatively constant and independent of incident solar radiation has also been questioned and it has been suggested that photorespiration can contribute to daytime respiration (Parkhill and Gulliver, 1999), as aforementioned. In addition, one of the greatest difficulties associated with the successful application of this approach is the estimation of an accurate gas transfer coefficient across the water surface.

1.6 Stable Isotope Theory

An isotope of a given element (nuclide) is defined by the number of neutrons in the nucleus, while the number of protons identifies the element itself. The atomic mass number is the sum of the protons and the neutrons. Even though there can be a large range of isotopes for a given element, the range is limited by the level of instability created by having either too many or too few neutrons (Clark and Fritz, 1997). Unstable, or radioactive, isotopes are subject to decay, whereas stable isotopes are not (Clark and Fritz, 1997). Isotopes of a particular element are denoted using the elemental symbol and the atomic mass number, for example, ^{18}O or ^{13}C. Oxygen has eight protons and eleven isotopes, ^{12}O to ^{20}O, but only ^{16}O, ^{17}O, and ^{18}O are stable (Clark and Fritz, 1997). Of the three stable isotopes, ^{18}O, ^{17}O, and ^{16}O are of most interest since ^{16}O is the most abundant, making up 99.76% of all O_2, where ^{18}O comprises 0.20%, and ^{17}O, 0.04%. Stable isotopes are measured as the ratio of the two most common isotopes of an element; in the case of oxygen it is ^{18}O:^{16}O.

When determining the isotopic signature of a substance, the ratio needs to be expressed in a format that is convenient and comparable among various laboratories. Rather than reporting a true ratio, the isotopic ratio is expressed relative to a known reference. For the ^{18}O:^{16}O of water, for example, the reference used is Vienna Standard Mean Ocean Water (VSMOW). Since the difference in isotopic ratio of a sample compared to a standard is very small, it is expressed in terms of parts per thousand, or permil (‰). This is referred to as delta (δ) notation:

$$\delta^{18}O_{sample} = \left(\frac{^{18}O{:}^{16}O_{sample}}{^{18}O{:}^{16}O_{reference}} - 1\right) * 1000 \quad (1.4)$$

If the $\delta^{18}O$ of a sample is positive, for example +5‰, it indicates that the sample contains 5 ‰ (or 0.5%) more ^{18}O as compared to the reference sample. A sample that has comparatively more of the heavier isotope is referred to as "heavy" or "enriched". Alternately, a more negative, "light" or "depleted" isotopic signature contains comparatively less of the heavy isotope and is negative in signature relative to the standard.

Even though isotopes of the same element have the same chemical attributes, various processes can change the isotopic ratio due to different reaction rates for each isotope. This is referred to as fractionation. The fractionation factor (α) is the ratio of the numbers of any two isotopes in one chemical compound A divided by the corresponding ratio for another chemical compound B:

$$\alpha = \frac{IR_A}{IR_B} = \frac{\delta_A + 1000}{\delta_B + 1000} \tag{1.5}$$

where IR is the isotopic ratio and δ is the corresponding isotopic signature in delta notation.

1.7 Characterization of Aquatic Ecosystem Oxygen Dynamics Using Stable Isotopes

There are several observations (Figure 1.1) that allow for the use of stable isotopes of O_2 as a tracer of biological activity (Quay et al., 1993). Photosynthesis produces O_2 with an isotopic signature similar to that of water because there is no fractionation associated with the photolysis of water (Guy et al., 1993). Atmospheric O_2 is isotopically more positive compared to VSMOW, with an $\delta^{18}O$-O_2 of +23.5 ± 0.3 due to the global Dole effect (Kroopnick and Craig, 1972). During gas dissolution, there is an equilibrium fractionation of approximately

0.7 ‰ at 20°C (Kroopnick and Craig, 1972; Wassenaar and Koehler, 1999), driving the $\delta^{18}O$-O_2 toward +24.2 ‰ in the dissolved phase at equilibrium. Meteoric waters are substantially more negative compared to atmospheric O_2, with $\delta^{18}O$-H_2O values usually less than 0 ‰. For example, the ^{18}O-H_2O of the Ottawa River water is approximately -10 ‰ (Wang and Veizer, 2000). Consequently, photosynthesis causes DO to become isotopically more negative as compared to DO at atmospheric equilibrium as relatively negative $\delta^{18}O$-O_2 is introduced to the water column reservoir. Another key observation is that respiring organisms consume the isotopically lighter ^{16}O molecules more rapidly than ^{18}O molecules (Kiddon et al., 1993) causing the $\delta^{18}O$-O_2 of the remaining DO to become more positive.

One of the initial attempts at using ^{18}O as a biological tracer used stable isotopes of O_2 to determine R:P (rather than P:R, the more commonly reported ratio), assuming steady state conditions (Quay et al., 1995). Quay et al. (1995) traced R:P within the Amazon River basin as a means for quantifying the heterotrophic state of the ecosystem. The Amazon River generally exhibits DO concentrations less than atmospheric saturation, implying that respiration exceeds photosynthesis. It was hypothesized that this was due to suspended sediments limiting photosynthesis. The DO concentrations were found to range from 20 to 90% saturation. The $\delta^{18}O$-O_2 values ranged from 24 to 30 ‰ in the main channel and tributaries, and from 14 to 24 ‰ in the floodplain lakes. The $\delta^{18}O$-O_2 signature indicated that respiration predominated in the rivers, while more depleted $\delta^{18}O$-O_2 values exhibited by the lakes were attributed to photosynthesis, even though the mean DO of the lakes was only 66 ± 29 % saturation. This illustrates the usefulness of $\delta^{18}O$-O_2 as a tracer of photosynthesis even when the ecosystem is strongly heterotrophic and DO is undersaturated (Quay et al., 1995).

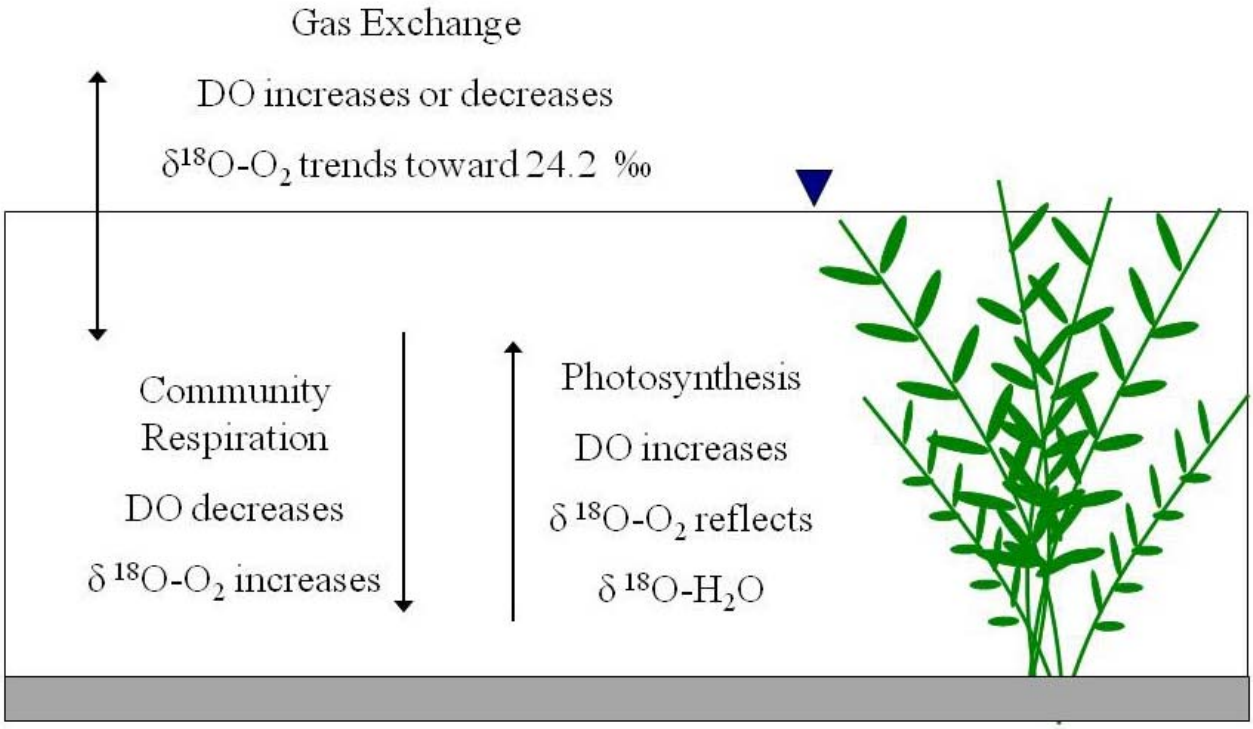

Figure 1.1 Conceptual model of DO and $\delta^{18}O\text{-}O_2$ dynamics in rivers.

The ratio of respiratory DO uptake to photosynthetic production (R:P) was calculated by Quay et al. (1995) using the following steady state equations:

$$R{:}P = \frac{^{18:16}O_w\alpha_p - {}^{18:16}O_g}{{}^{18:16}O\alpha_r - {}^{18:16}O_g} \tag{1.6}$$

and

$${}^{18:16}O_g = \frac{\alpha_g\left[{}^{18:16}O_a\alpha_s - \left({}^{DO}/_{DO_{sat}}\right){}^{18:16}O\right]}{\left[1 - \left({}^{DO}/_{DO_{sat}}\right)\right]} \tag{1.7}$$

where $^{18:16}O_w$ is the isotopic ratio of the water, α_p is the fractionation effect of photosynthesis, α_s is the solubility fractionation effect of ^{18}O:^{16}O in water, α_g is fractionation effect of gas transfer of ^{18}O:^{16}O, and $^{18:16}Og$ describes the ratio of the net air-water fluxes of ^{18}O and ^{16}O across the air-water interface multiplied by the fractionation factor due to the difference between respective isotopic gas transfer velocities.

Within the Quay et al. (1995) study, the R:P ranged from 1 to 1.7 for the lakes, 1.5 to 3 for the tributaries, and 2 to 4 in the main channel of the Amazon River. There was also a trend of lower $\delta^{18}O$-O_2 values as the R:P decreased (eg. as the rate of photosynthesis increased). It was hypothesized that the lakes exhibited the lowest R:P due to the settling of suspended sediment, allowing for higher rates of photosynthesis. From their findings, Quay et al. (1995) concluded that the O_2 isotopes can act as a unique tracer of photosynthesis and can provide a means of quantifying the heterotrophic state of freshwaters.

Wang and Veizer (2000) performed a similar study to evaluate the use of $\delta^{18}O$-O_2 as a tracer of photosynthesis and respiration in the Ottawa region, studying the Ottawa River,

Meech Lake, and Green Creek. Water samples were obtained approximately once or twice per month, over a period of one year. The calculation of R:P by Wang and Veizer (2000, 2004) followed the same model identified by Quay et al. (1995). The $\delta^{18}O\text{-}O_2$ values ranged from +19.2 to +25.2 ‰ in Meech Lake, where the DO ranged from 40 to 120 % saturation. In the Ottawa River, the DO ranged from 60 to 120 % saturation, with $^{18}O\text{-}O_2$ values from +21.1 to +26.0 ‰. Green Creek had DO levels from 70 to 120 % saturation, with $\delta^{18}O\text{-}O_2$ values of +18.4 to +32.3 ‰. All three water bodies were considered to be respiration dominated with R:P ranging from 1 to 5, except for during summer months, when R:P ratios fell due to enhanced P rates. Russ et al. (2004) also applied the Quay et al. (1995) steady-state approach in the study of R:P variations in Lake Superior. The $\delta^{18}O\text{-}O_2$ exhibited a range of approximately -2.0 to +0.7 ‰ compared to air, with DO concentrations from 85 to 110% saturation. The lake was found to be predominately net heterotrophic during April to October, with R:P ranging from 1.2-2.5 with brief periods of autrotrophy during summer stratification.

However, in non-steady state aquatic systems, more frequent sampling is required for $\delta^{18}O\text{-}O_2$ and DO to describe metabolic functioning. The condition of steady state assumes that neither DO nor $\delta^{18}O\text{-}O_2$ changes appreciably over the timeframe in which inferences are being made (Quay et al., 1993; Wang and Veizer, 2000, 2004). Dissolved O_2 concentrations in many aquatic systems follow a diel pattern of increasing concentrations during daylight hours due to photosynthesis, followed by decreases at night due to respiration. The $\delta^{18}O\text{-}O_2$ almost inversely mirrors the DO pattern, becoming more negative during the day due to photosynthetic inputs, and more positive at night as respiring communities consume the lighter isotopes (Roberts et al., 2000; Parker et al., 2005).

Diel fluctuations in DO and $\delta^{18}O\text{-}O_2$ have been more recently monitored to determine metabolic rates in aquatic systems (Parker et al., 2005; Tobias et al., 2007; Venkiteswaran et al., 2007; Poulson and Sullivan, 2009). Parker et al. (2005) conducted two diel sampling events during summer and fall in a relatively pristine headwater tributary located in Montana, USA. Diel $\delta^{18}O\text{-}O_2$ values were reported for each event, ranging from 12.4 to 25.5 ‰ and 18.7 to 26.4 ‰. The rates of photosynthesis, respiration, and gas exchange were estimated, however, using traditional DO curve fitting techniques adapted from Odum (1956). The calculated results were then applied to the Quay et al. (1995) model, to predict $\delta^{18}O\text{-}O_2$ and compared to the observed data.

Recently, the use of the stable isotopes of O_2 has shown some promise for quantifying the biogeochemical processes controlling DO in productive aquatic ecosystems (Tobias et al., 2007; Venkiteswaran et al., 2007). Tobias et al. (2007) examined the use of both steady state and non-steady state approaches to derive estimates of P, R, and P:R for six diel sampling events in a 2nd order, agriculturally impacted stream that exhibited a diel variation in $\delta^{18}O\text{-}O_2$ of approximately 10 ‰. Tobias et al. (2007) applied the steady state equation to both discrete values and mean daily values for DO and $\delta^{18}O\text{-}O_2$; the steady state solution method using daily means was in agreement with the dynamic approaches, but yields only P:R ratios, rather than metabolism rates. Applying discrete values was considered useless in productive waters, as there were non-unique values of $\delta^{18}O\text{-}O_2$ for a given DO saturation state. Tobias et al. (2007) also investigated two non-steady state approaches. The first involved using the changes in DO and $\delta^{18}O\text{-}O_2$ in a mass balance to solve directly for photosynthesis and respiration. However, this approach relies on accurately knowing both gas exchange rates and α_r to reduce the number of unknown variables, but has the advantage of allowing for the examination of

changes in respiration and photosynthesis within a diel cycle. The second approach was to perform time-forward numerical simulations to simulate changes in DO and $\delta^{18}O\text{-}O_2$ to compare to observed data. The time-forward simulation approach is useful for systems where α_r is unknown, or daily mean values for photosynthesis and respiration are sufficient.

Venkiteswaran et al. (2007) have also made recent advances in developing a transient model, similar to Tobias et al. (2007), to use the stable isotopes of O_2 in conjunction with DO concentration to quantify photosynthesis, respiration, and gas exchange in aquatic ecosystems. The application of the technique was tested in an upland reservoir, a wetland pond, and the South Saskatchewan River over diel cycles. The model was able to explain $\geq 87\%$ and $> 96\%$ of the variability in $\delta^{18}O\text{-}O_2$ and O_2, respectively. Further evaluation is still needed, however, to determine the applicability of a transient stable isotope modeling technique under variable geographical and seasonal conditions. The model developed by Venkiteswaran et al. (2007) has since been used by Poulson and Sullivan (2009) to model two diel events in the Upper Kalamath River, OR, demonstrating the potential of this technique for quantifying biogeochemical rates in large, slow moving rivers.

There is particular uncertainty associated with the isotopic fractionation factor for respiration, a critical parameter for resolving the isotopic mass balance for an ecosystem (Tobias et al., 2007). Quay et al. (1993) derived a respiration fractionation factor (α_r) from a series of models that budgeted the ^{16}O and ^{18}O of DO in ocean water. The α_r in the mixing layer was found to be 0.978 ± 0.006, which was in agreement with other surface seawater incubation studies. Quay et al. (1995) used dark bottle incubations of Amazon River water to calculate an α_r of 0.982 ± 0.003, which would be primarily representative of bacterial

respiration within the water column. The α_r found by Quay et al. (1995), determined from water sample incubations, was justified by comparing it to fractionation values found in marine systems. Both Wang and Veizer (2000) and Parker et al. (2005) used the α_r reported by Quay et al. (1995), but neither performed confirmatory experiments to determine if the α_r value was applicable to their systems. However, model-derived α_r values reported byTobias et al. (2007), Venkiteswaran et al. (2007), and Poulson et al. (2009) ranged from 0.979 to 0.994, indicating that fractionation is not likely to be a constant value as previously assumed.

A new method has also been introduced that uses ^{17}O:^{16}O and ^{18}O:^{16}O-O_2 in tandem with O_2 concentrations to determine net and gross production (Luz et al., 1999; Luz and Barken, 2005; Luz and Barken, 2009). Luz et al. (1999) have based this method on deviations from mass dependent fractionation, expressed as an ^{17}O anomaly ($\Delta^{17}O$). Mass dependent fractionation reactions (e.g., respiration) cause ^{17}O to fractionate half as much as ^{18}O relative to ^{16}O. However, some photochemical mass independent atmospheric reactions deviate from this relationship, causing the anomaly. The magnitude of $\Delta^{17}O$ in DO is affected by photosynthesis, gas exchange, but not by respiration; Luz and Barken et al. (2009) used the $\Delta^{17}O$ and the O_2:Ar ratio to calculate net production of O_2 in the Atlantic Ocean near Bermuda. This approach, however, requires estimates of k and precise measurements of $\delta^{17}O$ for application, and assumes steady state conditions.

In order to develop river management strategies, DO budget components must be adequately quantified and understood. From a river ecology perspective, much of the research focus has been centred on the structure and functioning of relatively unimpacted rivers and streams. Understanding how a river functions naturally is very important for providing an

ideal baseline level of ecosystem health. However, most of the world's major rivers are impacted by anthropogenic influences. In order to assess the effects of human influence on the structure and functioning of running waters, more information is needed on the response of systems impacted by organic and inorganic inputs, and flow regulation. Previous river metabolism studies have relied primarily on chamber incubation approaches, as well as a variety of diel DO curve-fitting techniques (Odum, 1956; Bott et al., 1985; Wiley et al., 1990; Marzolf et al., 1994; Williams et al., 2000). Potential inaccuracies of these techniques are associated with potential scale up error due to inferences made from closed system incubations, as well as uncertainty in air-water gaseous exchange estimates (Marzolf et al., 1994).

Supplementary information gained by $\delta^{18}O\text{-}O_2$ has the potential to provide unique information for reconciling aquatic DO budgets not otherwise obtainable by traditional means. The evaluation of $\delta^{18}O\text{-}O_2$ as a tool for characterizing aquatic metabolism has been based on relatively sparse and infrequent data collection (Quay et al, 1995; Wang and Veizer, 2000; Parker et al., 2005; Tobias et al., 2007). This is partly due to the fact that conventional techniques of extracting O_2 from air, soil, or water and the subsequent conversion of O_2 gas to CO_2 for isotope analysis were expensive, complex and very time consuming (Wassenaar and Koehler, 1999; Roberts et al., 2000). Recent techniques for the analysis of $\delta^{18}O\text{-}O_2$ have been developed, involving the use of a gas chromatograph coupled with a mass spectrometer allowing for more efficient sampling and analysis (Wassenaar and Koehler, 1999; Roberts et al., 2000). Additional investigation on the use of stable isotopes of O_2 for quantifying ecosystem metabolic rates is needed to evaluate this technique for applicability in dynamic systems that exhibit variable DO on a temporal basis.

1.8 Research Objectives

The objectives of this study are to:

1) Use the stable isotopes of O_2, in conjunction with DO concentrations, to quantify rates of respiration, photosynthesis, and gas exchange in the Grand River, Ontario, Canada,

2) Examine respiration, photosynthesis, and gas exchange trends within the Grand River relative to the environmental (e.g., physical, chemical) influences on DO, and

3) Evaluate the applicability and robustness of the isotopic technique for the quantification of DO dynamics in a large, impacted river.

Four main chapters will address the objectives. Chapter 3 focuses on the sensitivity and uncertainty the isotope modeling technique may express given its application to Grand River conditions. Chapters 4 and 5 concern the application of this modeling technique to quantify rates of gas exchange, photosynthesis, and respiration, and commentary is provided on the functioning of the Grand River with respect to DO consumption and production. Chapter 6 addresses the variability of respiratory isotopic fractionation factors reported in Chapter 5, and the mechanisms which may be affecting this phenonmenon. Conclusions regarding the identified objectives and associated recommendations are addressed in Chapter 7.

2.0 Site Description and Methods

2.1 The Grand River Watershed

The Grand River is a Canadian Heritage River located in southwestern Ontario. It originates approximately 20 km south of Georgian Bay at an elevation of 526 m above sea level and empties into Lake Erie at 355 m above sea level (Rott et al., 1998). The Grand River watershed, the largest in southern Ontario, covers an area of 6965 km^2, and the main channel measures about 290 km in length (Cooke, 2006). The watershed primarily drains agricultural land (76%), followed by wooded areas (17%). The central region of the watershed is characterized by urban development, which comprises about 5% of the total basin area. Most of the basin's population, over 900,000 people, reside in the cities of Kitchener, Waterloo, Cambridge, Guelph and Brantford.

Currently, the primary indicators of water quality in the Grand River Watershed used by the Grand River Conservation Authority (GRCA) are DO and nutrient concentrations (Cooke, 2006). The nutrient-rich conditions and depletion of DO have been identified as issues of concern in portions of the basin's watercourses. The river receives organic and nutrient inputs from 26 sewage treatment plants, on-site wastewater treatment systems, as well as non-point agricultural and urban sources, and serves as a source of drinking water and supports a significant recreational fishery. Inputs from both the treatment plants and non-point sources place DO demands on the receiving water body, and stimulate the growth of algae and other aquatic plants. Excess biomass of these can cause large daily fluctuations of pH and dissolved oxygen (Smith et al., 1999) due to algal photosynthesis during the day and

respiration at night. Hypoxic conditions can result in fish kills and loss of other aquatic biota and habitat (Carpenter et al., 1998).

The GRCA relies on a dynamic mass balance simulation model to predict DO concentrations in the Grand River under various management regimes (e.g., flow augmentation, loading inputs of sewage treatment plants). Dissolved O_2 concentrations derived from the GRCA's model are dependant on factors including O_2 demand, photosynthesis, and gas exchange with the atmosphere (GRCA, 1982). These parameters are calibrated using empirically-derived and theoretical coefficients. Additional information gained by the isotope technique may contribute to the level of confidence in model inputs and outputs.

Dissolved O_2 concentrations in areas of the Grand River can exhibit daily amplitudes of > 10 mg L^{-1} in the summer when plant biomass is high. The maximum growth season occurs from May to August, and during this time the diel DO cycle is the most pronounced, where the magnitude of the cycle is directly related to the density of aquatic weed growth (Draper and Weatherbe, 1995). The GRCA measures DO continuously at seven locations in the watershed as part of their real-time monitoring network, with the water quality objective of maintaining DO concentrations > 4 mg L^{-1}. From 2002 to 2006, DO concentrations generally exceeded quality objectives above the major urban areas of Kitchener-Waterloo, Cambridge, and Guelph (GRCA, 2007).

According to the GRCA (Cooke, 2006), the most serious pollution problems are found in the central part of the basin, where the municipalities of Waterloo, Kitchener, Cambridge, and Guelph are located. Generally, water quality tends to progressively deteriorate

downstream. Daily minimums frequently fall below 4 mg L^{-1} downstream of the urbanized central watershed, which receives wastewater from two large municipal treatment plants (GRCA, 2007). With respect to nutrients, index scores developed by the GRCA based on Canadian Council of Ministers of the Environment (CCME) guidelines indicate that the upper Grand and Speed River have the best water quality, rated as "good" to "fair". Sites monitored by the GRCA throughout the upper middle Grand River, as well as upper Conestogo River, lower Nith River and Whitemans Creek, scored in the "fair" category. Sites rated as "fair" have high levels of either phosphorus or nitrate. The middle and lower watershed were rated mainly in the "marginal" to "poor" categories, meaning that the river was characterized by very high concentrations of phosphorus, nitrate and ammonia. The combined effects of DO demand of organic wastes and diel DO fluxes, along with the physical choking of some river reaches with dense aquatic plant growth, render some sections of the river to be an unsuitable habitat for fish and other desirable aquatic organisms.

2.2 Sample Collection and Analysis

Three sampling locations (Figure 2.1) were chosen along the main channel of the Grand River, in what would be characterized as 5^{th} to 6^{th} order river sections in the central part of the basin: West Montrose (WM), Bridgeport (BRPT) and Blair (BLR). West Montrose is located upstream of the cities of Kitchener and Waterloo (population ca. 326,500) and is in a predominately agricultural landscape. Bridgeport, located downstream from WM, is subject to input from the Canagagigue Creek and the Conestogo River.

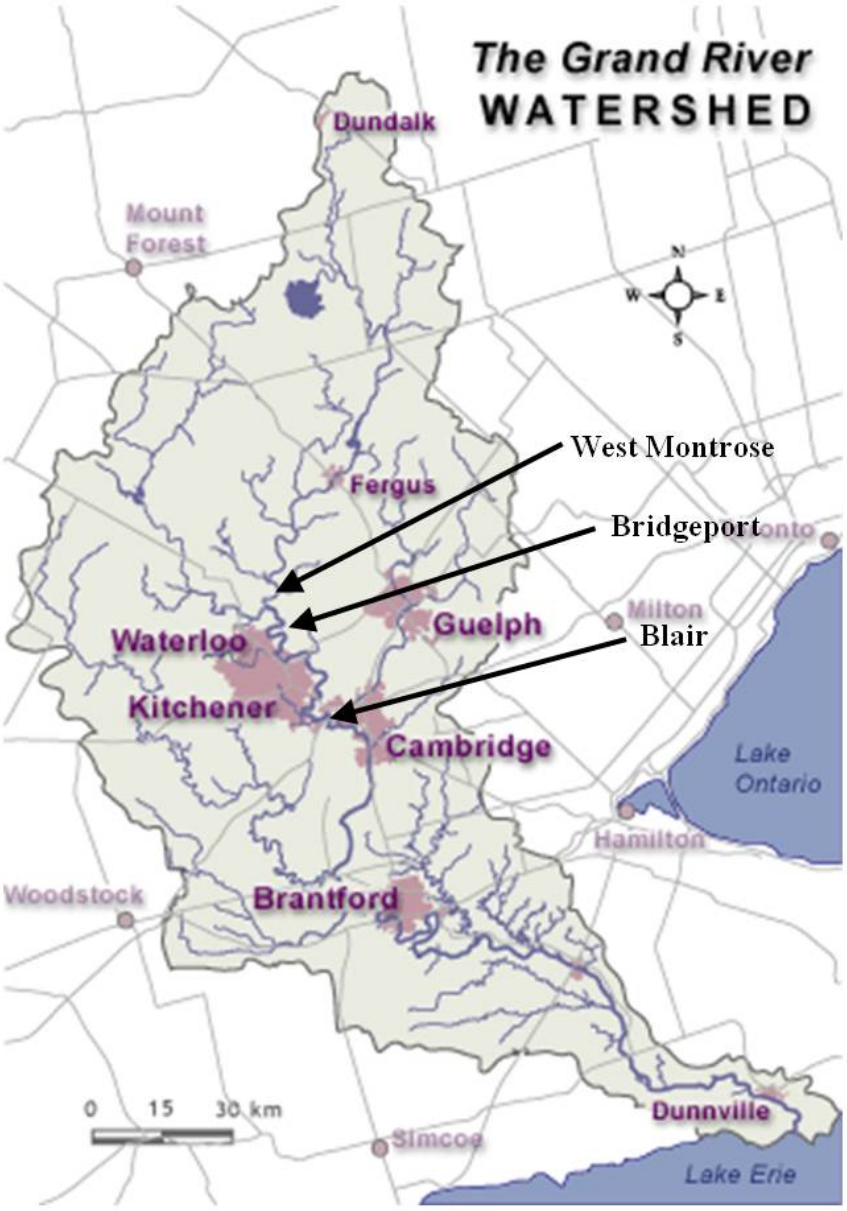

Figure 2.1 Map of the Grand River Watershed. The West Montrose, Bridgeport and Blair sampling locations are indicated. (image obtained and adapted from www.grandriver.ca)

High concentrations of chloride, total phosphorus, and nitrates occurring in these tributaries tend to negatively impact the Grand River, with levels significantly increasing between WM and BRPT (Cooke, 2006). Blair exhibits large diel DO fluctuations due to high productivity associated with abundant aquatic plant and algal growth (Cooke, 2006). The BLR sampling location is downstream of two major sewage treatment plant outfalls located in Kitchener and Waterloo, and is subject to substantial nutrient loadings and urban runoff.

The sampling protocol was intended to characterize changes in DO dynamics as the main channel moves from an agriculturally dominated basin into an urbanized setting, subject to impacts from sewage treatment plants and municipal runoff. A series of sampling events were conducted in order to capture the diel variability in DO and $\delta^{18}O\text{-}O_2$ in the Grand River. For the diel sampling events, samples were collected every 2 to 4 h over a 24 h period. In 2003, diel sampling was mainly focussed on the WM location, and additional diel sampling events at BLR and BRPT were added in 2004. Routine monitoring at the above locations was also conducted during 2003 and 2004, on an approximately monthly basis from May to December. During each routine monitoring event in 2003, samples were collected at three times during the day (early morning, midday, late afternoon) at each of the three locations. In 2004, the routine sampling was increased to four times per sampling event to provide more data points.

Water samples were collected for DO and $\delta^{18}O\text{-}O_2$, and temperature was recorded from within the main current of the channel at each location, at approximately mid-depth. Dissolved O_2 samples were collected in duplicate and titrated within 24 h of collection using the Winkler method (APHA, 1995). The precision of the Winkler analytical method is approximately ± 0.2

mg L^{-1}. Dissolved O_2 concentrations were also measured in situ using a YSI 556 MPS hand-held meter to serve as supplemental data to the collected DO samples. The $\delta^{18}O$-O_2 samples were collected, once per location per sample time, in 160 ml Wheaton serum bottles containing 0.3 g of sodium azide as a bactericide. Prior to sampling, the serum bottles were crimp sealed with butyl blue stoppers and then evacuated to <0.001 atm. The evacuated serum bottles were submerged and filled via an 18 gauge needle used to pierce the septum. After filling, the needle was removed while the bottle was still submerged to prevent atmospheric ^{18}O from invading the sample bottle. The $\delta^{18}O$-O_2 samples were prepared for analysis by removing 5 ml of water, inserting 5ml of He, followed by shaking to equilibrate the headspace. Headspace gas was analysed using a continuous flow gas chromatograph isotope ratio mass spectrometer, following Wassenaar and Koehler (1999), with an analytical error of approximately ± 0.3 ‰.

Samples were also collected via grab sample once per diel or routine event for the following parameters: $\delta^{18}O$-H_2O, dissolved inorganic carbon (DIC), dissolved organic carbon (DOC), nitrate nitrogen (NO_3-N), and phosphate phosphorus (PO_4-P). All water samples were kept on ice while being transferred to the laboratory, where they were refrigerated until analysis. Analyses for $\delta^{18}O$-H_2O were performed at the University of Waterloo Environmental Isotope Laboratory. Both DIC and DOC concentrations were measured using a Dohrmann DC-190 carbon analyzer. Samples for DIC, DOC, NO_3-N, and PO_4-P were pre-filtered and the DOC samples were acidified with 0.1 ml concentrated H_3PO_4 prior to analysis. Samples for NO_3-N and PO_4-P concentration were analyzed via ion chromatography using a Dionex ICS 90 chromatograph.

2.3 Model Description

To address the dynamic nature of DO in the Grand River, a non-steady state model was developed to describe the system, similar to the PoRGy model developed by Venkiteswaran et al. (2007). Two O_2 mass balances (DO and isotopic) were resolved based on the following equations:

$$\frac{dDO}{dt} = k(DOsat - DO) - CR + GPP \tag{2.1}$$

$$\frac{dDO * {}^{18}O}{dt} = {}^{18}OGE + {}^{18}OExch - CR\left({}^{18:16}O * \alpha_r\right) + GPP({}^{18:16}O_w * \alpha_p) \tag{2.2}$$

where CR is the community respiration rate (mg L^{-1} h^{-1}), GPP is gross primary production (mg L^{-1} h^{-1}), k is the gas exchange coefficient (h^{-1}), DOsat is the DO concentration under saturated conditions, $^{18:16}O$ refers to the ^{18}O:^{16}O of DO, , $^{18}O_w$ is ^{18}O:^{16}O of water, and fractionation factors for CR and GPP are represented by α_r and α_p respectively. DOsat was calculated based on temperature (Weiss, 1970), and corrected for the altitude (Radke et al., 1998) at each sampling location.

^{18}OGE and ^{18}OExch describe the mass flux of ^{18}O and ^{16}O due to exchange with the atmosphere. Under O_2 saturated conditions, the isotopes of O_2 will continue to exchange across the air-water interface if $\delta^{18}O$-O_2 is at disequilibrium. In undersaturated DO conditions, $\delta^{18}O$- O_2, will invade the water column with the appropriate fractionation factors associated with solubility and air-water transfer. However, in supersaturated DO conditions, ^{16}O will evade the water column preferentially to ^{18}O.

Therefore:

If (DOsat-DO) > 0 then:

$$^{18}OGE = k * \propto_k (DOsat - DO) * (^{18:16}O_a * \propto_s) \quad (2.3)$$

Else:

$$^{18}OGE = k * \propto_k (DOsat - DO) * (^{18:16}O / \propto_s) \quad (2.4)$$

where $^{18}O_a$ is the Ratio of ^{18}O to ^{16}O in air, α_s is the fractionation effect of the solubilisation of O_2 in water, and α_k is the fractionation factor associated with gas transfer. According to the equations, if DO is at equilibrium (DOsat-DO=0), ^{18}OGE would be nil. In order to allow for ^{18}O and ^{16}O to exchange across the air-water interface towards equilibrium independently of the bulk exchange of DO, even under saturated DO conditions, the following equation was used:

$$^{18}OExch = k * \propto_k * DO * [(^{18}O_{air} * \propto_s) - {}^{18}O] \quad (2.5)$$

The isotopic signature of atmospheric O_2 is assumed to be constant at 23.5‰ (Kroopnick and Craig, 1972). The solubility fractionation of ^{18}O-O_2 (α_s=1.0007) is due to the slightly different solubility between ^{18}O and ^{16}O, with negligible temperature effects (Benson and Krause, 1984). There is a kinetic fractionation effect associated with air-water transfer of ^{18}O-O_2 (α_k=0.9972), as the ^{18}O molecule is slightly larger than ^{16}O (Knox et al., 1992). Isotope values were modeled as ratios but will be reported in units of ‰ in δ-notation with respect to Vienna Standard Mean Ocean Water (VSMOW).

The effects of groundwater input were assumed to be negligible at the sample locations with respect to the large fluctuations in DO. Both k and CR values were varied with temperature within the model using the following relationships (McCutcheon, 1989; Chapra, 1997):

$$k_T = k_{20} * 1.024^{(T-20)} \quad (2.6)$$

$$CR_T = CR_{20} * 1.047^{(T-20)} \quad (2.7)$$

where T is temperature, measured in C, k_{20} and CR_{20} are k and CR at 20C.

Gross primary production was modeled as a half-sine wave, parameterized in terms of time and length of day (Chapra and DiToro, 1991):

$$GPP = Pmax * \sin\left(\frac{\pi t}{day\ length}\right) \quad (2.8)$$

where GPP is the rate of GPP at time t, Pmax is the maximum GPP rate, and the day length is the number of daylight hours. Pmax was the parameter adjusted in the model for each run.

2.4 Model Calibration

The model is composed of two mass balances, one for DO concentration, and the other for the associated isotopic signature. Modeling was performed using STELLA software, version

7.0.2, with a 15 min time-step using the non-steady state equations noted above. The unknowns in the model were CR, GPP, k, and α_r. Due to the dynamic state of the system, and because there are four unknowns and two mass balances, the model could not be solved directly. Therefore, the model was calibrated iteratively to optimize the goodness of fit between modeled and measured data. The goodness of fit statistic used was the root mean squared error (RMS) which compares the fitted and observed data, and provides a direct measure of model error (Thomann, 1982). The first data point for each modeling event was not included in the calculation of RMS as this point was used to initialize the model. The use of RMS as a goodness of fit statistic was also supported by visual examination comparing model output and observed data. Starting conditions for model runs were set using the DO, $\delta^{18}O\text{-}O_2$, and temperature measured at the time zero sampling data point for a particular model run.

To solve for the unknown parameters in the model, the data for the diel sampling events were divided into two portions, day and night. For the night portion of the diel data, GPP was assumed be zero. Potential k_{20} and CR_{20} values were first simulated and compared to observed DO concentration data. Model DO simulations that resulted in RMS values in approximately 0.2 or less (similar to the analytical error associated with Winkler titration), supported by visual examination, were used to constrain the potential range in input parameter values. The identified range of k_{20} and CR_{20} values were then modelled iteratively with a range of α_r, and compared to the observed $\delta^{18}O\text{-}O_2$ to determine the optimal fit.

To estimate GPP and α_r for each full diel sampling event, subsequent simulations were run using the night-time obtained k and CR with a range of Pmax and α_r. Optimal model fit

was determined by identifying values that minimize the RMS of both the DO and the $\delta^{18}O\text{-}O_2$ output. Estimation of unknown input parameter values for the routine day-only monitoring events was performed in a similar manner; the values obtained from the night-time determinations were used to constrain the possible range of input values for k_{20} and CR_{20} for the day-only models. For all sampling events, daily rates of CR were calculated by integrating the model output for the sampling period and extrapolating the result to a 24 h period. Equation 2.8 was used to generate the GPP rate over the day length using the model derived Pmax, and the output was integrated to obtain a daily rate of GPP.

3.0 Evaluation of the Isotope Technique Model for River Dissolved Oxygen Dynamics

3.1 Introduction

The use of O_2 isotopes to aid in the quantification of DO dynamics in aquatic ecosystems is relatively new. Previous applications have mainly focussed on representing ecosystem functioning by assuming steady state conditions, and that neither DO nor $\delta^{18}O\text{-}O_2$ varied considerably over the time period in question (Quay et al., 1995; Wang and Veizer, 2000, Russ et al., 2004). The steady state assumption, however, is not valid for systems that exhibit significant diel changes in DO and $\delta^{18}O\text{-}O_2$, such as in the Grand River.

Recently, there has been more research towards addressing the non-steady state conditions that are present in some freshwater systems. Parker et al. (2005) used conventional curve-fitting techniques to estimate k, CR and GPP, then applied these values to the steady state equations from Quay et al. (1995) to generate $\delta^{18}O\text{-}O_2$ values for comparison to observed data. However, this approach may result in inaccurate parameter estimates, as well as neglect the potential variability in α_r, as Parker et al. (2005) assumed α_r was constant and equal to 0.982. Numerical time-forward mass balance approaches that simulate changes in DO concentration and $\delta^{18}O\text{-}O_2$, while minimizing differences between simulated and observed data have been presented by Venkiteswaran et al. (2007) and Tobias et al. (2007). The model used in the current study is similar to the model presented by Venkiteswaran et al. (2007), in that it incorporates isotopic exchange with the atmosphere. Venkiteswaran et al. (2007) simulated GPP as a multiplier of irradiance data, whereas here GPP is presented as a half sinusoidal curve function.

There will always be a certain degree of uncertainty associated with model parameters that have been determined by fitting a multi-parameter mathematical model to observed data. Models generally fail to represent the complexity of the real world, and may assume that dynamic variables are constant in time and space. Complete verification and validation of models is inherently impossible when simulating complex, open, dynamic systems due to the impossibility of accurately representing all processes in a realistic manner (Oreskes et al., 1994). However, models of such systems have utility for increasing our understanding of cause-effect relationships, can sometimes replicate observed phenomena with an acceptable range of reality and predictive capacity, and allow us to strengthen our hypothesis or construct "what if" scenarios (Thomann, 1982; Oreskes, et al. 1994; Cox and Whitehead, 2005)

Evaluation of a model is generally performed by demonstrating agreement between observed and predicted data. To understand the general behaviour of the model, sensitivity analysis can be performed to demonstrate the effects of varying parameter magnitudes on the characteristics of the diel DO and $\delta^{18}O\text{-}O_2$ curves. Sensitivity analysis is useful for examining the effects of model input parameters on output results and how uncertainty in the parameters is likely to affect the simulation results. The use of sensitivity coefficients, which correct for differences in parameter units and scale, provided an indication of the relative magnitude with which input parameters contribute to the model output for both DO concentration and $\delta^{18}O\text{-}O_2$ values. The sensitivity coefficients presented represent the relative response of output characteristics to changes in an input parameter, as compared to the base, or default, modeling condition. A relatively high sensitivity coefficient would then indicate that for a unit change in input, there is a relatively large change in output. The magnitude of uncertainty in the input parameter value estimates also needs to be quantified to provide some context as to the

predictive capability of a given model. The objectives of this chapter were to identify individual input parameter influence on model output, provide some quantification of uncertainty regarding the fitted model input parameter estimates, and evaluate the benefit of the addition of the isotopic mass balance.

3.2 Methods

3.2.1 Sensitivity Analysis

Several approaches were adopted to evaluate the isotope and DO concentration mass balances model for describing DO dynamics in the Grand River, and to assess the confidence in the resulting estimates of input parameters. The DO and $\delta^{18}O\text{-}O_2$ measured at WM on August 13-14, 2003 was used as a case study to investigate model behaviour and parameter estimate uncertainty. This data set was characterized by a large diel change in both DO and $\delta^{18}O\text{-}O_2$, representative of productive, dynamic conditions. Data for this sampling event were collected on an approximately hourly time interval for the entire diel period to allow for a more precise comparison of model fit to observed data. Sensitivity analysis was performed according to Zheng and Bennett (2002). Sensitivity is a measure of the effect of change of a model parameter on the output response, with the sensitivity coefficient as a means of quantifying the effect. Sensitivity coefficients were calculated as follows:

$$SC = \frac{(y - y_b)}{\left[\frac{(x - x_b)}{x_b}\right]} \tag{3.1}$$

Where SC is the sensitivity coefficient, y is the output response for a given parameter

value, x, y_b is the output response for a base condition, and x_b is the associated parameter value at the base condition. Generally, a base condition should be chosen that is representative of mean model parameter values to provide a basis for comparison. Values for GPP, CR, and k, along with α_r, that provided the "best fit" to the WM August 13-14, 2003 event (Chapter 5) were used generate a theoretical base condition for DO and $\delta^{18}O\text{-}O_2$ for the sensitivity analyses. For simplification, a 12 h day length and constant temperature, 20C, was used. As the parameters in the current study model range in magnitude and are represented in different units of measure, the sensitivity quantification is normalized to a dimensionless form to allow for parameter comparison. The sensitivity coefficient is therefore representative of the change in model output in response to a percentage change in input parameter value compared to the base condition. The model output response characteristics of interest, to describe the resultant diel curves, were the minimum, maximum and amplitude of both the DO and $\delta^{18}O\text{-}O_2$ output for 24 h simulations.

Repeated forward simulations were conducted over the range of k, GPP, CR, and α_r (Table 3.1) to generate theoretical model outputs to illustrate how changes in each input parameter affects DO and $\delta^{18}O\text{-}O_2$. The range for each of these parameters was simulated one at a time, while holding the other parameters constant at the base condition. Each sensitivity model run was initiated with DO=6.23 mg L^{-1} and $\delta^{18}O\text{-}O_2$=27.93 ‰. The model was allowed to run until output was consistent over a 24 h cycle to create a theoretical steady-state diel model output. For instance, a given model run was allowed to simulate 72 h of diel changes, to create data output that was replicable on a 24 h cycle, representing a steady-state output.

Table 3.1 Model Simulation Conditions and Input Parameter Ranges for the Model Sensitivity Analyses. Base Conditions were representative of WM August 13, 2003 k, GPP, and CR.

Day Length = 12 h Temperature = 20 C $^{18}O_{H2O}$ = -10.6 ‰

Parameter Ranges

k (h^{-1})	k (d^{-1})	Pmax (mg L^{-1} h^{-1})	GPP (mg L^{-1} d^{-1})	CR (mg L^{-1} h^{-1})	CR (mg L^{-1} d^{-1})	α_r
0.19	4.5	2.6	19.89	0.66	15.8	0.968
0.23	5.5	3.1	23.7	0.76	18.2	0.973
0.27*	6.5*	3.6*	27.5*	0.86*	20.6*	0.978*
0.31	7.5	4.1	31.3	0.96	23.0	0.983
0.35	8.5	4.6	35.1	1.06	25.4	0.988

* Base Conditions

3.2.2 Uncertainty Analysis

As the model is dynamic in nature, the parameters of GPP, k, CR and α_r cannot be estimated independently of one another. As there were more unknowns than mass balance equations, direct calculation was not possible, and potential combinations of the parameters were simulated and compared against observed data. Optimal model fit to the observed data was chosen via both statistical means (e.g., RMS error) as well as visual interpretation for qualitative support. However, as there was scatter associated with the observed values as compared to the modeled output, the chosen optimal values for the model parameters carry with them a potential range of uncertainty.

The potential range of k, CR, GPP, and α_r that could describe the observed DO and $\delta^{18}O\text{-}O_2$ values were investigated using the data obtained from the sampling event conducted at WM on August 13-14, 2003. Two data points were removed from the original observed $\delta^{18}O\text{-}O_2$ data set as they were anomalous to the overall diel curve, in order to calculate RMS error that was not biased towards the anomalous data. To assess the range of potential parameter ranges that could explain the observed DO and $\delta^{18}O\text{-}O_2$ data, a series of simulations were conducted to examine the variability in potential input. The DO curve was initially used to confine the range of potential k, CR, and Pmax, that could explain measured concentrations. Simulated input ranges based on comparing DO output to observed data were confined to 0.2 to 0.35 h^{-1} for k_{20}, 0.8 to 0.9 mg O_2 L^{-1} h^{-1} for CR_{20}, and 3 to 3.7 mg O_2 L^{-1} h^{-1} for Pmax. For the uncertainty analysis, both day length and temperature conditions reflect the conditions during sampling were used. Combinations of input parameter values that resulted in model outputs exhibiting RMS errors of less than 1 mg L^{-1}compared to observed DO were then simulated with α_r ranging from 0.970 to 0.993. Model output was compared to the $\delta^{18}O\text{-}O_2$

data to find combinations of input parameters that could explain both the DO and $\delta^{18}O\text{-}O_2$ observed data. As with the sensitivity runs, each model run was simulated until a steady-state output over a diel basis was achieved. Day-time only sampling events were also conducted in the course of this study, as it was hypothesized at the beginning of this work that k and α_r would exhibit little variability and that full diel data sets were not always necessary. It was also assumed that CR_{20} does not differ from day to night. To test the effects of modeling only the day portion on input parameter estimates, the best model output fit to day data was also determined to compare results estimated by using the entire diel data set.

Traditional approaches have relied on only DO concentration mass balances for quantifying metabolism rates in rivers; k is often estimated using night-time regression techniques or empirical relationships with hydrology. Model simulations were conducted using the k_{20} value obtained via the night-time regression technique (Chapter 4) with varying CR_{20} and Pmax to compare input parameter estimates found using DO concentrations only to that found using the isotope modeling approach. Estimates were also obtained for CR, Pmax, and k using the best fit to DO concentration for the full range of input parameters simulated.

3.3 Results

3.3.1 Sensitivity Analyses

Increases in k caused a dampening effect in both the diel DO and $\delta^{18}O\text{-}O_2$ model output (Figure 3.1). Sensitivity coefficients (Tables 3.2 and 3.3) indicated that k controlled curve amplitudes by affecting both the maxima and minima.

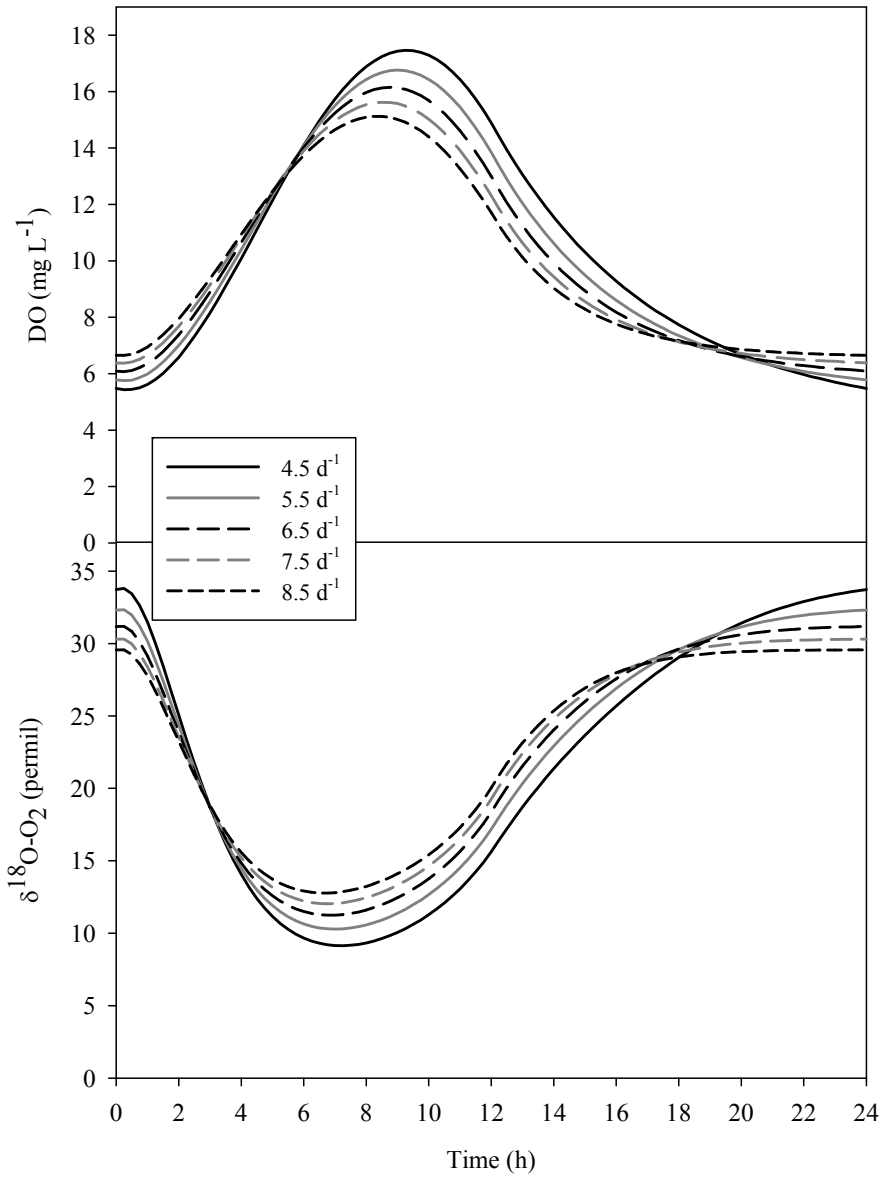

Figure 3.1 Diel model output of DO concentration and $\delta^{18}O\text{-}O_2$ for a range of k values, when GPP, CR, and α_r are held constant.

Table 3.2 Diel model output characteristics for DO concentration for ranges in k, GPP, CR, along with the associated sensitivity coefficients.

Model Output DO (mg/L)					
k (d^{-1})	**4.50**	**5.50**	**6.50**	**7.50**	**8.50**
Max	17.5	16.8	16.2	15.6	15.1
Min	5.43	5.75	6.07	6.37	6.64
Amplitude	12.0	11.0	10.1	9.25	8.48
GPP (mg L^{-1} d^{-1})	**19.9**	**23.7**	**27.5**	**31.3**	**35.1**
Max	13.3	14.7	16.2	17.6	19.0
Min	6.01	6.04	6.07	6.10	6.14
Amplitude	7.28	8.68	10.1	11.49	12.88
CR (mg L^{-1} d^{-1})	**15.8**	**18.2**	**20.6**	**23.0**	**25.4**
Max	16.9	16.5	16.2	15.8	15.4
Min	6.81	6.44	6.07	5.7	5.33
Amplitude	10.1	10.1	10.1	10.1	10.1
Sensitivity Coefficients – with DO as the Response Variable					
k (d^{-1})	**4.50**	**5.50**	**7.50**	**8.50**	**Mean**
Max	4.26	4.07	3.53	3.35	3.80
Min	2.08	2.13	2.00	1.85	2.02
Amplitude	6.34	6.20	5.53	5.20	5.82
GPP (mg L^{-1} d^{-1})	**19.9**	**23.7**	**31.3**	**35.1**	**Mean**
Max	10.3	10.3	10.4	10.3	10.3
Min	0.22	0.22	0.22	0.25	0.22
Amplitude	10.1	10.1	10.2	10.1	10.1
CR (mg L^{-1} d^{-1})	**15.8**	**18.2**	**23.0**	**25.4**	**Mean**
Max	3.18	3.18	3.18	3.14	3.17
Min	3.18	3.18	3.18	3.18	3.18
Amplitude	0	0	0	0.04	0.01

Table 3.3 Diel model output characteristics for $\delta^{18}O\text{-}O_2$ for ranges in k, GPP, CR, and α_r, along with the associated sensitivity coefficients.

Model Output $\delta^{18}O\text{-}O_2$ (‰)					
k (d^{-1})	**4.50**	**5.50**	**6.50**	**7.50**	**8.50**
Max	33.8	32.3	31.19	30.3	29.6
Min	9.14	10.29	11.2	12.0	12.8
Amplitude	24.7	22.1	20.0	18.3	16.8
GPP (mg L^{-1} d^{-1})	**19.9**	**23.7**	**27.5**	**31.3**	**35.1**
Max	31.2	31.2	31.19	31.19	31.19
Min	13.4	12.2	11.24	10.42	9.73
Amplitude	17.8	19.0	19.95	20.77	21.46
CR (mg L^{-1} d^{-1})	**15.8**	**18.2**	**20.6**	**23.0**	**25.4**
Max	29.51	30.35	31.19	32.03	32.87
Min	11.12	11.18	11.24	11.3	11.35
Amplitude	18.39	19.17	19.95	20.73	21.52
α_r	**0.968**	**0.973**	**0.978**	**0.983**	**0.988**
Max	34.83	33.01	31.19	29.38	27.58
Min	12.64	11.94	11.24	10.52	9.81
Amplitude	22.19	21.07	19.95	18.86	17.77
Sensitivity Coefficients – with $\delta^{18}O\text{-}O_2$ as the Response Variable					
k (d^{-1})	**4.50**	**5.50**	**7.50**	**8.50**	**Mean**
Max	8.48	7.67	5.93	5.30	6.85
Min	6.83	6.33	5.27	4.97	5.85
Amplitude	15.3	14.0	11.2	10.3	12.7
GPP (mg L^{-1} d^{-1})	**19.9**	**23.7**	**31.3**	**35.1**	**Mean**
Max	0	0	0	0	0
Min	7.85	7.06	5.90	5.44	6.56
Amplitude	7.85	7.06	5.90	5.44	6.56
CR (mg L^{-1} d^{-1})	**15.8**	**18.2**	**23.0**	**25.4**	**Mean**
Max	7.22	7.22	7.22	7.22	7.22
Min	0.52	0.52	0.52	0.47	0.51
Amplitude	6.71	6.71	6.71	6.75	6.72
α_r *	**0.968**	**0.973**	**0.983**	**0.988**	**Mean**
Max	8.01	8.01	7.96	7.94	7.98
Min	3.08	3.08	3.17	3.15	3.12
Amplitude	4.93	4.93	4.80	4.80	4.86

*Enrichment factors were used for coefficient calculations, due to the output being in delta notation

Diel curves for $\delta^{18}O\text{-}O_2$ exhibited greater sensitivity coefficients related to k than coefficients for DO, indicating a greater sensitivity in model output for a given change in k.

Photosynthesis rates (Figure 3.2) primarily controlled the daytime DO maximum and the associated $\delta^{18}O\text{-}O_2$ minima. Despite increases in GPP, the night time DO minima and $\delta^{18}O\text{-}O_2$ maxima remained constant. The sensitivity coefficients reflected this trend, with the curve amplitude being primarily attributable to the changes occurring in the day component of the DO and $\delta^{18}O\text{-}O_2$ curves. Increases in CR, however, tended to lead to a consistent downward shift in overall DO concentrations throughout the diel model curve (Figure 3.3); sensitivity coefficients were in agreement, as curve amplitude was not sensitive to changes in CR, while the DO maxima and minima were similarly, and consistently, sensitive to increases in CR. Increasing CR rates had almost no effect on $\delta^{18}O\text{-}O_2$ daytime output, but caused a consistent increase in estimates of $\delta^{18}O\text{-}O_2$ maxima. Respiratory fractionation factor inputs affected $\delta^{18}O\text{-}O_2$ in a consistent manner; as α_r increased from 0.968 to 0.988, the $\delta^{18}O\text{-}O_2$ became more negative (Figure 3.4). The $\delta^{18}O\text{-}O_2$ diel maxima were the most sensitive to changes in α_r, exhibiting a mean sensitivity coefficient about twice that of the diel minima and amplitude (Table 3.3).

The mean sensitivity coefficients calculated for the DO model output characteristics indicated that the maximum DO concentration appears to be primarily controlled by GPP, while the DO minimum is most sensitive to CR, with k expressing slightly less influence within the ranges tested (Figure 3.5). The $\delta^{18}O\text{-}O_2$ curve maximum appears to be equally sensitive to all input parameters, with GPP and k exerting the most influence on the diel minimum values (Figure 3.6).

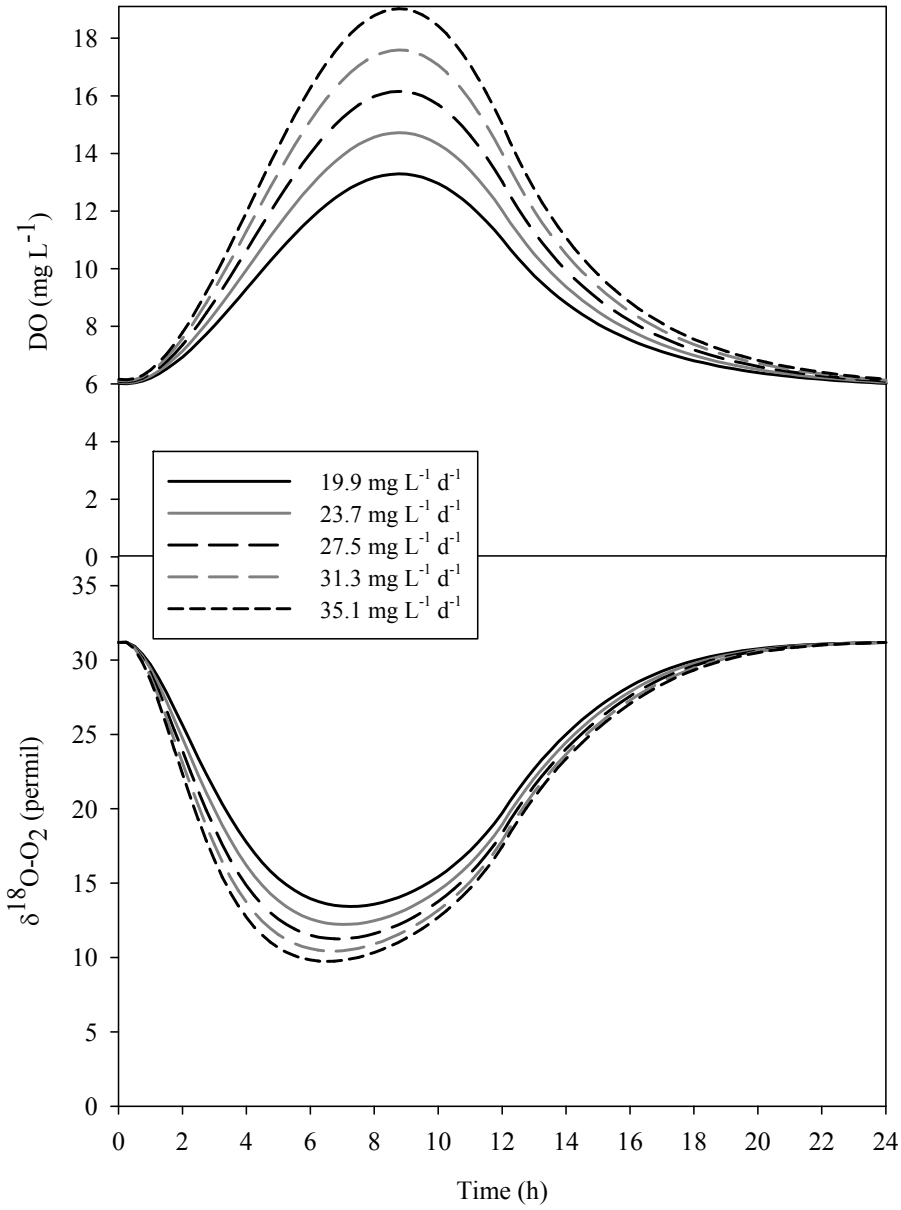

Figure 3.2 Diel model output of DO concentration and $\delta^{18}O\text{-}O_2$ for a range of GPP rates, when k, CR, and α_r are held constant.

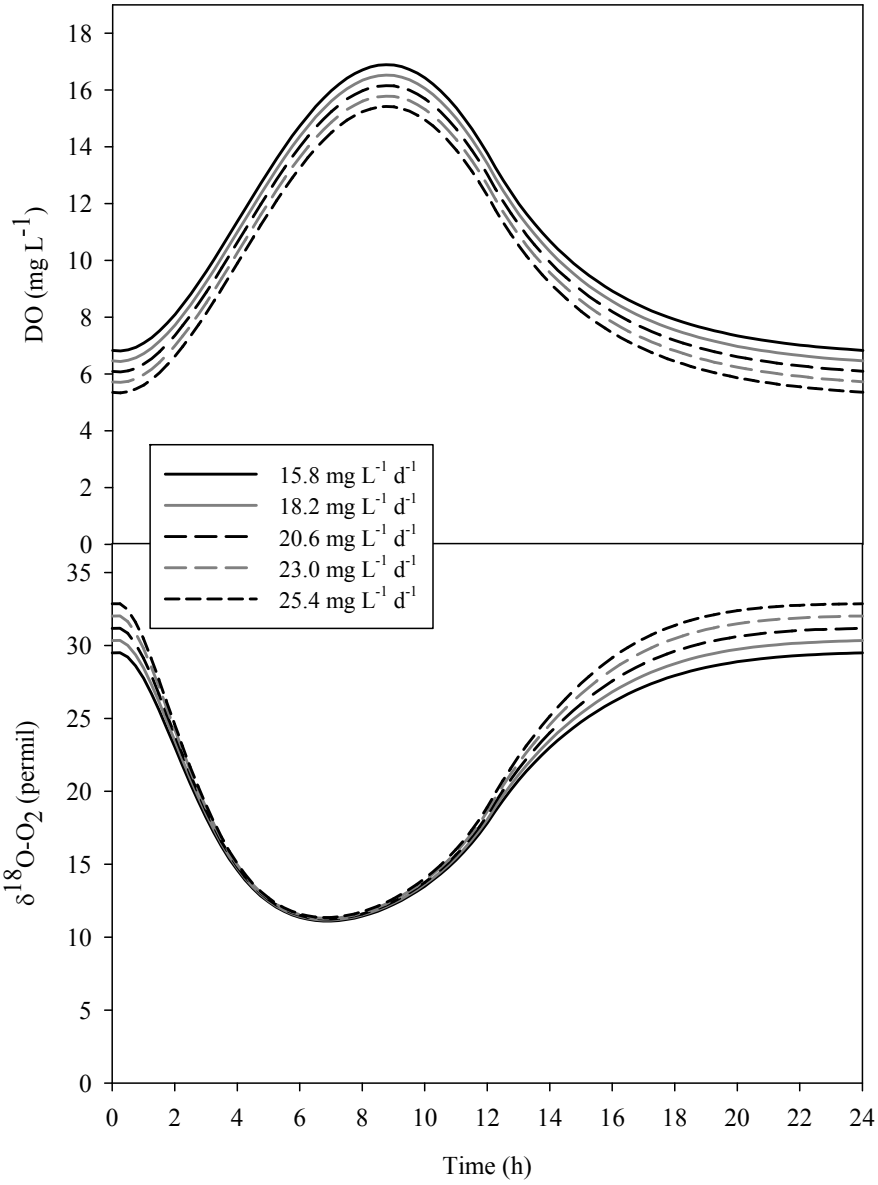

Figure 3.3 Diel model output of DO concentration and $\delta^{18}O\text{-}O_2$ for a range of CR rates, when GPP, k, and α_r are held constant.

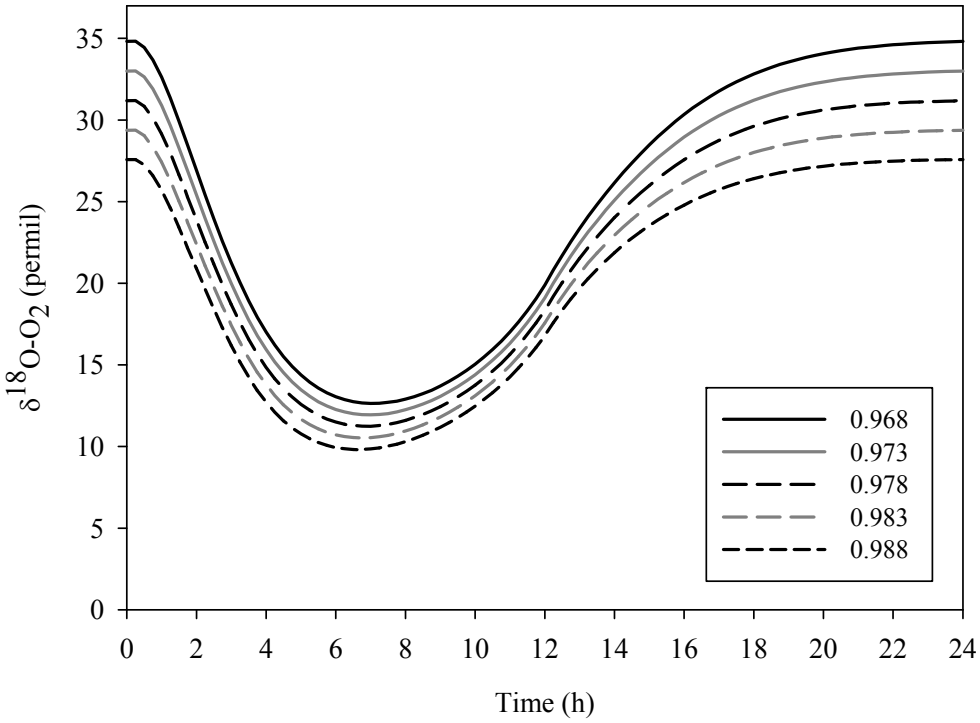

Figure 3.4 Diel model output of $\delta^{18}O\text{-}O_2$ for a range of α_r values, when GPP, CR, and k are held constant.

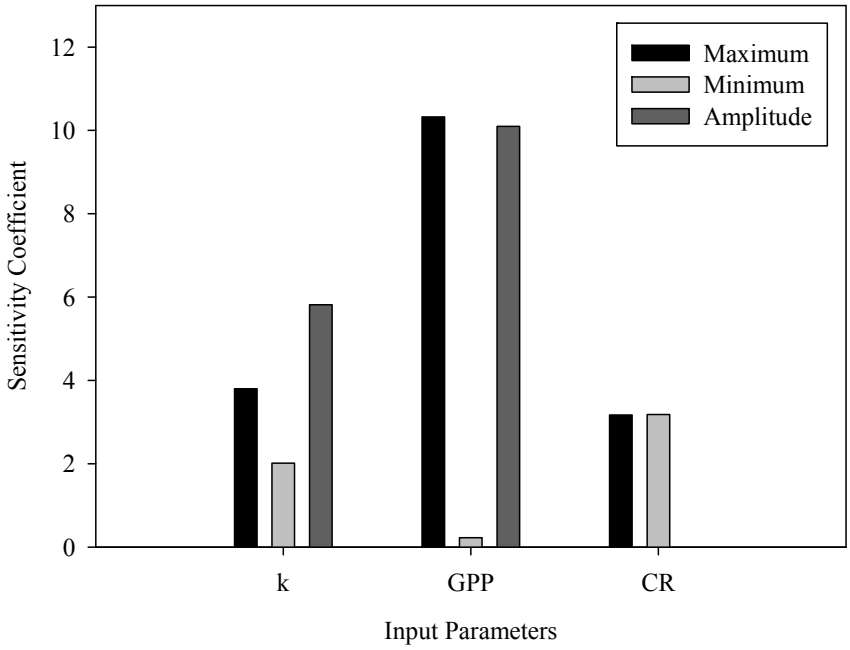

Figure 3.5 Mean sensitivity coefficients for diel DO characteristics, associated with the model input parameters.

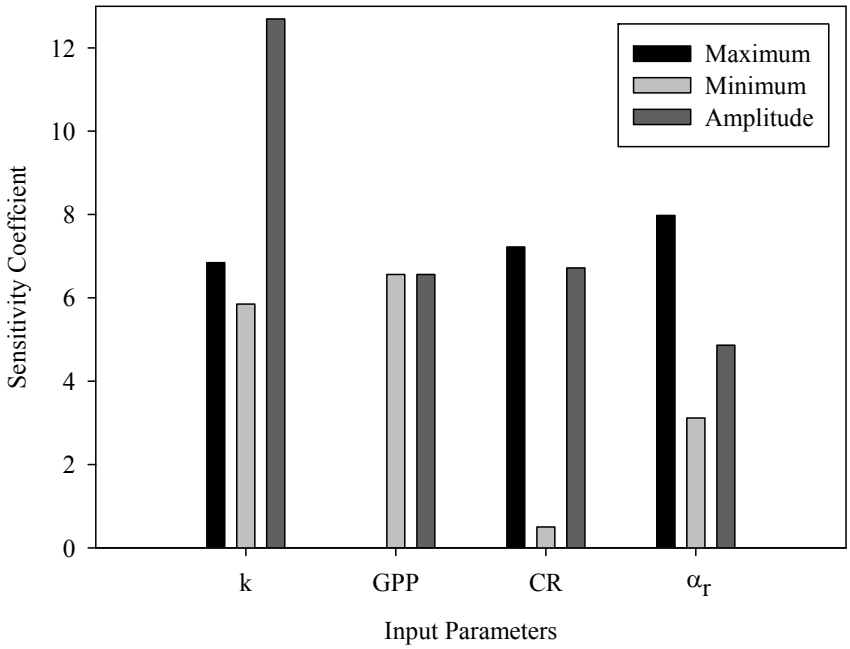

Figure 3.6 Mean sensitivity coefficients for diel $\delta^{18}O$-O_2 characteristics, associated with the model input parameters.

3.3.2 Input Parameter Uncertainty Analyses

When fitting DO and $\delta^{18}O\text{-}O_2$ model output to observed data in the current study, the "best-fit" input parameter estimates were chosen based on a combination of minimizing the RMS error for both mass balances, as well as visual observation. To examine how a range in model outputs relate to input parameter estimation, a series of model simulation outputs were identified (Table 3.4 and Figure 3.7). The intent of this exercise was to illustrate the range of input parameter values that could be estimated under different model fit approaches and biases. The model simulations chosen included the original fitted model parameter estimates (Simulation A), where k and CR were identified from fitting night portion of the data and used to calibrate Pmax and α_r for the full diel model curve (Chapters 4 and 5). In the original model fit procedure (Chapter 5), the model was initialized at the first data point and only simulated the time period for which data were observed. For each simulation, the model was allowed to reach diel steady state output in order to remove bias associated with using the first data point for model initialization.

To compare the validity of assuming k and CR obtained from the night data, the best overall fit (Simulation B) was identified by running a range of k, CR, α_r, and Pmax. Simulations C (low α_r value) and D (high α_r value) represent the range in input parameters that describe approximately twice the RMS error exhibited by the overall best fit to $\delta^{18}O\text{-}O_2$ data (Simulation E) taking into account the associated DO model fit. Simulation E represents biasing the model fit scenario towards minimizing the RMS error associated with $\delta^{18}O\text{-}O_2$. Simulation F is reflective of the best combined fit of DO and $\delta^{18}O\text{-}O_2$ model output to the day portion of the data. For model simulation of day time data, the absolute GE rate could not be

calculated via extrapolation since the model output would mainly be reflective of supersaturated conditions.

For all model simulations, GPP ranged from 11.4 to 12.4, and CR from 8.44 to 9.07 g O_2 m^{-2} d^{-1} despite the RMS ranging approximate two-fold. Using a range of α_r values from 0.970 (Simulation C) to 0.985 (Simulation D) did not appear to result in large changes in the best fit input parameter estimates. The ratio of P:R, as well as P:R:G, were also similar over the range of fitted input parameters. The model output and input parameter estimates were similar whether night-derived k and CR were assumed (Simulation A) or a range of potential parameters were applied to the entire diel curve (Simulation B), or only the day portion (Simulation F) of the data was used. The full diel curve best fits tended to predict a greater α_r value than when only day data was used, in agreement with the trends noted in Chapter 6. Biasing the model fit towards greatest agreement with observed $\delta^{18}O$-O_2 resulted in a slightly higher P:R ratio with parameter estimates similar to simulation C. However, given the range in GPP, CR, and k estimates found for the Grand River (Chapter 5), the uncertainty ranges in input parameter estimates were relatively small.

Using only the DO concentration data (Table 3.5 and Figure 3.9), and relying on night regression of changes in DO and associated saturation deficits to determine k, resulted in GPP and CR rates that were slightly higher than the best fit simulations (A and B), but with the same P:R, and slightly greater P:R:G. Making no assumptions for k and simulating a range of input estimates to determine model DO output that minimized the RMS error resulted in k, GPP and CR rates that were in also agreement with results found in simulations A and B.

Table 3.4 Range in input parameter characteristics for a diel DO and $\delta^{18}O\text{-}O_2$ observed data set collected at WM on August 13-14, 2003. Day length and temperature conditions present during observed data collection were used during the model simulations.

Simulation	**A**	**B**	**C**	**D**	**E**	**F**
Model Descriptors	Original Fitted Input Values	Best Fit Overall	Low α_r Value	High α_r Value	Best Fit to $\delta^{18}O\text{-}O_2$	Day Data Fit
RMS DO (mg L^{-1})	0.39	0.37	0.83	0.49	0.83	0.46
RMS $\delta^{18}O\text{-}O_2$ (‰)	2.25	1.97	2.06	2.76	1.64	1.91
k (h^{-1})	0.27	0.27	0.35	0.29	0.35	0.27
Pmax (mg O_2 L^{-1} h^{-1})	3.6	3.4	3.7	3.5	3.7	3.4
R_{20} (mg O_2 L^{-1} h^{-1})	0.86	0.80	0.80	0.82	0.80	0.80
α_r	0.978	0.977	0.970	0.985	0.976	0.971
k (d^{-1})	6.48	6.48	8.40	6.96	8.40	6.48
GPP (mg O_2 L^{-1} d^{-1})	32.6	30.7	33.5	31.7	33.5	30.7
CR (mg O_2 L^{-1} d^{-1})	24.5	22.8	22.9	23.4	22.8	23.3**
GE (mg O_2 L^{-1} d^{-1})	23.8	22.5	27.0	23.9	27.0	***
GPP* (g O_2 m^{-2} d^{-1})	12.1	11.4	12.4	11.7	12.4	11.4
CR* (g O_2 m^{-2} d^{-1})	9.07	8.44	8.47	8.66	8.44	8.62**
GE* (g O_2 m^{-2} d^{-1})	8.81	8.33	9.99	8.84	9.99	***
P:R	1.33	1.35	1.47	1.35	1.47	1.28
P:R:G	1.37:1.03:1	1.37:1.01:1	1.24:0.84:1	1.33:0.98:1	1.24:0.84:1	***

*Assuming a mean depth of 0.37 m

**Extrapolated to 24 h using CR output from modeled time period

***Removal of night data from model simulation precludes the estimation of diel GE flux

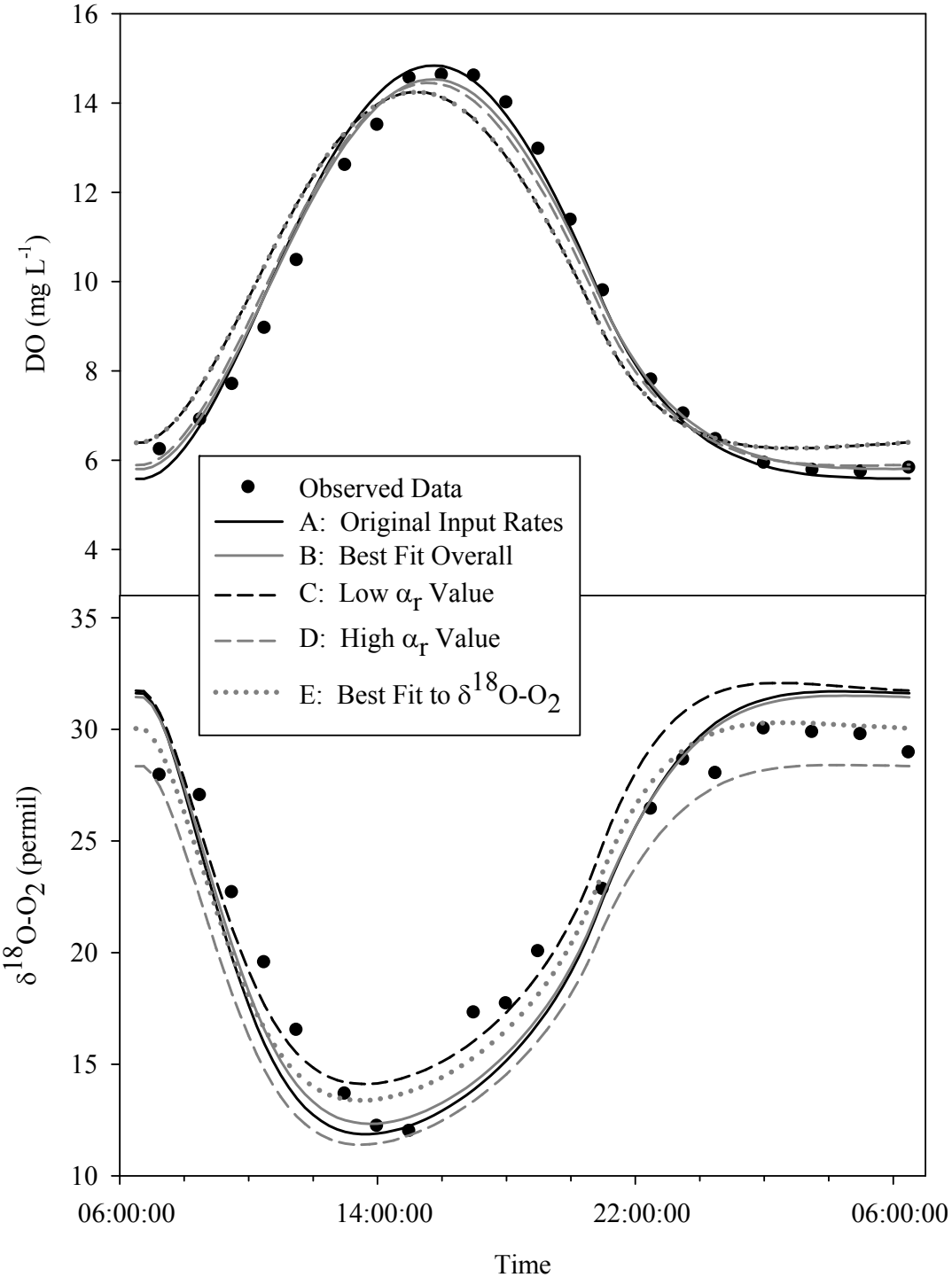

Figure 3.7 Output generated for various potential data modeling approaches using the WM August 13-14, 2003, DO and $\delta^{18}O\text{-}O_2$ data set.

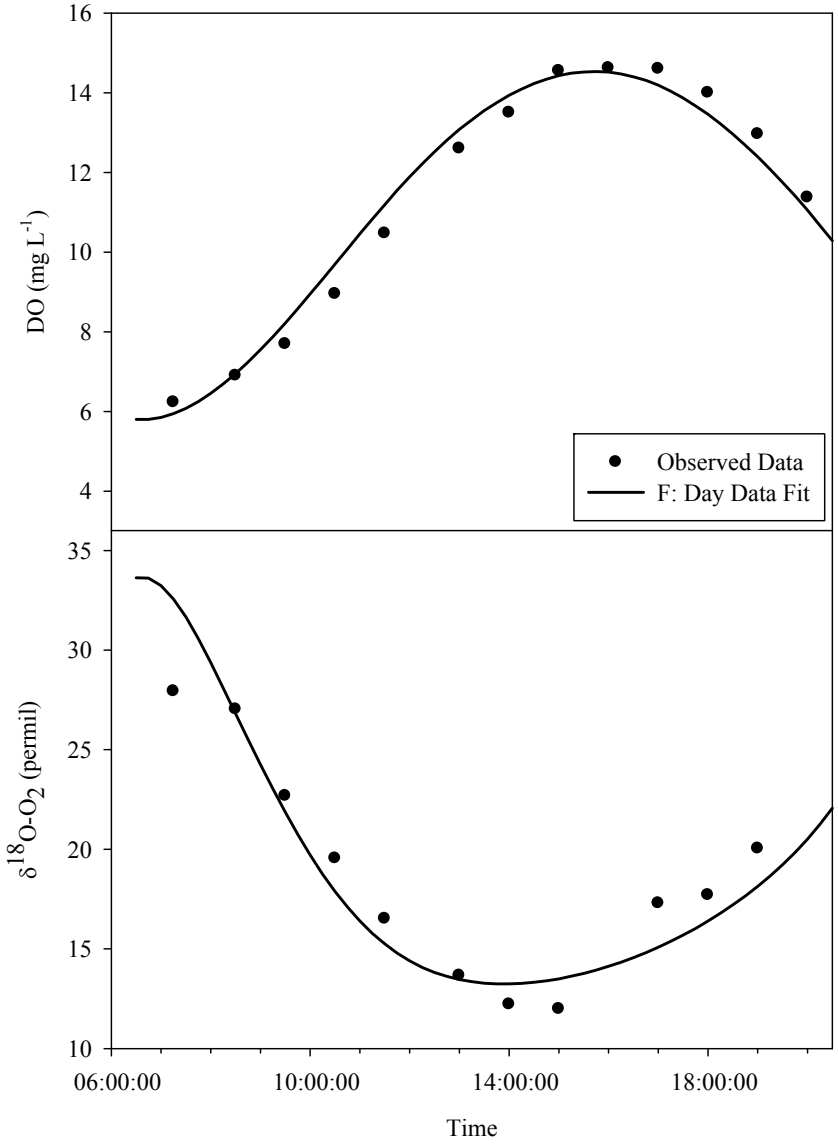

Figure 3.8 Output generated for the best model output fit to both DO and $\delta^{18}O\text{-}O_2$ for WM August 13-14, 2003, day data.

Table 3.5 Fitted input parameters and model output characteristics using k held at the value derived from night data regression, as well as a range of input rate permutations, using only diel observed DO data at WM for August 13-14, 2003.

Model Descriptors	Night-Regression k	Best Fit to DO Data
RMS DO (mg L^{-1})	0.64	0.25
k (h^{-1})	0.32	0.24
Pmax (mg O_2 L^{-1} h^{-1})	3.8	3.3
R_{20} (mg O_2 L^{-1} h^{-1})	0.90	0.80
k (d^{-1})	7.68	6.00
GPP (mg O_2 L^{-1} d^{-1})	34.4	29.8
CR (mg O_2 L^{-1} d^{-1})	25.7	22.8
GE (mg O_2 L^{-1} d^{-1})	26.8	20.7
GPP* (g O_2 m^{-2} d^{-1})	12.73	11.03
CR* (g O_2 m^{-2} d^{-1})	9.51	8.44
GE* (g O_2 m^{-2} d^{-1})	9.92	7.66
P:R	1.34	1.31
P:R:G	1.28:0.96:1	1.44:1.10:1

*Assuming a mean depth of 0.37 m

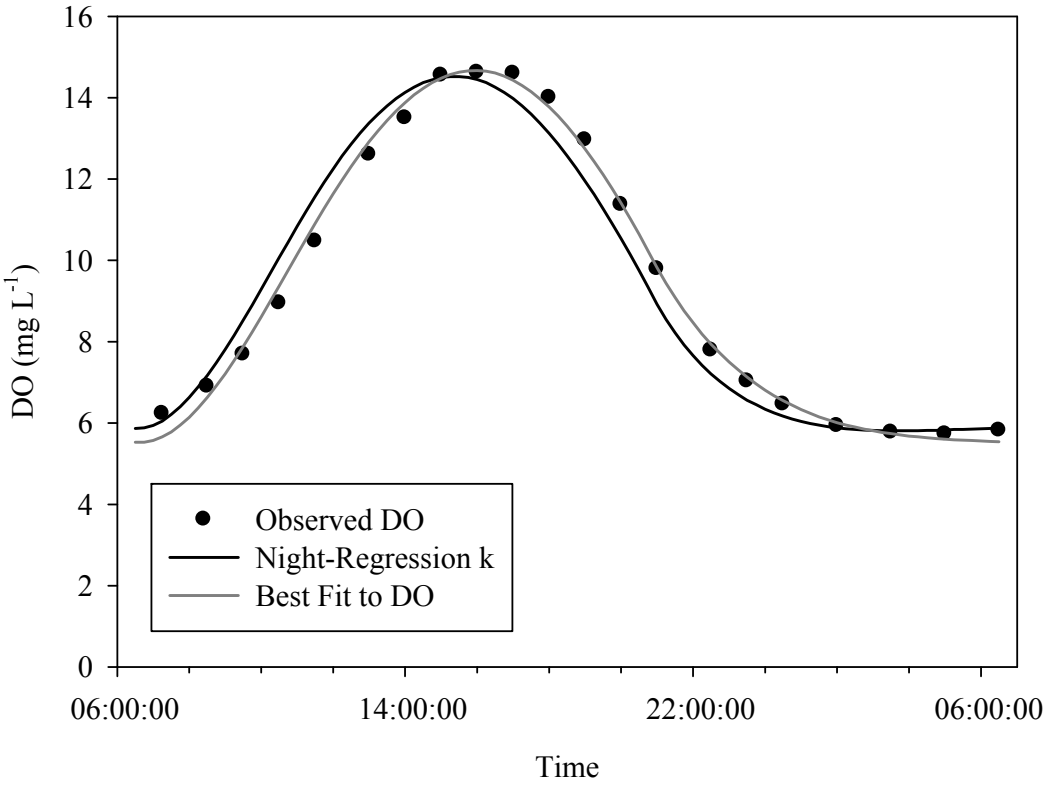

Figure 3.9 Output generated for the best model output fit to observed DO concentrations for WM August 13-14, 2003.

3.4 Discussion

3.4.1 Sensitivity of DO and $\delta^{18}O$-O_2 to Input Parameters

In general, the sensitivity analyses indicated that: 1) the amplitudes of the DO and $\delta^{18}O$-O_2 curves were most governed by k and GPP; 2) diel DO minimum and $\delta^{18}O$-O_2 maximum values are most sensitive to CR and k; and 3) DO maximum and $\delta^{18}O$-O_2 minimum are controlled by GPP and k. Gas exchange controls the overall amplitude of both DO and $\delta^{18}O$-O_2 by driving the values towards atmospheric equilibrium, as noted by Venkiteswaran et al. (2008). Curve amplitudes were sensitive to GPP, but the relatively high sensitivity coefficients were due to the strong effect of GPP on daytime DO maximum and $\delta^{18}O$-O_2 minimum. Gross primary production had a negligible effect on the night time portion of the curves. Decreasing the value of k also had the effect of shifting the timing of DO maximum, and $\delta^{18}O$-O_2 minimum, away from solar noon (Figure 3.1). The delay of the diel DO maximum from solar noon has been used as predictor of k, where shorter delays are indicative of greater k values (Chapra and Di Toro, 1991).

Photosynthetic rates did not affect the night-time values of DO and $\delta^{18}O$-O_2, regardless of the magnitude of GPP influence on the daytime DO maxima and $\delta^{18}O$-O_2 minima for the conditions tested. The entire DO curve shifted downward as CR rates increased, but appeared to only affect the night-time portion of the $\delta^{18}O$-O_2 output. Over a range of parameter values, day time DO is similarly sensitive to increasing GPP rates, but $\delta^{18}O$-O_2 becomes less sensitive to GPP as rates increase, as increasing GPP inputs of a given $\delta^{18}O$-H_2O cannot drive $\delta^{18}O$-O_2 past the endpoint value. In the Grand River, DO minima are primarily controlled by a balance of CR and k, with night time DO plateaus where CR is equal to gas exchange. Day time GPP

inputs appear to be insufficient to overcome k and high CR rates to affect night time low DO conditions. Changes in DO were simulated with the varying rates of GPP with a lower k of 2.4 d^{-1} (0.1 h^{-1}) and CR rate set at the base condition (Figure 3.10). In this case, increases in GPP cause subsequent increases in DO minima.

The α_r only affects $\delta^{18}O\text{-}O_2$, not DO concentration. Decreases in α_r values cause the overall diel curve to become more positive due to greater consumption preference for the lighter isotope (Figure 6.4). The amplitude of the diel $\delta^{18}O\text{-}O_2$ curve exhibited less sensitivity to α_r as compared to the other input parameters (Figure 6.6), and α_r appears to have more effect on night time $\delta^{18}O\text{-}O_2$ values than day time due to the greater effects of CR on the $\delta^{18}O\text{-}O_2$ mass balance at night. The diel $\delta^{18}O\text{-}O_2$ maximum was sensitive to changes in α_r, while the minimum had less sensitivity to α_r than to k and GPP . Venkiteswaran et al. (2008) also noted that $\delta^{18}O\text{-}O_2$ model output was sensitive to small changes in α_r. Parker et al. (2005) generated $\delta^{18}O\text{-}O_2$ data using a similar mass balance to compare to collected values, using net productivity and CR rates obtained from DO curve fitting techniques. Fractionation values ranging from 0.972 to 1.000 were tested using the assumed metabolism rates with no change in the calculated $\delta^{18}O\text{-}O_2$. However, the CR rate assumed by Parker et al. (2005) was equivalent to about 0.16 mg O_2 L^{-1} h^{-1}, which is about 5 times lower than rates reported in the current study at WM and for Venkiteswaran et al. (2007). The associated k used by Parker et al. (2005), 14.2 d^{-1}, was also much greater than those reported in the current study and by Venkiteswaran et al., (2007) of about 4 d^{-1}. Due to the relatively low CR rates in the Parker et al. (2005), and the high contribution of gas exchange, changes in α_r may have had a lesser effect on $\delta^{18}O\text{-}O_2$ output.

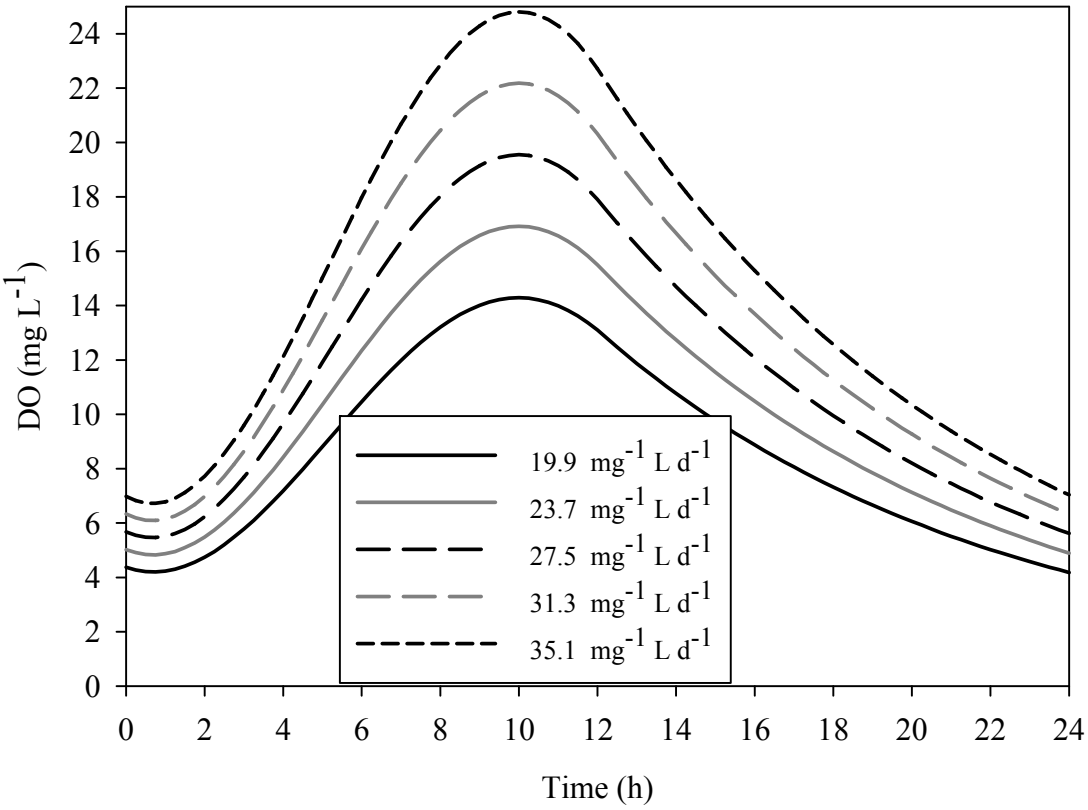

Figure 3.10 Diel model output of DO concentration for a range of GPP rates, when CR is held constant at the base condition and k was set at 2.4 d^{-1}.

3.4.2 Uncertainty in Predicting River Metabolism

Dissolved O_2 concentrations and $\delta^{18}O$-O_2 vary in the Grand River as a shifting balance between production and consumption of O_2, with gas exchange dampening the dynamics. Because DO and $\delta^{18}O$-O_2 are controlled by processes that vary simultaneously, the range over which a given parameter value could vary to result in a given output is dependent on the competing parameter values in the overall mass balance. The original input rates (Simulation A) did not differ greatly from the combined best fit using a range of input estimates (Simulation B), indicating that the technique of using the night portion of the data to calibrate k and CR for the diel model events was an acceptable approach.

The various fit simulations tested, based on different model assumptions and model fit scenarios, resulted in estimates of k ranging from 6.48 to 8.40 d^{-1}, as well as GPP and CR rates from 11.4 to 12.4 and 8.44 to 9.07 g O_2 m^{-2} d^{-1}. This range of uncertainty (~10% for GPP and CR) is in agreement with Venkiteswaran et al. (2007) who reported an uncertainty of approximately ± 5% of the metabolic rates in the South Saskatchewan River using the isotopic mass balance approach. The magnitude of uncertainty may be higher, however, for observed data sets that are characterized by less frequent sampling, or containing more scattered data points deviating from a model curve. However, fitting the model to only the day portion of the data set (Simulation F) yielded similar results to the best model fits obtained from the diel data (Simulations A and B).

Using only DO concentrations to estimate GPP, CR, and k resulted in rates that were similar (within ~10%) to those obtained by the isotope model approach (Table 3.5). Using k obtained from night data regression resulted in rates in the upper range of all estimates, while results from simply running a range of potential parameter values and fitting output to

observed DO were in the lower range of overall rate estimates. The range of parameter values to describe changes in DO in the Grand River may be unique and exhibit a relatively small range. This may not be the case in less impacted systems that generate less dynamic changes in DO.

Overall, the DO curves exhibited a better fit to observed data than the fit associated with $\delta^{18}O\text{-}O_2$, both in the simulations tested and in the results reported in Chapter 5. Deviation of observed $\delta^{18}O\text{-}O_2$ from modeled output is likely partially due to α_r. Adjusting α_r caused $\delta^{18}O\text{-}O_2$ output to vary considerably, as noted in Simulations C and D (Figure 6.7). However, adjusting values of α_r from 0.970 to 0.985 did not result in much change to the associated estimates for GPP and CR. Although α_r is a sensitive parameter in simulating $\delta^{18}O\text{-}O_2$, it does not appear to have a large influence on estimating metabolism, perhaps due to the need for reconciling dual mass balances (i.e., DO concentration and $\delta^{18}O\text{-}O_2$) which would limit the potential combinations of input parameters. In general, it appears that the $\delta^{18}O\text{-}O_2$ model response is more sensitive than DO to k and CR, with additional effects due to α_r. Day time DO appears to be more sensitive to GPP, and the associated the day-time $\delta^{18}O\text{-}O_2$ minimum was also sensitive to changes in GPP. The overall greater level of model error associated with $\delta^{18}O\text{-}O_2$ as compared to DO is likely due to the overall greater sensitivity to input parameters, as well as the assumptions of constant α_r and CR_{20} over a diel cycle.

4.0 Gaseous Exchange of Oxygen in the Grand River

4.1 Introduction

Gas exchange can be an important component of the DO balance in rivers. In turbulent streams, gas transfer can maintain DO near equilibrium and mitigate the effects of DO demand. Currently, the accurate determination of k is a topic of debate in DO modeling, and there are a wide variety of approaches for determining gas exchange rate (Section 1.2) including the application of tracers, regression of night time DO deficits, and using hydrology dependent equations. For instance, there are more than 34 empirical, semi-empirical, and theoretical formulas that have been proposed to predict k in rivers (McCutcheon, 1989) which vary in their uncertainty and applicability. Determining k is essential for modeling DO and estimating GPP and CR, as well as determining the assimilation capacity of rivers receiving organic inputs. It is of particular interest to investigate the applicability of using the stable isotopes of O_2 as a tool to determine k in large, impacted rivers, such as the Grand, where tracer techniques may be logistically difficult to use.

Previous studies using isotopic techniques for studying river DO dynamics have assumed steady state conditions with steady state gas exchange effects (Quay et al., 1995; Wang and Veizer, 2000), used DO concentration regression to obtain k (Parker et al, 2005), or conducted tracer addition experiments (Tobias et al., 2007). The objectives of this study were to 1) use the stable isotopes of O_2, in conjunction with measurement of DO concentration, to quantify the gas transfer coefficient in a large, impacted river 2) compare the results found using the isotope technique to other literature approaches and, 3) examine the variability of the gas transfer coefficient under a range of physical conditions.

4.2 Methods

4.2.1 Determination of Gas Transfer Coefficients

To investigate the application of the isotopic model technique for obtaining estimates of k, only the night portion of diel data was used to reduce the number of unknown variables; the effects of GPP were assumed to be zero and not included in the model simulations. In addition to the data collected in 2003 and 2004, an additional night sampling event was conducted in 2005 for WM and BLR to augment the previous years' data. Values for k were estimated using the iterative modeling routine described in Chapter 2, and the unknown input parameters were k, R and α_r.

4.2.2 Comparison to Traditional Gas Transfer Estimates

There are a large number of predictive equations available for k, high variability among their predictions, and no universally acceptable equation. Generally speaking, however, the most widely used equations (Chapra, 1997) include those by O'Connor and Dobbins (1956), Churchill et al. (1962), and Owens et al. (1964), and they are parameterized in terms of mean depth (D) and velocity (V) according to:

$$k_{20} = z\frac{V^x}{D^y} \tag{4.1}$$

where z, x, and y are the empirically calibrated constants (Table 4.1).

Table 4.1 Selected literature equation coefficients* for calculating k_{20} in rivers.

	Coefficients		
Equation	**z**	**x**	**y**
O'Connor and Dobbins (1958)	3.9	0.5	1.5
Churchill et al. (1962)	5.026	1	1.67
Owens et al. (1964)	5.32	0.67	1.85
Bennett and Rathburn (1972)	5.58	0.607	1.689

* $k_{20} = z\frac{V^x}{D^y}$

To put the k estimated by the isotope technique in context with other literature based estimates, hydrologic conditions were quantified for each sampling event. Discharge rates were obtained from the GRCA for each of the three sampling locations. Hydrologic data (i.e., discharge, mean depth, mean velocity) for the BLR sampling location were also obtained from stream gauging activities conducted by the GRCA. However, for the WM and BRPT locations, only discharge data were available. At the WM location, a topographic survey was performed to determine mean depth and velocity estimates as they relate to discharge. A topographical survey could not be conducted at BRPT due to channel access difficulties and deep water conditions at the sampling access point. Channel characteristics measured using surveying equipment at WM included cross-sectional geometry, and water surface slope. Two cross sections were surveyed along a uniform channel reach upstream from the sampling location. The cross-sectional geometry was used to compute cross sectional area, wetted perimeter and hydraulic radius of the channel for increasing fractions of bankfull flow, as the channel characteristics at various discharge rates were not measured directly. Manning's equation was used to express mean velocity (V) as a function of the hydraulic geometry (French, 1985):

$$V = \frac{1}{n} * R^{2/3} * s^{1/2} \tag{4.2}$$

where V is mean velocity (m s^{-1}), n is the assumed Manning's roughness coefficient equal to 0.035, R is the hydraulic radius (m), and s is the water surface slope (m m^{-1}) equal to 0.001. Water surface slope was calculated by the difference in water surface elevation over a distance of 30 m. Manning's roughness coefficient was assigned based on characteristics of the bed

(French, 1985). Hydraulic radius (HR) was calculated from, A, the cross-sectional area of flow (m^2) and P, the wetted perimeter (m):

$$HR = \frac{A}{P} \tag{4.3}$$

The relationships between discharge (Q) and both V and HR were then estimated by reconciling results from the estimates obtained by Manning's equation with the continuity equation:

$$Q = V * A \tag{4.4}$$

where Q is the discharge rate (m^3s^{-1}), as obtained from the GRCA. It was assumed that HR is equivalent to the mean depth (D) of the channel.

To develop an empirical equation to predict k in the Grand River, estimates of k found from the isotope modeling were related to hydrologic conditions using the non-linear regression routine in SigmaPlot v.6.0 (2000). The relationship was parameterized in terms of V and D according to the general form used in most gas transfer empirical equations (Eq. 4.1). Other stream characteristics such as slope, friction, and Reynolds number were not included as it has been found that they do not markedly increase the accuracy of predicted values (Churchill et al., 1962).

4.3 Results

4.3.1 Gas Transfer Coefficients in the Grand River

Dissolved O_2 concentrations declined at night due to respiration, with a concurrent enrichment of $\delta^{18}O\text{-}O_2$ (Figures 4.1, 4.2, and 4.3). The k values predicted from the isotope technique for the Grand River ranged from 3.6 to 8.6 d^{-1} (Table 4.2). Overall, the non-steady state model appears to satisfactorily reproduce the changes in both DO and $\delta^{18}O\text{-}O_2$ for most sampling days. RMS errors for the DO model output were near, or less than, the analytical error of 0.2 mg L^{-1} associated with Winkler titrations. There was greater variability associated with $\delta^{18}O\text{-}O_2$ model output, as indicated by greater RMS error.

There was a relatively poor model fit to $\delta^{18}O\text{-}O_2$ exhibited for the BLR July 29-30, 2005 data. During this sampling event, DO concentrations were very low, dipping to less than 2 mg L^{-1} at this location. Under the extremely low DO conditions, the model may not have been able to adequately represent CR or the fractionation processes. In addition, there may also have been analytical error associated with $\delta^{18}O\text{-}O_2$ due to the low levels of DO in the water sample. There appear to be greater RMS values associated with the BRPT and BLR as compared to WM. The high error in $^{18}O\text{-}O_2$ model fit at BRPT on August 30-31, 2004, appears to be attributable to an anomalous data point. Community respiration rates ranged from approximately 10 to 47 mg L^{-1} d^{-1}, with associated α_r values ranging from 0.971 to 0.996, with most values falling within the range of 0.980 to 0.989.

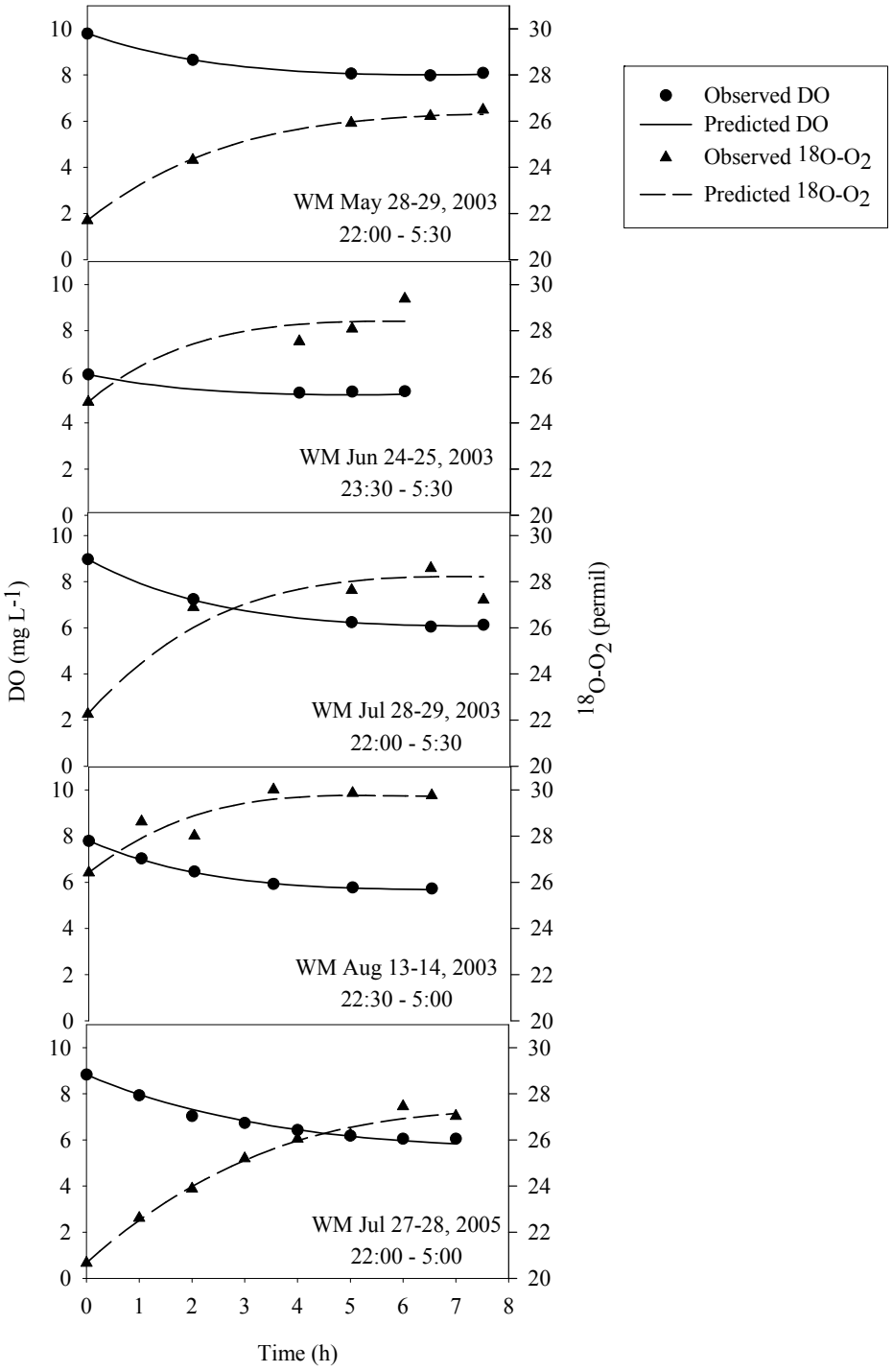

Figure 4.1 Changes in observed and model-predicted DO and $\delta^{18}O\text{-}O_2$ at the West Montrose location during the night-time sampling events plotted versus time.

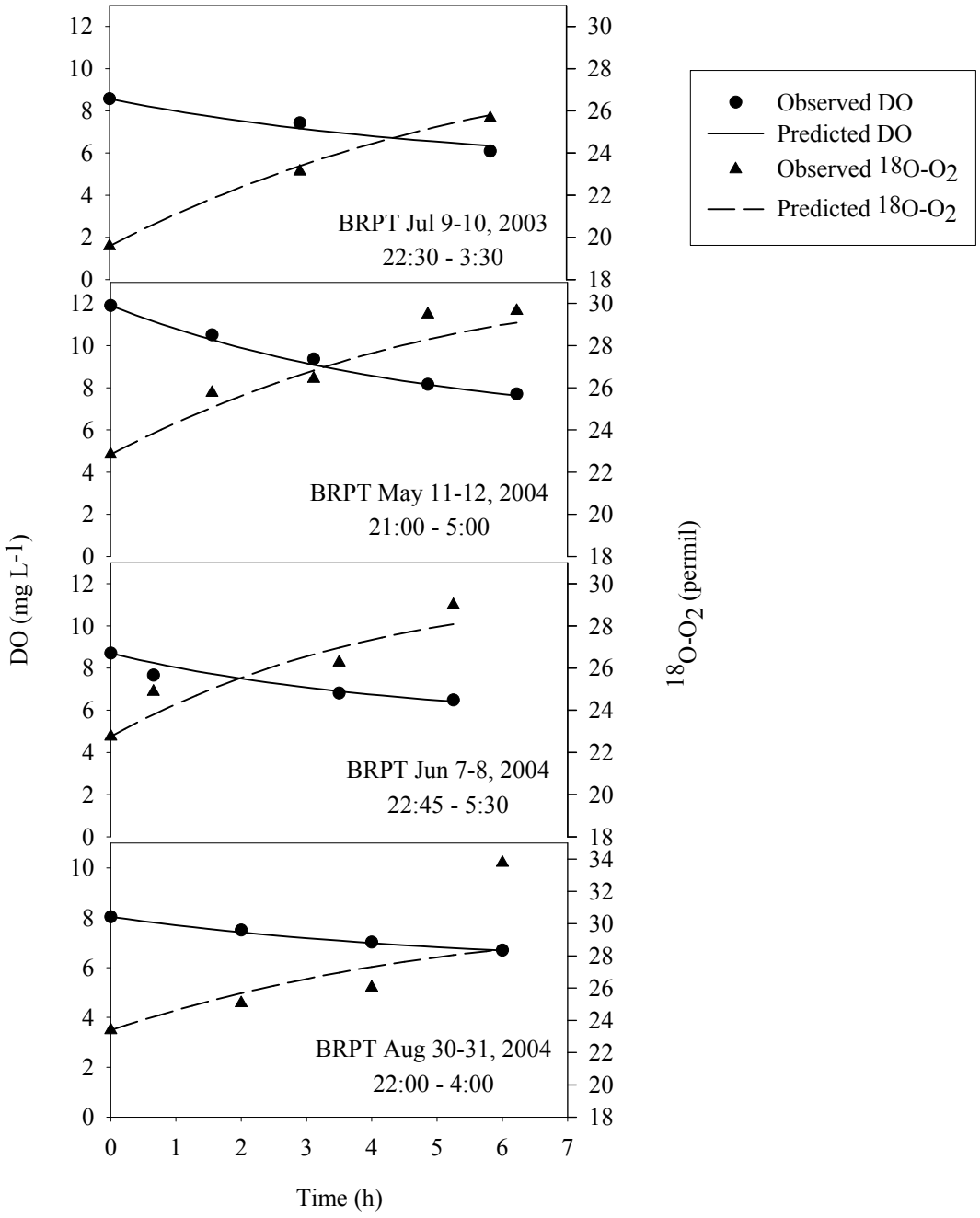

Figure 4.2 Changes in observed and model-predicted DO and $\delta^{18}O\text{-}O_2$ at the Bridgeport location during the night-time sampling events plotted versus time.

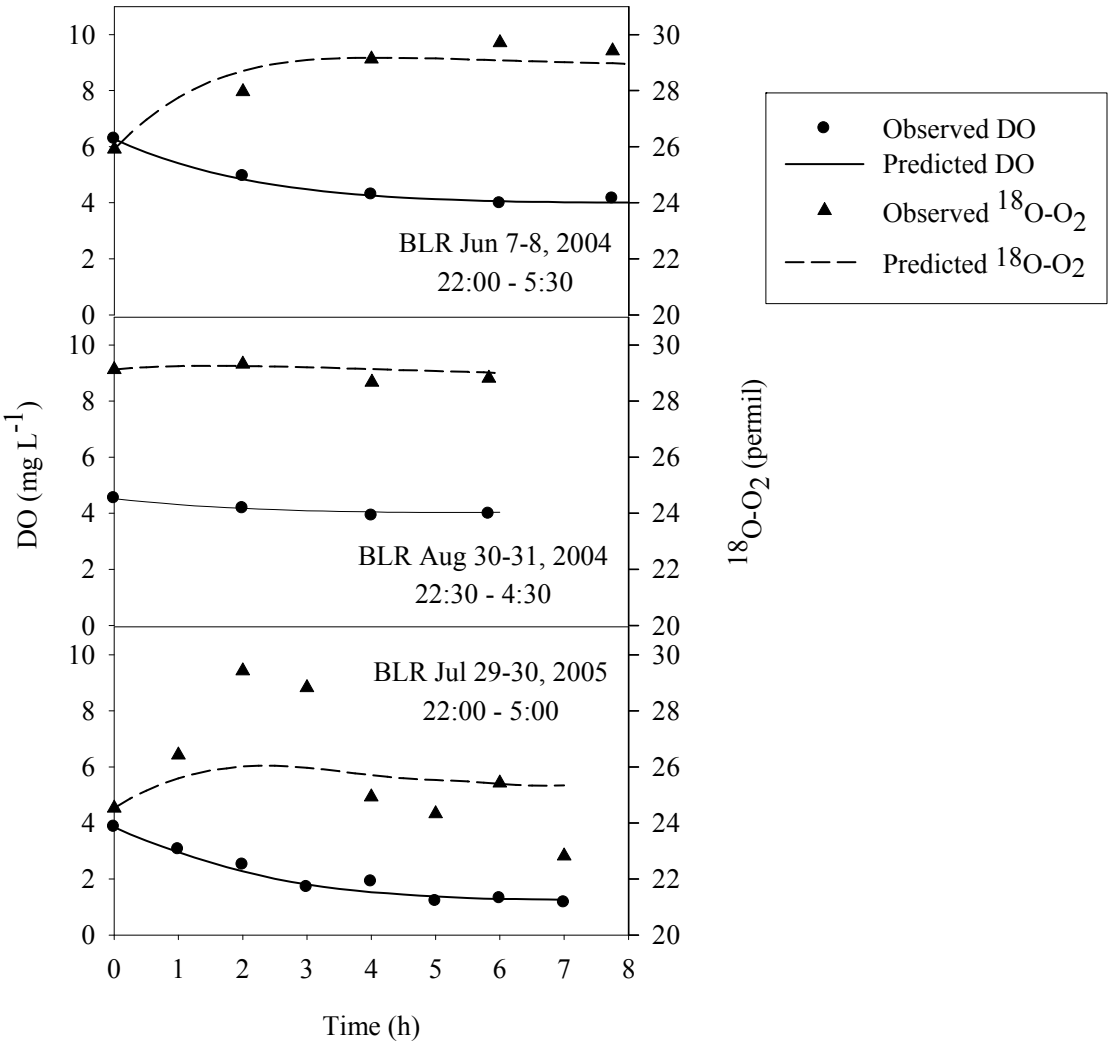

Figure 4.3 Changes in observed and model-predicted DO and $\delta^{18}O$-O_2 at the Blair location during the night-time sampling events plotted versus time.

Table 4.2 Fitted model input parameter results obtained from DO concentration and $\delta^{18}O\text{-}O_2$ night-time data modeling

Sampling Event		Model k* (d^{-1})	Model CR* (mg L^{-1} d^{-1})	Model α_r	RMS DO (mg L^{-1})	RMS $^{18}O\text{-}O_2$ (‰)
WM	May 28/03	**7.4**	22.8	0.988	0.03	0.10
	Jun 24/03	**6.0**	21.4	0.987	0.12	0.73
	Jul 28/03	**7.0**	23.0	0.986	0.04	0.72
	Aug 13/03	**6.7**	20.6	0.983	0.04	0.54
	Jul 27/05	**5.3**	23.8	0.990	0.16	0.27
BRPT	Jul 9/03	**3.6**	10.1	0.986	0.26	0.21
	May 11/04	**3.8**	13.8	0.980	0.18	0.77
	Jun 7/04	**3.6**	13.7	0.984	0.35	0.91
	Aug 30/04	**3.6**	11.5	0.971	0.05	3.21
BLR	Jun 7/04	**8.6**	43.2	0.989	0.09	0.53
	Aug 30/04	**7.2**	38.2	0.989	0.09	0.29
	Jul 29/05	**6.0**	46.8	0.996	0.19	2.04

*corrected to 20°C

4.3.2 Hydrologic Characteristics

The cross sectional geometry at WM (Figure 4.4) and hydrology characteristics (Table 4.3) were used to develop mean depth and velocity relationships to discharge rates (Figure 4.5). Discharge rates calculated using the geometry of the channel at WM for 25 to 50% of bankfull discharge were within the range of discharges reported by the GRCA during the course of this study. For the BLR location, mean discharge-depth and velocity relationships were developed as the average of a series of cross-sectional stream gauging events conducted by the GRCA upstream of this location (Figure 4.6).

The mean of the curves obtained for WM and BLR were used to calculate mean depth and velocity changes based on discharge for the BRPT location (Figure 4.7). The river channel upstream (e.g. width, depth) at each of these sites appear be consistent with the respective location where hydrologic characteristics were measured. The BRPT location is located at roughly the mid-point on the longitudinal main channel continuum between WM and BLR, and it was assumed that the BLR region of the watershed would exhibit hydrologic characteristics that were the average of that in the areas of WM and BLR.

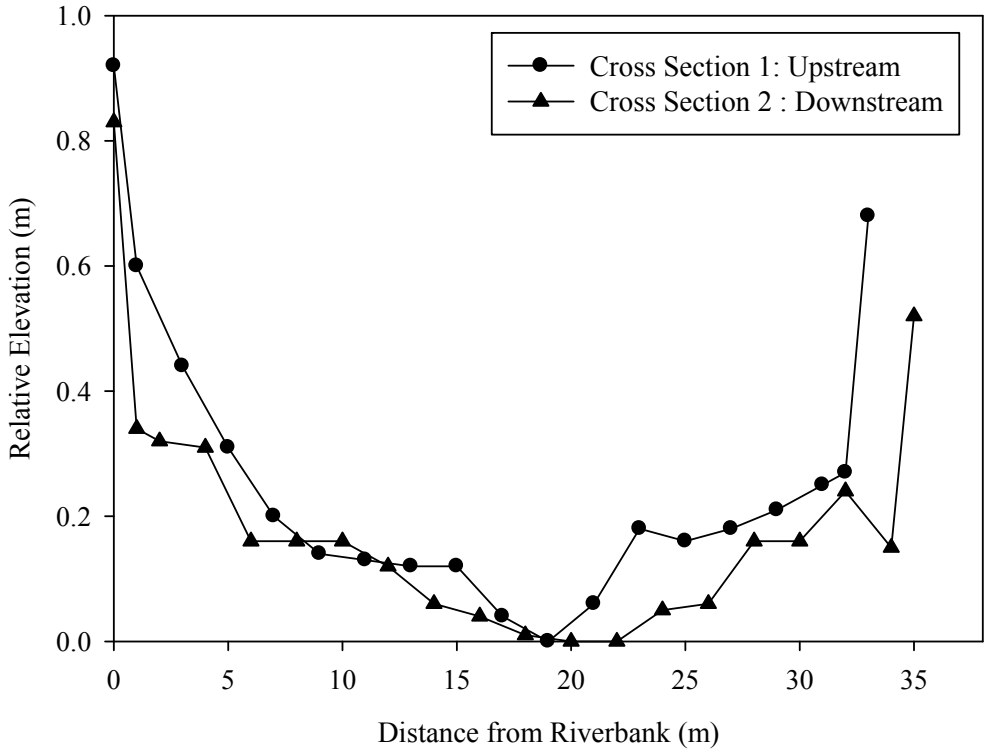

Figure 4.4 Cross-sectional topography of the Grand River as measured at West Montrose.

Table 4.3 Hydrologic characteristics for the Grand River at WM based on stream-bed geometry.

	Fraction of Bankfull Discharge	**Cross Section 1**	**Cross Section 2**
Cross Sectional Area (m^2)	100%	24.4	24.8
A	75%	16.8	17.3
	50%	9.22	10.4
	25%	2.86	3.64
Wetted Perimeter (m)	100%	34.2	36.2
P	75%	32.4	34.8
	50%	29.5	34.0
	25%	23.6	28.9
Mean Depth (m) measured as Hydraulic Radius	100%	0.72	0.68
HR=A/P	75%	0.52	0.50
	50%	0.31	0.31
	25%	0.12	0.13
Manning's Mean Velocity (m s^{-1})	100%	0.72	0.70
$V=1/n * R^{2/3} s^{1/2}$	75%	0.58	0.57
n = 0.035	50%	0.42	0.41
s = 0.001	25%	0.22	0.23
Mean Discharge (m^3s^{-1})	100%	17.66	17.35
Q=V*A	75%	9.81	9.78
	50%	3.84	4.29
	25%	0.63	0.83

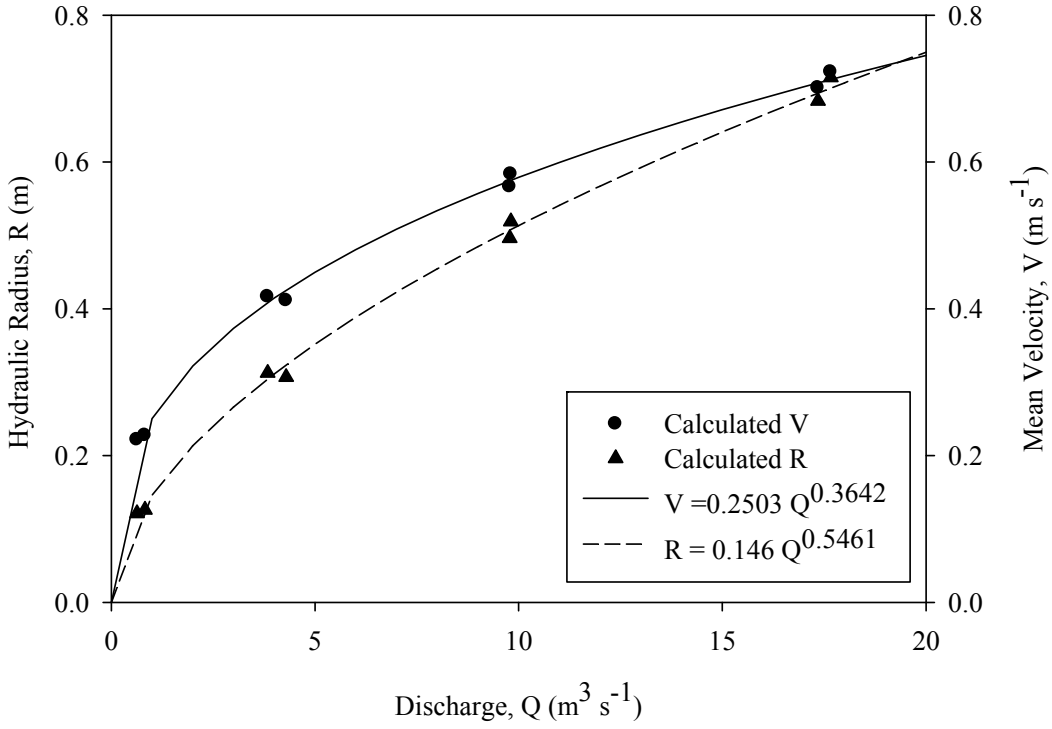

Figure 4.5 Hydraulic radius, (equivalent to mean depth) and velocity relationships to discharge rates at the WM location.

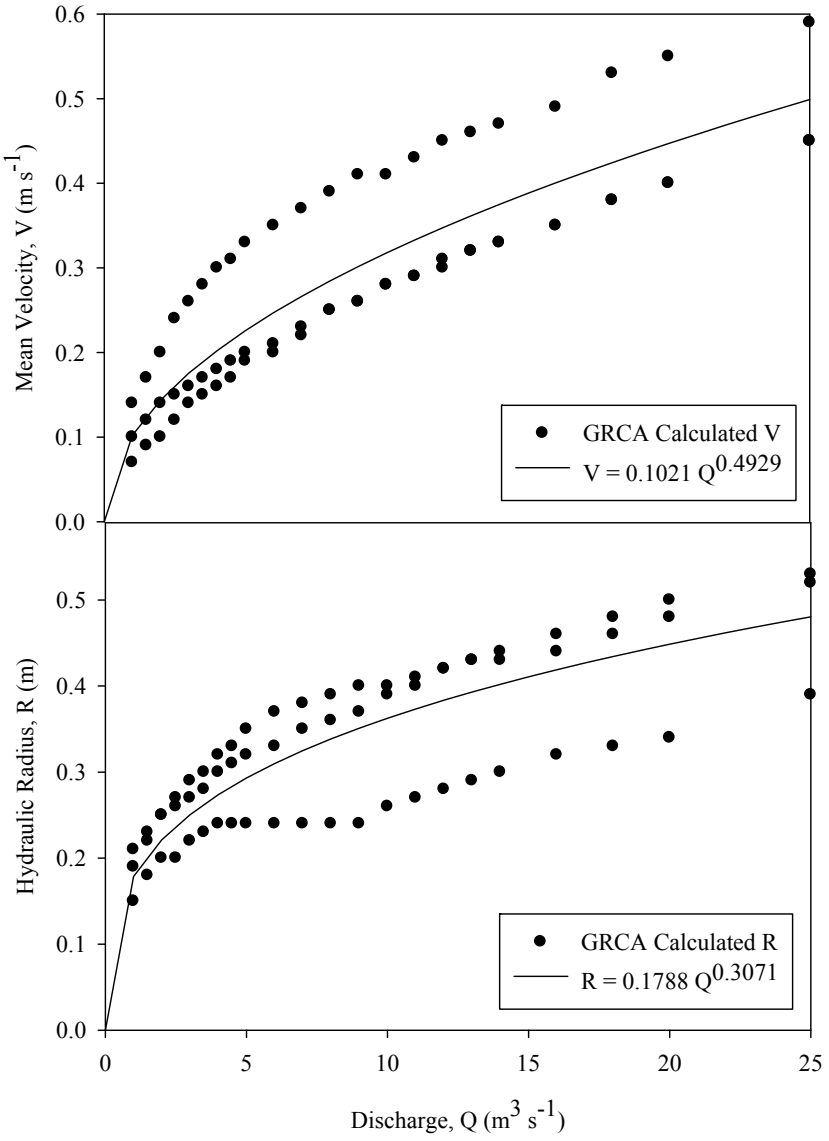

Figure 4.6 Hydraulic radius (equivalent to mean depth) and velocity relationships to discharge rates at the BLR location; discharge relationships were taken as the mean of a series of GRCA conducted stream gauging events conducted at cross sections upstream of this site.

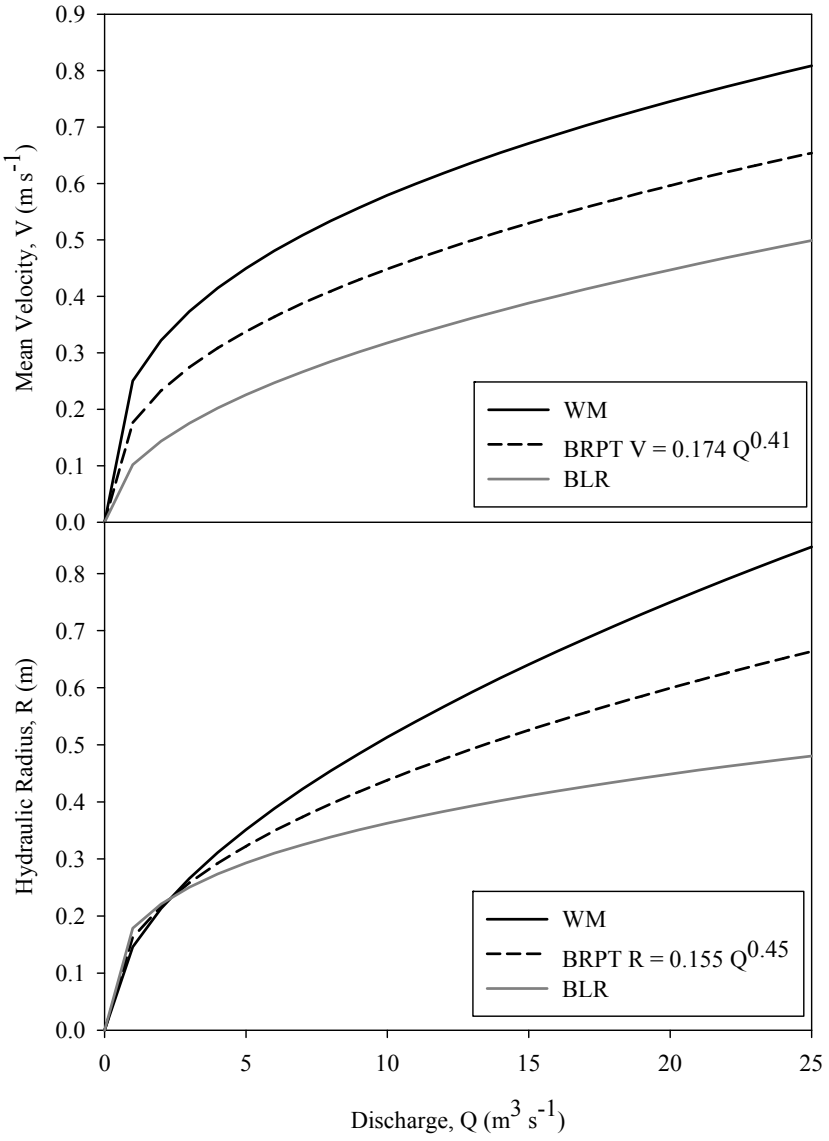

Figure 4.7 Hydraulic radius (equivalent to mean depth) and velocity relationships to discharge rates. At the BRPT location, discharge relationships were taken as the mean of the results obtained for the WM and BLR locations.

Gas transfer coefficients in the Grand River appear to be fairly constant for all locations over changes in mean depth and velocity during sampling events. There was also no relationship between discharge and k (R^2=0.24%; Figure 4.8). When an empirical equation similar to the form commonly used in gas exchange equations, based on changes in mean velocity and depth, is fitted to the Grand River k data via non-linear regression, the resulting expression is:

$$k_{20} = 8.55 \frac{V^{-0.38}}{D^{-0.60}} \qquad (4.5)$$

The R^2 for this equation was 0.20%, indicating that the traditional approach of using mean velocity and depth to predict k were not appropriate for the Grand River under the conditions observed (Figure 4.9). The coefficients associated with V and D in literature equations (Table 4.1) are usually positive; the negative coefficients noted in equation 4.5 are likely due to the poor relationship between k and hydrologic characteristics in the Grand River. The k at BRPT on May 11/04 was not included in Figure 4.8 or fitting Equation 4.5 to avoid biasing the regressions, as the discharge (73 $m^3 s^{-1}$) was anomalously greater than the other discharges observed.

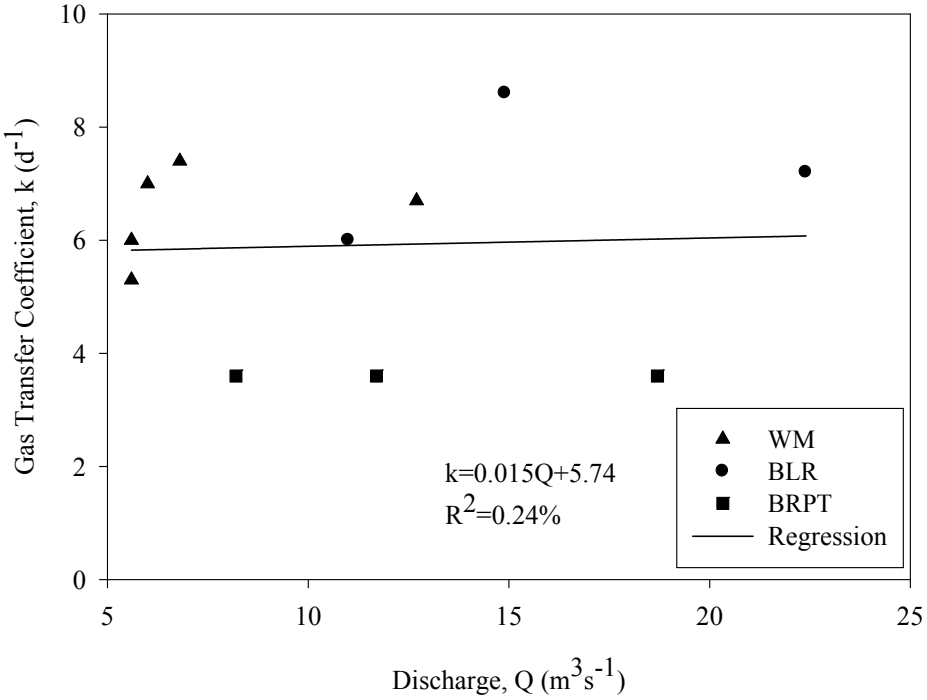

Figure 4.8 Plot and linear regression of the modeled k versus discharge for the sampling locations examined in the Grand River.

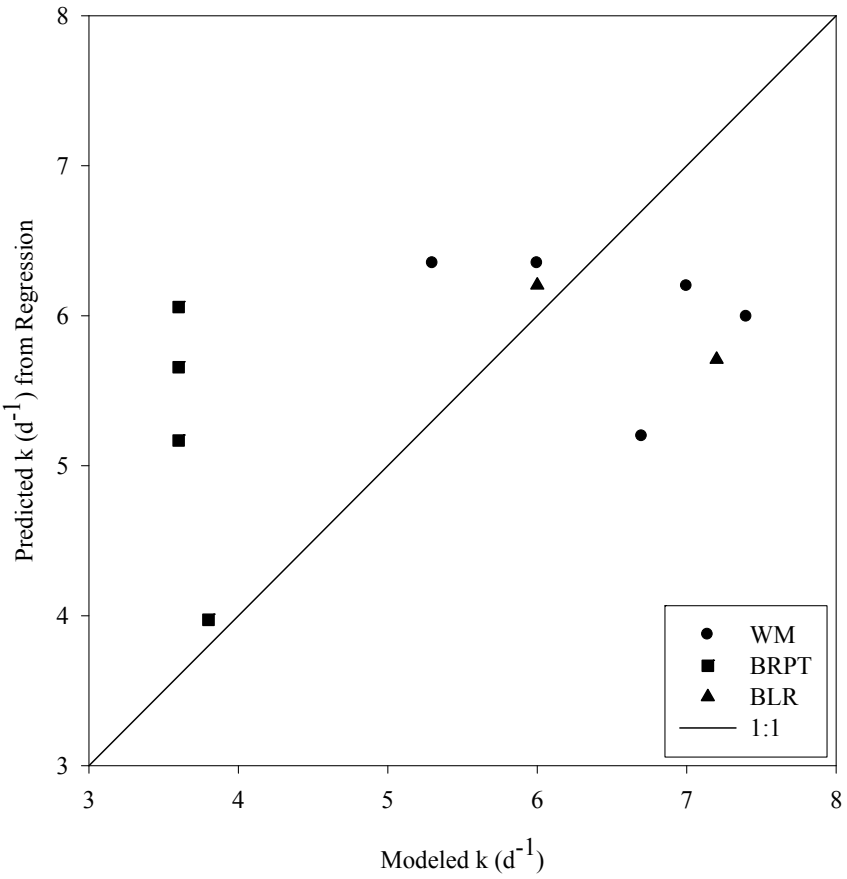

Figure 4.9 Plot of k values as predicted by non-linear regression (Eq. 4.5) versus k obtained from the isotope modeling technique.

4.3.3 Comparison to Other Approaches

The hydrology data for each sampling location (Figures 4.4, 4.5 and 4.6) were used to calculate k from other published equations based on mean depth and velocity (Table 4.4). Regressions using night DO concentration data were also performed to obtain estimates of k (Odum and Hoskin, 1958). The rate of change of DO concentration was regressed against DO deficit (relative to saturation) to obtain the slope of the regression which is an estimate of k. The DO deficit was averaged between the two time points that were used to calculate a given rate of change in DO.

Gas transfer coefficient estimates obtained from the isotope modeling approach were found to be lower than those predicted by the other approaches (Table 4.4 and Figure 4.10). The difference was, on average, 5.2 d^{-1} less than k calculated from the hydrology dependant equations. The closest k estimates obtained by other hydrology-dependant approaches to that obtained using the isotope model were from the O'Connor and Dobbins (1958) equation, followed by Bennett and Rathburn (1972), and then Owens et al. (1964). Gas transfer coefficients obtained via night-time regressions were generally closest to, but on average 1.6 d^{-1} greater than, the coefficients obtained by modeling.

Table 4.4 Comparison of model derived k to selected traditional approaches

Sampling Event	Q ($m^3 s^{-1}$)	D (m)	V ($m s^{-1}$)	Model k* (d^{-1})	O'Connor and Dobbins (1958)	Churchill et al. (1962)	Owens et al. (1964)	Bennett and Rathburn (1972)	Night-time regression (Odum and Hoskin, 1958)*
WM May 28/03	6.8	0.42	0.50	**7.4**	10.1	10.7	16.6	15.9	9.6
WM Jun 24/03	5.6	0.37	0.47	**6.0**	11.9	12.4	20.2	18.9	12.1
WM Jul 28/03	6.0	0.39	0.48	**7.0**	11.1	11.6	18.6	17.5	8.1
WM Aug 13/03	12.7	0.58	0.63	**6.7**	7.0	7.9	10.7	10.6	7.7
WM Jul 27/05	5.6	0.37	0.47	**5.3**	11.9	12.4	20.2	18.9	8.0
BRPT Jul 9/03	8.2	0.40	0.41	**3.6**	9.9	9.5	15.9	15.3	5.0
BRPT May 11/04	73.1	1.07	1.01	**3.8**	3.5	4.5	4.7	5.0	2.9
BRPT Jun 7/04	11.7	0.47	0.48	**3.6**	8.4	8.5	13.2	12.8	9.5
BRPT Aug 30/04	18.7	0.58	0.58	**3.6**	6.7	7.2	10.1	10.1	2.5
BLR Jun 7/04	14.9	0.41	0.39	**8.6**	9.3	8.5	14.7	14.2	9.0
BLR Aug 30/04	22.4	0.46	0.47	**7.2**	8.6	8.6	13.5	13.1	8.1
BLR Jul 29/05	11.0	0.37	0.33	**6.0**	10.0	8.7	15.9	15.3	6.0

*corrected to 20°C

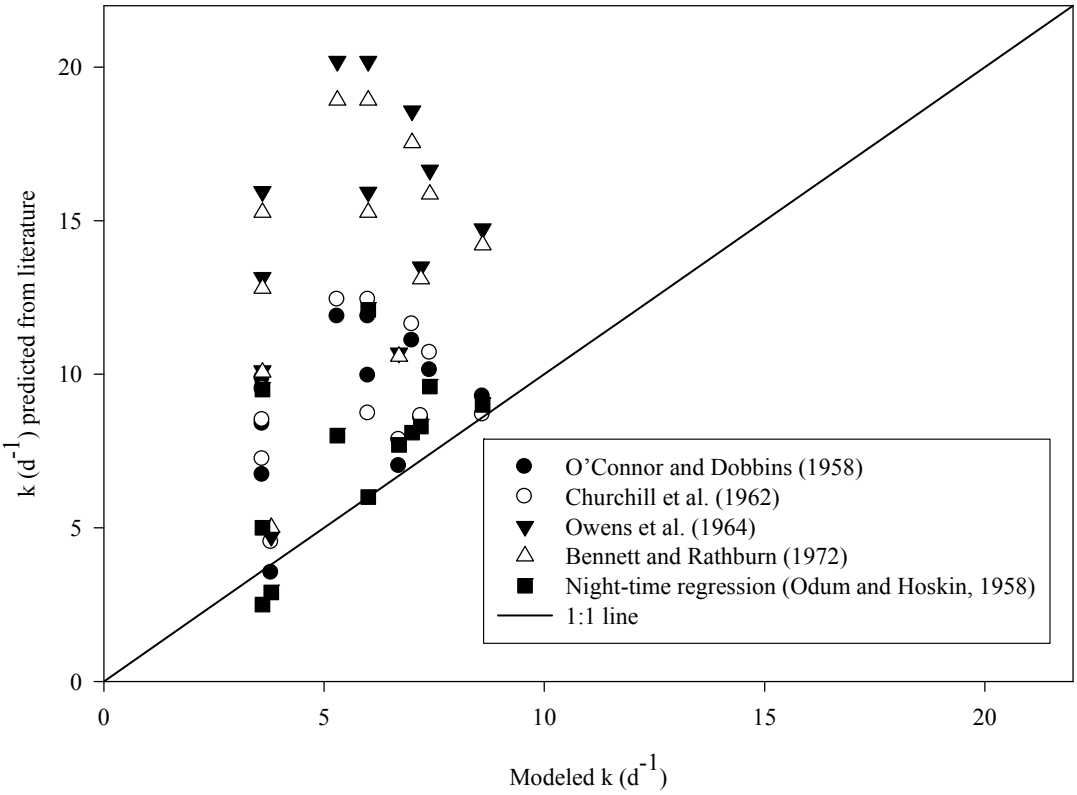

Figure 4.10 Plot of k values as predicted by other selected published approaches versus modeled k values in the Grand River.

4.4 Discussion

The model uses one rate of CR_{20} and k_{20}, over the modeled time period, and short-term variability in either of these terms beyond what is attributable to the temperature correction could potentially lead to deviations from the modeled DO and ^{18}O-O_2 output. This study was undertaken as a single-station approach, common to other DO modeling studies (Servais et al, 1984; Edwards and Meyer, 1987; Livingstone, 1991; Pearson and Crossland, 1996; Wilcock et al, 1998; Williams et al., 2000). As a result, the findings obtained for a particular location are an integrated measure of processes occurring in the watershed upstream from that point. For instance, as k can be considered as a first order rate constant, the "half life" of a unit of DO undergoing exchange can be calculated as:

$$t_{0.5} = \frac{\ln(2)}{k} \tag{4.6}$$

Using mean k at each site to calculate $t_{0.5}$, and multiplying by mean velocity (Table 4.2), the half life travel distance for gas exchange would be on the order of 5, 10, and 3 km at WM, BRPT and BLR, respectively. Gas transfer coefficients at BRPT were roughly half of the estimates for WM and BLR, which exhibited similar k. Gas exchange in rivers is mainly influenced by upstream physical attributes of the channel. At WM and BLR, the river upstream consists of main channel, with no confluences with other major tributaries or reservoirs within the turnover distances, which may lead to similar k values among these locations. However, BRPT is located approximately 12 km downstream from the Conestoga river confluence, one of the major tributaries in the watershed, and about 6 km downstream from Snyder's Flats. Gas transfer upstream of BRPT may be influenced by Conestoga river

input which could exhibit lower k values. Snyder's Flats is a floodplain area that was once a site for gravel mining; this section of the Grand River may be an area of groundwater discharge of a magnitude great enough to affect the DO budget, which was not accounted for in the model. In addition, if the channel morphology upstream of BRPT was less consistent with WM and BLR, if there was less turbulence for example, rates of k may be lower.

The fit of the model to observed data was generally poorest at BLR, as compared to WM and BRPT. Error in associated model fits may be due to short-term temporal variation in upstream processes that are not accounted for in the model, as constant rates of CR_{20} and an idealized GPP half sine curve were assumed. Blair is located downstream of two major sewage treatment plants that would have a daily pattern of discharge which could cause small temporal variability in model parameters. Pulsed inputs of DO consuming substances could cause short-term variability in observed DO and $\delta^{18}O\text{-}O_2$. Community respiration rates tend to be greater at BLR than upstream, with lower DO minima at night. As DO concentration declines at BLR, associated decline in the rate of CR could also be occurring as the system approaches hypoxic conditions.

The range in k observed in the Grand River (3.6 to 8.6 d^{-1}) is well within ranges measured in other similarly sized rivers. Wilcock (1988) found k values of 6.34 to 8.54 d^{-1} obtained from gas tracer experiments for a river with mean annual discharge and velocity of 30 $m^3\ s^{-1}$, and 0.8 m s^{-1}. Using the isotopic approach similar to the present study, Venkiteswaran et al. (2007) reported a k value of 3.96 d^{-1} in the South Saskatchewan River, which was characterized as having a mean depth of 0.65 m and mean velocity of 0.21 m s^{-1}. O'Connor

and Dobbins (1956) estimated re-aeration k values ranging from 0.03 to 4.8 d^{-1} in rivers with mean depths of 0.27 to 11 m, where shallower rivers exhibited greater k values.

The relatively constant nature of k in the Grand River is likely due to the shape of the river channel, which tends to be rectangular with a relatively flat bottom along the main channel at all three locations. As discharge rates increase, both mean depth and velocity increased at similar rates (Figures 4.5 and 4.6); increases in depth and velocity would effectively cancel one another, since k tends to be proportional to velocity divided by depth (Melching and Flores, 1999). A mean depth and velocity dependant equation specific to Grand River conditions is inappropriate as there was not a strong relationship between k and hydrologic conditions (Figure 4.8 and 4.9). Other studies that have derived an empirical predictive k equation have analyzed data sets covering k values in various settings that range by two to three orders of magnitude (Bowie et al., 1985). The variation in k for the Grand River is relatively small and not very changeable under the hydrologic conditions used during this study. Genereux and Hemond (1992) measured k in a first order stream using a petroleum gaseous tracer technique, and found that measured k was relatively constant with increases in flow. Melching and Flores (1999) have also noted no relationship between k and discharge in a data set complied of 493 reaches in 166 streams across the U.S that exhibited discharges from <0.01 to >100 m^3 s^{-1}.

Of the empirical equations, the O'Connor and Dobbins (1958) equation provided best fit to the k obtained from isotope modeling. O'Connor and Dobbins (1958) developed a theoretical equation, based on fundamental turbulence parameters, and tested it over a wide range of depth and velocity conditions. As a result, the equation tends to have the widest

applicability for a range of flow conditions, although it is most appropriate for moderate to deep streams with moderate to low velocities (Chapra, 1997). Bennett and Rathburn (1972) also found that O'Connor and Dobbins (1958) was the formula that best fit the entire range of existing gas transfer data sets that they reviewed, and the Churchill et al. (1962) formula provided the best fit to natural stream data. The equation subsequently developed by Bennett and Rathburn (1972) was a result of re-analyzing data collected from the literature.

Overall, k values obtained in the present study were lower than predicted using hydrology-dependant empirical equations. Rathburn (1977) has also noted that there is a tendency for k values calculated from empirical equations to be larger than observed values obtained by tracer techniques. The discrepancy was partially attributed to possible effects of wind or substances in a stream (e.g, detergents, pollutants from sewage treatment plants). The Grand River receives nutrient loading from both point and non-point sources along the main channel at both locations studied, has a very high macrophyte biomass, and is considered to be a highly impacted system, possibly resulting in depressed k coefficients. Parkhurst and Pomeroy (1972) noted that the presence of impurities results in a more stable surface film, thus reducing turbulence at the surface. The effect is a decrease in k as compared to pure water. The authors cited research conducted by Kehr (1938) which showed that sewage additions as low as 0.5 % to tap water reduced k by 10 %. In addition, there can be a substantial amount of variability when comparing observed to calculated k values associated with k-estimation equations. The standard error of estimate was reported to range from 44 to 61% when comparing equation estimates developed by Melching and Flores (1999) to direct k results from tracer-gas techniques. Rathburn (1977) reported standard errors of estimate ranging from 3.0 to 7.2 d^{-1} when comparing results using the equations addressed in the current study (Table

4.4) to tracer derived estimates, using a composite of results of five US rivers. Churchill et al. (1962) had the lowest error, followed by O'Connor and Dobbins (1958), Bennett and Rathburn (1972), and Owens et al. (1964).

The night-time regression technique (Odum and Hoskin, 1958) was in closest agreement with model derived k using DO and $\delta^{18}O\text{-}O_2$. That method directly uses DO concentration to derive k, which differs from the other literature approaches that rely on hydrologic parameters to predict the rate of gas transfer. Discrepancy between the k found by regression and the isotope technique are likely due to factors such as assumptions of constant CR and k, as well as error that would occur in averaging DO deficit and the change in DO over large time steps when performing the regression. The isotopic approach accounts for changes in temperature when fitting the input parameters. It is not surprising that a simple regression of DO rate of change and magnitude of undersaturation would result in a k different than that obtained using dynamic model calibration. The water temperature in the Grand River was not constant, resulting in varying DO_{sat} conditions and CR rates during the regression time periods. The temperature declined by between 0.8 to 4.7 C during a given night-time sampling event, with an average decline of 2.7 C. A decline in 2.7 C corresponds to a change in DOsat of approximately 0.5 mg L^{-1}, and a change in CR of about 1.6 mg O_2 L^{-1} d^{-1} (given a mean CR rate of 24 mg O_2 L^{-1} d^{-1}). This variation may be enough to cause a change in k estimation using a regression technique which would rely on constant DOsat and CR for accurate prediction. In addition, Odum and Hoskin (1958) used hourly DO concentration data to obtain estimates of k, CR, and GPP. Data of this resolution were only available for the WM August 15, 2003 sampling event.

In theory, night-time regression should predict an accurate k, based on the DO deficit and dDO/dt under steady state CR, temperature, and k conditions. In order to test this, DO concentration data were generated for 15 minute time steps using STELLA 7.0.2, assuming the conditions present for the BLR August 30, 2004 sampling event. Community respiration was assumed to be 38.2 mg O_2 L^{-1} d^{-1} at 20 C, k was set to 7.2 d^{-1} at 20 C (mean k = 7.1 d^{-1} under modeled temperature conditions), the initial DO concentration was 4.52 mg L^{-1}, and temperature declined from 20 to 18.8 C during the model run. Night-time regression of the generated DO data resulted in a calculated k of 8.8 d^{-1}, which was 1.6 d^{-1} greater than the theoretical k (Figure 4.11). The model was also run assuming a constant T of 19.4 C, which resulted in a k of 7.2 d^{-1} calculated from the night-time regression that matched the theoretical k used to simulate DO changes (Figure 4.12). The regression results were also similarly matched to the theoretical values when only hourly data points were used (Figure 4.13).

The DO concentration only declined by 0.5 mg L^{-1} during the model run under the assumed BLR conditions. To examine the ability of night-time regression to predict k under more dynamic DO decline, DO concentration data was generated to simulate the WM August 13 to 14, 2003, sampling event. The initial DO concentration was set at 7.8 mg L^{-1}, with temperatures declining from 24.9 to 21.1 C over the model run. Community respiration was assumed to be 20.6 mg L^{-1} d^{-1} at 20 C, and k was set to 6.7 d^{-1} at 20C (mean k = 7.2 d^{-1} under modeled temperature conditions). Night-time regression of the generated DO data resulted in a calculated k_{20} of 8.3 d^{-1}, which was 1.1 d^{-1} greater than the theoretical k (Figure 4.14) similar to the BLR trial. The model was re-run assuming a constant T of 22.7 C, which resulting a calculated k of 7.0 d^{-1}, in closer agreement to the theoretical value (Figure 4.15).

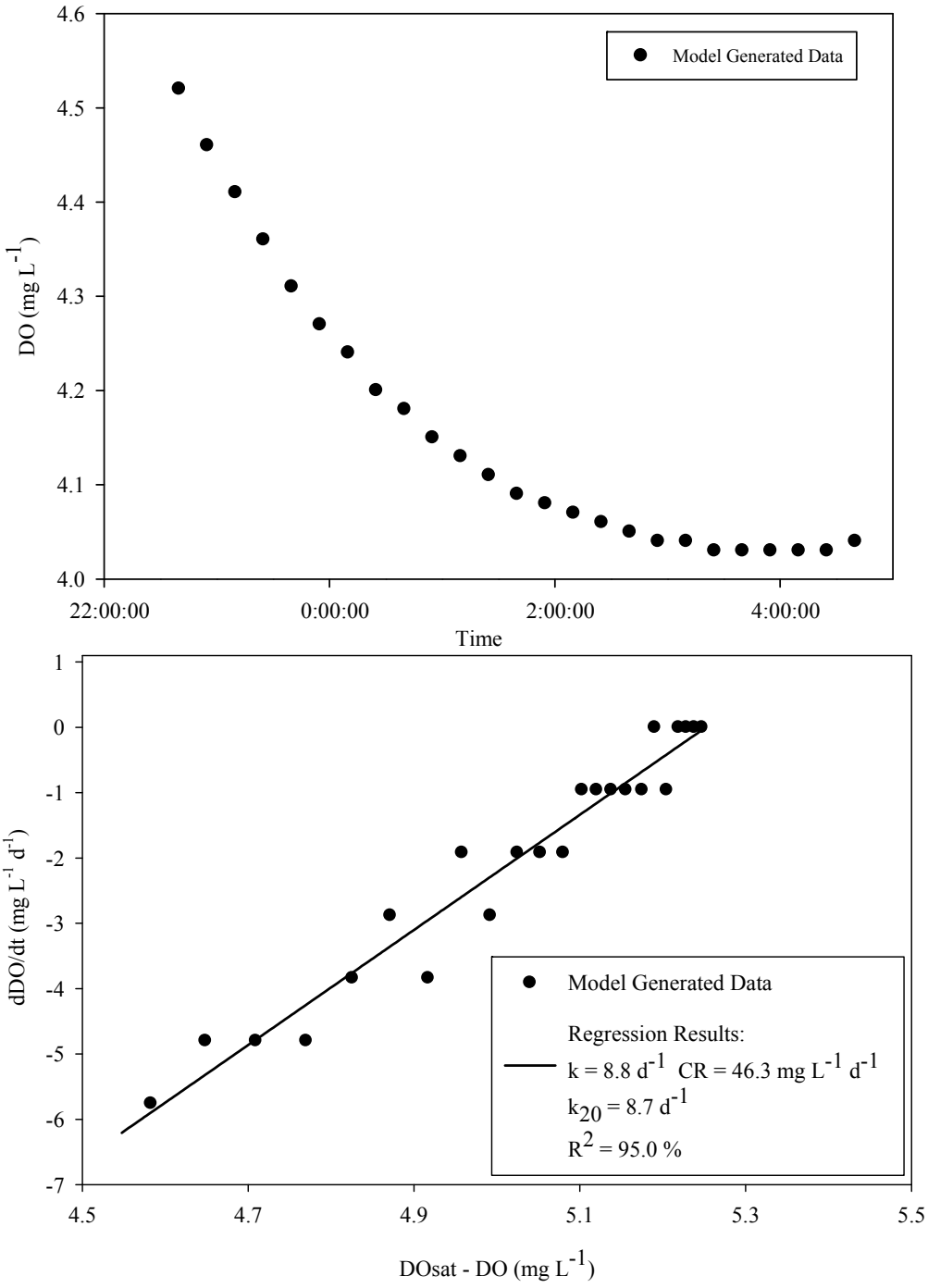

Figure 4.11 Night-time regression results from model generated data representative of the BLR August 30, 2004 sampling event conditions. The theoretical value of k was set to 7.2 d^{-1} (k_{20} = 7.1 d^{-1}), with a mean CR of 37.2 mg O_2 L^{-1} d^{-1} (CR_{20} = 38.2 mg O_2 L^{-1} d^{-1}), with temperature conditions measured during the August 30, 2004 event.

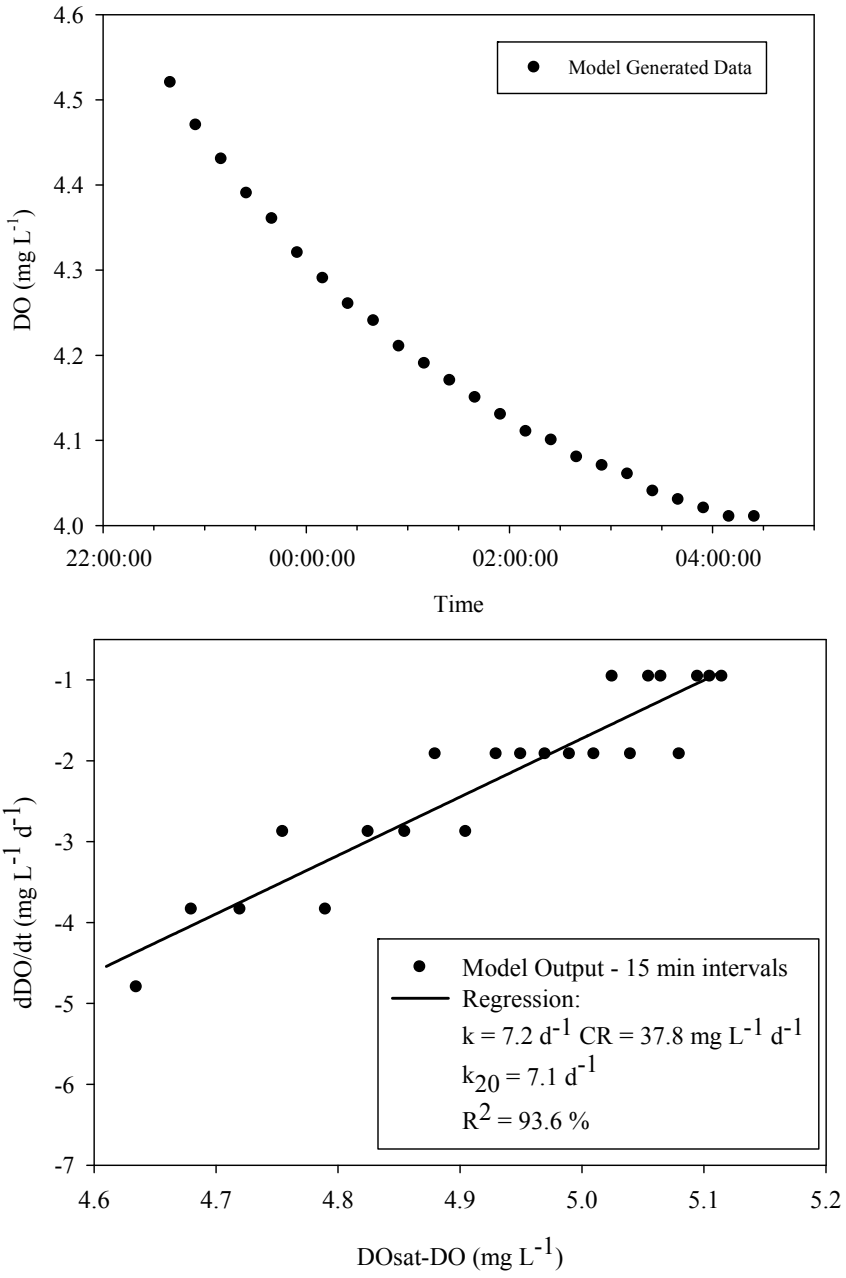

Figure 4.12 Night-time regression results from model generated data representative of the BLR August 30, 2004 sampling event conditions, where mean CR = 37.2 mg O_2 L^{-1} d^{-1} (CR_{20} = 38.2 mg O_2 L^{-1} d^{-1}) and k of 7.2 d^{-1} , but assuming a constant temperature of 19.4 C.

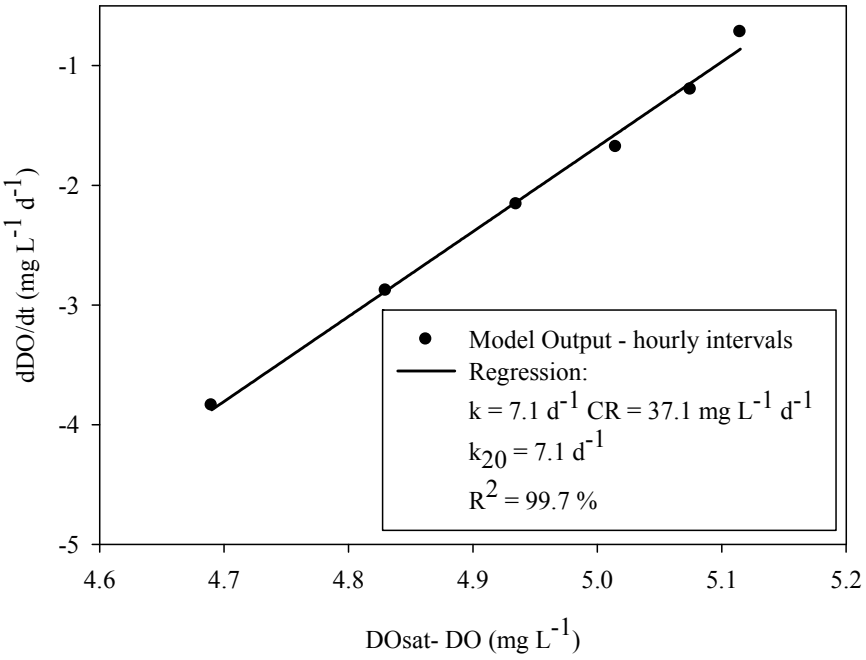

Figure 4.13 Night-time regression results from model generated hourly data representative of the BLR August 30, 2004 sampling event conditions, where mean CR = 37.2 mg O_2 L^{-1} d^{-1} (CR_{20} = 38.2 mg O_2 L^{-1} d^{-1}) and k of 7.2 d^{-1}, and assuming a constant temperature of 19.4 C.

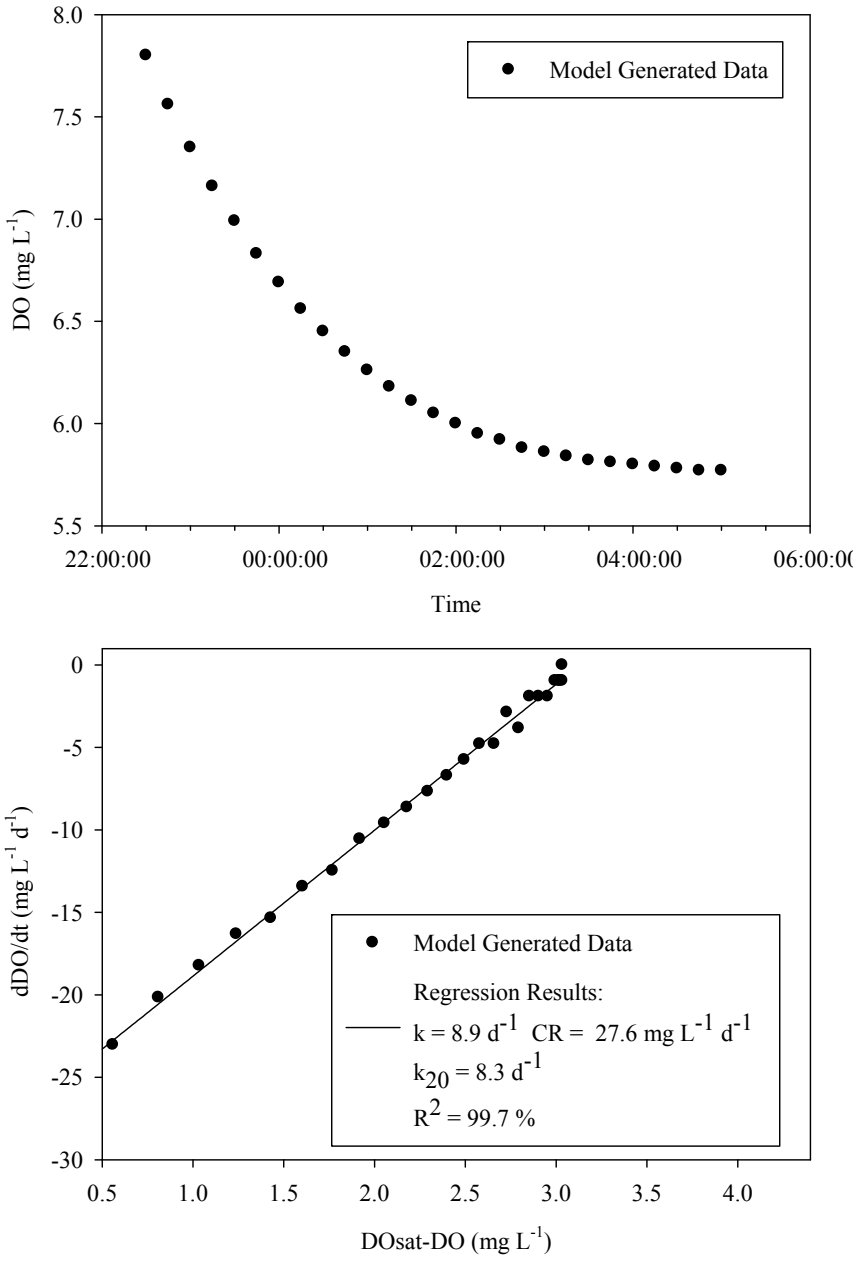

Figure 4.14 Night-time regression results from model generated data representative of the WM August 13, 2003 sampling event conditions. The theoretical value of k was set to 7.2 d^{-1} (k_{20} = 6.7 d^{-1}), with a mean CR of 23.4 mg O_2 L^{-1} d^{-1} (CR_{20} = 20.6 mg O_2 L^{-1} d^{-1}), with temperature conditions measured during the August 13, 2003 event.

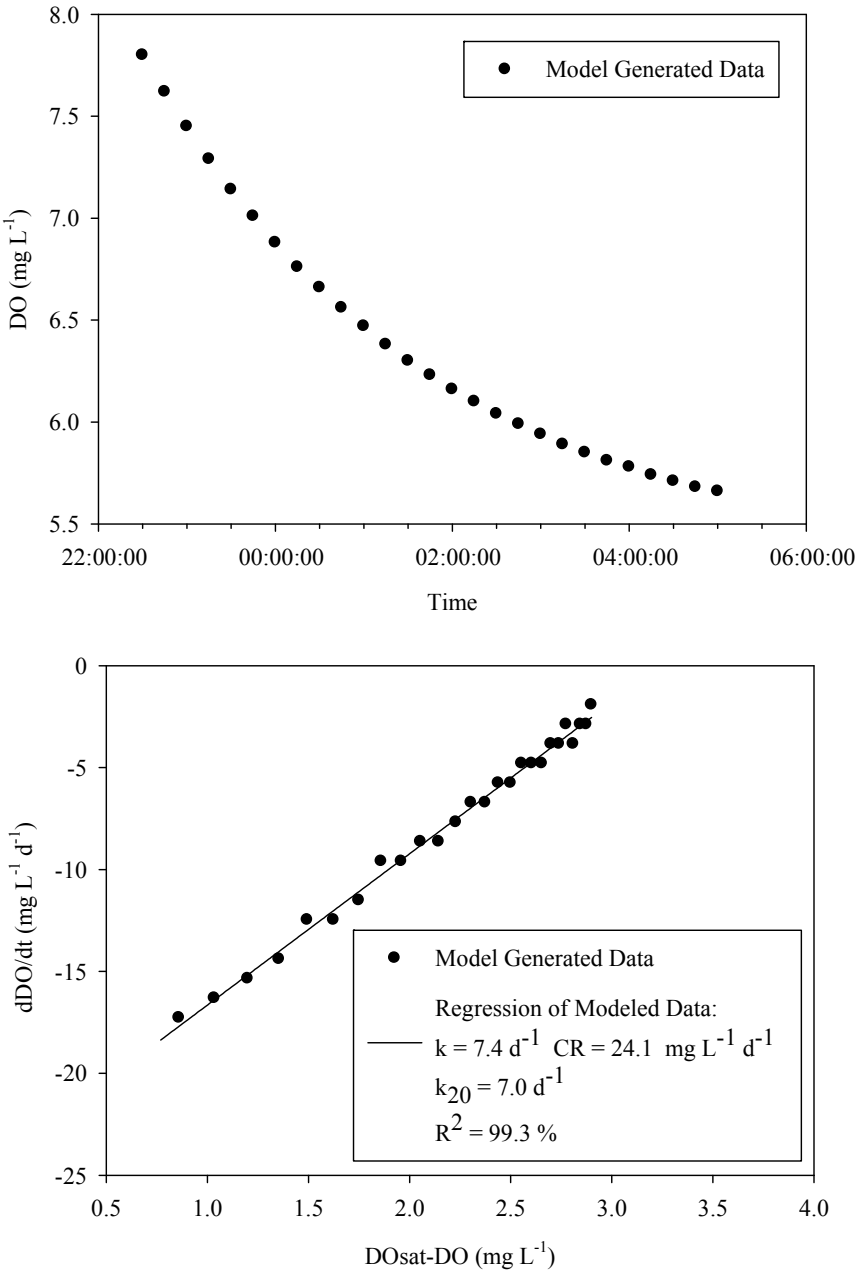

Figure 4.15 Night-time regression results from model generated data representative of the WM August 13, 2003 sampling event conditions, where mean CR = 23.2 mg O_2 L^{-1} d^{-1} (CR_{20} = 20.6 mg O_2 L^{-1} d^{-1}) and k of 7.2 d^{-1}, and assuming a constant temperature of 22.7 C.

Changes in temperature over the regression time period appear to cause a consistent over-prediction in k using the night-time regression versus the isotopic model. In the BLR and WM simulation trials above, the over-prediction was 1.6 and 1.1 d^{-1}, which is similar to the average over-prediction of night-time regressed k compared to isotope model derived k obtained from the sampling events (Table 4.4). This suggests that the k values estimated from the isotope modeling are likely representative of *in situ* conditions and that the deviation from night-time regression estimates lies in: 1) the paucity of data points collected to perform night-time regression analyses and 2) the varying temperature.

Overall, k values obtained with the isotope model for the Grand River were found to be 1) relatively constant, 2) not dependent on hydrologic conditions, and 3) lower than predicted by the other approaches evaluated, highlighting the importance of determining site-specific values of k, as opposed to relying on empirical equations derived from other river systems. The potential over-estimation of k in large, impacted rivers should be taken into consideration when making management decisions, as it could lead to error in respiration estimates, and under-prediction of DO deficits. For example, using an overestimate of k would predict a higher concentration of DO at night; sensitivity analysis in Chapter 2 indicated that an increase in k of 4 d^{-1} resulted in an increase in the DO minimum by about 1 mg L^{-1} under CR and GPP conditions typical of the Grand River. Accurately predicting k is essential for assessing the capacity of a river to assimilate DO demands and ensure adequate concentrations to support aerobic organisms. The non-steady state isotope modeling technique appears to offer an advantage in simulating dynamic changes in O_2 regime as compared to traditional regression techniques due to account made for changes in temperature conditions. The fitted model outputs were able to explain the changes in both DO and ^{18}O-O_2. The addition of the isotopic

mass balance to the DO concentration model provided a constraint on the potential range of model parameters that could generate a particular DO pattern, allowing for the selection of parameters that optimize the fit of both models to the observed field data.

The gas transfer coefficients ranged from 3.6 to 8.6 day^{-1}, over discharges mainly ranging from 5.6 to 22.4 with one high-flow event of 73.1 m^3s^{-1}. The k values were relatively constant over the range of discharge conditions studied. The range in discharge observed is mainly representative of non-storm and summer low-flow events; a greater range in k might be observed under a wider range of hydrologic conditions. However, from a water quality management perspective, low-flow conditions are the times of highest concern where gas transfer would be a key factor in mitigating DO deficits due to O_2 demands.

5.0 Characterization of Dissolved Oxygen Dynamics in the Grand River

5.1 Introduction

Primary production and respiration are key factors determining ecosystem biomass and are the central regulators of nutrient cycling in aquatic environments on both local and regional scales (Bott et al., 1985; Mulholland et al., 2001; Tobias et al., 2007). Gross primary production (GPP) is the organic matter produced within an ecosystem, while community respiration (CR) is indicative of all DO consuming reactions from both authochthonous (within ecosystem) and allochthonous (outside ecosystem) influences (Mulholland et al., 2001). Quantification of DO mass balance components are integral for the development of river management strategies, and to understand the functioning of the river system. From a river ecology perspective, much of the research focus has been centred on the structure and functioning of relatively unimpacted rivers and streams. In order to assess the effects of anthropogenic impacts on the structure and functioning of running waters, more information is needed on the response of systems impacted by organic and inorganic inputs, and flow regulation.

Previous reach and watershed-scale investigations of river metabolism have been primarily based on Odum's (1956) initial work, where GPP and CR have been estimated by monitoring changes in DO, accounting for the transfer of DO between the water column and the atmosphere via gas exchange (Marzolf et al., 1994; Edwards and Meyer, 1987; Mulholland et al., 2001). The study of DO dynamics in aquatic ecosystems has recently incorporated the use stable isotopes of O_2 in the measurement of metabolism rates. Previous to Tobias et al. (2007) and Venkiteswaran et al. (2007), the focus was on using the $\delta^{18}O$-O_2 technique to determine P:R under steady state assumptions (Quay et al., 1995; Russ et al., 2004; Parker et

al., 2005). Impacted waters, such as the Grand River, often exhibit strong diel fluctuations in DO concentrations, requiring a non-steady state modeling approach. The objective of this chapter is to examine watershed-scale community metabolism along a longitudinal gradient in the Grand River, obtained by dual mass balance approach using DO concentration and the stable isotopes of O_2.

5.2 Methods

Field data from the three sampling locations, WM, BRPT, and BLR, were collected and subjected to the diel and day-time modeling procedures as outlined in sections 2.2, 2.3, and 2.4. The resultant optimal model fits were compared to observed data to calculate associated RMS and coefficients of determination (R^2) as descriptors of goodness of model fit. The first data point in a given model event was not included in RMS or R^2 calculations as these values were used to initialize the model. Coefficients of determination were not calculated for the daytime model events due the low number of data points. The associated hydrologic data collection and calculations that were used to estimate mean depth are outlined in Chapter 4. All statistical analyses were performed using Minitab 15 Statistical Software (2007).

5.3 Results

5.3.1 Modeled and Observed Data

The $\delta^{18}O\text{-}O_2$ signature varied inversely with the DO concentrations (Figures 5.1 through 5.8). Greatest DO concentrations were measured in the mid afternoon, a few hours after solar noon, where the time lag was likely associated with levels of gas exchange (Chapra and Di Toro, 1991). At WM and BLR, DO maximums occurred approximately 2-2.5 h after solar noon and exhibit similar k values (Chapter 4). Time lags at BRPT were longer, about 3-3.5 h, and this site also exhibited lower k values which agrees with Chapra and Di Toro's (1991) theory that lag time increases at lower k. Dissolved O_2 concentrations in the Grand River ranged from approximately 1.2 to 15 mg L^{-1}, while the $\delta^{18}O\text{-}O_2$ trended between 10 and 30 ‰. The model, on average, was in good agreement with observed DO concentrations where RMS values for all modeling events were ≤ 0.72 mg L^{-1} and R^2 were $\geq 93\%$ for the diel models (Table 5.1). The model outputs were in poorer agreement with observed $\delta^{18}O\text{-}O_2$, with RMS values ranging from 0.03 to 4.35 ‰ (mean=1.6 ‰) and R^2 were between 56 and 97% (mean= 83%) for the diel models (Table 5.1).

The poorest fits appear to be associated with the diel sampling events, where the $\delta^{18}O\text{-}O_2$ appeared to be underestimated during the day, and overestimated at night (e.g., Figs.5.1, 5.3, and 5.3). Rates of CR_{20} are assumed to be constant and only temperature corrections are applied over a given modelling event. Overall poorer fits for $\delta^{18}O\text{-}O_2$, are likely due to uncertainty associated with input parameters, potential error with assuming constant values of CR_{20} and α_r over a modelling time period, compounded by the greater sensitivity of $\delta^{18}O\text{-}O_2$ to the input parameters as noted in Chapter 4. In addition, the model assumes that GPP follows a

sinusoidal curve and does not account for cloud cover. Variability in CR beyond the temperature corrections, and changes in α_r within the diel cycle, would lead to deviations from the modeled values. The potential variability of α_r is addressed in more detail in Chapter 6. The $\delta^{18}O\text{-}O_2$ simulated by the model on at BLR on July 9, 2003 (Figure 5.3) exhibited a relatively extreme plateau, which coincided with an anomalously low DO minimum at BLR location on that date, less than 1.5 mg L^{-1}. The CR rate on this date was also elevated compared to sampling occasions. Values for $\delta^{18}O\text{-}O_2$ could not be quantified, due to the low concentration of DO, and the model was likely unable to describe the changes in $\delta^{18}O\text{-}O_2$ under extremely low DO conditions, as it assumes constant CR_{20} and α_r despite very low DO concentrations.

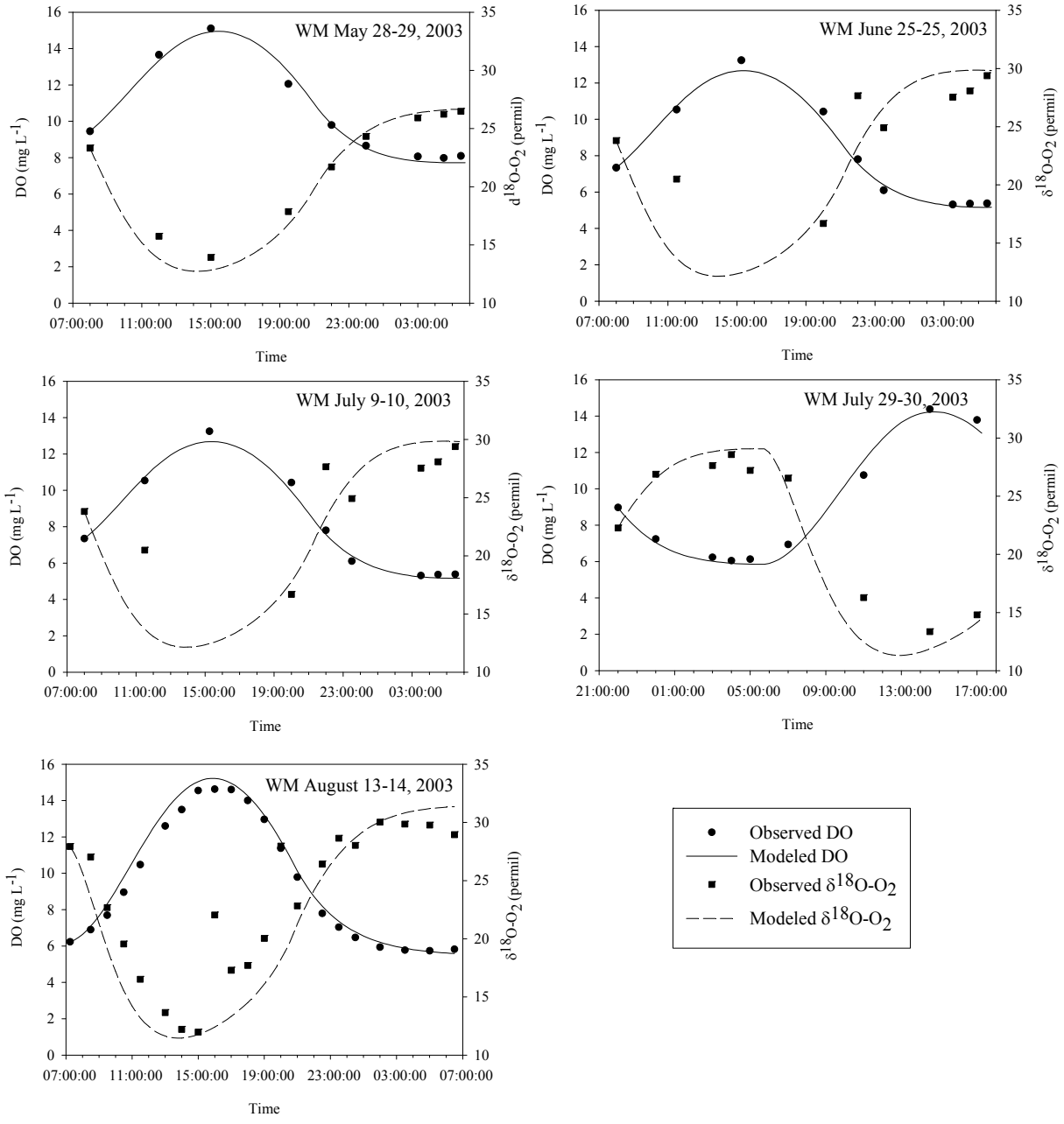

Figure 5.1 Best fit model output and observed data for the diel sampling events at the WM location.

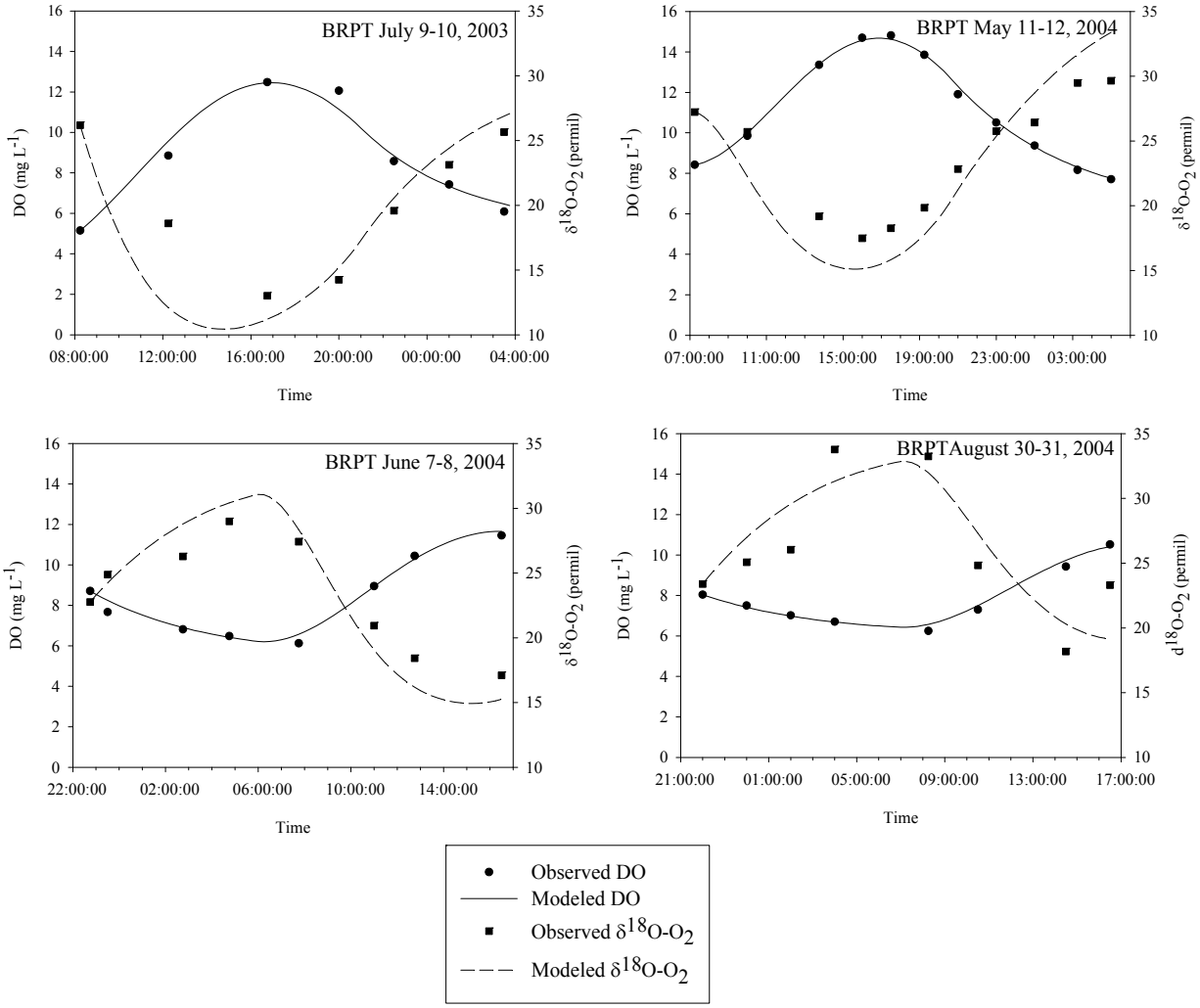

Figure 5.2 Best fit model output and observed data for the diel sampling events at the BPRT location.

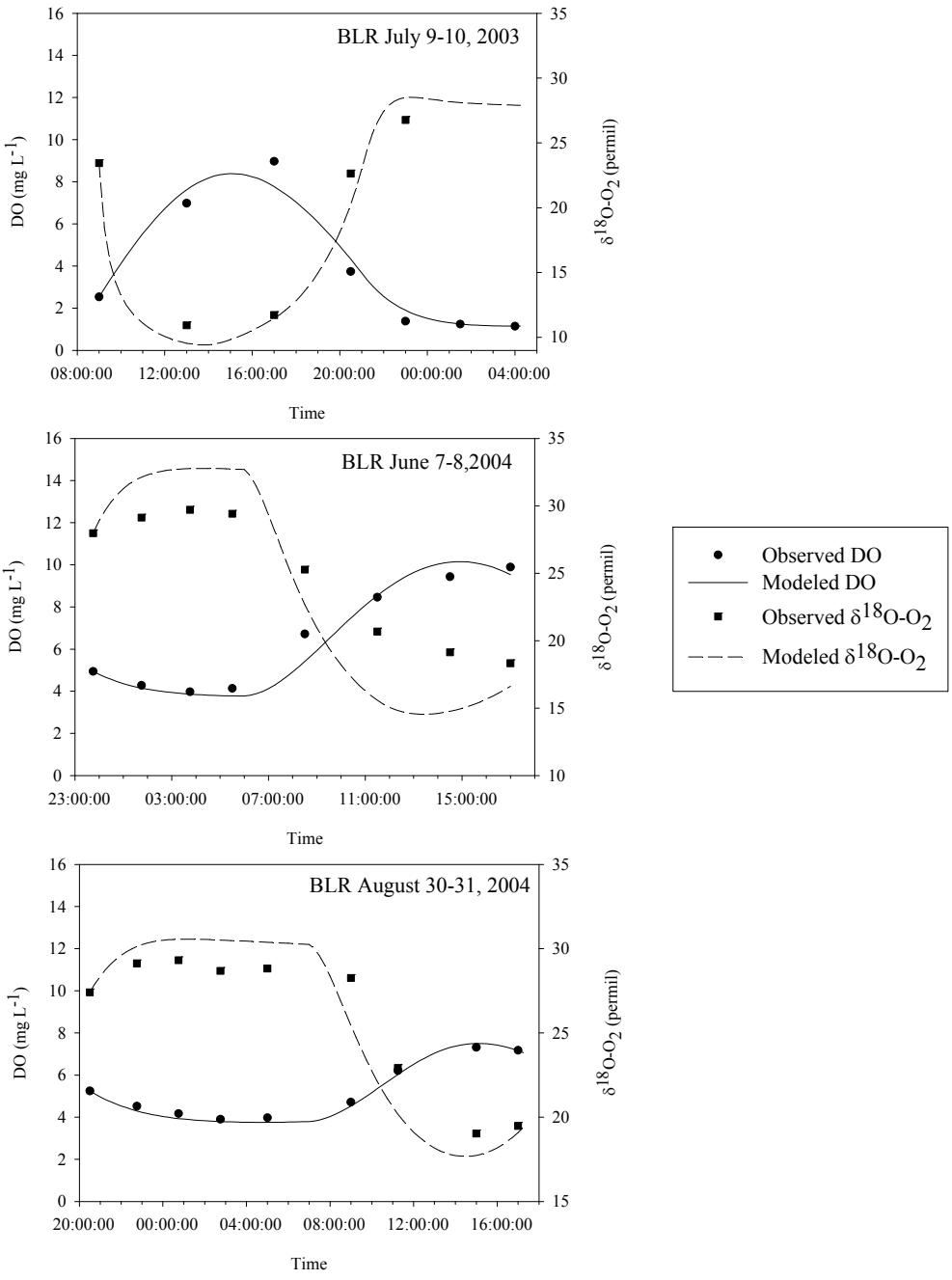

Figure 5.3 Best fit model output and observed data for the diel sampling events at the BLR location.

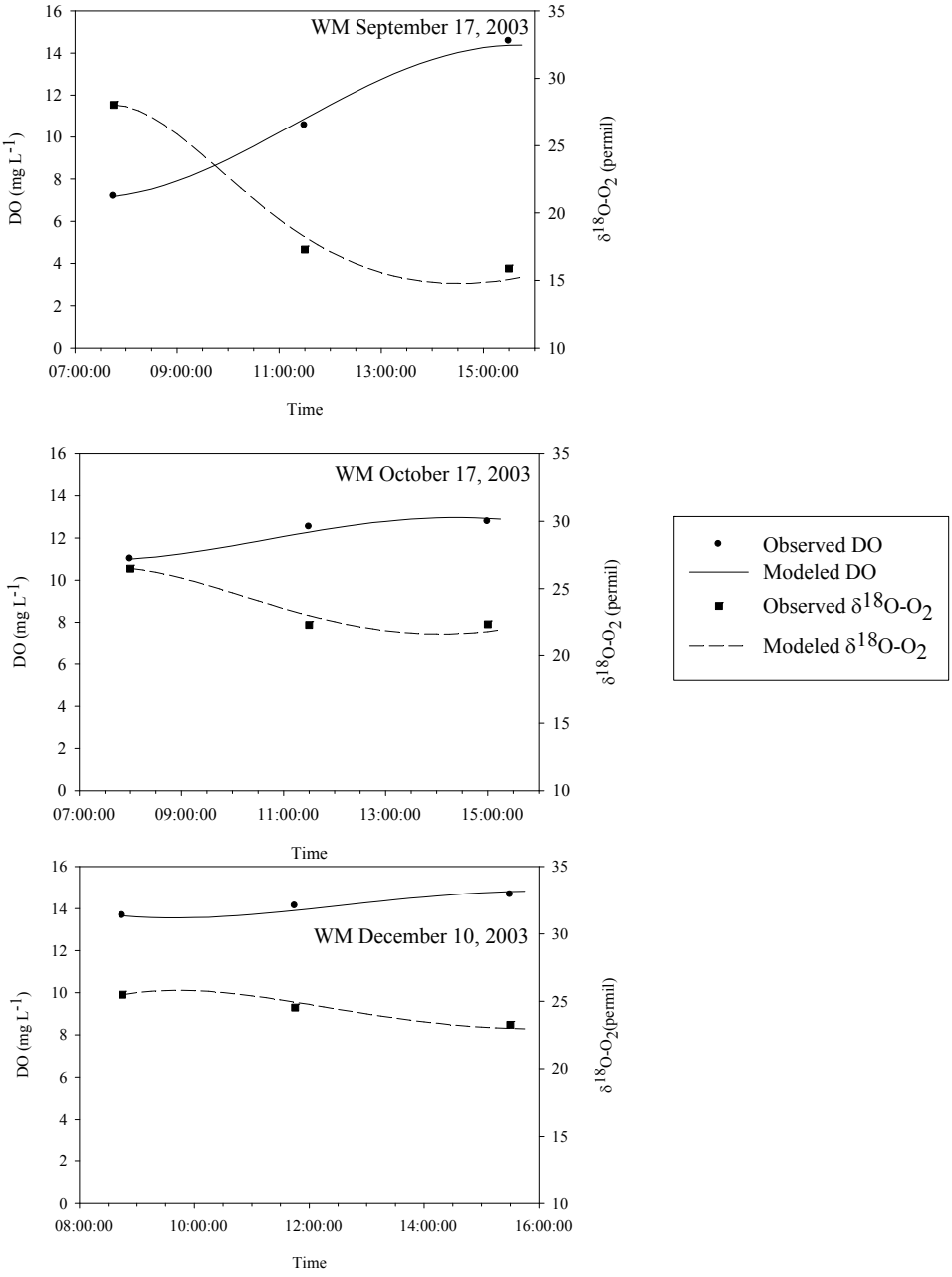

Figure 5.4 Best fit model output and observed data for the 2003 routine day time sampling events at the WM location.

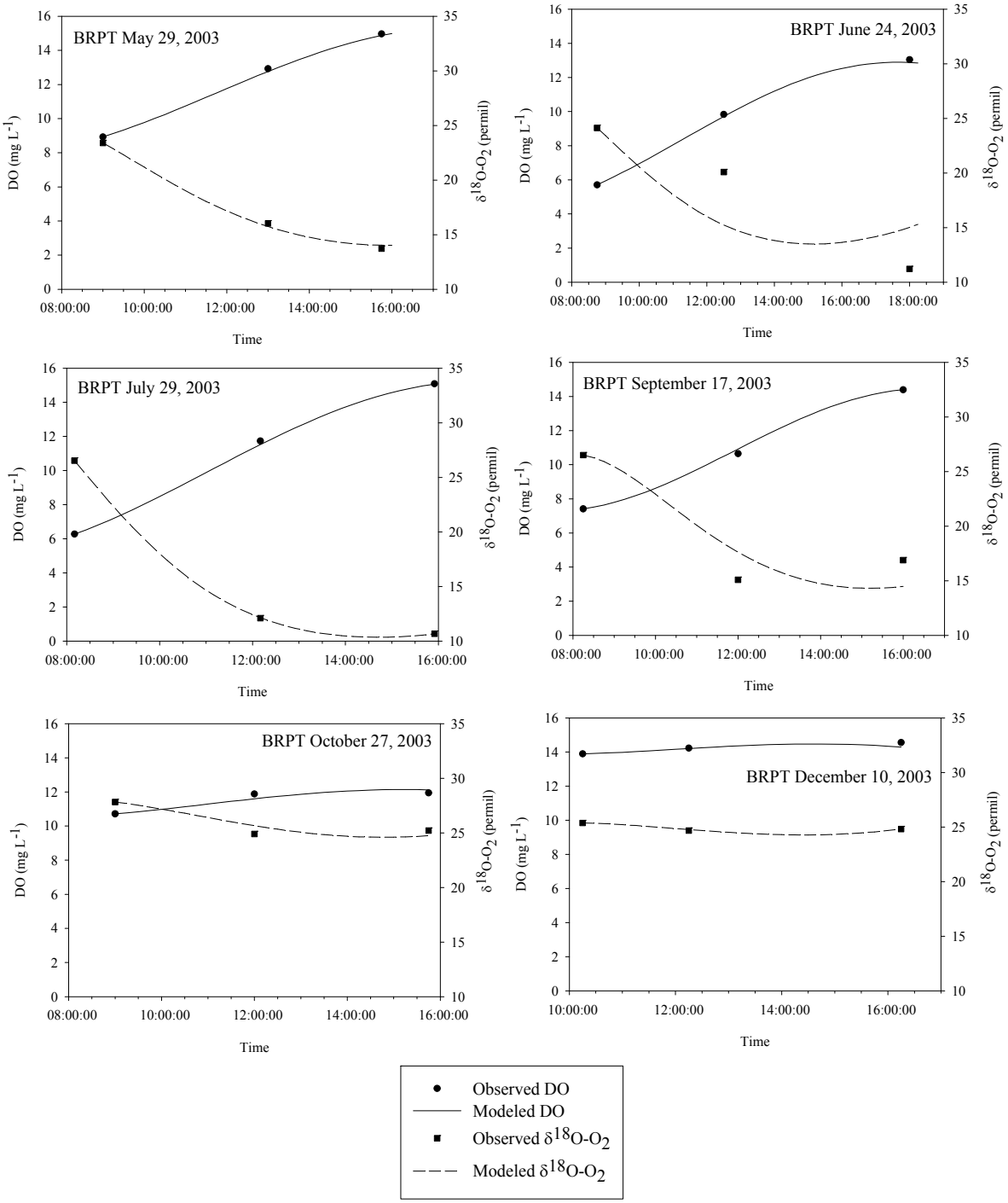

Figure 5.5 Best fit model output and observed data for the 2003 routine day time sampling events at the BRPT location.

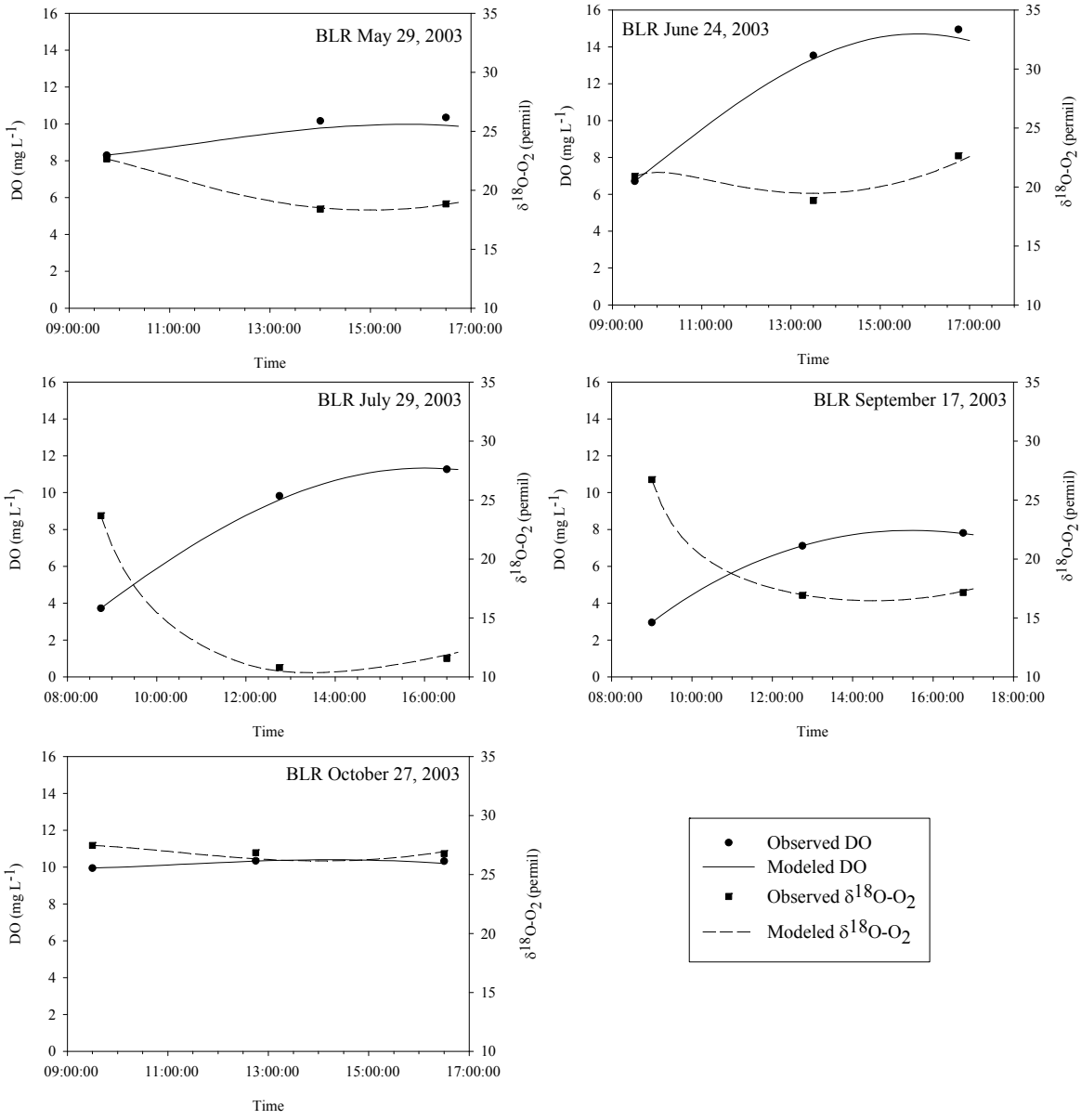

Figure 5.6 Best fit model output and observed data for the 2003 routine day time sampling events at the BLR location.

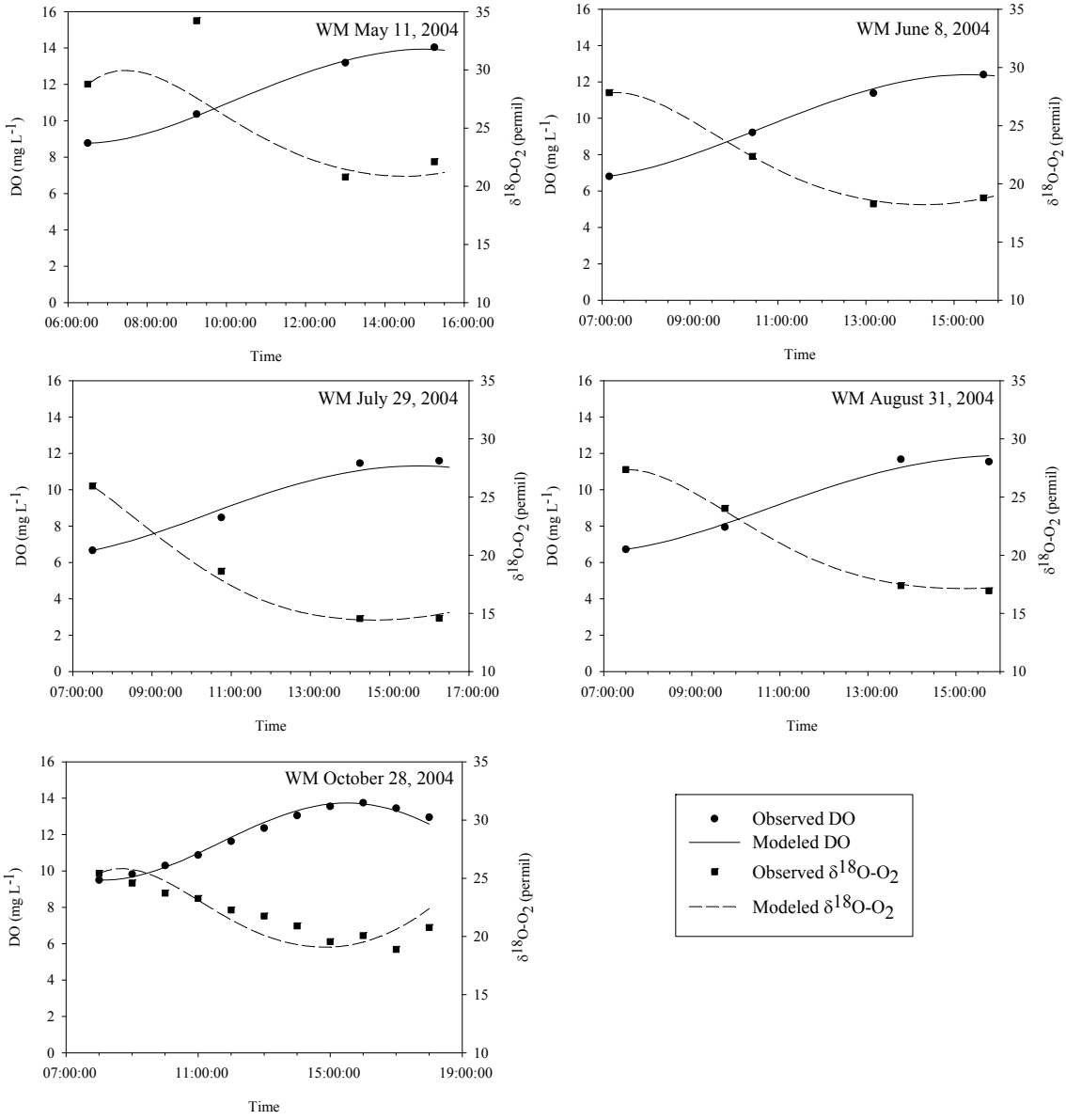

Figure 5.7 Best fit model output and observed data for the 2004 routine day time sampling events at the WM location.

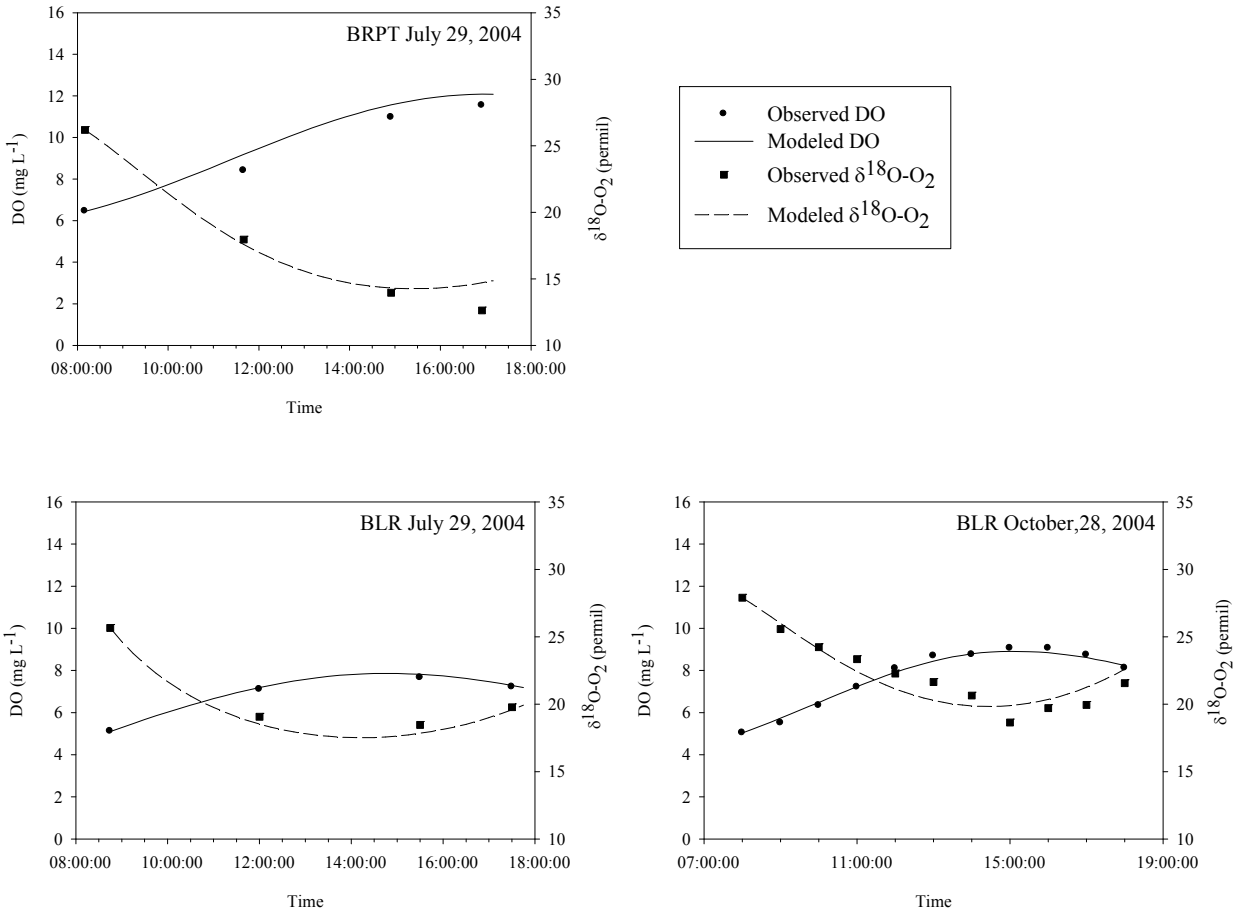

Figure 5.8 Best fit model output and observed data for the 2004 routine day time sampling events at the BPRT and BLR locations.

Table 5.1 Best fit model input parameters, and associated model fit statistics for each sampling event.

Location	Date	DO RMS (mg L^{-1})	DO R^2 (%)	$\delta^{18}O$-O_2 RMS (‰)	$\delta^{18}O$-O_2 R^2 (%)	k_{20} (h^{-1})	R_{20} (mg O_2 L^{-1} h^{-1})	P_{max} (mg O_2 L^{-1} h^{-1})	α_r
WM	May 28, 2003*	0.33	98.6	0.92	97.3	0.31	0.95	2.60	0.987
	Jun 24, 2003*	0.32	99.1	3.11	55.6	0.25	0.89	2.60	0.984
	Jul 9, 2003*	0.33	98.9	2.83	85.9	0.20	0.75	2.50	0.981
	Jul 29, 2003*	0.41	98.7	1.71	94.6	0.29	0.96	3.20	0.984
	Aug13, 2003*	0.50	99.4	3.87	80.1	0.27	0.86	3.60	0.978
	Sept 17, 2003	0.27		0.87		0.22	0.74	2.50	0.964
	Oct 27, 2003	0.20		0.61		0.36	0.82	1.00	0.964
	Dec 10, 2003	0.18		0.34		0.41	0.82	1.00	0.942
	May 11, 2004	0.11		3.91		0.36	0.80	2.25	0.924
	Jun 8, 2004	0.06		0.08		0.23	1.00	2.25	0.960
	Jul 29, 2004	0.48		0.75		0.20	0.74	1.75	0.982
	Aug 31, 2004	0.11		3.91		0.32	0.92	2.25	0.972
	Oct 28, 2004	0.21		1.21		0.20	0.88	1.50	0.962
BRPT	May 29, 2003	0.13		0.30		0.11	0.55	1.70	0.964
	Jun 24, 2003	0.14		4.35		0.11	0.35	1.70	0.952
	Jul 9, 2003*	0.51	93.8	2.91	76.9	0.15	0.42	1.90	0.983
	Jul 29, 2003	0.15		0.03		0.17	0.43	2.50	0.976
	Sept 17, 2003	0.19		2.47		0.14	0.55	2.10	0.960
	Oct 27, 2003	0.23		0.63		0.20	0.43	0.50	0.948
	Dec 10, 2003	0.19		0.05		0.15	0.51	0.50	0.944
	May 11, 2004*	0.72	99.6	2.60	84.6	0.16	0.58	1.80	0.968
	Jun 7, 2004*	0.30	97.9	1.75	91.1	0.15	0.57	1.70	0.976
	Jul 29, 2004	0.66		1.23		0.11	0.45	1.50	0.970
	Aug 30, 2004*	0.19	98.5	2.72	66.9	0.15	0.48	1.10	0.968
BLR	May 29, 2003	0.41		0.08		0.27	1.80	1.80	0.976
	Jun 24, 2003	0.36		0.56		0.25	1.40	4.20	0.938
	Jul 9, 2003*	0.64	94.9	1.63	95.6	0.35	2.28	3.50	0.993
	Jul 29, 2003	0.15		0.31		0.29	1.00	2.60	0.992
	Sept 17, 2003	0.02		0.10		0.35	1.00	1.00	0.998
	Oct 27, 2003	0.09		0.39		0.27	1.00	0.40	0.970
	Jun 7, 2004*	0.59	95.1	3.46	80.6	0.36	1.80	3.10	0.983
	Jul 29, 2004	0.09		0.43		0.29	1.20	1.40	0.986
	Aug 30, 2004*	0.18	98.8	1.78	88.8	0.30	1.59	1.50	0.987
	Oct 28, 2004	0.16		0.98		0.31	1.40	0.80	0.990

* Diel sampling event

5.3.2 Areal Metabolic Rates in the Grand River

In order to compare the sampling sites over time and to other locations, rates of volumetric CR and GPP (Table 5.1) were multiplied by estimates of mean water depth (Table 5.2) to estimate rates on an areal basis (Table 5.3). The daily CR rates reported in Table 4.3 are representative of rates occurring under the observed water temperatures during which the sampling event was conducted. Gross primary production ranged from 3.3 - 19.9, 2.2 - 17.9, and 2.0 - 15.0 g O_2 m^{-2} d^{-1} at WM, BRPT, and BLR, respectively (Table 5.3). When examining the trends in GPP among the three sites over time (Figure 5.9 and Table 5.4), the GPP ranges are somewhat similar among sites, with the highest rates in the spring/early summer followed by a decline towards the end of the growing season in the autumn.

Community respiration rates (Figure 5.10) were more constant throughout the sampling period, with the exception of an elevated CR rate at BLR in Jul 9, 2003. The measured night-time DO minimum was very low at BLR location on that date, less than 2 mg L^{-1} and lower than the DO minima observed on other sampling occasions, indicating that there may have been anomalously high DO demand during this sampling event. In 2004, there appears to be a slight downward trend in CR from May to November. Rates of CR were overall slightly higher at WM than at BRPT, and BLR exhibited the greatest CR rates (Table 5.4). In 2003, there appears to be less separation of CR on both a spatial and temporal basis. Overall, the CR rates ranged from 4.2-13.8, 4.0-12.7, 7.1-29.6 g O_2 m^{-2} d^{-1} at WM, BRPT, and BLR, respectively (Table 5.3).

Table 5.2 Environmental and hydrologic conditions at each location during sampling events.

Location	Date	Day Length (h)	Incoming Radiation** (W m^{-2} d^{-1})	Mean Temperature	Discharge (m^3s^{-1})	Mean Depth (m)	Mean Velocity (m s^{-1})	$\delta^{18}O$-H_2O (‰)
WM	May 28, 2003*	15.1	229.1	14.1	6.8	0.42	0.50	-11.62
	Jun 24, 2003*	15.4	331.5	21.8	5.6	0.37	0.47	-11.49
	Jul 9, 2003*	15.2	278.8	22.9	6.0	0.39	0.48	-11.53
	Jul 29, 2003*	14.7	293.3	20.6	12.7	0.58	0.63	-11.15
	Aug 13, 2003*	14.2	232.5	23.7	5.6	0.37	0.47	-10.61
	Sept 17, 2003	12.4	214.2	17.7	4.7	0.34	0.44	-9.73
	Oct 27, 2003	10.5	52.5	6.7	8.8	0.48	0.55	-10.11
	Dec 10, 2003	9.0	34.8	2.3	18.1	0.71	0.72	-10.62
	May 11, 2004	14.6	312.4	14.1	31.1	0.95	0.88	-10.90
	Jun 8, 2004	15.3	236.2	19.1	7.9	0.45	0.53	-9.59
	Jul 29, 2004	14.6	238.1	20.8	10.0	0.51	0.58	-9.37
	Aug 31, 2004	13.2	234.1	18.5	9.5	0.50	0.57	-8.81
	Oct 28, 2004	10.4	120.4	9.3	4.4	0.33	0.43	-8.32
BRPT	May 29, 2003	15.1	312.0	14.6	15.3	0.53	0.53	-11.96
	Jun 24, 2003	15.4	331.5	23.8	8.10	0.40	0.41	-11.31
	Jul 9, 2003*	15.2	278.8	25.5	8.20	0.40	0.41	-10.99
	Jul 29, 2003	14.7	293.3	22.1	8.10	0.40	0.41	-11.12
	Sept 17, 2003	12.4	214.2	18.9	8.10	0.40	0.41	-9.70
	Oct 27, 2003	10.5	42.1	6.9	29.6	0.71	0.70	-10.03
	Dec 10, 2003	9.0	34.8	2.3	35.8	0.78	0.75	-10.56
	May 11, 2004*	14.6	312.4	16.6	73.1	1.07	1.01	-10.62
	Jun 7, 2004*	15.3	225.2	21.5	11.7	0.47	0.48	-9.42
	Jul 29, 2004	14.6	238.1	22.0	19.0	0.58	0.58	-9.37
	Aug 30, 2004*	13.2	104.9	19.4	18.7	0.58	0.58	-8.42
BLR	May 29, 2003	15.1	312.0	15.5	22.0	0.46	0.47	-11.08
	Jun 24, 2003	15.4	331.5	25.4	10.1	0.36	0.32	-11.01
	Jul 9, 2003*	15.2	278.8	25.4	14.9	0.41	0.39	-10.60
	Jul 29, 2003	14.7	293.3	23.0	9.2	0.35	0.30	-10.95
	Sept 17, 2003	12.4	214.2	20.0	9.4	0.36	0.31	-9.61
	Oct 27, 2003	10.5	42.1	7.6	33.0	0.52	0.57	-10.02
	Jun 7, 2004*	15.3	225.2	21.7	22.4	0.46	0.47	-9.45
	Jul 29, 2004	14.6	238.1	22.2	21.7	0.46	0.47	-9.44
	Aug 30, 2004*	13.2	104.9	19.9	11.0	0.37	0.33	-8.52
	Oct 28, 2004	10.4	120.4	11.2	11.0	0.37	0.33	-9.03

* Diel sampling event

** Obtained from the University of Waterloo weather station (http://weather.uwaterloo.ca)

Table 5.3 Grand River metabolism parameters from results generated by the fitted models. The rates of GPP, CR, and NP have been calculated on an areal basis.

Location	Date	K_{20} (d^{-1})	α_r	GPP ($g\ O_2\ m^{-2}\ d^{-1}$)	CR ($g\ O_2\ m^{-2}\ d^{-1}$)	NP** ($g\ O_2\ m^{-2}\ d^{-1}$)	P:R
WM	May 28, 2003*	7.44	0.987	10.5	7.5	3.0	1.40
	Jun 24, 2003*	6.00	0.984	9.4	9.0	0.5	1.05
	Jul 9, 2003*	4.80	0.981	9.4	8.1	1.3	1.16
	Jul 29, 2003*	6.96	0.984	17.4	13.7	3.7	1.27
	Aug13, 2003*	6.48	0.978	12.1	7.6	4.4	1.58
	Sept 17, 2003	5.28	0.964	6.7	5.4	1.4	1.25
	Oct 27, 2003	8.64	0.964	4.1	6.2	-2.1	0.66
	Dec 10, 2003	9.84	0.942	4.1	6.2	-2.1	0.66
	May 11, 2004	8.64	0.924	19.9	13.8	6.1	1.45
	Jun 8, 2004	5.52	0.960	9.9	10.1	-0.2	0.98
	Jul 29, 2004	4.80	0.982	8.4	9.6	-1.3	0.87
	Aug 31, 2004	7.68	0.972	9.5	10.2	-0.8	0.93
	Oct 28, 2004	4.80	0.962	3.3	4.2	-1.0	0.77
BRPT	May 29, 2003	2.64	0.964	8.6	5.5	3.2	1.58
	Jun 24, 2003	2.64	0.952	6.6	4.1	2.6	1.63
	Jul 9, 2003*	3.60	0.983	7.3	5.2	2.1	1.40
	Jul 29, 2003	4.08	0.976	9.3	4.6	4.7	2.03
	Sept 17, 2003	3.36	0.960	6.6	5.0	1.6	1.33
	Oct 27, 2003	4.80	0.948	2.4	4.0	-1.7	0.59
	Dec 10, 2003	3.60	0.944	2.2	4.2	-2.0	0.53
	May 11, 2004*	3.84	0.968	17.9	12.7	5.2	1.41
	Jun 7, 2004*	3.60	0.976	7.8	6.8	1.0	1.15
	Jul 29, 2004	2.64	0.970	8.2	6.9	1.3	1.19
	Aug 30, 2004*	3.60	0.968	5.4	6.3	-1.0	0.85
BLR	May 29, 2003	6.48	0.976	8.0	16.3	-8.3	0.49
	Jun 24, 2003	6.00	0.938	15.0	14.6	0.4	1.03
	Jul 9, 2003*	8.40	0.993	13.9	29.6	-15.7	0.47
	Jul 29, 2003	6.96	0.992	8.6	9.7	-1.1	0.88
	Sept 17, 2003	8.40	0.998	2.8	8.5	-5.7	0.33
	Oct 27, 2003	6.48	0.970	1.4	7.1	-5.7	0.20
	Jun 7, 2004*	8.64	0.983	13.9	21.3	-7.4	0.65
	Jul 29, 2004	6.96	0.986	6.0	14.8	-8.8	0.41
	Aug 30, 2004*	7.20	0.987	4.7	13.9	-9.2	0.34
	Oct 28, 2004	7.44	0.990	2.0	9.0	-7.1	0.22

* Diel sampling event

** Net Production = GPP – CR

Table 5.4 Site characteristics* associated with each the Grand River sampling locations, along with the descriptive statistics associated with the model-derived metabolism parameter results*.

		WM	BRPT	BLR
Descriptive Statistics (N=9)				
GPP (g O_2 m^{-2} d^{-1})	Mean	9.48	6.91	8.25
	Standard Deviation	3.56	2.07	5.05
	Range	4.1 -17.4	2.4 -9.3	1.4-15
CR (g O_2 m^{-2} d^{-1})	Mean	8.87	5.37	15.1
	Standard Deviation	2.47	1.09	6.96
	Range	5.4-13.7	4-6.9	7.1-29.6
P:R	Mean	1.06	1.3	0.53
	Standard Deviation	0.08	0.14	0.09
	Range	0.2-1.4	0.59-2.04	0.66-1.03
NP (g O_2 m^{-2} d^{-1})	Mean	0.60	1.54	-6.84
	Standard Deviation	1.94	1.97	4.71
	Range	-2.1-3.7	-1.7-4.7	-15.7-0.4
Mean Site Characteristics				
	Discharge (m^3 s^{-1})	8.0	14.1	17.1
	Depth (m)	0.45	0.50	0.42
	Velocity (m s^{-1})	0.53	0.50	0.40
	Temperature (C)	18.0	19.4	20.1
	TN (mg L^{-1})	2.52	3.26	5.24
	TP (mg L^{-1})	0.03	0.03	0.07
	DIC (mg L^{-1})	44.3	45.6	48.7
	DOC (mg L^{-1})	7.96	6.71	6.62

*Data associated with the Aug 13/03, Dec 10/03, May 11/04, and Oct 28/04 sampling events were not included in order to remove bias, as not all of the locations were monitored on each of these dates.

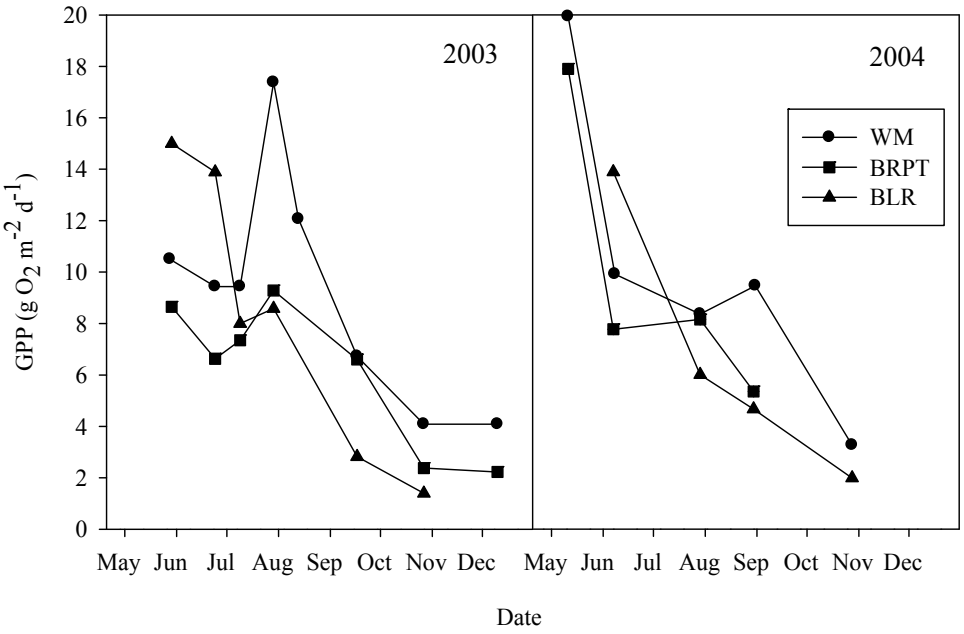

Figure 5.9 Gross primary production rates at each sampling location in the Grand River. Error associated with the estimates is approximately 10% (Chapter 3).

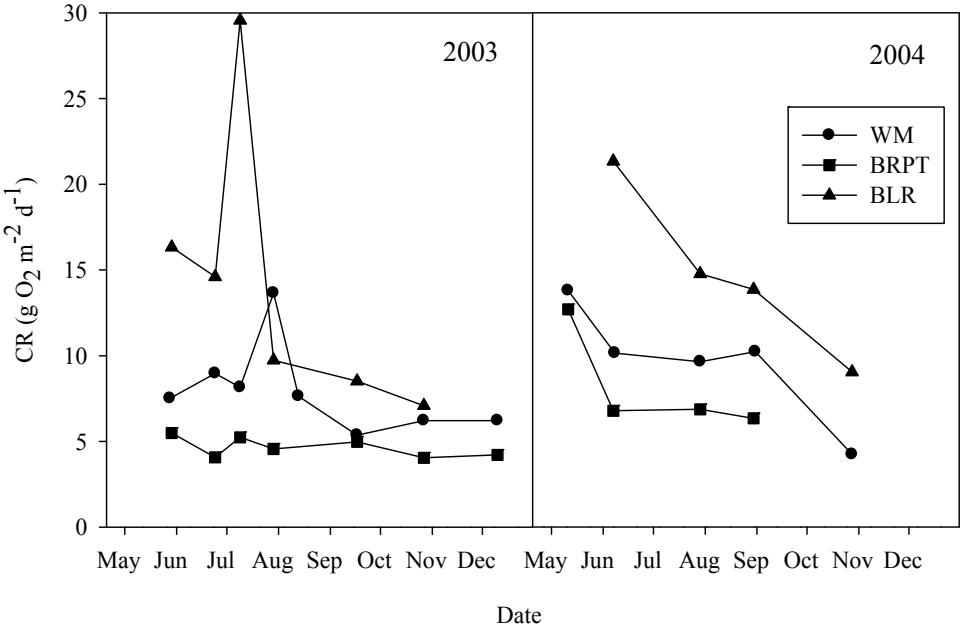

Figure 5.10 Community respiration rates at each sampling location in the Grand River. Error associated with the estimates is approximately 10% (Chapter 3).

Metabolic differences among the three sites are evident in the NP rates (Figure 5.37) and P:R (Figure 5.12) ratios. The ratio of GPP to CR (P:R), first suggested by Odum (1956), has been classically used to describe the trophic status of aquatic systems, based on the relative dominance of autotrophic production introducing DO over the heterotrophic consumption of DO. Net production (NP, calculated as GPP-CR) were also calculated, to use along with P:R, as indices of how the Grand River produces and consumes organic matter. The NP rate is generally indicative of whether the Grand River is acting as a net producer or consumer of organic matter and O_2.

Net production rates at WM and BRPT were similar, with positive rates from May to October 2003 followed by net consumption in the late autumn. In 2004, a similar decreasing trend with time prevailed, but levelled off at a balanced NP from June onward at both WM and BRPT. The Grand River exhibited a seasonal variation in P:R with the highest ratios occurring in the spring and summer, with subsequent declines in the fall. Upstream of the wastewater treatment plants, WM and BRPT exhibited similar trends in P:R with values near 1.0 or above throughout the spring and summer, with declines to less than 1.0 in the fall which coincided with declines in GPP (Figure 5.12).

The P:R was greater in early 2003 than in 2004; this reflects the greater GPP and lower CR rates in early 2003 compared to 2004. At WM and BRPT in 2003, the elevated rates of P:R during the spring and summer indicate that there may have been greater proportion of organic matter that was either being stored or exported from the system.

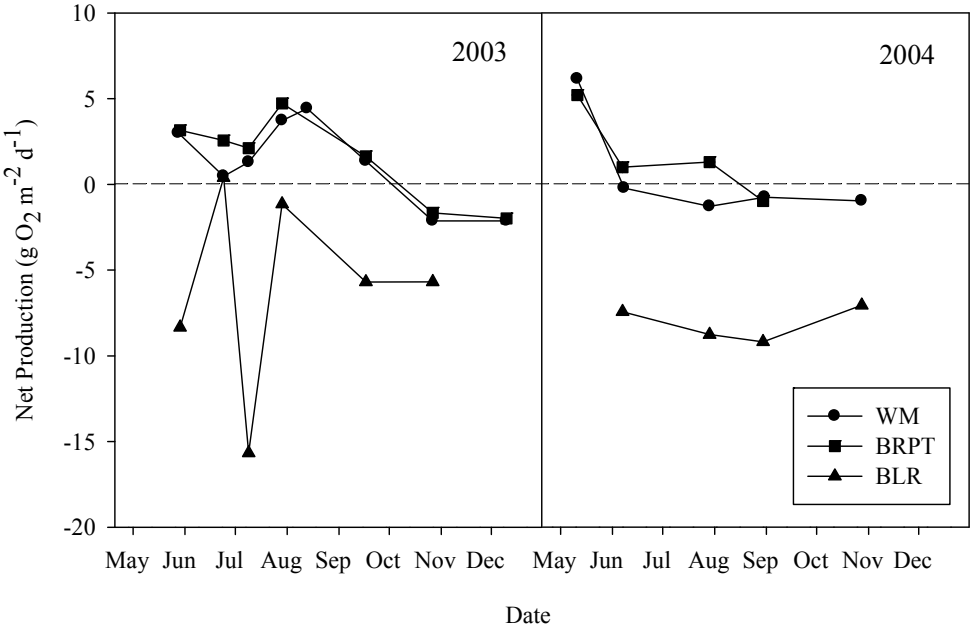

Figure 5.11 Net Production (GPP – CR) at each sampling location in the Grand River.

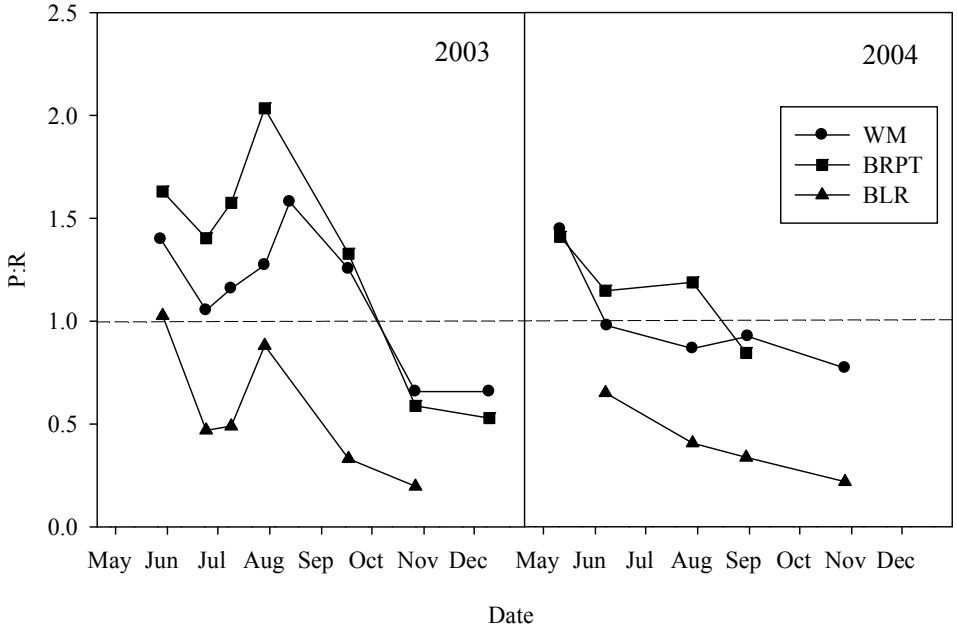

Figure 5.12 P:R at each sampling location in the Grand River.

The BLR location, however, exhibited consistently negative NP rates in both 2003 and 2004, indicating that there is a net consumption of DO at this location. The P:R shows the same relationship, with BLR having a ratio consistently less than 1. As in the NP trends, WM and BRPT have the same temporal trends in P:R, with some positive longitudinal gradient from May to October of 2003.

5.3.3 Factors Relating to Grand River Metabolism

In order to relate the river metabolism rates to physical and environmental factors in the Grand River watershed, GPP, CR, and NP from all sites together were correlated (Table 5.5) with selected water quality parameters, as well as mean temperature, day length, and incoming radiation. Water quality parameters collected (Table 4.6) during sampling events did not include all the nitrogen or phosphorus forms. However, the Ontario Ministry of the Environment oversees a provincial water quality monitoring network (PWQMN), which routinely monitors locations including WM, BPRT, BLR.

The PWQMN data (Table 5.7) did not directly correspond to the modeled sampling events; for correlation purposes, the closest corresponding PWQMN sampling data were used. Gross primary production rates were most highly correlated with day length and incoming radiation (Figures 5.13 and 5.14), which likely explains the seasonal decline in GPP from May to December noted in Figure 5.9. Both GPP and CR were significantly correlated with mean temperature. Community respiration rates exhibited a positive linear relationship with mean daily temperature (Figure 5.15), but the R^2 was only 13%.

Table 5.5 Results of correlation analysis between descriptors of metabolism and selected environmental conditions. The Pearson correlation coefficents are presented with the associated p-values in parentheses (assuming a confidence level of 95%).

	n	GPP ($g\ O_2\ m^{-2}\ d^{-1}$)	CR ($g\ O_2\ m^{-2}\ d^{-1}$)	NP ($g\ O_2\ m^{-2}\ d^{-1}$)	P:R
CR	34	0.549* (0.001)			
NP	34	0.351* (0.042)	-0.590* (<0.001)		
P:R	34	0.512* (0.002)	-0.318 (0.067)	0.851* (<0.001)	
Day length (h)	34	0.681* (<0.001)	0.410* (0.016)	0.198 (0.261)	0.508* (0.002)
Mean Temperature	34	0.480* (0.004)	0.365* (0.034)	0.055 (0.758)	0.380* (0.027)
Incoming Radiation ($W\ m^{-2}\ d^{-1}$)	34	0.715* (<0.001)	0.333 (0.054)	0.318 (0.067)	0.592* (0.002)
Discharge ($m^3\ d^{-1}$)	34	0.218 (0.218)	0.173 (0.328)	0.017 (0.924)	-0.121 (0.496)
Mean Depth (m)	34	0.311 (0.074)	0.019 (0.917)	0.279 (0.109)	0.072 (0.687)
Mean Velocity ($m\ s^{-1}$)	34	0.299 (0.085)	-0.074 (0.676)	0.373* (0.030)	0.142 (0.425)
Water Quality Data Collected During Sampling Events ($mg\ L^{-1}$)					
NO_3-N	25	-0.391 (0.053)	-0.190 (0.364)	-0.135 (0.519)	-0.353 (0.084)
PO_4-P	18	-0.104 (0.680)	0.113 (0.656)	-0.222 (0.376)	-0.183 (0.467)
DIC	28	-0.033 (0.868)	0.057 (0.771)	-0.098 (0.621)	-0.360 (0.060)
DOC	33	0.161 (0.372)	0.003 (0.986)	0.151 (0.401)	0.214 (0.233)
PWQM Water Quality Data ($mg\ L^{-1}$)					
NH_4-N	29	-0.329 (0.082)	0.176 (0.362)	-0.526* (0.003)	-0.329 (0.082)
NO_3-N	29	0.014 (0.944)	0.296 (0.120)	-0.273 (0.153)	0.014 (0.944)
TON	29	-0.156 (0.420)	0.161 (0.403)	-0.325 (0.085)	-0.114 (0.556)
TIN	29	-0.033 (0.865)	0.361 (0.054)	-0.386* (0.038)	-0.298 (0.116)
TN	29	-0.048 (0.806)	0.355 (0.059)	-0.396* (0.033)	-0.291 (0.126)
TP	29	-0.067 (0.730)	0.087 (0.654)	-0.157 (0.417)	0.073 (0.707)

* denotes statistical significance

Table 5.6 Water quality data results collected during sampling events. All parameter values are presented in mg L^{-1}.

Location and Date	NO3-N	PO4-P	DIC	DOC
WM				
May 28, 2003		0.01	38.77	8.42
June 24, 2003	1.81	0.48	51.42	7.98
July 9, 2003	1.61	0.01	40.65	8.71
July 29, 2003		<0.01		8.60
August 13, 2003				8.38
September 17, 2003	4.14	<0.01	42.82	8.09
October 27, 2003				7.36
December 10, 2003	3.45	0.02	55.69	8.31
May 11, 2004	2.27	0.01	53.91	6.39
Jun 8, 2004	2.03	0.04	46.68	
July 29, 2004	1.19	<0.01	44.83	7.58
August 31, 2004	1.26	<0.01	44.77	6.91
October 28, 2004	1.21	0.09	50.21	7.49
BRPT				
May 29, 2003		0.02	40.17	6.34
June 24, 2003	2.04	<0.01	48.68	6.73
July 9, 2003	1.56	0.02	38.68	7.36
July 29, 2003	0.59	<0.01		7.00
September 17, 2003		<0.01	41.49	6.06
October 27, 2003		<0.01	58.86	6.70
December 10, 2003	4.83	0.01	53.38	6.51
May 11, 2004	0.43	0.02	55.36	5.69
June 7, 2004	2.50	<0.01	52.95	6.38
July 29, 2004	1.68	0.18	51.13	6.54
August 30, 2004	1.75	0.01	46.11	7.30
BLR				
May 29, 2003		0.16	44.27	7.06
June 24, 2003	2.55	0.01	51.29	7.00
July 9, 2003	2.04	0.07	43.43	7.90
July 29, 2003	1.32	<0.01		6.95
September 17, 2003		<0.01	44.83	6.23
October 27, 2003		<0.01		5.42
June 7, 2004	0.65	<0.01	53.78	6.29
July 29, 2004			52.16	6.09
August 30, 2004	1.42	0.26	51.37	6.66
October 28, 2004	3.47	0.01	55.03	6.83

Table 5.7 Water quality data obtained from the Ontario Ministry of the Environment Provincial Water Quality Monitoring Network for 2003-2004. All parameters are presented in mg L^{-1}.

Location and Date	NH_4-N	NO_3-N	TON*	TIN***	TN**	TP
WM						
May 12, 2003	0.01	3.69	0.77	3.73	4.49	0.03
June 24, 2003	0.02	1.66	0.85	1.69	2.54	0.02
August 6, 2003	0.01	1.80	0.82	1.83	2.65	0.05
August 12, 2003	0.02	1.78	0.83	1.82	2.65	0.03
September 16, 2003	0.01	0.75	0.76	0.77	1.53	0.02
October 28, 2003	0.01	2.98	0.92	3.00	3.93	0.02
May 12, 2004	0.01	2.65	0.67	2.67	3.35	0.02
June 8, 2004	0.01	1.97	0.81	1.99	2.80	0.02
July 6, 2004	0.02	1.76	0.65	1.79	2.43	0.02
August 10, 2004	0.01	0.99	0.66	1.01	1.67	0.03
September 7, 2004	0.01	0.89	0.61	0.91	1.52	0.02
October 19, 2004	0.01	1.09	0.58	1.10	1.68	0.02
October 28, 2004	0.01	1.22	0.59	1.24	1.83	0.02
BRPT						
May 12, 2003	0.02	5.76	0.86	5.82	6.68	0.07
June 24, 2003	0.02	1.85	0.90	1.90	2.80	0.03
August 12, 2003	0.06	2.93	1.33	3.03	4.36	0.25
September 16, 2003	0.01	1.20	0.76	1.22	1.98	0.02
October 28, 2003	<0.01	3.41	0.93	3.44	4.37	0.05
May 12, 2004	<0.01	4.10	0.67	4.13	4.79	0.03
June 8, 2004	0.02	3.14	0.78	3.18	3.96	0.02
July 6, 2004	0.02	2.55	0.68	2.58	3.26	0.03
August 10, 2004	0.01	1.40	0.64	1.42	2.06	0.02
September 7, 2004	0.01	1.38	0.72	1.40	2.12	0.03
October 19, 2004	<0.01	1.51	0.58	1.52	2.10	0.02
October 28, 2004	0.01	1.91	0.64	1.93	2.57	0.02
BLR						
May 13, 2003	0.24	6.22	1.21	6.54	7.75	0.14
June 25, 2003	0.46	2.80	0.95	3.94	4.89	0.06
August 13, 2003	0.01	3.54	0.91	3.55	4.47	0.14
September 17, 2003	0.45	3.71	1.03	4.72	5.75	0.06
October 29, 2003	0.31	3.44	1.11	3.87	4.98	0.07
May 13, 2004	0.48	4.06	0.78	4.73	5.51	0.04
June 9, 2004	0.02	3.85	1.05	4.43	5.49	0.06
July 7, 2004	0.25	3.18	0.73	3.82	4.55	0.04
August 11, 2004	0.18	2.25	0.84	2.68	3.53	0.07
September 8, 2004	0.25	3.09	0.92	3.76	4.68	0.09
October 20, 2004	0.98	3.63	0.75	4.82	5.57	0.06

* Calculated from TON = Total Kjeldahl N – NH_4-N

** Calculated from TN = Total Kjeldahl N + NO_3-N + NO_2-N

*** Calculated from TIN = TN - TON

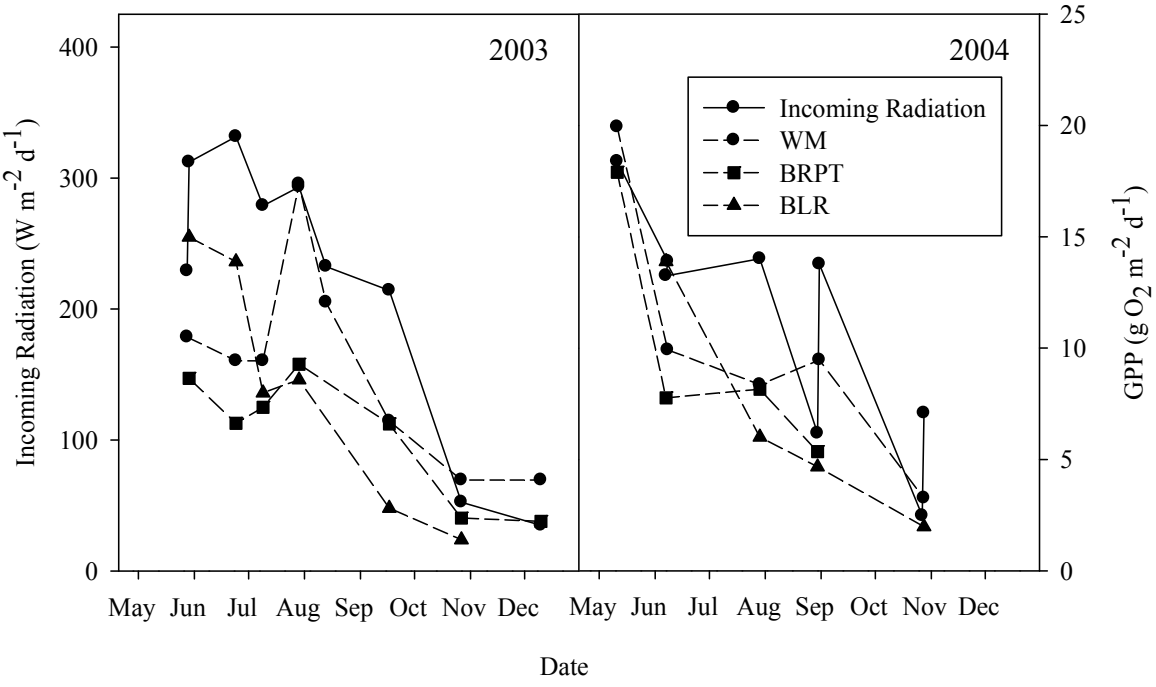

Figure 5.13 Incoming radiation plotted with GPP rates in the Grand River watershed for the sampling periods in 2003 and 2004.

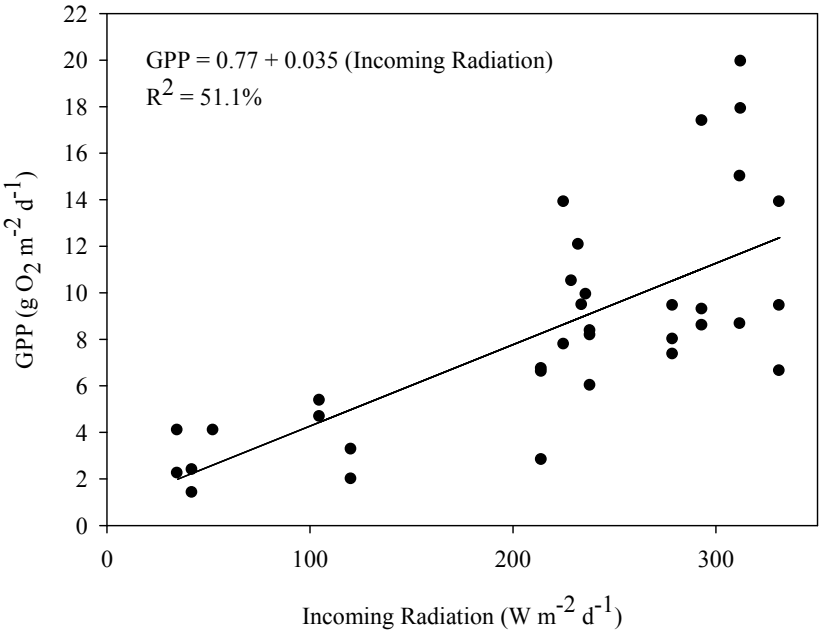

Figure 5.14 Plot of GPP rates regressed against incoming radiation in the Grand River.

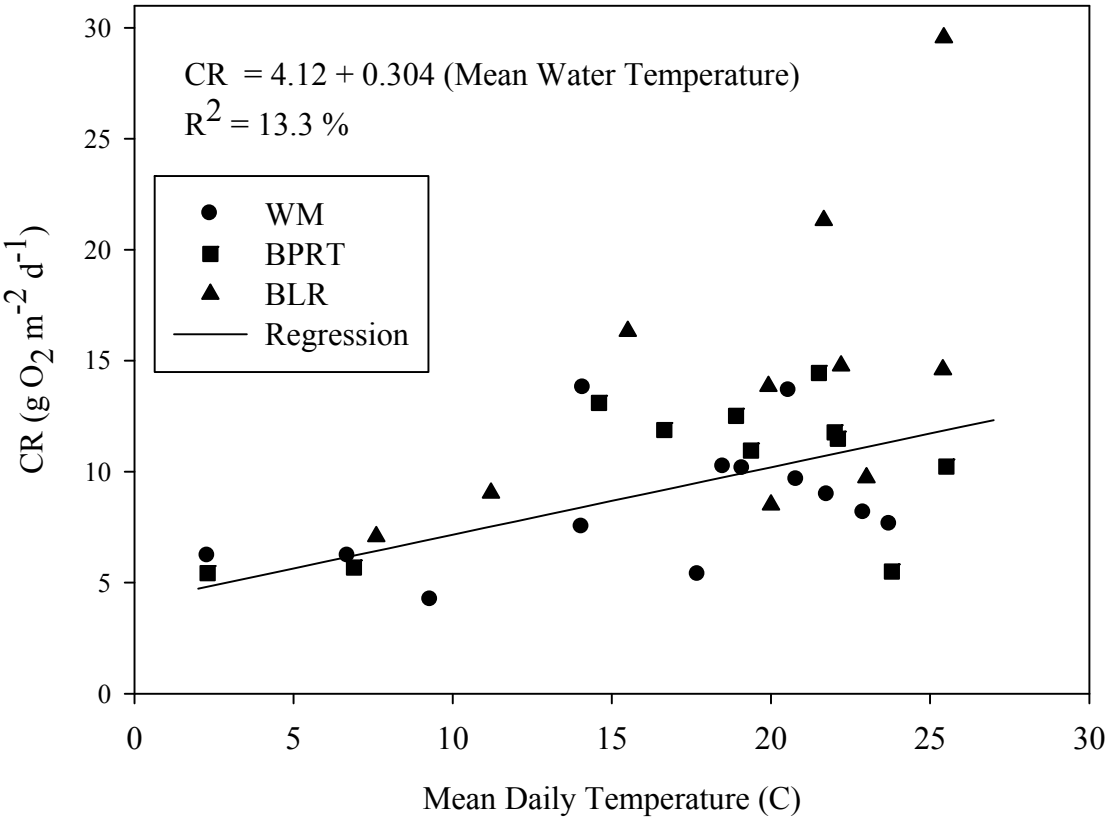

Figure 5.15 Plot of areal CR rates regressed against mean daily water temperature in the Grand River.

P:R ratios were also significantly correlated with temperature, day length and incoming radiation due to the relatively high correlations of these factors to GPP. There were no significant correlations noted between GPP, CR, and nutrient concentrations. Net production was negatively correlated with PWQM-measured ammonium nitrogen (NH_4-N), total inorganic nitrogen (TIN), and total nitrogen (TN), driven by the elevated concentrations and low NP at BLR. Nitrogen concentrations, PO_4-P as well as both dissolved inorganic and organic carbon (DIC and DOC, respectively) were relatively consistent between WM and BRPT (Table 5.6 and 5.7). Blair exhibited higher TIN, TON (Figure 5.16) and TP (Figure 5.17) concentrations with the exception of elevated TON and TP concentrations observed at BRPT on Aug 12, 2003.

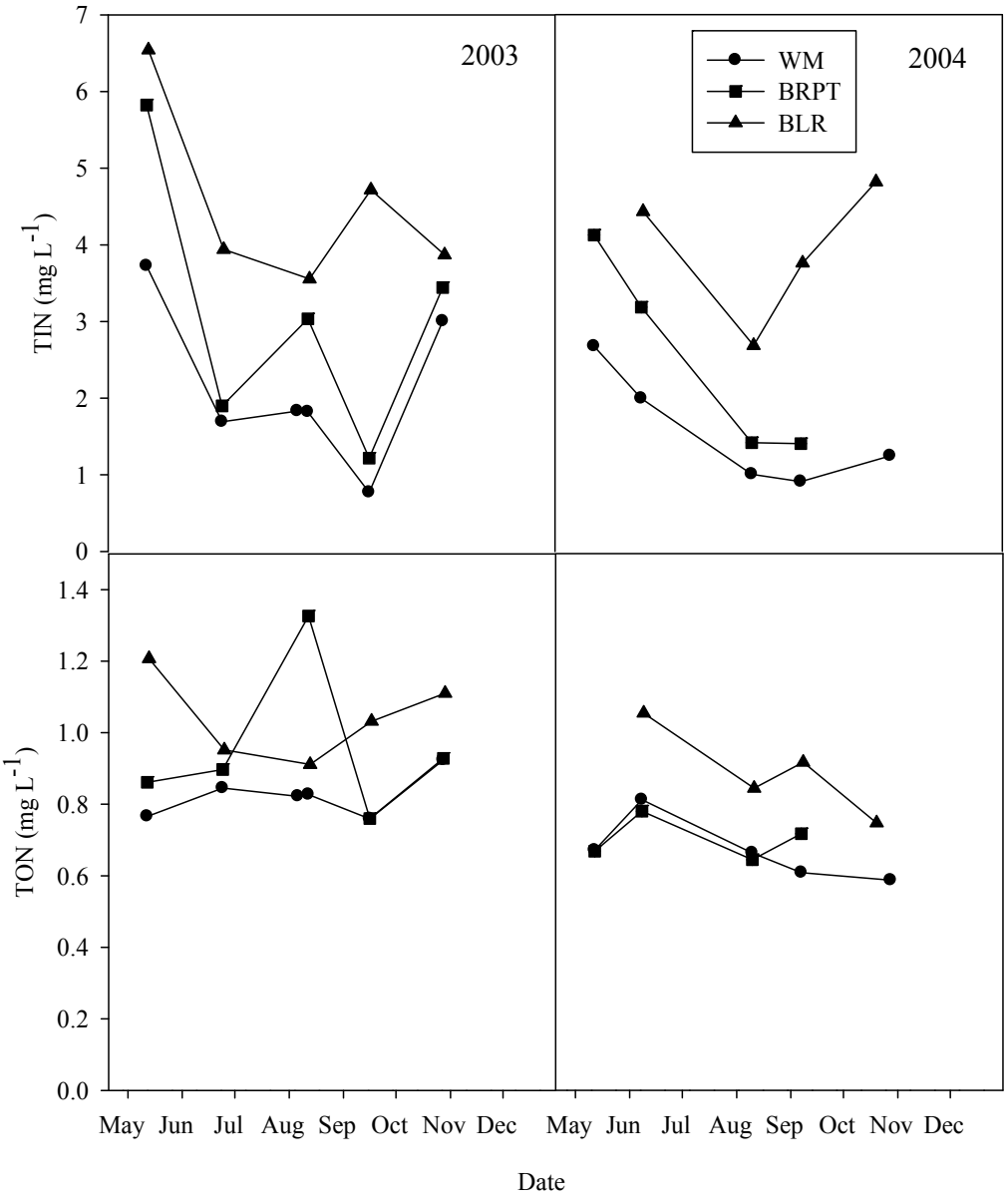

Figure 5.16 Total organic and inorganic nitrogen concentrations in the Grand River for WM, BRPT, and BLR, obtained from the Ontario Ministry of the Environment Provincial Water Quality Monitoring Network for 2003-2004.

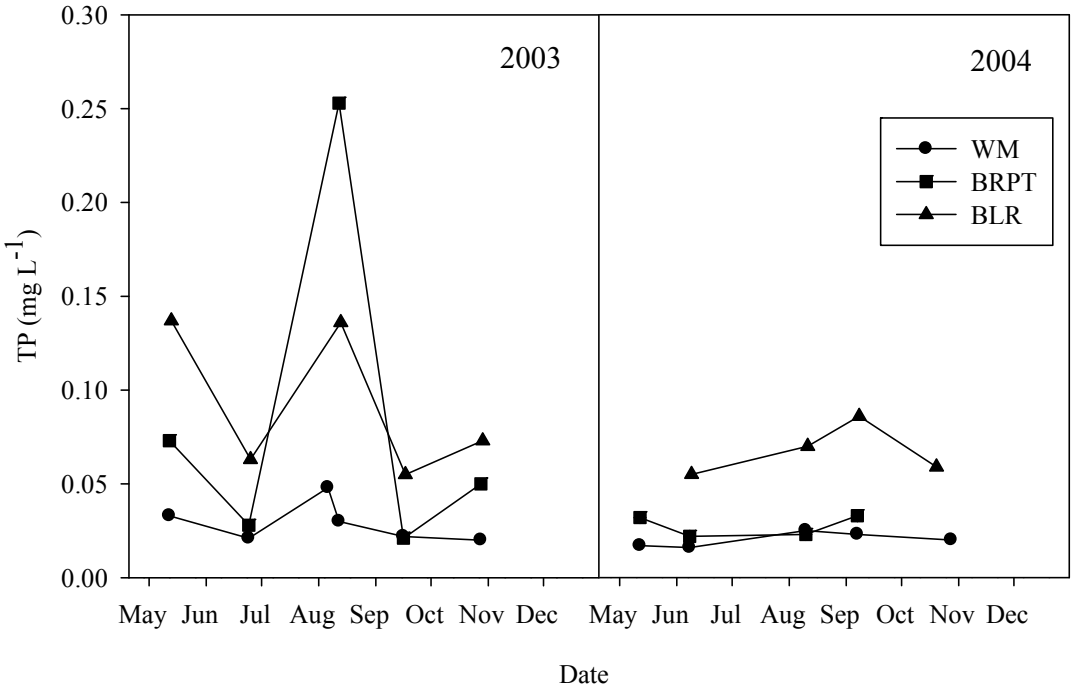

Figure 5.17 Total phosphorus concentrations in the Grand River for WM, BRPT, and BLR, obtained from the Ontario Ministry of the Environment Provincial Water Quality Monitoring Network for 2003-2004.

5.4 Discussion

5.4.1 Community Metabolism Rates

The metabolic rates (Table 5.3 and 5.4) in the Grand River (GPP = 2.2 to 19.9 and CR = 4.0 to 29.6 g O_2 m^{-2} d^{-1}) were found to be much higher than previous estimates in relatively unimpacted, large, rivers. Naiman (1983) measured whole system metabolism rates in an undisturbed boreal forested watershed located in eastern Quebec. In the two open canopy streams of 5th and 6th order, similar in size to the Grand River, metabolism rates were up to an order of magnitude less than in the Grand River, with GPP ranging from 0.3 to 4.0, and CR from 0.4 to 2.7 g O_2 m^{-2} d^{-1}, as measured from April to November. Net production rates in these rivers were consistently between 0 and 1 g O_2 m^{-2} d^{-1}, indicating that the larger rivers were autotrophic. The Ogeechee River, a 6th order blackwater river located in the southeastern USA, however, exhibited GPP rates of 0.49 to 13.99 and CR rates of 3.70 to 11.75 g O_2 m^{-2} d^{-1} (Edwards and Meyer, 1987). The Ogeechee river is not affected by major sources of pollution or other disturbances, but does receive large quantities of organic matter from surrounding hardwood forests during flood periods. Bott et al. (1985) reported seasonal mean GPP rates of 0.37 to 0.96 and CR rates of 0.34 to 0.72 O_2 m^{-2} d^{-1} for the McKenzie River, a 7th order river located in Oregon with a coniferous forest drainage basin.

Rivers that are impacted by agricultural and urban land uses, however, exhibit comparable metabolism rates to the Grand River. The Kalamazoo River, a 5th order river located in a rural agricultural watershed in Michigan, USA, exhibited high GPP (1.76 to 6.39 g O_2 m^{-2} d^{-1}) and CR (1.37 to 5.79 g O_2 m^{-2} d^{-1}) rates from May to December (Bott et al., 1985). Uehlinger (2006) measured monthly rates of GPP and CR of 3.9 to 6.1 and 4.1 to 8.8 g O_2 m^{-2}

d^{-1}, respectively, over a 15 yr period in a 7th order Swiss river receiving sewage treatment plant inputs. Wilcock et al. (1998) monitored 23 lowland streams in agriculturally developed catchments in New Zealand that were considered to be in "poor condition." Rates of GPP were between 0.5 and 29.2, with CR rates of 3.5 to 55 g O_2 m^{-2} d^{-1}. The Erpe, a 3rd order urban stream located in Germany, was monitored upstream and downstream of wastewater treatment plant discharges (Gucker et al., 2006). Upstream of the treatment plant, the river exhibited GPP rates of 0.1, 2, and 32 g O_2 m^{-2} d^{-1} in winter, spring, and summer, respectively. Downstream, GPP rates were similar, <0.1, 2, and 47 g O_2 m^{-2} d^{-1}. Rates of CR were 6, 11, and 32 g O_2 m^{-2} d^{-1} upstream of the treatment plant, and increased to 18, 24, and 59 g O_2 m^{-2} d^{-1} downstream of the plant. The South Saskatchewan River, located 50 km downstream from Saskatoon, SK, showed mid-July GPP and CR rates of 10.2 and 9.2 g O_2 m^{-2} d^{-1}, respectively (Venkiteswaran, 2007). The metabolism rates for South Saskatchewan River were determined using a dynamic isotopic model and exhibited $\delta^{18}O$-O_2 values that ranged from a maximum of approximately 23‰ at night to a minimum of around 8‰ during early afternoon.

5.4.2 Trends and Influences on Community Metabolism

Total P concentrations, which ranged from 20 to 250 μg L^{-1} (Tables 5.5 and 5.6), indicated that the Grand River is meso-eutrophic to eutrophic at all three sampling locations according to the trophic trigger ranges suggested by the CCME (2007), which was in agreement with long term Grand River water quality trends noted by Cooke (2006). There were no significant correlations between water quality and GPP rates. As major nutrient concentrations were consistently above levels considered to be limiting, the lack of correlation between GPP and

water quality is not surprising. Nutrient effects on GPP may be more apparent over a wider range of TP concentrations, or when concentrations are limiting (Young and Huryn, 1996; Mulholland et al., 2001). There appears to be a seasonal influence on GPP at all three sampling locations along the Grand River, with the highest rates recorded in the spring and early summer, with subsequent declines in the late summer and fall (Figure 5.9). Naiman (1983) also noted that their study sites showed seasonal variations, with an annual minimum at ice breakup, followed by GPP and CR increasing to their annual maximum by late June or July, and a gradual seasonal decrease to winter levels occurring between August and November. Uehlinger (2006) recorded annual rate maxima in GPP and CR in May, with a subsequent decline to minimum values in the winter months. The overall ranges in GPP were similar at all three sampling locations (Table 5.4 and Figure 5.9). Seasonal variation in GPP in the Grand River is most highly correlated with incoming radiation, day length, and with temperature (Table 5.5). Biomass of primary producers may have been an important correlative factor, but was not measured.

The GPP seasonal pattern clearly paralleled light availability (Figure 5.13), and irradiance explained 51% of the variability in production rates (Figure 5.14). Differences among the seasonal trends reported in 2003 and 2004 may be due to irradiance. There was greater incoming radiation during the summer of 2003, which coincided with higher GPP during this period, as compared to 2004. Greater NP rates and P:R also occurred in the summer of 2003 than in 2004, due to greater GPP rates. Light availability tends to be a function of stream size (Minshall, 1978; Vannote et al., 1980), with larger streams having more open canopies, as was the case for the 5 to 6th order Grand River where the sampling areas were located.

Other studies have also shown that light and temperature are the primary determinants of GPP (Naiman, 1983; Servais et al., 1984; Bott et al., 1985; Young and Huryn, 1999; Uehlinger et al., 2000; Mulholland et al., 2001). As temperature and irradiance vary in a regular manner annually, distinct seasonal variation in GPP should be expected. Negative correlations between GPP and both water depth and DOC concentrations have been noted in other studies (Edwards and Meyer 1987) due to their influence on light at the river bottom. However, neither hydrology nor DOC concentrations showed a relationship with production rates in the Grand River possibly due to that fact that monitoring was conducted during non-storm flow periods, and the water column did not appear to exhibit colouring due to DOC concentrations.

The CR rates were less variable seasonally than GPP rates, with only a moderate declining trend from May to December in both 2003 and 2004. Community respiration rates were significantly correlated with mean temperature and day length (Table 5.4). Daylength was significantly correlated with temperature (Pearson $r = 0.847$, $p < 0.001$), where longer day lengths are associated with greater mean temperatures, causing higher CR rates. As CR and GPP were also significantly correlated, greater CR associated with longer day lengths could be also in part due to greater biomass leading to higher respiration rates. Water temperature influences CR rates, but at different magnitudes in different systems. The Pearson correlation of 0.365 for CR and temperature in the Grand River was in the range reported by Hill et al. (2002), who reported correlations ranging from 0.33 to 0.37, while Bott et al. (1985) found a higher correlation coefficient of 0.572. Mean temperatures measured in the Grand River during this study ranged from 2.3 to 25.5 C (Table 5.2). Linear regression analysis of the Grand River CR rates showed a positive relationship between mean daily temperature and CR,

but explained only 13.3 % of the variability (Figure 5.15) indicating that other factors were also responsible for CR variability, such as biomass, limited CR at low DO concentrations, or effects of non-temperature dependant DO consuming processes. Water temperature may also not be an appropriate predictor of CR rate if DO consumption was occurring in regions of the river channel that may have a different, more stable, thermal regime (e.g., sediments). Uehlinger et al. (2000) found that temperature was a significant predictor of CR, explaining 22% of the variation. Mulholland et al. (2001) and Hedin (1990), however, both found no evidence of an effect of water temperature on CR.

Compared to WM and BRPT, BLR is characterized by elevated concentrations of both nitrogen (Figure 5.16) and phosphorus (Figure 5.17). Correlations between CR rates at all locations and TN and NH_4-N were borderline non-significant, but TN, TIN, and NH_4-N were all significantly correlated with NP. When comparing the three sampling sites along the longitudinal gradient of the Grand River, BLR exhibits the highest rates of CR, most notably in 2004 (Figure 5.11 and Table 5.4). Community respiration rates at BLR were on average 7.2 g O_2 m^{-2} d^{-1} higher than measured upstream. As mentioned, changes in DO at BLR are due to the integrated effects of upstream influences. The consistently elevated CR rates at BLR compared to the other sites are likely due to the additional input of nutrients and O_2 consuming substances from upstream urban influences.

Metabolic response of rivers and streams to wastewater loading has not been frequently researched since the pervasive implementation of secondary and tertiary treatment plants (Gucker et al., 2006). However, Ruggiero et al. (2006) recently measured mean CR rates of 5.4 upstream, and 29.3 g O_2 m^{-2} d^{-1} downstream, of two wastewater treatment plants located

on a Mediterranean 3rd order stream. Gross primary production rates were low, 1.3 g O_2 m^{-2} d^{-1} upstream of the treatment plant, and almost nil downstream. Similar wastewater plant effluent effects were observed by Gucker et al. (2006) in a 3rd order stream in Germany, where CR increased from an annual mean of 16 upstream to 34 g O_2 m^{-2} d^{-1} downstream of the plant. Ruggiero et al. (2006) and Gucker et al. (2006) both reported that GPP rates were relatively consistent between upstream and downstream locations.

A portion of the total DO consumption occurring at BLR may be due to demands associated with NH_4 oxidation via nitrificiation. Long term water quality trends indicate that total NH_4 concentrations at BLR are among the highest in the watershed (Cooke, 2006). Wastewater flowing into the treatment plant serving Kitchener-Waterloo undergoes coagulation, ozonation, and filtration processes, but the plant does not provide more advanced treatment involving the oxidation of NH_4^+ and organic matter. Gowda (1983) modeled nitrification effects on the DO regime in the Speed River, a major tributary in the Grand River watershed that receives inputs from the Guelph wastewater treatment plant. Gowda (1983) determined the maximum DO depletion attributable to nitrogenous demand was close to 4.5 mg L^{-1}. The reach studied exhibited similar hydrology characteristics as the WM location, and received wastewater treatment plant loadings serving a population of approximately 68,000 people.

During 2003 and 2004, the Waterloo Water Pollution Control Plant discharged 220 and 218 tonnes of NH_4^+, while the plant in Kitchener discharged 527 and 533 tonnes (NPRI, 2007). This translates to a mean total loading of about 750 tonnes y^{-1} of NH_4^+ (~2 tonnes d^{-1}) into the Grand River upstream of BLR. Subsequent nitrification to NO_3^- would place additional DO

demands on the River downstream of these plants, compared to WM and BRPT. Assuming a mean discharge of 16.5 $m^3 s^{-1}$, and a mean depth of 0.41 m, approximately 0.6 g $m^{-2} d^{-1}$ of NH_4^+ discharged from the upstream treatment plants would be available for nitrification. Assuming that oxidation of each g of NH_4^+ requires about 4 g of DO, about 2.7 g $m^{-2} d^{-1}$ of the DO could be consumed via nitrification due to Kitchener-Waterloo wastewater NH_4^+ inputs to the Grand River. Thuss (2008) suggests that nitrification is a significant source of NO_3^- in the Grand River downstream of the Kitchener and Waterloo Water Pollution Control Plants, and that the diel variations in DO are linked to nitrogen cycling processes in the river. Thuss (2008), however, found that the nitrification effects attributable to the Kitchener plant are apparent before the river reaches the BLR location. As the 3 km half-life for k at this location (Chapter 4) would suggest, DO consumption effects due to treatment plant inputs would have been mainly attenuated before reaching the BLR location, which is located approximately 20 km downstream of the Kitchener plant outfall.

Elevated DO consumption upstream of BLR would likely be attributable to organic matter degradation, both by the bacterial oxidation of the suspended and dissolved organic matter, and demand associated with the sediment and benthic deposits. Total nitrogen concentrations paired with particulate organic matter, have been found to predict CR in river sediments, explaining up to 90% of variation (Fuss and Smock, 1996). Oxygen demand associated with organically-enriched sediments typically range from about 1 to 10 g $m^{-2} d^{-1}$ (Chapra, 1997). Particle inputs could include wastewater treatment plant outfalls, plant matter, and eroded organic sediments (Chapra, 1997). The land use upstream of BLR is characterized by cities of both Kitchener and Waterloo, which would be a source of nutrient and organic inputs via run-off from urban and residential areas, as well as from recreational sources such as

parks and golf courses. As only the dissolved forms of organic C were measured during the course of this study, factors potentially more correlative with CR may have been overlooked (e.g., total and particulate organic matter, biomass).

5.4.3 Trophic Indicators

Downstream of the wastewater treatment plants, P:R at BLR is consistently below 1.0 in both years due to greater rates of CR, as GPP rates are similar to the upstream locations. These same trends are reflected in the NP rates (Figure 5.11), where WM and BRPT exhibit either a balanced or net production of O_2, while BLR consistently exhibits net consumption. Autotrophic production appears to be a more dominant energy base upstream from the wastewater treatment plants, as indicated by the greater P:R values, lower CR rates and more positive NP rates, as compared to BLR. As the P:R values are greater than one at WM and BRPT during the growing season, organic matter produced within the system is likely being stored or exported downstream. When rates of GPP are plotted against CR (Figure 5.18), the trophic separation between the upstream and downstream of the treatment plants is evident. The WM and BRPT sampling sites plot on the same GPP to CR tangent near to, or above, the 1:1 line, as areas of overall net production of organic matter. The BLR location also follows a linear trend, but consistently below the 1:1 line, indicative of the additional oxygen consuming inputs upstream.

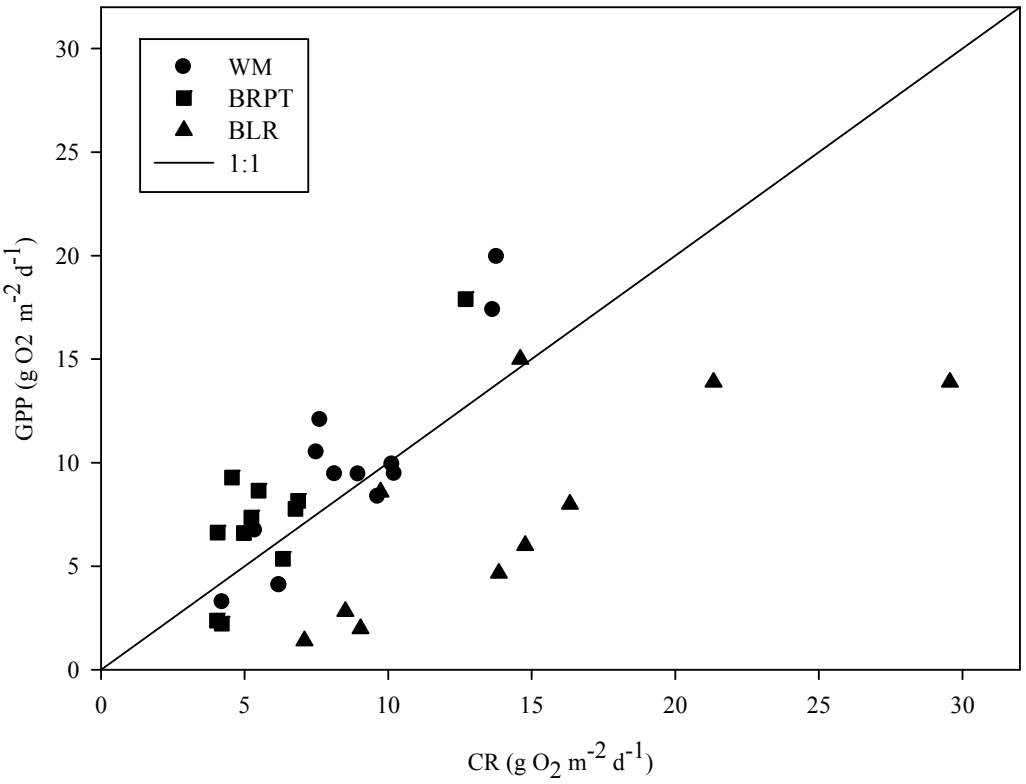

Figure 5.18 Plot of areal GPP to CR for each sampling location on the Grand River.

Quay et al. (1995) first attempted to use $\delta^{18}O\text{-}O_2$ as an ecological indicator of trophic status, by plotting $\delta^{18}O\text{-}O_2$ against fraction of DO saturation in the water column. Plotting all $\delta^{18}O\text{-}O_2$ and DO data collected during this study on a similar cross-plot (Figure 5.19), separation with sampling location similar to that noted in Figure 5.18 occurs where WM and BRPT plots are located in similar regions on the diagram. The data from BLR, however, are shifted towards lower DO saturation along with higher $\delta^{18}O\text{-}O_2$. Quay et al. (1995) linked P:R to the cross-plot of $\delta^{18}O\text{-}O_2$ and DO saturation, with lower P:R systems plotting towards the upper left quandrant, and higher P:R systems trending towards the bottom right hand quadrant. A similar relationship is exhibited in the cross-plotted data for the Grand River, where WM and BRPT trended further into the bottom right hand quadrant than BLR.

Steady state conditions were assumed by Quay et al. (1995) for the Amazon lakes and rivers monitored, with one data point representing the diel condition. In the Grand River system, however, the $\delta^{18}O\text{-}O_2$ and DO follow an elliptical shape on a diel basis (Figure 5.20), similar to the diel DO and $\delta^{18}O\text{-}O_2$ trends noted by Venkiteswaran et al. (2007). Due to the strong diel cycle present in the Grand River, a single point analysis is not representative of the ecosystem conditions. Venkiteswaran et al. (2008), have suggested that the elliptical cross-plots of $\delta^{18}O\text{-}O_2$ and DO as % saturation may provide some insight for assessing the status of aquatic metabolism and ecosystem health. Venkiteswaran et al. (2008) also presented P:R ratios that were corrected for the absolute rate of gas exchange, denoted as P:R:G. As gas exchange mitigates the amplitude of diel O_2 dynamics, effects of GPP and CR on a given water body is modified by exchange with the atmosphere.

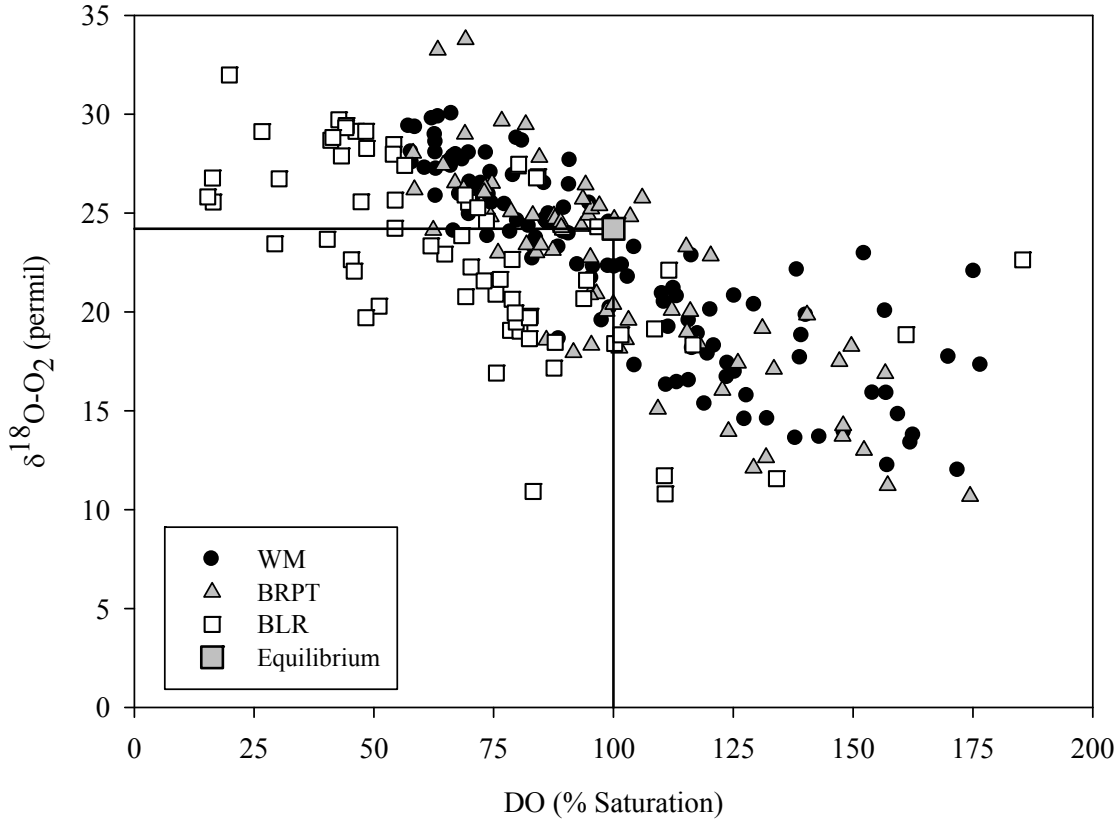

Figure 5.19 Cross plots of DO saturation and $\delta^{18}O\text{-}O_2$ data obtained from all samples collected in the Grand River. Equilibrium is indicated by a grey square at the point of where both DO and $\delta^{18}O\text{-}O_2$ are at atmospheric equilibrium (DO = 100% saturation and $\delta^{18}O\text{-}O_2 = 24.2$ ‰).

The relative magnitudes of P:R:G in the Grand River (Table 5.8) indicate that gas exchange in the Grand River plays a comparatively large role in the overall balance of DO. Despite the high rates of GPP and CR in the Grand River, the rates relative to gas exchange were in the range of 0.5 to 1.9 for CR, and 0.8 to 1.9 for GPP. For comparison, Venkiteswaran et al. (2007) reported P:R:G values of 9.28:11.9:1 for a northwestern Ontario experimental lake and 2.5:3.5:1 in a Saskatchewan wetland. Both GPP (~2.5 to 3 g O_2 m^{-2} d^{-1}) and CR (~3.5 to 4 g O_2 m^{-2} d^{-1}) at these sites were much lower than in the Grand River, and gas exchange rates (~ 0.3 to 1.0 g O_2 m^{-2} d^{-1}) comprised a lower portion of the overall DO mass balance. The South Saskatchewan River exhibited a P:R:G of 1.97:1.78:1 (Venkiteswaran et al., 2007), which was closer to the range noted in the current study for the Grand River. The South Saskatchewan River exhibited k (3.96 d^{-1}), GPP (10.2 g O_2 m^{-2} d^{-1}) and CR (9.2 g O_2 m^{-2} d^{-1}) rates similar to the Grand River.

Values of P:R:G (Table 5.8) indicated that GPP, relative to gas exchange, was greatest upstream of BRPT, while relative CR rates were highest upstream of BLR. Even though GPP rates were similar at all three sites, BRPT exhibited the lowest k, allowing for greater relative effects of GPP inputs. The P:R:G values in the Grand River (Table 5.8) followed the same trend as the NP rates, where as NP declined so did the relative influence of CR versus GPP in the P:R:G ratios.

Table 5.8 Aquatic metabolism characteristics obtained from the diel modeling results at WM, BRPT and BLR. Gas exchange (GE) has been calculated as the absolute gross flux of DO across the air-water interface.

Location	Date	GPP*	CR*	GE*	NP*	P:R	P:R:G
WM	May 28,2003	10.5	7.51	7.71	2.99	1.40	1.4:1.0:1
	Jun 24, 2003	9.44	8.97	6.42	0.47	1.05	1.5:1.4:1
	Jul 9, 2003	9.44	8.15	5.61	1.29	1.16	1.7:1.5:1
	Jul 29, 2003	17.4	13.7	12.7	3.72	1.27	1.4:1.1:1
	Aug 13, 2003	12.1	7.64	9.01	4.43	1.58	1.3:0.8:1
BRPT	Jul 09, 2003	7.35	5.24	3.92	2.11	1.40	1.9:1.3:1
	May 11, 2004	17.9	12.7	9.41	5.20	1.41	1.9:1.3:1
	Jun 07, 2004	7.77	6.77	4.91	0.99	1.15	1.6:1.4:1
	Aug 30, 2004	5.36	6.34	3.41	-0.98	0.85	1.6:1.9:1
BLR	Jun 07, 2004	13.9	21.3	12.4	-7.44	0.65	1.1:1.7:1
	Jul 09, 2003	13.9	29.6	13.6	-15.67	0.47	1.0:2.2:1
	Aug 30, 2004	4.67	13.9	9.83	-9.19	0.34	0.5:1.4:1

* units: g O_2 m^{-2} d^{-1}

The cross-plot location of the diel ellipses (Figure 5.20) in the Grand River appears to be mostly related to the NP rates and P:R; as P:R and NP decline and CR becomes more dominant, the ellipses trend from the lower right towards the upper left quadrant on the diagram. The ellipses that exhibit the most "balanced" CR and GPP centre around the atmospheric equilbrium values. There did not appear to be dominant controls on the shape of the individual ellipses found from the Grand River diel data. Venkiteswaran et al. (2008) noted that k values tend to control the overall shape of the ellipses, affecting the length and difference between the daytime and nighttime portions of the ellipsis. Gas transfer coefficients at the three sampling locations along the Grand River were relatively consistent, and this effect may also be evident in Figure 5.20 as many of ellipses were of a similar size and width.

Both BRPT and BLR exhibited smaller ellipses on August 30, 2004; the amplitude of DO saturation and $\delta^{18}O\text{-}O_2$ were comparatively low on these sampling occasions, and did not appear to be directly linked to any one factor. As the parameters influencing $\delta^{18}O\text{-}O_2$ and DO (e.g., temperature, GPP, CR, $^{18}O\text{-}H_2O$, k and α_r) are variable and interactive, specific controls on ellipses shape and size were not clear. However, the diel data exhibited a wide range in DO saturation values and $\delta^{18}O\text{-}O_2$ during almost all sampling events, which would lead to ellipses that exhibit similar sizes among events.

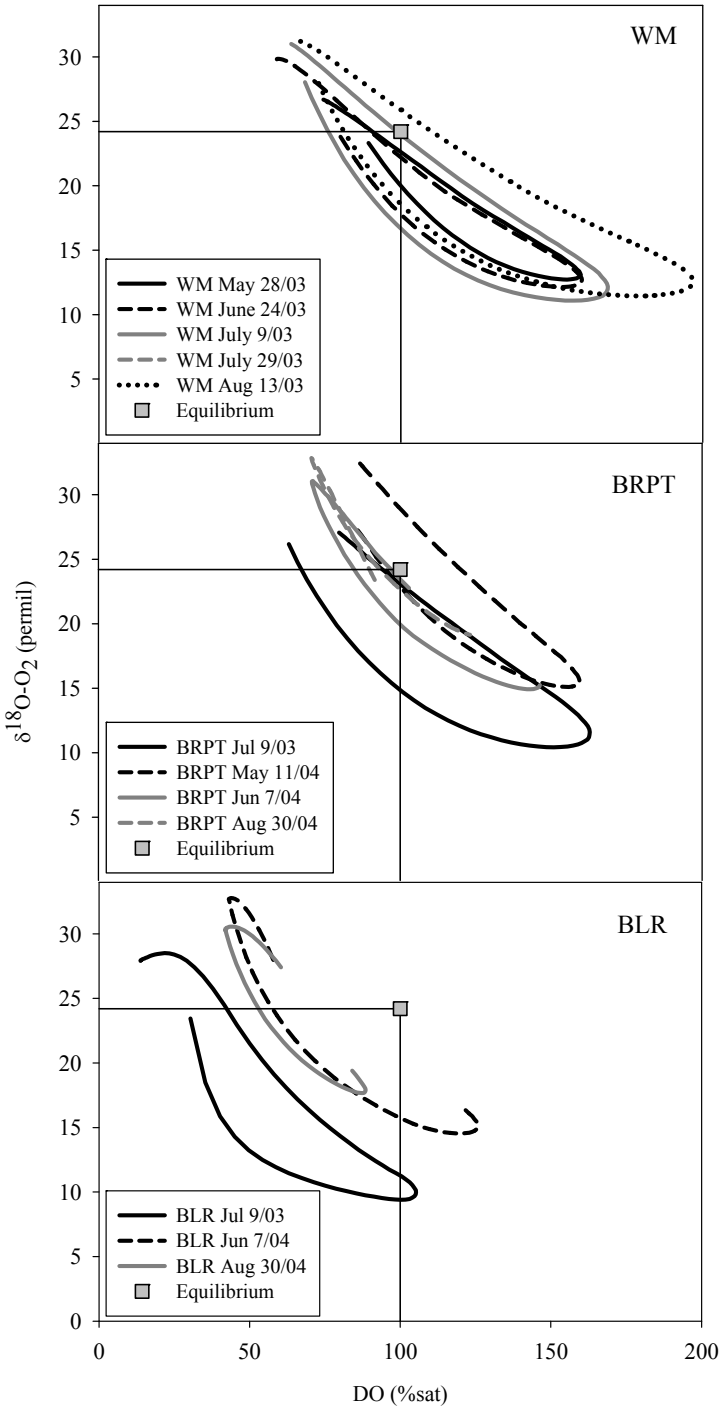

Figure 5.20 Fitted model output for the diel sampling events, plotted as the $\delta^{18}O\text{-}O_2$ in delta notation and DO as % of atmospheric saturation. The theoretical atmospheric equilbria for both $\delta^{18}O\text{-}O_2$ and DO are shown by the squares.

One of the key indicators of environmental stress on aquatic ecosystems is the diel DO minimum. The Ontario provincial water quality objective (at 20 C) is 4 mg L^{-1} for warm water biota and 5 mg L^{-1} for cold water biota (OMOE, 1994) and the Canadian water quality guidelines for the protection of aquatic life set minimum DO at 5.5 mg L^{-1} for warm-water biota at non-early life stages and 6.5 mg L^{-1} for non-early life stage cold-water biota (CCME, 2007). Minimum DO concentrations from the Grand River were observed to be below these guidelines at the BLR location for all three diel sampling events (Figure 5.3).

The depressed DO minima are associated with P:R values of less than one, when R>P in the P:R:G ratios, and when the span of ellipses fall mainly in the left upper and lower quadrants of the $\delta^{18}O\text{-}O_2$ and DO cross-plot (Figure 5.20). For P:R:G and P:R ratios associated with both WM and BRPT, P was generally close to or greater than R. However, this was not the case for conditions upstream of BLR; the P component in the P:R:G ratios was less than R, and trended between 0.5 ant 1.1. This indicates that both P and G are contributing a similar absolute magnitude mediating the DO flux upstream of BLR. When considering P:R, P:R:G, and NP values for these sites, it appears that gas exchange plays a greater role in mitigating DO minimums upstream of BLR as compared to WM and BRPT. If events were to occur that would cause lower rates of k, such as very deep water conditons or changes in river morphology, or if the P:R ratio was further depressed, DO in the river in the BLR region would likely continue to decline, or become anoxic.

Overall, results in main the Grand River indicated that the watershed is experiencing effects from both agricultural and urban inputs from the surrounding land base. Rates of GPP and CR were found to be elevated compared at all locations to relatively unimpacted systems (Table 1.1). For comparison, Naiman (1983) found that similarly sized, unimpacted rivers in Eastern Canada had much lower GPP (0.3 to 4.0 g O_2 m^{-2} d^{-1}) and CR (0.4 to 2.7 g O_2 m^{-2} d^{-1}) rates than in the Grand River (Table 5.4), and consistently positive NP values. Metabolism rates in the Grand River were in agreement, however, with systems impacted by agricultural and urbanized drainage basins (Wilcock et al., 1998; Williams et al., 2000; Ruggiero et al., 2006; Gucker et al., 2006).

The most notable indication of increased disturbance is the marked increase in CR downstream of Kitchener-Waterloo, greater than two-fold at BLR, since GPP rates at all three sites were relatively similar (Table 5.4) when averaged across all sampling events. Both Mulholland et al. (2005) and Hornberger (1977) found that CR rates as ecological indicators show a more consistent relationship with impact than GPP. The upstream locations of WM and BRPT tended to exhibit similar characteristics in both P:R, $\delta^{18}O$-O_2 and DO cross plot ellipses, while BLR exhibited a distinctly different profile that indicated that the upstream oxidative demands exceed DO inputs to the system.

5.4.4 Predicting River DO Dynamics Using the Isotopic Modeling Approach

In the current study, the $\delta^{18}O\text{-}O_2$ was used to supplement DO concentration monitoring for the quantification of DO dynamics in a large impacted river. The technique was applied to three sampling locations that were subject to increasing levels of impact due to agricultural and urban influences, in an attempt to provide a more in-depth, comprehensive evaluation than provided by previous research. Mass-balance based, diel time-forward simulation of DO and $\delta^{18}O\text{-}O_2$ has been successfully applied to other dynamic systems ranging from smaller 1st and 2nd order tributaries (Parker et al., 2005; Tobias et al., 2007) to larger rivers (Venkiteswaran et al., 2007; Poulson and Sullivan, 2009). As compared to traditional modeling approaches, measuring $\delta^{18}O\text{-}O_2$ provides a second mass balance that further constrains the potential range in input parameter values that can describe the DO dynamics.

The best fit results from the diel sampling events indicated that the model explained > 93% of the variability in DO concentrations, but there was greater uncertainty associated with $\delta^{18}O\text{-}O_2$. The model assumes that CR, k, and α_r are constant (except that k and CR are corrected for temperature) and that GPP followed a sinusoidal curve. Deviations from these assumptions would contribute to the inability of the model to describe the observed data. As $\delta^{18}O\text{-}O_2$ tends to exhibit a greater sensitivity to most of the input parameters, as compared to DO, any uncertainty associated with the individual variables would then have a greater accumulative effect on $\delta^{18}O\text{-}O_2$ model output.

Factors causing model deviation from observed data could include: α_r and CR_{20} may not be constant on a diel basis; the mass balance may be missing a process that causes a shift in $\delta^{18}O\text{-}O_2$; GPP could deviate from the prescribed half-sinusoidal function; groundwater inputs are also not accounted for. Fractionation during DO consumption is not likely to be constant in

the Grand River, as discussed in Chapter 6. According to the sensitivity analysis (Chapter 3), $\delta^{18}O\text{-}O_2$ exhibited little sensitivity, whereas DO was more responsive, to changes in GPP. Deviations from the GPP sinusoidal function would therefore likely cause lack of fit of the model to daytime DO, which was not evident.

Tobias et al. (2007) considered three possible groundwater cases, oxic, anoxic, and no groundwater, in their isotopic modeling approaches. They found that groundwater inputs shifted P:R values approximately 15%, and that CR values were affected while GPP estimates were only minimally influenced. From their exact solution isotope modeling results, a cyclical diel pattern in CR was noted, where CR increased during the day to a peak afternoon value of approximately 1.3 times that of the night value. The use of a temperature function to explain changes in CR was only able to partially explain the changes in CR, with deviations occurring mainly during day time conditions. Tobias et al. (2007) reasoned that high day time CR could be a response to labile DOC produced during GPP, or photorespiration accompanying high day time irradiance and DO conditions. Nitrification has also been shown to have diel variability (Thuss, 2008). However, overall daily metabolism results reported by Tobias et al. (2007) varied only by about 10 to 15 % between the exact solution and time-forward modeling approaches, including the different groundwater input assumptions. The exact inverse solution provided additional information such as inter-diel variability in GPP and CR, but requires sampling intervals at fine temporal resolution relative to changes in DO and $\delta^{18}O\text{-}O_2$, and is very sensitive to the choice of α_r.

It should be noted that in the current study monitoring was conducted at a given sampling point over time, and model results reflect an integration of all upstream influences affecting the DO dynamics of the system. Given the dynamic nature of DO production and

consumption processes in the Grand River, and the spatial scale over which inferences are being made, the isotopic mass balance approach presented in the current study exhibited a good fit to observed DO and $\delta^{18}O\text{-}O_2$. The addition of the isotopic mass balance is of value, as it provides a corroboration of the input parameter estimates between the two balances, and constrains the range of potential input values. As illustrated in Chapter 3, the range of parameter rates that provide an optimal fit to both DO and isotopic mass balances is narrow. The extra mass balance can then provide a greater level of confidence in the selection of model input values compared to traditional curve fitting methods or calibration procedures. Sampling in the current study was mainly conducted every 2 to 4 hours due to travel times between the locations studied on the watershed for a given sampling period. In some cases, $\delta^{18}O\text{-}O_2$ and DO exhibited scatter and deviation from a mean trend over time. Visual examination of model output to complement the statistical measure of fit (RMS error) was performed to minimize the bias of model fit results towards anomalous data. However, more frequent sampling may lower the risk of anomalous points affecting parameter estimation. This problem was greatest in the routine daytime only sampling events due to fewer data.

The sampling and analysis for $\delta^{18}O\text{-}O_2$ cannot be automated at present time, however, and can be labourious and expensive. Dissolved O_2, on the other hand, can be easily measured continuously via *in situ* monitoring equipment. Daytime sampling for $\delta^{18}O\text{-}O_2$ may not be necessary; the isotopic technique may still be useful with only nighttime $\delta^{18}O\text{-}O_2$ data, which would minimize the number of samples to be collected. In Chapter 3, Simulation A, which assumed k and CR obtained from night DO and $\delta^{18}O\text{-}O_2$ model fitting, resulted GPP, CR, and k rates that were within 10% of that obtained by modeling the full diel data set (Simulation B). Using night data of DO and $\delta^{18}O\text{-}O_2$ to estimate k and CR, and determining GPP using diel the

DO concentration data may be most efficient application for using the isotope technique. Values of α_r also exhibited a smaller range associated with night undersaturated conditions, allowing for less labourious modeling and parameter estimation.

Input parameter uncertainty and sensitivity (i.e., potential variability in input parameters that explain observed data) most likely reflect the dynamic processes occurring in the Grand River watershed. In the current study, model error appears to be primarily linked to the ability of the isotopic mass balance to describe observed $\delta^{18}O\text{-}O_2$ data. Uncertainty in α_r presents some complication in using the isotopic model mass balance approach to predict $\delta^{18}O\text{-}O_2$ in systems where α_r is unknown, or variable. A better understanding of processes affecting $\delta^{18}O\text{-}O_2$, to improve the capability of the model to replicate observed data, would improve the prediction of metabolic processes in impacted rivers. Despite these shortcomings, however, the isotopic approach has the potential to improve the ability to characterize DO dynamics and metabolism in highly impacted watersheds due to the provision of corroboration to estimates obtained by DO concentration alone.

6.0 Isotopic Fractionation during Dissolved Oxygen Consumption

6.1 Introduction

In living systems, biological consumption of O_2 preferentially uses ^{16}O at a slightly more rapid rate than ^{18}O, causing an isotope fractionation and subsequent enrichment of the remaining pool of ^{18}O. Kinetic fractionation of O_2 exhibits a range of values in different organisms and varying environments. Lane and Dole (1956) were among the first researchers to quantify the respiratory fractionation of O_2 isotopes in different circumstances and found fractionation factors ranging from 0.971 to 0.994 for animals, plants, bacteria and fungi. Other literature values ranged from 0.971 to 0.998 for a variety of aquatic organisms and ecocommunities (Table 6.1).

Information regarding to what extent O_2 fractionates during community respiration in rivers is sparse. Previous researchers using $\delta^{18}O\text{-}O_2$ to study community metabolism in lotic systems (Quay et al., 1993; Wang and Veizer, 2000; Parker et al., 2005) have assumed that α_r maintains a relatively constant value of 0.982 based on bottle incubations conducted in the Amazon River (Quay et al., 1993). This fractionation factor is representative of DO consumption associated with the water column and may not be applicable to systems that have proportionally greater consumption occurring in sediments or via different organisms and consumption pathways. Under some circumstances, DO consumption may also include photochemical DO demand, nitrification, or other DO consuming processes. Experiments incubating cores and slurries from a Midwestern USA agricultural stream yielded fractionations varying from 0.982 to 0.991. Results based on the optimal fit of models for this same stream averaged about 0.987 (Tobias et al., 2007).

Table 6.1 Summary of estimated respiratory fractionation factors from various sources.

Organism/Environment	Mean α_r	Range	Method	Source
Homo sapiens	0.982	0.981-0.985	Incubations	Lane and Dole (1956)
Crab	0.990	0.989-0.991		
Frog	0.993	0.991-0.994		
Molds	0.982	0.981-0.983		
Bacteria	0.984	0.971-0.992		
Plants (Spinach, Potato, Mushroom)	0.976	0.971-0.978		
Pacific Ocean - Surface Water	0.979	0.968-0.988	Incubations	Kroopnick (1975)
Pacific Ocean - Deep Water	0.990	0.990-0.995	Model Derived	Kroopnick and Craig (1976)
Pacific Ocean - Deep Water	0.987	0.982-0.996	Model Derived	Bender (1990)
Pacific Ocean - Surface Water	0.982	0.975-0.990	Model Derived	Knox (1993)
Bacteria	0.980	0.978-0.982	Incubations	Kiddon et al. (1993)
Microalgae	0.977	0.974-0.981		
Protozoa	0.981	0.977-0.986		
Mollusk	0.992	0.992-0.993		
Fish	0.993	0.992-0.995		
Amazon Basin - River and Lake Water	0.982	0.980-0.986	Incubations	Quay et al. (1995)
Lake Kinneret	0.977	0.971-0.980	Incubations	Luz et al. (2002)
Northern Gulf of Mexico	0.978	0.978-0.979	Incubations	Quinones-Rivera et al. (2007)
2nd Order Agricultural Creek -	0.987	0.982-0.991	Incubations	Tobias et al.
Midwestern USA	0.989	0.986-0.993	Model Derived	(2007)
Reservoir – Ontario	0.979		Model Derived	Venkiteswaran et al.
Wetland - Saskatchewan	0.985		Model Derived	(2007)
South Saskatchewan River	0.998		Model Derived	
Upper Kalamatch River, OR	0.992	0.990-0.994	Model Derived	Poulson et al. (2009)
Overall	0.985			

In a large impacted watershed such as the Grand River, DO consumption would occur in the water column, on surfaces, and in the sediments. Variation in the contribution of each to the total could result in different fractionation values. As noted in Chapter 2, model $\delta^{18}O\text{-}O_2$ was very sensitive to changes in α_r, contrary to Parker et al. (2005); insensitivity of α_r in this case may have been due to the low GPP and CR rates in the system studied. As the Grand River exhibits high rates of production and consumption, α_r has a much greater effect on changes in $\delta^{18}O\text{-}O_2$. In order to reconcile the mass balances of DO and $\delta^{18}O\text{-}O_2$ used to quantify biotic and physical controls on DO in the Grand River, accurate respiratory fractionation factors are therefore necessary. A series of *in vitro* and *in situ* investigations were conducted with the objective of empirically quantifying respiratory fractionation of O_2 under Grand River conditions.

6.2 Methods

6.2.1 Bottle Incubations

Dark incubations of water samples have typically been used to estimate fractionation during the consumption of DO in a variety of aquatic environments (Quay et al., 1995; Luz et al., 2002; Quinones-Rivera et al., 2007). In the Grand River, however, respiration could occur in both the water column and on or in substrate. Sampling location may also have an effect on α_r. For example, at the West Montrose location, DO dynamics reflect the upstream communities that are primarily impacted by agriculture. However, the Blair location is subjected to DO consuming materials from wastewater treatment plants and urban runoff, and generally has lower DO levels. Therefore, water and substrate were used from both of these locations for incubations measuring α_r.

Two bottle incubation trials were conducted; during August and September, 2004, water was sampled from approximately mid-channel in 20-L containers. The river channel substrate is a mixture of fine sediments and gravel. Therefore, the substrate was collected using a metal spade from random locations within the channel in attempt to minimize the effects of heterogeneity within the system. The samples were immediately transported back to the laboratory. Once in the laboratory, the water was transferred to reservoirs and all materials were placed in the dark. Water from each location was sparged with air for 30 minutes to ensure that the initial DO conditions were close to saturation before being transferred to the incubation bottles.

Four sets of 1-L bottles were assembled for each experiment. One set contained water from West Montrose, with another set containing water from Blair. The third and fourth sets contained both water and substrate from these locations. For the water incubations, the bottles were gently filled simultaneously by submerging them in the water reservoirs. The bottles were capped underwater and the bottles remained submerged in the dark for the remainder of the incubation. The remaining water in each reservoir was then immediately analysed for DO and a sample was collected for $\delta^{18}O\text{-}O_2$ to obtain time zero conditions. For the substrate/water incubations, approximately 150-200 g of sediment (wet weight) were added to each bottle and the bottles were immediately filled with water, capped, and re-submerged in a reservoir for incubation. The remaining water was also then immediately analysed for DO and a sample was collected for $\delta^{18}O\text{-}O_2$. The bottles were then sampled over time on a sacrificial basis and analysed for DO and $\delta^{18}O\text{-}O_2$. All incubations were performed in the dark at 20C.

In order to sample $\delta^{18}O\text{-}O_2$ from the incubation bottles, Tygon tubing and a three-way stopcock were used. A 10-ml syringe was attached to one stopcock port, an 18 gauge needle was attached to the second port, and the tubing was attached to the final port. Approximately 10 ml of water from the incubation bottle was drawn through the apparatus to remove any air and to purge the sample needle. The sample needle was then used to fill a 160 mL serum vial that had been sealed with butyl blue stopper and evacuated to 0.1 atm. A similar procedure was used to sample for DO. The 10 ml syringe was replaced by a 60 ml syringe. Water was drawn from the same incubation bottle using the syringe and tubing, and then gently expelled down the side of the titration bottle, so as not to introduce DO into the sample via atmospheric exchange. This was repeated until the 300 ml titration bottle was filled. Dissolved O_2 analyses were immediately performed by the Winkler titration method with an azide modification (APHA, 1995).

Dissolved O_2 and $\delta^{18}O\text{-}O_2$ were measured at the beginning and in each bottle sacrificed over time. The changes in DO concentration and $\delta^{18}O\text{-}O_2$ were applied to the Rayleigh distillation equation (Clark and Fritz, 1997) in order to determine α_r:

$$\ln\left(\frac{\delta+1000}{\delta_o+1000}\right) = (\alpha_r - 1) * \ln f \qquad (6.1)$$

Where δ is the isotopic signature of $\delta^{18}O\text{-}O_2$ in permil, δ_o is the initial isotopic signature of $\delta^{18}O\text{-}O_2$ at time zero, and f is the fraction of DO remaining in the reservoir. Changes in $\delta^{18}O\text{-}O_2$ and DO from the bottle incubation trials were subjected to linear regression using the

Rayleigh distillation equation (equation 6.1) to estimate α_r for each experimental trial. The intercept was set at zero, and the slope of the regression (equal to α_r-1) was used to calculate α_r.

6.2.2 Submerged Chamber Incubations

Chamber incubation experiments were also conducted *in situ*. The chambers were constructed by removing the bottom from 9-L polycarbonate bottles, similar to Scott et al. (1999). The chambers were covered with aluminum foil to create a dark interior, and equipped with a submersible motorized propeller assembly that rotated at 15 rpm to prevent concentration gradients from forming. Three locations on the Grand River watershed were studied: Swan Creek, Carroll Creek, and the main channel at BLR (Figure 6.1). Incubations could not be conducted in the main channel at WM or BRPT due to the composition of the stream bed which was characterized by gravel and rocks which made it impossible to install water-tight chambers. Swan Creek and Carroll Creek, both tributaries, were chosen due to their soft sediments and close proximity upstream to WM.

Two chambers were deployed simultaneously at the water sediment interface; the open bottom of each chamber was driven approximately 5 cm into the sediment layer and weighed down to isolate the chamber. Initial samples were collected for both DO and $\delta^{18}O\text{-}O_2$ via a sampling port located at the midpoint on the side of the vessel. Dissolved O_2 samples were collected with a 60 ml glass syringe fitted with an 18-gauge needle, and DO was analyzed via Winkler titration. An evacuated 160 ml serum vial and a two-way needle assembly were used to collect $\delta^{18}O\text{-}O_2$. The chambers were allowed to incubate for 2 to 3 h before collecting end-point DO and $\delta^{18}O\text{-}O_2$.

6.2.3 Model Calibrations

In addition to the *in vitro* and *in situ* incubation empirical approaches, the isotopic mass balance model was also used to determine α_r. Initial modeling simulations were conducted (Chapter 4) using the night portion of the diel data sets to remove P as an unknown variable; by removing one of the unknowns from the mass balance models, a smaller range of parameter combinations could be run to obtain an optimal model fit to observed DO and data. These k and CR rates from the night-time simulations were used, along with a range of Pmax and α_r values, to fit the observed DO and $\delta^{18}O\text{-}O_2$ values for a given full diel dataset (Chapter 5). Additional model-obtained α_r estimates were acquired from routine day sampling events (Chapter 5).

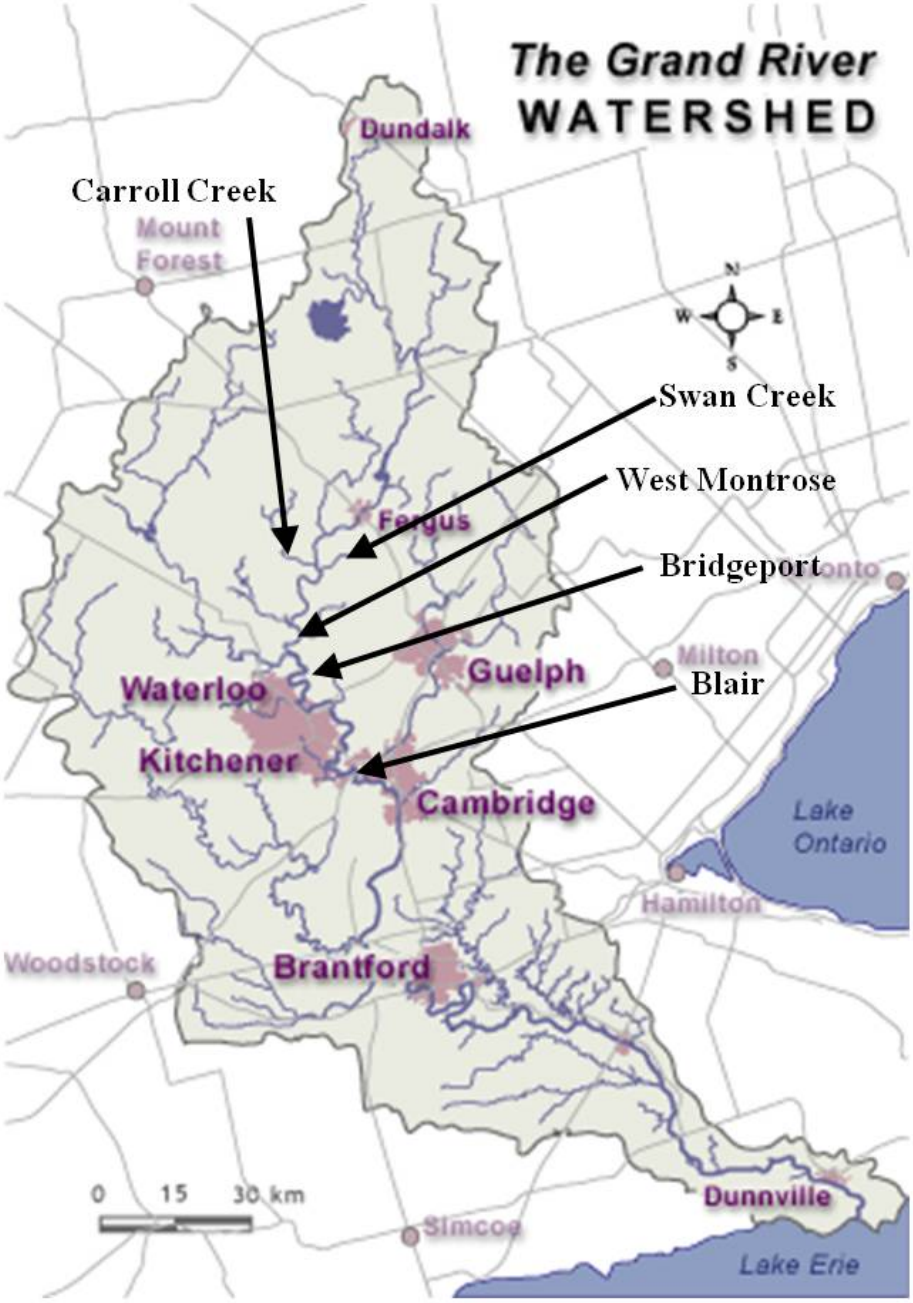

Figure 6.1 Locations studied for the estimation of α_r in the Grand River Watershed.

6. 3 Results

The calculated α_r obtained from the bottle incubation trials ranged from 0.988 to 0.998 and 0.991 to 0.998 for the first and second bottle incubation experiments, with an overall mean of 0.994 (Table 6.2 and Figures 6.2 and 6.3). The observed data were generally a poor fit to the regressions, with only three trials exhibiting R^2 values > 80%. The first bottle incubation experiment consisted of only three data points for regression, and had the highest variability (Figure 6.2). Incubations of bottles containing both water and substrate material appeared to exhibit greater variability compared to the water incubations according to results of the second experiment. In the experimental trials conducted using in situ submerged chambers, there was little to no isotopic enrichment detected with respect to $^{18}O\text{-}O_2$, despite declines observed in DO concentrations (Table 6.3).

Model derived α_r values (Table 6.4) appeared to exhibit some discernable trends. Pooling the data among the three sampling locations, the α_r values found from the diel and night data were similar. Fractionation values derived from the day data were significantly smaller than the night α_r values (two sample $t = -4.70$, and $p < 0.001$; Figure 6.4). Box-plots of the data (Figure 6.4) show that BLR α_r values tend to be closer to one, as compared to WM and BRPT which exhibit similar α_r. There were several anomalously low α_r estimates; 0.924 (WM May 11, 2004) and 0.952 (BRPT June 24, 2003) were associated with the greatest RMS error for $\delta^{18}O\text{-}O2$. However, overall, α_r derived from modeling day time data exhibited a wider range than α_r obtained from the night and diel model scenarios.

Table 6.2 Isotopic fractionation results obtained from the bottle incubation experiments.

Incubation Materials		Time (h)	DO (mg L^{-1})	$\delta^{18}O$-O_2 (‰)	f	α_r*	R^2 (%)
Experiment 1:	WM Water	0	8.18	20.30	1.00	0.988	18.9
		18.00	7.75	23.50	0.948	±0.025	
		44.75	7.25	23.63	0.887		
		115.75	5.58	24.10	0.682		
	BLR Water	0	7.85	21.62	1.00	0.995	91.9
		18.00	7.23	21.56	0.92	±0.003	
		44.75	6.10	22.80	0.78		
		115.75	5.00	23.96	0.64		
	WM	0	8.25	24.78	1.00	0.998	30.5
	Substrate + Water	1.75	5.00	25.18	0.61	±0.001	
		5.50	4.10	26.96	0.50		
		18.50	4.15	25.72	0.50		
	BLR	0	7.70	21.89	1.00	0.994	58.0
	Substrate + Water	1.25	6.00	22.06	0.78	±0.004	
		5.00	5.85	23.84	0.76		
		18.00	4.85	25.62	0.63		
Experiment 2:	WM Water	0.00	8.13	27.84	1.00	0.995	87.5
		118.50	6.05	28.97	0.74	±0.001	
		139.50	5.90	30.15	0.73		
		165.50	5.30	30.79	0.65		
		188.50	4.90	30.58	0.60		
		262.50	4.40	30.32	0.54		
		354.75	3.10	32.21	0.38		
		378.75	2.50	33.86	0.31		
	BLR Water	0.00	8.10	26.48	1.00	0.991	83.8
		67.00	5.90	29.28	0.73	±0.001	
		68.75	5.85	29.69	0.72		
		90.75	5.05	31.61	0.62		
		91.00	4.60	33.08	0.57		
		118.50	4.35	31.57	0.54		
		139.75	4.20	32.67	0.52		
		165.50	3.80	33.52	0.47		
	WM	0.00	8.18	27.86	1.00	0.998	59.2
	Substrate + Water	2.00	6.75	28.79	0.83	±0.002	
		18.50	5.45	28.73	0.67		
		19.25	4.20	32.18	0.51		
		25.50	4.10	30.10	0.50		
		44.00	0.50	31.11	0.06		
		44.75	3.35	34.34	0.41		
		68.00	1.40	30.83	0.17		
		69.25	2.20	33.14	0.27		
	BLR	0.00	8.50	27.02	1.00	0.995	27.2
	Substrate + Water	18.50	4.00	35.32	0.47	±0.003	
		25.00	3.10	31.34	0.36		
		43.75	4.35	29.40	0.51		
		44.00	4.25	31.12	0.50		
		67.75	2.70	31.32	0.32		

* ± standard deviation

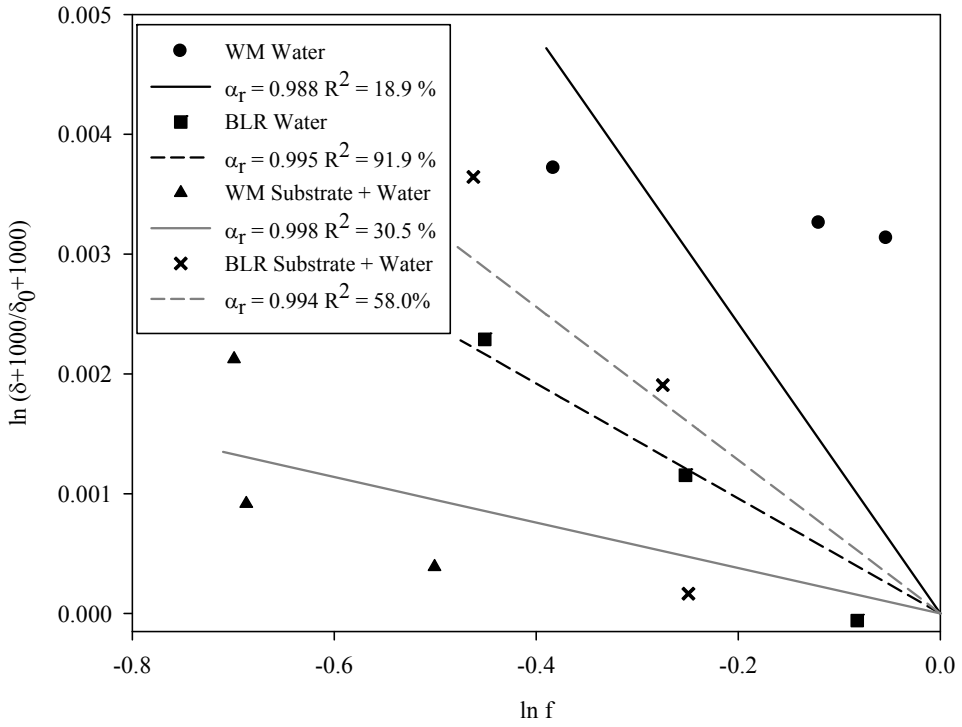

Figure 6.2 Regression results from the first bottle incubation experiment.

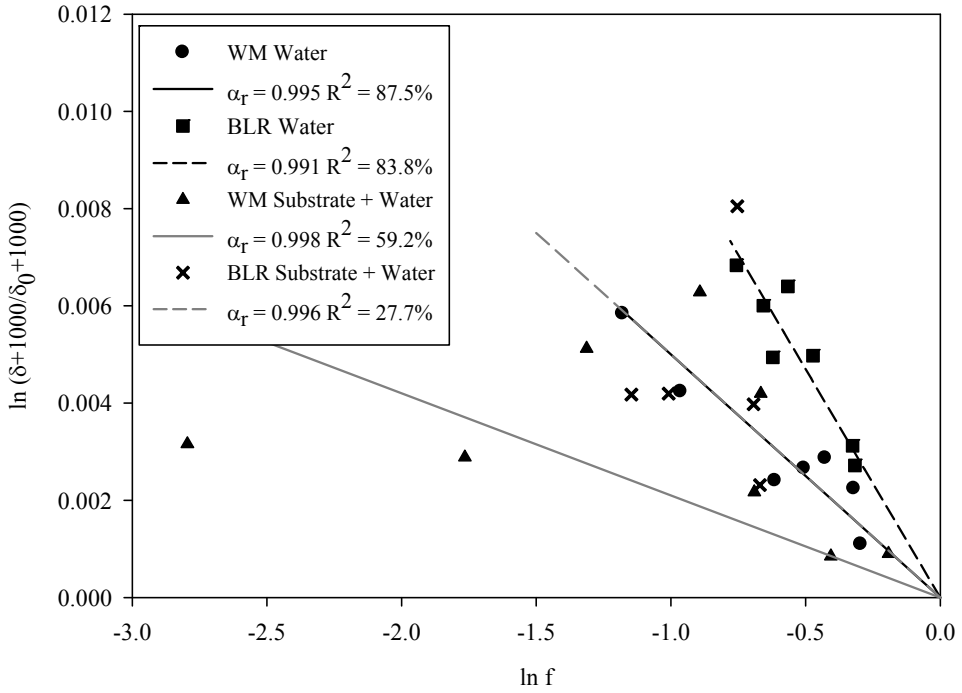

Figure 6.3 Regression results from the second bottle incubation experiment.

Table 6.3 Isotopic fractionation results obtained from submerged chamber trials.

Location			**DO** ($mg\ L^{-1}$)	**$\delta^{18}O$-O_2** (‰)	**f**	**α_r**
Swan Creek	Trial 1	Initial	9.60	14.3	0.77	1.002
		Final	7.35	13.7		
	Trial 2	Initial	15.3	9.88	0.84	1.000
		Final	8.10	9.86		
Carroll Creek	Trial 1	Initial	8.78	21.3	0.75	0.998
		Final	7.20	21.9		
	Trial 2	Initial	9.55	20.0	0.91	1.009
		Final	8.75	19.1		
Blair	Trial 1	Initial	9.78	11.5	0.80	0.996
		Final	7.65	12.4		
	Trial 2	Initial	9.60	12.2	0.74	1.004
		Final	7.15	11.0		
					Mean	1.002
					Standard Deviation	0.005

Table 6.4 Isotopic fractionation estimates from modeling data obtained form the day only and diel DO and $\delta^{18}O$-O_2 sampling events.

	Location	Date	α_r	Mean DO (mg L^{-1})	Mean DOsat (mg L^{-1})	Mean % DOsat	Mean $\delta^{18}O$-O_2 (‰)	RMS DO (mg L^{-1})	RMS $\delta^{18}O$-O_2 (‰)
Day	WM	Sept 17, 2003	0.964	11.14	9.15	121.8	19.33	0.27	0.87
		Oct 27, 2003	0.964	12.19	11.75	103.7	23.42	0.20	0.61
		Dec 10, 2003	0.942	14.11	13.18	107.1	24.49	0.18	0.34
		May 11, 2004	0.924	11.67	9.88	118.1	24.70	0.11	3.91
		Jun 8, 2004	0.960	9.98	8.89	112.3	21.76	0.06	0.08
		Jul 29, 2004	0.982	9.52	8.59	110.8	17.66	0.48	0.75
		Aug 31, 2004	0.972	9.55	9.00	106.1	21.00	0.11	3.91
		Oct 28, 2004	0.962	12.02	11.03	109.0	21.80	0.21	1.21
	BRPT	May 29, 2003	0.964	12.15	9.80	124.0	17.28	0.13	0.30
		Jun 24, 2003	0.952	10.20	8.13	125.5	16.19	0.14	4.35
		July 29, 2003	0.976	11.09	8.40	132.1	14.65	0.15	0.03
		Sept 17, 2003	0.960	11.11	8.95	124.2	18.61	0.19	2.47
		Oct 27, 2003	0.948	11.16	11.72	95.20	25.74	0.23	0.63
		Dec 10, 2003	0.944	14.26	13.21	107.9	24.69	0.19	0.05
		Jul 29, 2004	0.970	9.69	8.41	115.2	17.80	0.66	1.23
	BLR	May 29, 2003	0.976	9.38	9.64	97.29	19.63	0.41	0.08
		Jun 24, 2003	0.938	12.13	7.92	153.2	20.45	0.36	0.56
		Jul 29, 2003	0.992	8.91	8.28	107.6	12.76	0.15	0.31
		Sep 17, 2003	0.998	6.58	8.78	74.92	18.26	0.02	0.10
		Oct 27, 2003	0.970	10.24	11.56	88.56	26.62	0.09	0.39
		Jul 29, 2004	0.986	7.10	8.41	84.41	19.34	0.09	0.43
		Oct 28, 2004	0.990	7.73	10.61	72.85	22.10	0.16	0.98
Diel Night	WM	May 28, 2003	0.988	8.44	10.10	83.56	25.01	0.03	0.10
		Jun 24, 2003	0.987	5.44	8.71	62.46	27.52	0.12	0.73
		Jul 29, 2003	0.986	6.84	8.98	76.17	26.74	0.04	0.72
		Aug 13, 2003	0.983	6.26	8.58	72.96	29.01	0.04	0.54
		Jun 27, 2005	0.990	6.90	9.28	74.35	24.89	0.16	0.27
	BRPT	Jul 9, 2003	0.986	7.45	7.88	94.54	24.17	0.26	0.21
		May 11, 2004	0.980	9.65	9.23	104.6	27.22	0.18	0.77
		Jun 7, 2004	0.984	7.24	8.60	84.19	26.17	0.35	0.91
		Aug 30, 2004	0.971	7.06	8.92	79.15	28.56	0.05	3.21
	BLR	Jun 7, 2004	0.989	4.55	8.94	50.89	28.66	0.09	0.53
		Aug 30, 2004	0.989	4.16	9.18	45.31	29.16	0.09	0.29
		Jul 29, 2005	0.996	1.98	8.78	22.58	25.58	0.19	2.04
Full Diel	WM	May 28, 2003	0.987	11.21	9.70	115.6	19.36	0.33	0.92
		Jun 24, 2003	0.984	8.91	8.20	108.6	20.26	0.32	3.11
		Jul 9, 2003	0.981	9.49	8.13	116.6	19.34	0.33	2.83
		Jul 29, 2003	0.984	9.43	8.53	110.6	20.31	0.41	1.71
		Aug 13, 2003	0.978	9.82	8.02	122.4	21.18	0.50	3.87
	BRPT	Jul 9, 2003	0.983	9.36	7.78	120.3	17.24	0.51	2.91
		May 11, 2004	0.968	11.32	9.36	120.9	22.40	0.72	2.60
		Jun 7, 2004	0.976	8.29	8.44	98.15	23.55	0.30	1.75
		Aug 30, 2004	0.968	7.68	8.88	86.55	27.22	0.19	2.72
	BLR	Jul 9, 2003	0.993	4.65	8.05	57.77	18.45	0.64	1.63
		Jun 7, 2004	0.983	6.45	8.33	77.44	23.68	0.59	3.46
		Aug 30, 2004	0.987	5.06	8.73	57.97	25.78	0.18	1.78

Table 6.5 Descriptive statistics for Grand River α_r obtained from the fitted model results.

Modeling Event	Location	N	Mean	Standard Deviation	Minimum	Maximum	Median
Day	WM	8	0.959	0.019	0.924	0.982	0.963
	BRPT	7	0.959	0.012	0.944	0.976	0.960
	BLR	7	0.979	0.020	0.938	0.998	0.986
Night	WM	5	0.987	0.003	0.983	0.990	0.987
	BRPT	4	0.980	0.007	0.971	0.986	0.982
	BLR	3	0.991	0.002	0.989	0.996	0.989
Diel	WM	5	0.983	0.003	0.978	0.987	0.984
	BRPT	4	0.974	0.004	0.968	0.983	0.972
	BLR	3	0.988	0.005	0.983	0.993	0.987
All Locations	Day	22	0.965	0.019	0.924	0.998	0.964
	Diel	12	0.981	0.007	0.968	0.993	0.983
	Night	12	0.986	0.006	0.971	0.996	0.986

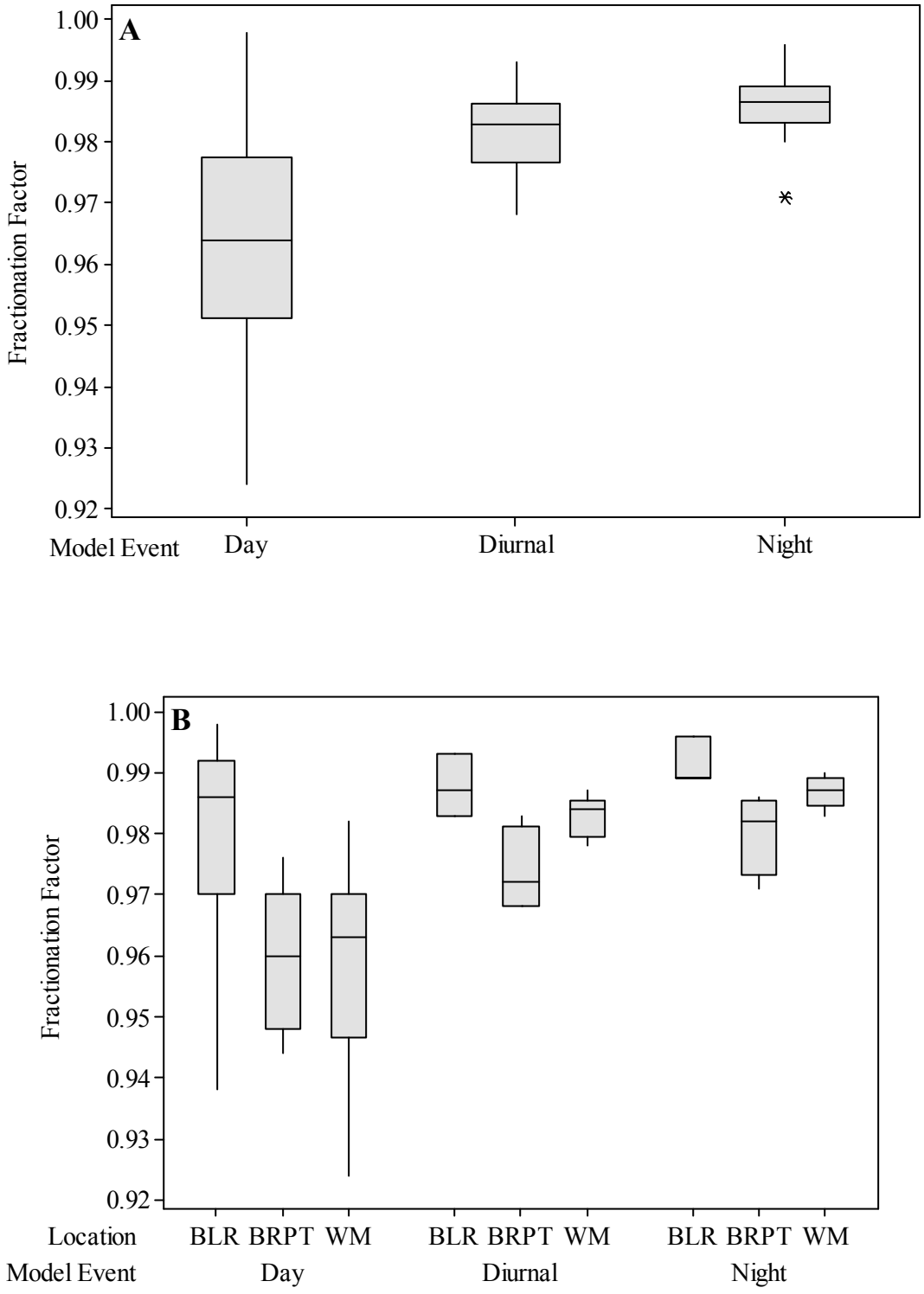

Figure 6.4 Box and whisker plots of Grand River α_r obtained from the fitted model results, by model event (A) and subdivided by sampling location (B). * indicates an outlier in the data.

6.4 Discussion

Laboratory bottle incubations, submerged chamber trials, and model simulations yielded a wide range in α_r values. The α_r estimates obtained from the bottle incubations overall tended to be greater than values previously reported for other river systems. Minimal fractionation was also observed in the chamber trials at all sites studied. Amazon River water incubations yield α_r values from 0.980 to 0.986 (Quay et al., 1995), while Tobias et al., (2007) estimated a range of 0.982 to 0.991 from incubations of core and slurry samples from a mid-western agricultural stream.

The lack of apparent preference of the DO consuming community for the lighter DO isotope in the submerged chambers, and bottles containing substrate, may be due to diffusion limitation. Water in the submerged chambers, despite the addition of the propeller apparatus, would not be mixing in the same manner as in an unconfined state. Respiratory fractionation values approaching 1.0 have been associated with deep ocean environments (Kroopnick and Craig, 1976) as well as coastal marine sediments (Brandes and Devol, 1997). Bender (1990) notes that α_r can theoretically be as high as 1.000 in sediments and particle aggregates if DO is totally consumed. Brandes and Devol (1997) noted an average α_r of 0.997 in coastal marine sediments and reasoned that respiration in the deposits was occurring in discrete microsites surrounded by diffusive layers. In order for DO consuming bacteria to alter the isotopic composition of the overlying DO reservoir, sediment $\delta^{18}O\text{-}O_2$ would have to be altered by consumption in the sediments but exchanging with the water column. However, if all DO diffusing into the sediments is consumed, there would be no influence on the pool in the water column.

Preliminary modeling attempts indicated that the range in α_r measured via the incubations did not replicate the observed $\delta^{18}O\text{-}O_2$ data. Fractionation characteristics of DO consumption in confined small-scale bottles did not reflect field-scale DO consumption, likely due to disturbance of river substrates, inadequate representation of the entire respiring community, and artificial *in vitro* conditions regarding conditions such as hydrology, temperature, CR rates, and DO regime. The rate of DO decline in the water incubation bottles (average of 0.6 mg O_2 L^{-1} d^{-1}) were an order of magnitude slower than in bottles containing substrate and observed in the field data, and did not represent DO consumption occurring at the community level. Community DO consumption in the Grand River is likely occurring at a higher rate on surfaces and in the bed substrate than in the water column. Faster rates of DO decline (average of 9 mg O_2 L^{-1} d^{-1}) were noted in the incubation bottles containing both substrate material and water, but the associated α_r were still greater than 0.994, and not in agreement with the range of α_r noted from the modeling events.

Other studies of this nature (Tobias et al., 2007; Venkiteswaran et al., 2007) have used model optimization as a means to obtain system-appropriate α_r in the absence of precise empirical estimates. Grand River α_r values (Table 6.4) obtained from the diel and night time model optimizations spanned the entire range of, but were in agreement with, findings noted in other investigations. The overall model-derived α_r values ranged from 0.942 to 0.998 (Table 6.5). The Grand River exhibits high rates of DO consumption and high variability in DO concentration (Chapter 5). The modeled α_r and DO consumption characteristics noted in the present study are representative of upstream influences which would integrate a variety of reactions and transport characteristics that may lead to a wide range in α_r. Reported α_r for a number of biological O_2 consuming pathways include microbial and larger organism

respiration, ranging from around 0.971 to 0.995, depending on enzyme or diffusion limitations (Table 6.1), as well as plant respiration pathways which exhibit a range around 0.975-0.985 (Guy et al., 1989; Raven and Beardall, 2005).

Box plot analysis, separating the α_r results by location and modeling time period (Figure 6.4), indicated that the WM and BRPT locations were similar to one another, and tended to exhibit stronger fractionation than BLR. The fractionation similarities between WM and BRPT are consistent with the two sites also exhibiting similar DO metabolism characteristics, as noted in Chapter 5. The BLR location is characterized (Chapter 5) by greater CR rates, lower overall DO minima, and greater heterotrophy than the upstream sites. The river upstream of BLR would be subject to additional biological, nitrogenous, and inorganic DO demands due to effluent loadings from the upstream wastewater treatment plant inputs and urban runoff. Considering that Clark and Fritz (1997) report that there is also no significant fractionation associated nitrification, higher α_r values at BLR may be attributable to factors nitrification of NH_4-N inputs, and a greater influence of sedimentary respiration with little associated fractionation (Bender, 1990; Brandes and Devol, 1997).

Modeling the day sampling data yielded a wider range in α_r estimates than for night or diel simulations, containing values that were much lower than have been reported previously. The lowest published instances of α_r , about 0.969, have been attributed to plant respiration via the alternative oxidase pathway (Robinson, 1992). At the community level, the lowest measurements of α_r were in Pacific Ocean surface water (0.968, Kroopnick, 1975) and in Lake Kinneret (0.971, Luz et al., 2002). Visual examination of the diel model fitted curves (Chapter 5) indicated that for events with greater $\delta^{18}O$-O_2 RMS values (Table 6.4) the observed data

were underestimated by the model during the day, and overestimated at night, despite the model having good agreement with DO concentration data. When fitting the diel model scenarios, a constant α_r was used; this would represent an average daily fractionation. In order to force the model to better mimic the observed $\delta^{18}O\text{-}O_2$, α_r would have to be lower during the day and higher at night (Table 6.6), which would coincide with the discrepancy between the night and day model derived α_r trends noted in Figure 6.4.

Dissolved O_2 concentrations and day time conditions appear to affect the range of α_r exhibited by the Grand River. The discrepancy of α_r among the day and night model simulations may be related to changes in DO concentrations during each of these time periods (Figure 6.5). There were weak relationships between DO and diel α_r (R^2=19.2%) and the night portion of the diel data (R^2=35.4%). However, the relationship between α_r and DO appears to be more pronounced under day time conditions. When modeling the day and night portion of the diel models separately, mean DO appears to exhibit a greater influence on day time α_r than night time α_r (Table 6.6; Figure 6.5). The R^2 (62.9%) and slope associated with regressing α_r against mean DO were greatest for the routine day sampling results. Guy et al. (1989) noted a linear increase in soybean respiration discrimination for ^{16}O as mean O_2 concentration increased. Bender (1990) also noted a trend in community α_r, with greater fractionation ($\alpha_r \sim$ 0.987) occurring in moderately undersaturated regimes (DO > 74% saturation) with less fractionation ($\alpha_r \sim 0.996$) associated at greater undersaturations. As mean DO concentrations increase, the preference for the lighter ^{16}O isotope may rise, leading to a lower inferred α_r value.

Table 6.6 Comparison of model-obtained α_r values obtained from fitting the $\delta^{18}O\text{-}O_2$ output to the full, night portion, and day portion of diel data sets, assuming the same k, CR, and GPP conditions.

Location	Date	α_r Fitted to Full Diel	Mean Diel DO (mg L^{-1})	α_r Fitted to Night Portion	Mean Night DO (mg L^{-1})	α_r Fitted to Day Portion	Mean Day DO (mg L^{-1})
WM	May 28, 2003	0.987	11.21	0.988	8.44	0.980	13.10
	Jun 24, 2003	0.984	8.91	0.987	5.44	0.975	10.85
	Jul 29, 2003	0.984	9.43	0.986	6.84	0.972	11.04
	Aug 13, 2003	0.978	9.82	0.983	6.9	0.965	12.00
BRPT	Jul 9, 2003	0.983	9.36	0.986	7.45	0.977	10.17
	May 11, 2004	0.968	11.32	0.980	9.65	0.942	12.36
	Jun 7, 2004	0.976	8.29	0.984	7.24	0.966	8.96
	Aug 30, 2004	0.968	7.68	0.971	7.06	0.965	8.23
BLR	Jul 9, 2003	0.993	4.65	0.989	4.55	0.991	6.59
	Jun 7, 2004	0.983	6.45	0.989	4.16	0.973	7.67
	Aug 30, 2004	0.987	5.06	0.996	1.98	0.984	6.02

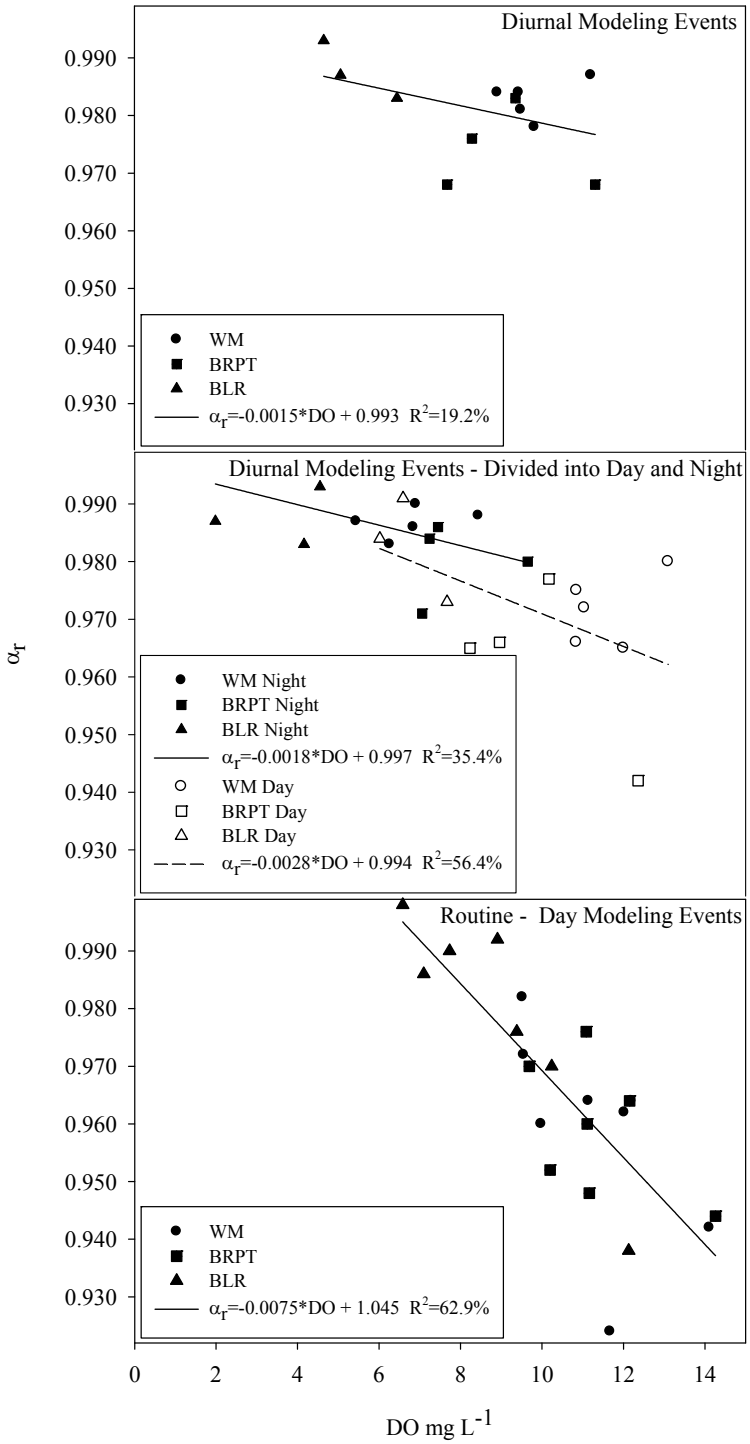

Figure 6.5 Relationship between α_r and mean concentration of DO in the Grand River. Each data point was calculated based on the α_r paired with the mean DO concentration calculated for a particular modeling time period.

Day time data tended to exhibit higher mean DO concentrations than at night, which may be leading to greater α_r values. Diel model results would represent the mean of day and night conditions, and appear to be around the mid-point of the full range in DO and α_r values. Mean DO concentrations also tended to be lower at the BLR location, which coincided with higher α_r values (Figure 6.5), providing an additional explanation for the sampling location separation noted in the box-plot analysis (Figure 6.4).

For each model event, a wide range of parameter magnitudes were tested across a full range of α_r values. Due to the coupling of two mass budgets, DO concentration and $\delta^{18}O\text{-}O_2$, the optimal-fit α_r values were relatively narrow in range when paired with a range of potential k, CR and Pmax values, under the model assumptions of constant CR_{20} and k_{20}. The routine day modeling events were based on relatively sparse data, and model outputs were fitted to only 3 or 4 observed data points. The lower α_r estimates obtained for the routine day modeling events could possibly be an artifact of the modeling approach used; for example, if CR was underestimated for a given time period (and thus GPP underestimated to maintain the same balance in DO concentration) a lower α_r value would have to then be assumed to reconcile the $\delta^{18}O\text{-}O_2$ budget. There also may be processes occurring during day time conditions that are contributing to the DO and $\delta^{18}O\text{-}O_2$ dynamics, such as photorespiration and photodegradation, that could cause shifts in α_r estimates.

The model obtained α_r values appear to be within the range reported in the literature up to mean DO of approximately 9 mg L^{-1} in the Grand River, which would mainly represent undersaturated and relatively lower DO conditions. The Grand River watershed has been shown in Chapter 4 to exhibit uniquely high DO production and consumption rates as

compared to a number of other systems that are less impacted. During the daylight hours in the Grand River, productivity levels are great enough to induce DO supersaturated conditions, with maxima reaching up to approximately 15 mg L^{-1}, while night DO minima can fall to less than 2 mg L^{-1}. In such a dynamic system, a constant diel α_r may not be sufficient to adequately represent the mechanisms at hand. Isotopic fractionation under very high DO, or supersaturated, conditions has not yet been identified or addressed in published literature. Under high DO conditions, the respiring communities could exhibit lower α_r values simply due to the fact that there is an abundance of lighter isotopes for consumption. The model derived α_r values presented in this study are reflective of DO consumption occurring at the community level; it would be reasonable to assume that under varying conditions α_r may also change. Nevertheless, isotopic fractionation mechanisms under highly productive systems are still an enigmatic subject that requires further investigation.

7.0 Conclusions and Recommendations

The primary goals of this research were to investigate the applicability of using $\delta^{18}O\text{-}O_2$, along with DO concentrations, to quantify rates of CR, GPP, and k in a large impacted river. Primary production and respiration are key factors determining ecosystem biomass and are the central regulators of nutrient cycling in aquatic environments on both local and regional scales (Bott et al., 1985; Mulholland et al., 2001; Tobias et al., 2007).

There is a general shortage of information on the functioning of heavily impacted rivers and streams with respect to the production and consumption of DO. The characterization of DO dynamics in aquatic ecosystems has recently incorporated the use of stable isotopes of O_2 as quantitative support for measuring rates of metabolism. Previous reach and watershed-scale investigations of river metabolism have been primarily based on Odum's (1956) initial technique (Marzolf et al., 1994; Edwards and Meyer, 1987; Mulholland et al., 2001) that relies on monitoring changes in DO, accounting for atmospheric exchange.

The use of O_2 isotopes to aid in the quantification of DO dynamics in aquatic ecosystems is relatively new. Previous applications have assumed steady state conditions where neither DO nor $\delta^{18}O\text{-}O_2$ varied considerably over the given time period in question (Quay et al., 1995; Wang and Veizer, 2000; Russ et al., 2004), or used DO curve-fitting techniques to estimate k, CR and GPP, then applied these values to the steady state equations to generate $\delta^{18}O\text{-}O_2$ values for comparison to observed data (Parker et al., 2005). However, these approaches are not valid for impacted systems that exhibit a large variation in DO over a given time period of interest. Recently, numerical time-forward mass balance approaches that simulate changes in DO concentration and $\delta^{18}O\text{-}O_2$, while minimizing differences between

simulated and observed data have been presented by Venkiteswaran et al. (2007) and Tobias et al. (2007).

The focus of this study was the Grand River watershed, the largest watershed in southwestern Ontario. The Grand River receives discharges from sewage treatment plants, as well as non-point inputs from agricultural and urban sources. Due to the agricultural and urban impacts, the Grand River exhibits strong diel fluctuations in both $\delta^{18}O\text{-}O_2$ values and DO concentrations. Much of the non-steady state $\delta^{18}O\text{-}O_2$ modeling work has been based on only a few diel sampling events, and in either smaller or less impacted systems than in the Grand River. There also appears to be a shortage of information relating to the metabolic response of rivers and streams upstream and downstream of wastewater treatment plant loading (Gucker et al., 2006; Ruggiero et al., 2006). The current study was a unique opportunity to both 1) investigate the applicability of the $\delta^{18}O\text{-}O_2$ approach in a dynamic system, with frequent sampling events conducted over a longitudinal gradient, and 2) gather information on the metabolic functioning of a river impacted by both agricultural and urban catchment influences.

The three monitoring locations in this study, West Montrose (WM), Bridgeport (BRPT), and Blair (BLR), were chosen to study DO dynamics as the river moved from a predominately agricultural landscape to areas of increasing inputs from urban activity. A non-steady state dual mass-balance model was developed and the data collected were used to calibrate the model in order to quantify GPP and CR rates, and k values. This study represents the first published estimates of GPP, CR, and k for the Grand River. In addition, this is the first research containing both DO and $\delta^{18}O\text{-}O_2$ data collected from early spring through December over several years, and that attempted to use both diel changes as well as a limited number of sampling points to quantify metabolism rates.

7.1 Summary of Main Conclusions and Contributions to Research

7.1.1 Gas Exchange

Gas exchange can be an important component of the DO balance in rivers, maintaining DO balances near equilibrium and mitigating the effects of high demand for O_2. There is a wide variety of approaches for estimating gas transfer coefficients (k) in rivers that yield varying results. Previous studies using isotopic techniques for studying river DO dynamics have assumed steady state conditions (Quay et al., 1995; Wang and Veizer, 2000), used DO concentration regression to obtain k (Parker et al., 2005), or conducted concurrent tracer addition experiments (Tobias et al., 2007). It is of particular interest to investigate the applicability of using the stable isotopes of O_2 as a tool to determine k in large, impacted rivers where tracer techniques may be considered to be difficult to use.

Gas transfer coefficients were estimated using the isotopic approach on the night portion of data obtained during diel sampling events; this was done to remove the effects of GPP in order to narrow the range of k and CR that could explain changes in DO and $\delta^{18}O\text{-}O_2$. Grand River k ranged from 3.6 to 8.6 day^{-1} and were relatively constant at each location over the range of discharge conditions studied. The range in discharge observed is mainly representative of non-storm and summer low-flow periods; a greater range in k might be observed under a wider range of hydrologic conditions. However, from a water quality management perspective, low-flow conditions are the times of highest concern where gas transfer would be a key factor in mitigating DO deficits due to O_2 demand.

The k values obtained with the isotope model for the Grand River were found to be generally lower than predicted by various hydrology-dependent equations and by the DO night

regression technique. Varying temperature appears to cause k obtained from night regression analysis to deviate from that estimated via the isotope approach. Thus, the non-steady state isotope modeling technique appears to offer an advantage in simulating dynamic changes in DO regime as compared to traditional regression techniques. The fitted model outputs were able to explain the changes in both DO and $\delta^{18}O\text{-}O_2$. These findings highlight the importance of determining site-specific values of k, as opposed to relying on empirical equations derived from other river systems.

The potential over-estimation of k in large, impacted rivers should be taken into consideration when making management decisions, as it could lead to error in respiration estimates, and under-prediction of DO deficits. The addition of the isotopic mass balance to the DO concentration model provided a constraint on the potential range of model parameters that could generate a particular DO pattern, allowing for the selection of parameters that optimize the fit of both models to the observed field data.

7.1.2 Dissolved O_2 Dynamics and River Metabolism

Overall, the results in the main channel of Grand River indicated that both agricultural and urban inputs from the surrounding area are impacting the watershed. Rates of GPP and CR at all locations were found to be elevated compared to relatively unimpacted systems. The metabolism rates in the Grand River (GPP = 2.2 to 19.9 and CR = 4.0 to 29.6 g O_2 m^{-2} d^{-1}) were much higher than published estimates for relatively undisturbed systems. There was a seasonal variation in GPP, most strongly correlated with irradiance, at all three sampling locations along the Grand River.

The CR rates were more seasonally consistent than GPP rates, with only a moderate declining trend from May to December in both 2003 and 2004. There was a positive relationship between community respiration and mean daily temperature, but temperature explained only 13.3 % of the variability, likely due to other factors influencing CR, such as biomass. The BLR site exhibited the highest rates of CR, on average 7.2 g O_2 m^{-2} d^{-1} higher than measured upstream at WM and BRPT, due to the additional input of nutrients and DO consuming substances from upstream wastewater treatment plant discharges and urban runoff.

The upstream locations of WM and BRPT tended to exhibit similar characteristics in both P:R, as well as $\delta^{18}O$-O_2 and DO cross plot ellipses, while BLR exhibited a distinctly different profile due to increased impact. There was a seasonal variation in P:R with the highest ratios occurring in the spring and summer, and subsequent declines in the fall. Autotrophic production appears to be a more important energy base upstream of WM and BRPT, as indicated by the greater P:R values, as well as more positive NP rates, as compared to upstream of BLR, where net production was consistently below zero. As evident by the low DO concentrations at BLR, DO inputs are not sufficient to overcome the oxidative demands upstream of this location to maintain adequate minimum DO concentrations during summer months.

This research has provided some insight into how DO in the Grand River could be effectively managed. Gas exchange processes do not appear to be large enough to mitigate DO deficits; therefore physical hydrological control management strategies are likely not to be effective. The Grand River exhibits nutrient concentrations that exceed meso-eutrophic and eutrophic trigger levels, as well as elevated GPP and CR rates, indicating that nutrient loading is having an important impact on the metabolism and functioning of the river. A combination

of agricultural and urban beneficial management practices would need to be applied throughout the watershed in order to address these issues. Specific beneficial management practices would have to be evaluated on a sub-catchment level, but could include practices such as nutrient management planning, treatment plant upgrades, buffer zones, and storm water treatment systems.

7.1.3 Isotopic Fractionation During DO Consumption

Information regarding to what extent O_2 fractionates during community respiration in rivers is sparse. Previous researchers using $\delta^{18}O\text{-}O_2$ to study community metabolism in lotic systems (Quay et al., 1993; Wang and Veizer, 2000; Parker et al., 2005) have assumed that α_r maintains a relatively constant value of 0.982 based on bottle incubations conducted in the Amazon River (Quay et al., 1993). This α_r is representative of DO consumption associated with the water column and may not be applicable to systems that have proportionally greater consumption occurring in sediments or via different organisms and consumption pathways. Fractionation of O_2 exhibits a range of values in different organisms and varying environments. Published values have been reported from 0.971 to 0.998 for a variety of aquatic organisms and communities.

In a large impacted watershed such as the Grand River, variation in the contribution of processes occurring in the water column, on surfaces, and in the sediments to total DO consumption could result in different α_r. In order to reconcile the mass balances of DO and $\delta^{18}O\text{-}O_2$ used to quantify biotic and physical controls on DO in rivers, more information as to the extent to which O_2 fractionates when consumed is needed. A series of *in vitro* and *in situ*

investigations were conducted with the objective of quantifying α_r under Grand River conditions.

In general, the α_r estimates obtained from the bottle incubations tended to be greater than values previously reported for other river systems. The α_r calculated from the bottle incubation experiments with the lowest experimental regression errors ranged from 0.991 to 0.995. In the submerged chambers, there was little to no isotopic enrichment detected with respect to $\delta^{18}O\text{-}O_2$, despite declines observed in DO concentrations. The lack of apparent preference of the DO consuming community for the lighter DO isotope may have been due to diffusion limitation and low DO concentrations. The model-derived α_r values mainly ranged from 0.942 to 0.998. The BLR α_r values tended to be closer to one, as compared to WM and BRPT which exhibited lower, and similar, α_r. Higher α_r values at the BLR site may be attributable to a combination of higher rates of CR, nitrification, low DO concentrations, and a greater influence of sedimentary respiration with little associated fractionation. Model derived α_r values found from the diel and night data were similar (as they were obtained from the same sampling events), while α_r derived from the routine day modeling were markedly lower.

The discrepancy of α_r among the day and night model simulations may be related to changes in DO concentrations or due to DO consumption characteristics under day conditions. There were weak relationships between DO and diel α_r (R^2=19.2%) and the night portion of the diel data (R^2=35.4%). However, the relationship between α_r and DO is more pronounced for the routine sampling events that were conducted under day conditions (R^2=62.9%). The model derived α_r values presented in this study are reflective of DO consumption occurring at the community level; it would be reasonable to assume that under varying DO regimes that α_r may also change. Isotopic fractionation under high DO conditions has not yet been identified or

addressed in published literature. Under high DO conditions, the respiring communities could exhibit lower α_r values due to the abundance of the lighter isotopes for consumption. The lower α_r estimates obtained for the routine day modeling events could also possibly be an artifact of the modeling approach used; for example, if CR was underestimated for a given time period (and thus GPP underestimated to maintain the same balance in DO concentration) a lower α_r value would have to then be assumed to reconcile the $\delta^{18}O\text{-}O_2$ budget. There may be processes also occurring during high irradiance conditions that are contributing to the DO and $\delta^{18}O\text{-}O_2$ dynamics that may cause shifts in α_r estimates, such as photorespiration and photodegradation, which were not reflected in the model assumptions. Isotopic fractionation mechanisms under highly productive systems are still a subject that requires further investigation.

7.1.4 Evaluation of the Isotope Technique for DO Modeling

In the current study, the applicability of using $\delta^{18}O\text{-}O_2$ to supplement DO concentration monitoring for the quantification of DO dynamics in a large impacted river was assessed. The technique was applied to a series of sampling locations on a longitudinal gradient that were subject to increasing levels of impact due to agricultural and urban influences, in an attempt to provide a more in-depth, comprehensive evaluation than provided by previous research. There will always be a certain degree of uncertainty associated with model parameters that have been determined by fitting a multi-parameter mathematical model to observed data. Evaluation of the isotope-modeling approach was performed by demonstrating agreement between observed and predicted data, as well as by sensitivity analysis to understand the general behaviour of the

model. The effects of uncertainty were also quantified to provide some context as to the predictive capability of the approach.

The model fit results from the diel sampling events indicated that the model explained >93% of the variability in DO concentrations but there was greater uncertainty associated with $\delta^{18}O\text{-}O_2$. The uncertainty analysis indicated that using k obtained from night data regression resulted in metabolism rates in the upper range of all isotope model estimates, while results obtained from simply running a range of potential parameter values and fitting output to observed DO led to lower estimates of GPP and CR. The range of parameter values to describe changes in DO in the Grand River may be unique and exhibit a relatively small range. The overall error in CR and GPP associated with the isotopic modeling technique appears to be approximately 10% when RMS error < 0.83 mg L^{-1} for DO and < 2.76‰ for $\delta^{18}O\text{-}O_2$. This may not be the case in less impacted systems that generate less dynamic changes in DO.

Model deviation from the observed data could be due to 1) the assumption of constant α_r and CR_{20}, 2) GPP does not follow the assumed sinusoidal curve, or 3) the model may be missing a process that causes a shift in $\delta^{18}O\text{-}O_2$. For example, CR rates could be changing over a diel cycle beyond that due to temperature changes due to responses to labile DOC produced during GPP, or increases in photorespiration accompanying high day time irradiance and DO conditions. Input parameter uncertainty and sensitivity most likely reflect the dynamic processes occurring in the Grand River watershed. As sampling was conducted at one point over time, the model results reflect an integration of all upstream influences affecting the DO dynamics of the system. Given the dynamic nature of DO production and consumption processes in the Grand River, and the spatial scale over which inferences are being made, and

invoking rates that vary only with temperature, the isotopic mass balance approach presented here models the variability in DO and $\delta^{18}O\text{-}O_2$ reasonably well.

The advantage of the isotope technique is the provision of a corroboration of the input parameter estimates between the two balances, which constrains the range of potential input values. The extra mass balance is able to then provide a greater level of confidence in the selection of model input values compared to traditional curve fitting methods or calibration procedures. A current drawback to this approach is that sampling can be labourious and expensive. Dissolved O_2 concentrations, however, can be easily measured continuously via *in situ* monitoring equipment. Day time collection of $\delta^{18}O\text{-}O_2$ may not be necessary, if full diel data collection is not feasible. Therefore, monitoring DO continuously, supplemented with night data of $\delta^{18}O\text{-}O_2$ to estimate k and CR, then determining GPP with day time DO concentration data may be most efficient application for using the isotope technique. Testing various model simulation scenarios resulted in about a 10% variability in parameter estimates, indicating that a night $\delta^{18}O\text{-}O_2$ calibration approach may be useful when this level of uncertainty is acceptable. There was also a smaller range of α_r values associated with undersaturated night DO conditions, which may allow for more efficient modeling and parameter estimation. In situations where DO declines to a plateau, it also may be more appropriate to model only the portion previous to DO levelling off.

In this study, model error appears to be primarily linked to the ability of the isotopic mass balance to describe observed $\delta^{18}O\text{-}O_2$ data. Uncertainty in α_r presents some complication in using the isotopic model mass balance approach to predict $\delta^{18}O\text{-}O_2$ in systems where α_r is unknown, or variable. A better understanding of processes affecting $\delta^{18}O\text{-}O_2$, would improve the capability of the model to replicate observed data, and provide more

confidence in predicting metabolic processes in impacted rivers. Despite these shortcomings, however, the isotopic approach has the potential to improve the ability to characterize DO dynamics and metabolism in highly impacted watersheds due to the provision of qualitative and quantitative corroborative support to information obtained by measuring DO concentration alone.

7.2 Recommendations for Future Research

- There is still uncertainty surrounding isotopic fractionation during the consumption of DO. Questions remain regarding the specific controls on α_r, the role of different O_2 and O_2 consuming pathways (e.g., nitrification, photorespiration, water column respiration versus that taking place on surfaces or in sediments, photochemistry, chemical oxygen demand etc.).

- Downstream of the wastewater treatment outfalls was characterized by lower net production, lower P:R, and higher fractionation factors compared to the upstream, more agriculturally dominant catchment. Further work is suggested in locations downstream of urban influences to determine 1) the assimilative capacity of the river for receiving pollution inputs and 2) the relative proportion of O_2 demanding reactions responsible for heterotrophic conditions (e.g., nitrification vs. biological oxygen demand).

- Using the isotope approach for the quantification of gas exchange appears promising. Assessing this approach for finding k should be tested under various hydrologic

regimes and locations. Comparison to results obtained via tracer experiments would also aid in determining the relative accuracy of the isotope approach.

- Groundwater influences were assumed to be negligible in the DO mass balance; this assumption may not be appropriate for some locations. Investigation into the importance of groundwater-surfacewater interactions may be important in relatively high groundwater discharge areas.

- The metabolic functioning and DO dynamics results presented in this study represented an integration of influences upstream of a given sampling site. Reach-scale, or two point, investigations may more precise information on catchment characteristics or environmental conditions affecting river DO production and consumption. Evaluation of potential management practices to mitigate impacts should also be conducted on a reach-scale or sub-catchment basis.

References

Allan, J. 1995. Stream Ecology: Structure and Function of Running Waters. Kluwer Academic Publishers, Dordecht, The Netherlands, 388pp.

American Public Health Association (APHA). 1995. Standard methods for the examination of water and wastewater. 19th ed. American Public Health Association, Inc., New York.

Bennett, J.P. and R.E. Rathburn. 1972. Reaeration in Open-Channel Flow. U.S. Geological Survey Professional Paper 737.

Bender, M.L. 1990. The $\delta^{18}O$ of dissolved O_2 in seawater: a unique tracer of circulation and respiration in the deep sea. J. Geophys. Res. 95: 22,243-22,252.

Benson, B.B. and D.J. Krause. 1984. The concentration and isotopic fractionation of oxygen dissolved in fresh water and seawater in equilibrium with the atmosphere. Limnol. Oceanogr. 29: 620-632.

Bicudo, J.R. and A. James. 1989. Measurement of reaeration in streams: comparison of techniques. J. Environ. Eng. 115: 992-1010.

Bott, T.L., J.T. Brock, C.S. Dunn, R.J. Naiman, R.W. Ovink, and R.C. Petersen. 1985. Benthic community metabolism in four temperate stream systems: an inter-biome comparison and evaluation of the river continuum concept. Hydrobiologia. 123: 3-45.

Bowie, G.L., W.B. Mills, D.B. Porcella, C.L. Campbell, J.R. Pagenkopf, G.L. Rupp, K.M. Johnson, P.W.H. Chan, S.A. Gherini, and C.E. Chamberlain. 1985. Rates, Constants, and Kinetic Formulations in Surface Water Modeling. U.S. Environmental Protection Agency, ORD, Athens, GA, ERL, EPA/600/3-85/040.

Brandes, J.A. and A. H. Devol. Isotopic fractionation of oxygen and nitrogen in coastal marine sediments. Geochim. Cosmochim. Acta 61: 1793-1801.

Canadian Council of Ministers of the Environment (CCME). 2007. Canadian water quality guidelines for the protection of aquatic life: summary table. Updated December 2007. In: Canadian environmental quality guidelines, 1999, Canadian Council of Ministers of the Environment, Winnipeg.

Carpenter, S.R., N.F. Caraco, D.L. Correll, R.W. Howarth, A.N. Sharpley and V.H. Smith. 1998. Nonpoint pollution of surface waters with phosphorus and nitrogen. Ecol. Appl. 8: 559-568.

Chapra, S.C. 1997. Surface Water-Quality Modeling. McGraw-Hill Companies, Inc. New York, NY, 844 pp.

Chapra, S.C. and D.M. Di Toro. 1991. Delta method for estimating primary production, respiration, and reaeration in streams. J. Environ. Eng. ASCE 117: 640-655.

Churchill, M.A., H.L. Elmore, and R.A. Buckingham. 1962. The prediction of stream reaeration rates. J.San. Engr. Div. ASCE SA 4:1, Proc. Paper 3199.

Clark, I. and P. Fritz . 1997. Environmental Isotopes in Hydrogeology. Lewis Publishers, Inc., Boca Raton, Fla, 320 pp.

Clark, J.F., H.J. Simpson, W.M. Smethie, Jr., and C. Toles. 1992. Gas exchange in a contaminated estuary inferred from chlorofluorocarbons. Geophys. Res. Lett. 19:1133-1136.

Cole, G.A. 1994. Textbook of Limnology. 4th Ed. Waveland Press, Inc. Prospect Heights, Ill, 418 pp.

Cooke, S. 2006. Water Quality in the Grand River: A Summary of Current Conditions (2000-2004) and Long Term Trends. Grand River Conservation Authority, Cambridge, ON. 88 pp. http://www.grandriver.ca/Water/2006_WaterQuality_complete.pdf

Cosby, B.J. and G.M. Hornberger. 1984. Identification of photosynthesis-light models for aquatic systems. I. Theory and simulations. Ecol. Model. 23: 1-24.

Cox, B.A. and P.G. Whitehead. 2005. Parameter sensitivity and predictive uncertainty in a new water quality model, Q^2. J. Environ. Eng. ASCE 131: 147-157.

Danckwerts, P.V. 1951. Significance of liquid-film coefficients in gas absorption. Ind. Eng. Chem. 43: 1460-1467.

D.W. Draper & Associates Ltd. and Donald G. Weatherbe Associates Inc. 1995. Review of Surface Water Quality Protection Measures. Report for the Regional Municipality of Water Engineering Department, Water Services Division. Final Report.

Edwards, R.T. and J.L. Meyer. 1987. Metabolism of sub-tropical low gradient blackwater river. Fresh. Biol. 17: 251-263.

Even, S., M. Poulin, J.M. Mouchel, M. Seidl, and P. Servais. 2004. Modelling oxygen deficits in the Seine River downstream of combined sewer overflows. Ecol. Model. 173: 177-196.

French, R.H. 1985. Open-Channel Hydraulics, McGraw-Hill, USA, 739 pp.

Fuss, C.L. and L.A. Smock. 1996. Spatial and temporal variation of microbial respiration rates in a blackwater stream. Fresh. Biol. 36: 339-349.

Garnier, J., G. Billen, and A. Cebron. 2007. Modelling nitrogen transformations in the lower Seine river and estuary (France): impact of wastewater release on oxygenation and N_2O emission. Hydrobiologia 588: 291-302.

Genereux, D.P. and H.F. Hemond. 1992. Determination of gas exchange rate constants for a small stream on Walker Branch Watershed, Tennessee. Wat. Resour. Res. 28: 2365-2374.

Giller, P.S. and B. Malmqvist. 1998. The Biology of Streams and Rivers. Oxford University Press Inc., New York, 296 pp.

Gowda, T.P.H. 1983. Modelling nitrification effects on the dissolved oxygen regime of the speed river. Water Res. 17: 1917-1927.

Grand River Conservation Authority (GRCA). 1982. Grand River Basin Management Study. Grand River Implementation Committee, Grand River Conservation Authority, Cambridge, ON. 8 pp.
http://www.grandriver.ca/Water/2007_WaterQuality_boardreport.pdf

Grand River Conservation Authority (GRCA). 2007. State of Water Quality in the Grand River (2002-2006). Report No. CW-09-07-72 Grand River Conservation Authority, Cambridge, ON.

Gucker, B., M. Brauns, and M. Pusch. 2006. Effects of wastewater treatment plant discharge on ecosystem structure and function of lowland streams. J. N. Benthol. Soc. 25: 313-329.

Guy, R.D., J.A. Barry, M.L. Fogel, and T.C. Hoering. 1989. Differential fractionation of oxygen by cyanide-resistant and cyanide-sensitive respiration in plants. Planta 177:483-491.

Guy, R.D., M.L. Fogel, and J.A. Berry. 1993. Photosynthetic fractionation of the stable isotopes of oxygen and carbon. Plant Physiol. 101: 37-47.

Hedin, L. 1990. Factors controlling sediments community respiration in woodland stream ecosystems. Oikos 57: 94-105.

Hill, B.H., A.T. Herlihy, and P.R. Kaufmann. 2002. Benthic microbial respiration in Appalachian Mountain, Piedmont, and Coastal Plains streams of the eastern U.S.A. Fresh. Biol. 47: 185-194.

Hornberger, G.M., M.G. Kelly, and B.J. Crosby. 1977. Evaluating eutrophication potential from community productivity. Water Res. 11: 65-69.

Howarth, R.W., R. Marino, R. Garritt, and D. Sherman. 1992. Ecosystem respiration and organic carbon processing in a large, tidally influenced river: the Hudson River. Biogeochemistry 16: 83-102.

Hunter, R.G. and J.H. Carroll. 1985. Estimation of community metabolism in a polluted stream using the Velz oxygen model. Proc. Okla. Acad. Sci. 65:19-23.

Kehr, R.W. 1938. Measures of natural oxidation in polluted streams. IV. Effect of sewage on atmospheric reaeration rates under stream flow conditions. Sewage Works J. 10:228-240.

Kiddon, J., M.L. Bender, J. Orchardo, D.A. Caron, J.C. Goldman, and M. Dennett. 1993. Isotopic fractionation of oxygen by respiring marine organisms. Global Biogeochem. Cycl. 7: 679-694.

Knox, M., P.D. Quay, and D.O. Wilbur. 1992. Kinetic isotopic fractionation during air-water gas transfer of O_2, N_2, CH_4, and H_2. J. Geophys. Res. 97: 20335-20343.

Kosinski, R.J. 1984. A comparison of the accuracy and precision of several open-water productivity techniques. Hydrobiologia. 119: 139-148.

Kroopnick, P.M. 1975. Respiration, photosynthesis, and oxygen isotope fractionation in oceanic surface water. Limnol. Oceanogr. 20: 988-992.

Kroopnick, P. and H. Craig. 1972. Atmospheric oxygen: isotopic composition and solubility fractionation. Science 175: 54-55.

Kroopnick, P. and H. Craig. 1976. Oxygen isotope fractionation in dissolved oxygen in deep sea. Earth Plant. Sci. Lett. 32: 375-388.

Lane, G.A. and M. Dole. 1956. Fractionation of oxygen isotopes during respiration. Science 123: 574-576.

Lewis, W.K. and Whitman, W.G. 1924. Principles of gas absorption. Ind. Eng. Chem. 16:1215-1220.

Livingstone, D.M. 1991. The diel oxygen cycle in three subalpine Swiss streams. Arch. Hydrobiol. 120: 457-479.

Luz, B. and E. Barkan. 2005. The isotopic ratios $^{17}O/^{16}O$ in molecular oxygen and their significance in biogeochemistry. Geochim. Cosmochim. Acta 69: 1099-1110.

Luz, B. and E. Barkan. 2009. Net and gross oxygen production from O_2/Ar, $^{17}O/^{16}O$, and $^{18}O/^{16}O$ ratios. Aquat. Microb. Ecol. 56: 133-145.

Luz, B., E. Barkan, M. L. Bender, M.H. Thiemens, and K.A. Boering. 1999. Triple-isotope composition of atmospheric oxygen as a tracer of biosphere productivity. Nature 400: 547-550.

Luz, B., E. Barkan, Y. Sagi. 2002. Evaluation community respiratory mechanisms with oxygen isotopes: a case study in Lake Kinneret. Limnol. Oceanogr. 47: 33-42.

Marzolf, E.R., P.J. Mulholland, and A.D. Steinman. 1994. Improvements to the diel upstream-downstream dissolved oxygen change technique for determining whole-stream metabolism in small streams. Can. J. Fish. Aquat. Sci. 51: 1591-1599.

McCutcheon, S.C. 1989. Water Quality Modeling: Volume I Transport and Surface Exchange in Rivers. CRC Press, Inc., Boca Raton Fla. 334 pp.

Melching. C.S., and H. E. Flores. 1999. Reaeration equations derived from U.S. geological survey database. J. Environ. Eng. 125: 407-414.

Meyer, J.L. and R.T. Edwards. 1990. Ecosystem metabolism and turnover of organic carbon along a blackwater river continuum. Ecology 71:668-677.

Meyer, J.L., M.J. Paul, and W.K. Taulbee. 2005. Stream ecosystem function in urbanizing landscapes. J. N. Benthol. Soc. 24: 602-612.

Minshall, G.W. 1978. Autotrophy in stream ecosystems. BioScience 28:767-771.

Minshall, G.W., R.C. Petersen, K.W. Cummins, T.L. Bott, J.R. Sedell, C.E. Cushing, R.L. Vannote. 1983. Interbiome comparison of stream ecosystem dynamics. Ecol. Mono. 53: 1-25.

Minshall, G.W., K.W. Cummins, R.C. Petersen, C.E. Cushing, D.A. Bruns, J.R. Sedell, and R.L. Vannote. 1985. Developments in stream ecosystem theory. Can. J. Fish. Aquat. Sci. 42: 1045-1055.

Minshall, G.W., R.C. Petersen, T.L. Bott, C.E. Cushing, K.W. Cummins, R.L. Vannote, and J.R. Sedell. 1992. Stream ecosystem dynamics of a Salmon River, Idaho; an 8th-order system. J. North. Am. Benthol. Soc. 11: 111-137.

Mulholland, P.J., C.S. Fellows, J.L. Tank, N.B. Grimm, J.R. Webster, S.K. Hamilton, E. Marti, L. Ashkenas, W.B. Bowden, W.K. Dodds, W.H. McDowell, M.J. Paul, and B.J. Peterson. 2001. Inter-biome comparison of factors controlling stream metabolism. Fresh. Biol. 46: 1503-1517.

Naiman, R.J. 1983. The annual pattern and spatial distribution of aquatic oxygen metabolism in boreal forest watersheds. Ecol. Monogr. 53: 73-94.

National Pollutant Release Inventory (NPRI), Environment Canada. 2007. http://www.ec.gc.ca/pdb/npri/npri_home_e.cfm. (Accessed January 2009)

O'Connor, D.J. and Dobbins, W.E. 1956. Mechanism of reaeration in natural streams. ASCE Trans. 86: 35-55.

Odum, H.T. 1956. Primary production in flowing waters. Limnol. Oceanogr. 1: 102-117.

Odum, H.T. and C.M. Hoskin. 1958. Comparative studies on the metabolism of marine waters. Publs. Inst. Mar. Sci. Univ. Texas 5: 15-46.

Ontario Ministry of Environment and Energy (OMOE). 1994. B-1-2 Water Management - Policies, Guidelines, Provincial Water Quality Objectives. Publication #3303e

http://www.ene.gov.on.ca/envision/gp/3303e.pdf

Oreskes, N., K. Shrader-Frechette, and K. Belitz. 1994. Verification, validation, and confirmation of numerical models in the earth sciences. Science 263: 641-646.

Osmond, C.B. 1981 Photorespiration and photoinhibition: Some implications for the energetic of photosynthesis. Biochim. Biophys. Acta 639: 77-98.

Osmond, C.B., and S.C. Grace. 1995. Perspectives on photoinhibition and photorespiration in the field – quintessential inefficiencies of light and dark reactions of photosynthesis. J. Exp. Bot. 46: 1351-1362.

Owens, M. 1974. Methods of measuring production rates in running water. In R.A. Vollenweider (ed.), A manual on methods of measuring primary production in aquatic environments. IBP Handbook 12, Blackwell Scientific Publishers, Oxford: 111-119.

Owens, M., R.W. Edwards, and J.W. Gibbs. 1964. Some reaeration studies in streams. Int. J. Air Wat. Poll. 8: 469-486.

Parker, S.R., S.R. Poulson, C.H. Gammons, and M.D. Degrandpre. 2005. Biogeochemical controls on diel cycling of stable isotopes of dissolved O_2 and dissolved inorganic carbon in the Big Hole River, Montana. Environ. Sci. & Technol. 39: 7134-7140.

Parkhurst, J.D. and R.D. Pomeroy. 1972. Oxygen absorption in streams. J. Sanit. Eng. Div. ASCE 98: 101-124.

Parkhill, K.L. and J.S. Gulliver. 1998. Modeling the effect of light on whole-stream respiration. Ecol. Model. 117: 333-342.

Paul, M.J. and J.L. Meyer. 2001. Streams in the urban landscape. Annu. Rev. Ecol. Syst. 32: 333-365.

Pearson, N. and N.O. Crossland. 1996. Measurement of community photosynthesis and respiration in outdoor artificial streams. Chemosphere 32: 913-919.

Poulson, S.R and A.B. Sullivan. 2009. Assessment of diel chemical and isotope techniques to investigate biogeochemical cycles in the upper Kalamath River, Oregon, USA. Chem. Geol. 266: 114-122.

Quay, P.D., S. Emerson, D.O. Wilbur, C. Stump, and M. Knox. 1993. The $\delta^{18}O$ of dissolved O_2 in the surface waters of the Subarctic Pacific: a tracer of biological productivity. J. Geophys. Res. 98: 8447-8458.

Quay, P.D., D.O. Wilbur, J.E. Richey, A.H. Devol, R. Brenner, and B.R. Forsberg. 1995. The ^{18}O:^{16}O of dissolved oxygen in rivers and lakes in the Amazon Basin: Determining the ratio of respiration to photosynthesis rates in freshwaters. Limnol. Oceanogr. 40: 718-729.

Quinones-Rivera, Z., B. Wissel, D. Justic, and B. Fry. 2007. Partitioning oxygen sources and sinks in a stratified, eutrophic coastal ecosystem using stable oxygen isotopes. Mar. Ecol. Prog. Ser. 342: 69-83.

Radtke, D.B., White, A.F., Davis, J.V., and Wilde, F.D., 1998, National field manual for the collection of water-quality data--dissolved oxygen: U.S. Geological Survey Techniques of Water-Resources Investigations, book 9, chap. A6, sect. 6.2

Rathburn, R.E. 1977. Reaeration coefficients of streams – state of the art. J. Hydraul. Div. ASCE 103: 409-424.

Raven, J.A. and Beardall, J. 2005. Respiration in Aquatic Photolithotrophs. In: Respiration in Aquatic Ecosystems. Ed. By P.A. del Giorgio and P. J. Le B. Williams. Oxford University Press, pp. 36-46

Roberts, B.J., M.E. Russ, and N.E. van Ostrom. 2000. Rapid and precise determination of the $\delta^{18}O$ of dissolved and gaseous dioxygen via gas chromatography - isotope ratio mass spectrometry. Environ. Sci. Technol. 34: 2337-2341.

Robinson, S.A., D. Yakir, M. Ribas-Carbo, L. Giles, C.B. Osmond, J.N Siedow, and J.A. Barry. 1992. Measurements of the engagement of cyanide-resistant respiration in the crassulacean acid metabolism plant *Kalanchoe daigremontiana* with the use of on-line oxygen isotope discrimination. Plant Physiol. 100: 1087-1091.

Rosenfield, J.S., R.J. Mackay. Assessing the food base of stream ecosystems: alternatives to the P/R ratio. Oikos 50: 141-147.

Rott, E., H.C. Duthie, and E. Pipp. 1998. Monitoring organic pollution and eutrophication in the Grand River, Ontario, by means of diatoms. Can. J. Fish Aquat. Sci. 55: 1443-1453.

Ruggiero, A., A.G. Solimini, G. Carchini. 2006. Effects of a waste water treatment plant on organic matter dynamics and ecosystem functioning in a Mediterranean stream. Ann. Limnol. – Int. J. Lim. 42: 97-107.

Russ, M.E., N.E. Ostrom, H. Gandhi, P.H. Ostrom, and N.R. Urban. 2004. Temporal and spatial variations in R:P ratios in Lake Surperior, and oligotrophic freshwater environment. J. Geophys. Res. 109: C10S12.

Scott, K.J., C.A. Kelly, and J.W.M. Rudd. 1999. The importance of floating peat to methane fluxes from flooded peatlands. Biogeochemistry 42: 187-202.

Servais, P., E. Debecker, and G. Billen. 1984. Annual cycle of gross primary production and respiration in the Viroin River (Belgium). Hydrobiologia. 111: 57-63.

Smith, V.H., G.D. Tilman, and J.C. Nekola. 1999. Eutrophication: Impacts of excess nutrients on freshwater, marine, and terrestrial ecosystems. Environ. Poll. 100: 179-196.

Thomann, R.V. 1982. Verification of water quality models. J. Environ. Eng. ASCE 108: 923-940.

Thuss, S. 2008. Nitrous oxide production in the Grand River, Ontario, Canada: new insights from stable isotope analysis of dissolved nitrous oxide. M.Sc. Thesis. University of Waterloo, ON. 185 pp.

Tobias, C. R., J.K. Bohlke, and J.W. Harvey. 2007. The oxygen-18 isotope approach for measuring aquatic metabolism in high-productivity waters. Limnol. Oceanog. 51: 1439-1453.

Tsivoglou, E.C. and L.A. Neal. 1976. Tracer measurements of reaeration: III. Predicting the reaeration capacity of inland streams. J. Water Poll. Control Fed. 48: 2669-2689.

Uehlinger, U. 2006. Annual cycle and inter-annual variability of gross primary production and ecosystem respiration in a floodprone river during a 15-year period. Fresh. Biol. 51: 938-950.

Uehlinger, U., C. Konig, and P. Reichert. 2000. Variability of photosynthesis-irradiance curves and ecosystem respiration in a small river. Fresh. Biol. 44: 493-507.

Venkiteswaran J.J., L.I. Wassenaar, and S.L. Schiff. 2007. Dynamics of dissolved isotopic ratios: a transient model to quantify primary production, community respiration, and air-water exchange in aquatic ecosystems. Oecologia 153: 385-398.

Venkiteswaran, J.J., S.L. Schiff, and L.I. Wassenaar. 2008. Aquatic metabolism and ecosystem health assessment using dissolved O_2 stable isotope diel curves. Ecol. App. 18: 965-982.

Walsh, C.J., A.H. Roy, J.W. Feminella, P.D. Cottingham, P.M. Groffman, R.P. Morgan II. 2005. The urban stream syndrome: current knowledge and the search for a cure. J. N. Am. Benthol. Soc. 24: 706-723.

Wang, X. and J. Veizer. 2000. Respiration-photosynthesis balance of terrestrial aquatic ecosystems, Ottawa area, Canada. Geochim. Cosmochim. Acta 64: 3775-3786.

Wang, X. and J. Veizer. 2004. Erratum to Wang, X. and J. Veizer. 2000. Respiration-photosynthesis balance of terrestrial aquatic ecosystems, Ottawa area, Canada. Geochim. Cosmochim. Acta 64: 3775-3786. Geochim. Cosmochim. Acta 68: 933-944.

Wanninkhof, R., P.J. Mulholland and J.W. Elwood. 1990. Gas Exchange rates for a first-order stream determined with deliberate and natural tracers. Water Resour. Res. 26: 1621-1630.

Wassenaar, L.I. and G. Koehler. 1999. An on-line technique for the determination of the $\delta^{18}O$ and $\delta^{17}O$ of gaseous and dissolved oxygen. Anal. Chem. 71: 4965-4968.

Weiss, R.F. 1970. Solubility of nitrogen, oxygen and argon in water and seawater. Deep-Sea Res. 17: 721-735.

Westlake, D.F. 1978. Measurements on non-isolated natural communities. In R.A. Vollenweider (ed.), A manual on methods of measuring primary production in aquatic environments. IBP Handbook 12, Blackwell Scientific Publishers, Oxford: 110-111.

Wilcock, R.J., J.W. Nagels, G.B. McBride, K.J. Collier. 1998. Characterisation of lowland streams using a single-station diel curve analysis model with continuous monitoring data for dissolved oxygen and temperature. New Zeal. J. Mar. Fresh. 32: 67-79.

Wiley, M.J., L.L. Osborne, and R.W. Larimore. 1990. Longitudinal structure of an agricultural prairie rivers system and its relationship to current stream ecosystem theory. Can. J. Fish Aquat. Sci. 47: 373-384.

Williams, R.J., C. White, M.L. Harrow, C. Neal. 2000. Temporal and small-scale variations of dissolved oxygen in the Rivers Thames, Pang, and Kennet, UK. Sci. Total Environ. 251/252: 497-510.

Vannote, R.L., G.W. Minshall, K.W. Cummins, J.R. Sedell, and C.E. Cushing. 1980. The river continuum concept. Can. J. Fish Aquat. Sci. 37: 30-37.

Young, R.G. and A.D. Huryn. 1999. Effects of land use on stream metabolism and organic matter turnover. Ecol. App. 9:1359-1376.

Zheng, C. And G.D. Bennett. 2002. Applied Contaminant Transport Modeling. 2nd Ed. John Wiley & Sons, Inc. New York, 621 pp.

Appendix A. Temperature, DO, and $\delta^{18}O\text{-}O_2$ data collected at WM, BRPT, and BLR that has not been reported in the main body of thesis.

Table A1. Diel DO, $\delta^{18}O\text{-}O_2$, and temperature data collected.

Location	Date	Time	Temperature (C)	DO (mg L^{-1})	$\delta^{18}O\text{-}O_2$ (‰)
WM	28-May-03	8:00	11.3	9.45	23.32
WM	28-May-03	12:00	14.0	13.65	15.75
WM	28-May-03	15:00	16.2	15.10	13.92
WM	28-May-03	19:30	16.8	12.05	17.86
WM	28-May-03	22:00	15.9	9.79	21.70
WM	29-May-03	0:00	14.8	8.65	24.32
WM	29-May-03	3:00	13.2	8.06	25.92
WM	29-May-03	4:30	12.4	7.98	26.22
WM	29-May-03	5:30	12.0	8.09	26.49
WM	24-Jun-03	8:00	17.3	7.34	23.81
WM	24-Jun-03	11:30	19.4	10.54	20.49
WM	24-Jun-03	20:00	25.9	10.42	16.68
WM	24-Jun-03	22:00	24.9	7.80	27.65
WM	24-Jun-03	23:30	24.0	6.10	24.91
WM	25-Jun-03	3:30	21.4	5.31	27.53
WM	25-Jun-03	4:30	20.8	5.36	28.08
WM	25-Jun-03	5:30	20.2	5.37	29.38
WM	25-Jun-03	6:30	19.6	5.76	27.25
WM	9-Jul-03	7:30	19.5	5.99	28.04
WM	9-Jul-03	11:30	20.7	10.52	16.41
WM	9-Jul-03	15:30	24.7	13.27	15.88
WM	9-Jul-03	19:30	25.9	11.80	19.82
WM	9-Jul-03	22:00	24.8	7.79	23.93
WM	10-Jul-03	0:30	23.1	6.29	25.83
WM	10-Jul-03	3:00	21.7	5.35	29.32
WM	28-Jul-03	22:00	22.6	8.97	22.26
WM	29-Jul-03	0:00	21.5	7.24	26.89
WM	29-Jul-03	3:00	19.8	6.24	27.63
WM	29-Jul-03	4:30	19.0	6.05	28.58
WM	29-Jul-03	5:30	18.4	6.13	27.21
WM	29-Jul-03	7:15	17.6	6.94	26.54
WM	29-Jul-03	11:30	18.7	10.75	16.28
WM	29-Jul-03	15:00	23.1	14.38	13.36
WM	29-Jul-03	17:30	24.4	13.78	14.79
WM	13-Aug-03	7:15	20.8	6.23	27.93
WM	13-Aug-03	8:30	20.8	6.90	27.03
WM	13-Aug-03	9:30	20.9	7.69	22.67
WM	13-Aug-03	10:30	21.4	8.95	19.54

WM	13-Aug-03	11:30	22.1	10.47	16.52
WM	13-Aug-03	13:00	23.4	12.60	13.66
WM	13-Aug-03	14:00	24.8	13.50	12.22
WM	13-Aug-03	15:00	25.6	14.55	11.98
WM	13-Aug-03	16:00	26.4	14.62	22.04
WM	13-Aug-03	17:00	26.9	14.60	17.29
WM	13-Aug-03	18:00	27.1	14.00	17.70
WM	13-Aug-03	19:00	26.9	12.96	20.03
WM	13-Aug-03	20:00	26.4	11.37	27.96
WM	13-Aug-03	21:00	25.9	9.79	22.83
WM	13-Aug-03	22:30	24.9	7.79	26.42
WM	13-Aug-03	23:30	24.2	7.03	28.63
WM	14-Aug-03	0:30	23.5	6.46	28.02
WM	14-Aug-03	2:00	22.6	5.93	30.01
WM	14-Aug-03	3:30	21.8	5.77	29.86
WM	14-Aug-03	5:00	21.2	5.73	29.76
WM	14-Aug-03	6:30	20.8	5.82	28.94
BRPT	9-Jul-03	8:15	23.3	5.15	26.18
BRPT	9-Jul-03	12:15	24.4	8.85	18.60
BRPT	9-Jul-03	16:45	27.2	12.48	13.00
BRPT	9-Jul-03	20:00	27.5	12.06	14.25
BRPT	9-Jul-03	22:30	26.4	8.57	19.58
BRPT	10-Jul-03	1:00	25.2	7.43	23.12
BRPT	10-Jul-03	3:30	24.4	6.09	25.65
BRPT	26-Feb-04	7:40	0.2	13.13	24.74
BRPT	26-Feb-04	10:06	0.3	12.39	24.95
BRPT	26-Feb-04	13:07	0.3	12.61	24.57
BRPT	26-Feb-04	15:19	0.3	12.92	23.95
BRPT	26-Feb-04	17:50	0.3	13.45	22.93
BRPT	26-Feb-04	20:15	0.3	14.00	22.35
BRPT	26-Feb-04	22:45	0.3	14.32	21.81
BRPT	27-Feb-04	1:10	0.3	14.13	22.15
BRPT	27-Feb-04	4:10	0.3	13.47	23.45
BRPT	11-May-04	7:15	14.6	8.42	27.24
BRPT	11-May-04	10:00	14.6	9.85	25.71
BRPT	11-May-04	13:45	16.1	13.36	19.17
BRPT	11-May-04	16:00	17.0	14.69	17.49
BRPT	11-May-04	17:30	17.4	14.82	18.26
BRPT	11-May-04	19:15	17.6	13.85	19.85
BRPT	11-May-04	21:00	17.5	11.90	22.83
BRPT	11-May-04	23:00	17.4	10.51	25.76
BRPT	12-May-04	1:00	17.2	9.37	26.43
BRPT	12-May-04	3:15	17.0	8.16	29.48
BRPT	12-May-04	5:00	16.7	7.71	29.65
BRPT	7-Jun-04	18:45	22.4	11.30	17.41

BRPT	7-Jun-04	20:45	22.0	10.43	18.98
BRPT	7-Jun-04	22:45	21.4	8.71	22.76
BRPT	7-Jun-04	23:30	21.0	7.66	24.88
BRPT	8-Jun-04	2:45	20.5	6.81	26.27
BRPT	8-Jun-04	4:45	20.1	6.48	28.99
BRPT	8-Jun-04	7:50	19.5	6.12	27.42
BRPT	8-Jun-04	11:00	20.7	8.95	20.92
BRPT	8-Jun-04	13:50	23.0	10.44	18.41
BRPT	8-Jun-04	16:25	24.7	11.45	17.10
BRPT					
BRPT	30-Aug-04	18:00	20.2	9.36	20.38
BRPT	30-Aug-04	19:45	20.0	8.93	20.88
BRPT	30-Aug-04	22:00	19.6	8.04	23.39
BRPT	31-Aug-04	0:00	19.2	7.50	25.07
BRPT	31-Aug-04	2:00	18.9	7.02	26.04
BRPT	31-Aug-04	4:00	18.5	6.70	33.77
BRPT	31-Aug-04	8:15	17.6	6.25	33.24
BRPT	31-Aug-04	10:30	17.9	7.30	24.82
BRPT	31-Aug-04	14:30	20.4	9.43	18.17
BRPT	31-Aug-04	16:30	21.4	10.52	23.29
BLR	9-Jul-03	9:00	24.1	2.53	23.44
BLR	9-Jul-03	13:00	25.7	6.98	10.92
BLR	9-Jul-03	17:00	27.6	8.97	11.72
BLR	9-Jul-03	20:30	26.7	3.73	22.64
BLR	9-Jul-03	23:00	25.5	1.38	26.77
BLR	10-Jul-03	1:30	24.5	1.24	
BLR	10-Jul-03	4:00	24.0	1.14	
BLR	26-Feb-04	8:30	0.6	13.61	24.58
BLR	26-Feb-04	10:56	1.3	14.16	24.37
BLR	26-Feb-04	13:53	2.7	14.00	23.68
BLR	26-Feb-04	16:06	2.5	13.37	24.30
BLR	26-Feb-04	18:30	2.5	13.08	26.18
BLR	26-Feb-04	20:50	1.9	13.05	25.67
BLR	26-Feb-04	23:40	1.5	13.24	26.46
BLR	27-Feb-04	1:40	1.3	13.21	26.93
BLR	27-Feb-04	4:40	0.9	13.47	25.73
BLR	7-Jun-04	19:45	22.2	8.46	21.60
BLR	7-Jun-04	21:45	21.5	6.27	25.91
BLR	7-Jun-04	23:45	21.2	4.94	27.97
BLR	8-Jun-04	1:45	20.6	4.28	29.13
BLR	8-Jun-04	3:45	20.3	3.97	29.71
BLR	8-Jun-04	5:30	20.0	4.14	29.42
BLR	8-Jun-04	8:35	20.0	6.71	25.27
BLR	8-Jun-04	11:35	21.9	8.46	20.67
BLR	8-Jun-04	14:30	23.8	9.43	19.14
BLR	8-Jun-04	17:10	25.1	9.89	18.33

BLR	30-Aug-04	18:45	20.8	6.30	23.86
BLR	30-Aug-04	20:30	20.4	5.24	27.41
BLR	30-Aug-04	22:40	20.0	4.52	29.13
BLR	31-Aug-04	0:40	19.5	4.17	29.32
BLR	31-Aug-04	2:45	19.2	3.90	28.68
BLR	31-Aug-04	4:35	18.8	3.97	28.82
BLR	31-Aug-04	9:00	18.2	4.71	28.26
BLR	31-Aug-04	11:15	18.8	6.21	22.92
BLR	31-Aug-04	15:00	21.5	7.31	19.03
BLR	31-Aug-04	17:00	22.0	7.17	19.48

Table A2. Daytime Routine DO, $\delta^{18}O\text{-}O_2$, and temperature data collected.

Location	**Date**	**Time**	**Temperature (C)**	**DO (mg L^{-1})**	**$\delta^{18}O\text{-}O_2$ (‰)**
WM	17-Sep-03	7:45	15.8	7.18	28.02
WM	17-Sep-03	11:30	16.6	10.54	17.28
WM	17-Sep-03	3:30	20.8	14.55	15.87
WM	27-Oct-03	8:00	6.2	11.00	26.49
WM	27-Oct-03	11:30	6.8	12.51	22.30
WM	27-Oct-03	15:00	7.2	12.77	22.35
WM					
WM	10-Dec-03	8:45	1.9	13.66	25.48
WM	10-Dec-03	11:45	2.2	14.12	24.52
WM	10-Dec-03	15:30	2.8	14.66	23.25
WM	11-May-03	6:30	12.8	8.77	28.77
WM	11-May-03	9:15	12.4	10.37	34.22
WM	11-May-03	13:00	14.7	13.19	20.79
WM	11-May-03	15:15	16.4	14.04	22.11
WM					
WM	8-Jun-04	7:10	16.1	6.81	27.84
WM	8-Jun-04	10:20	17.2	9.22	22.36
WM	8-Jun-04	13:15	20.1	11.38	18.27
WM	8-Jun-04	15:40	22.9	12.41	18.79
WM	29-Jul-04	7:30	18.0	6.66	25.94
WM	29-Jul-04	10:45	19.3	8.47	18.62
WM	29-Jul-04	14:15	22.4	11.46	14.55
WM	29-Jul-04	16:15	23.7	11.59	14.58
WM	31-Aug-04	7:30	16.3	6.72	27.36
WM	31-Aug-04	9:45	16.5	7.94	24.02
WM	31-Aug-04	13:45	20.0	11.67	17.39
WM	31-Aug-04	15:45	21.2	11.54	16.95

WM	28-Oct-04	8:00	8.0	9.50	25.42
WM	28-Oct-04	9:00	8.0	9.83	24.59
WM	28-Oct-04	10:00	8.0	10.30	23.72
WM	28-Oct-04	11:00	8.0	10.88	23.26
WM	28-Oct-04	12:00	8.5	11.63	22.27
WM	28-Oct-04	13:00	9.0	12.35	21.75
WM	28-Oct-04	14:00	9.5	13.05	20.91
WM	28-Oct-04	15:00	10.0	13.55	19.55
WM	28-Oct-04	16:00	11.0	13.75	20.08
WM	28-Oct-04	17:00	11.0	13.45	18.88
WM	28-Oct-04	18:00	11.0	12.95	20.77
BRPT	29-May-03	9:00	13.0	8.93	23.40
BRPT	29-May-03	13:00	14.5	12.93	16.04
BRPT	29-May-03	15:45	16.4	14.96	13.72
BRPT	24-Jun-03	8:45	21.4	5.71	24.13
BRPT	24-Jun-03	12:30	23.6	9.83	20.09
BRPT	24-Jun-03	16:00	26.6	13.04	11.22
BRPT	29-Jul-03	8:10	20.2	6.27	26.53
BRPT	29-Jul-03	12:00	21.8	11.73	12.10
BRPT	29-Jul-03	15:45	24.3	15.08	10.67
BRPT	17-Sep-03	8:15	17.3	7.41	26.51
BRPT	17-Sep-03	12:00	18.2	10.65	15.08
BRPT	17-Sep-03	4:00	21.1	14.40	16.88
BRPT	27-Oct-03	9:00	6.6	10.71	27.82
BRPT	27-Oct-03	12:00	7.0	11.88	24.90
BRPT	27-Oct-03	15:45	7.1	11.94	25.21
BRPT	10-Dec-03	10:15	2.0	13.89	25.38
BRPT	10-Dec-03	12:15	2.3	14.22	24.69
BRPT	10-Dec-03	16:15	2.6	14.56	24.82
BRPT	29-Jul-04	8:10	20.1	6.45	26.20
BRPT	29-Jul-04	11:30	21.3	8.40	17.95
BRPT	29-Jul-04	14:45	23.1	10.96	13.96
BRPT	29-Jul-04	16:50	23.7	11.53	12.63
BLR	29-May-03	9:45	14.4	8.30	22.65
BLR	29-May-03	14:00	16.1	10.16	18.40
BLR	29-May-03	16:30	15.9	10.34	18.84
BLR	24-Jun-03	9:30	22.6	6.71	20.90
BLR	24-Jun-03	13:30	25.6	13.54	18.85
BLR	24-Jun-03	16:45	27.9	14.95	22.63

BLR	29-Jul-03	8:45	20.7	3.72	23.67
BLR	29-Jul-03	12:45	22.8	9.82	10.79
BLR	29-Jul-03	16:30	25.6	11.27	11.56
BLR	17-Sep-03	9:00	17.9	2.95	26.73
BLR	17-Sep-03	12:45	19.7	7.11	16.91
BLR	17-Sep-03	4:45	22.5	7.81	17.15
BLR	27-Oct-03	9:30	7.3	9.95	27.46
BLR	27-Oct-03	12:45	7.8	10.33	26.84
BLR	27-Oct-03	16:30	7.7	10.32	26.77
BLR					
BLR	29-Jul-04	8:45	19.9	5.10	25.65
BLR	29-Jul-04	12:00	21.7	7.10	19.07
BLR	29-Jul-04	15:30	23.7	7.65	18.46
BLR	29-Jul-04	17:30	23.6	7.21	19.78
BLR	28-Oct-04	8:00	10.0	5.03	27.89
BLR	28-Oct-04	9:00	10.0	5.50	25.57
BLR	28-Oct-04	10:00	10.0	6.33	24.23
BLR	28-Oct-04	11:00	10.0	7.20	23.34
BLR	28-Oct-04	12:00	10.5	8.08	22.27
BLR	28-Oct-04	13:00	11.0	8.68	21.65
BLR	28-Oct-04	14:00	12.0	8.75	20.64
BLR	28-Oct-04	15:00	12.5	9.05	18.64
BLR	28-Oct-04	16:00	12.5	9.05	19.71
BLR	28-Oct-04	17:00	12.5	8.73	19.95
BLR	28-Oct-04	18:00	12.0	8.10	21.56